

School of Optometry and Vision Sciences
Cardiff University

Quantifying Perception and Oculomotor Instability in Infantile Nystagmus

Matt J Dunn

2014

A thesis submitted to Cardiff University for the degree of Doctor of Philosophy

Supervisors:

JT Erichsen

TH Margrain

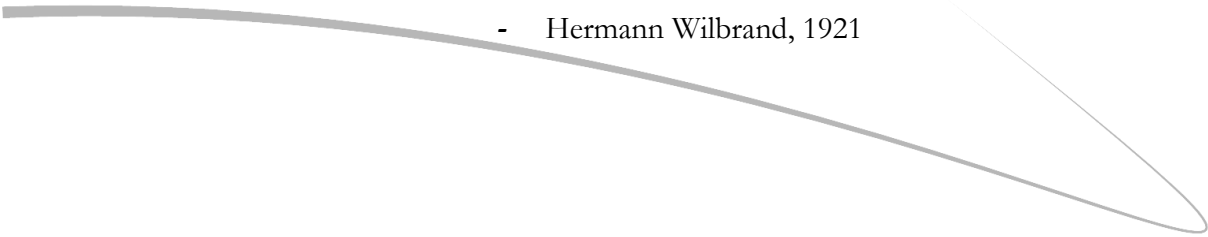
JM Woodhouse

Advisor:

FA Ennis

“Never write about nystagmus, it will lead you nowhere”

- Hermann Wilbrand, 1921



Acknowledgements

First, thanks must go to my supervisors, Jon Erichsen, Maggie Woodhouse and Tom Margrain, whose suitably varied perspectives and insights have shaped the entire project. I am grateful for the freedom I have been given to direct the work and their gentle persuasion whenever anything too crazy was suggested! Fergal Ennis has been an excellent mentor, providing input into the experiments above and beyond his role as an advisor.

One particularly crucial figure in these studies taking shape is John Sanders – not only due to the support provided by Nystagmus Network, but for the countless hours John has spent piloting the many bizarre experiments we've run at the Research Unit over the years. I'm extremely grateful to each and every person who has participated in the experiments, for giving up their time and traveling from the far reaches of the country in order to contribute to the work presented here.

The many friends I have made in the office have made the years far more enjoyable than any optometry practice: Diti, Hanim, Allannah, Rachel, Ally, Claire, Tamsin, Nikki and Grant. I am especially grateful for the guidance and support of Phil Jones, Ashley Wood, Tony Redmond, Robin O'Donovan and of course Chris Harris who has contributed in some way to almost every study in this report.

Thank you also to my project students, who have kept me focussed on getting projects ready in good time: Nikki, Nicolás, Elan and Laura. Thanks to Lee and Flors for discovering so many bugs in my code! From the nystagmus research community I'd also like to extend my gratitude to Jonathan Jacobs and Joost Felijs for helpful discussions in understanding the NAFX and NOFF algorithms. Crispin, Ami, Meg and Jason definitely deserve a mention for keeping my mind off the thesis in my spare time, instead encouraging me to spend much of my time dangling off ropes in remote parts of South Wales...

Of course, big thanks go to my mum, dad and brother (Stephen). Thanks for putting up with the endless typing when I came to visit and with me not having a 'proper' job all these years! And thanks to you, for reading (but I won't blame you if you don't read further than the acknowledgments ☺)

- **Matt**

Table of contents

Declaration	i
Acknowledgements	i
Table of contents	iii
List of tables	ix
List of figures	x
Acronyms.....	xviii
A note on CEMAS nomenclature.....	xviii
Summary	xix
Chapter 1 Background.....	1
1.1 Eye movements.....	1
1.1.1 Why do we move our eyes?.....	1
1.1.2 Neuromuscular control and classification of eye movements	1
1.1.3 Saccades	3
1.1.4 Optokinetic nystagmus	6
1.1.5 Vestibulo-ocular reflex.....	7
1.1.6 Smooth pursuit	7
1.1.7 Fixation maintenance movements	8
1.1.8 Vergence	9
1.2 Nystagmus.....	10
1.2.1 Physiological nystagmus	10
1.2.2 Acquired nystagmus	10
1.2.3 Early-onset nystagmus	11
1.3 Infantile nystagmus.....	12
1.3.1 Waveforms of infantile nystagmus.....	13
1.3.2 Baseline oscillation	16
1.3.3 Head shaking.....	16
1.3.4 Visual and oculomotor development in infantile nystagmus	16

1.3.5	Pathogenesis	17
1.3.6	Periodic alternating nystagmus	20
1.3.7	Idiopathic infantile nystagmus	21
1.3.8	Motor control in infantile nystagmus	24
1.3.9	Visual perception in infantile nystagmus	28
1.3.10	Treatments for infantile nystagmus	32
1.3.11	Appropriate measures of visual function	37
1.4	Eye movement recording	38
1.4.1	Scleral search coil	39
1.4.2	Electro-oculography	39
1.4.3	Photo-oculography	39
1.5	Summary	41
Chapter 2	Automated waveform analysis	43
2.1	Introduction	43
2.1.1	The problem with calibration	43
2.1.2	Foveations are not the same in all individuals	44
2.1.3	Complete waveform analysis	46
2.1.4	Waveform analysis: existing solutions	49
2.1.5	Existing methods for automated saccade detection	50
2.1.6	Aims	53
2.2	Materials and methods	54
2.2.1	Eye tracking apparatus	54
2.2.2	Software design	56
2.2.3	Participants and procedures	67
2.2.4	Display equipment	68
2.2.5	Ethics	68
2.2.6	Validation	69
2.3	Results	70

2.3.1	Participants and exclusions	70
2.3.2	Software output	71
2.3.3	Verification	73
2.4	Discussion	77
2.4.1	Verification	77
2.4.2	Redefinition of ‘foveation’	79
2.4.3	Saccade detection algorithm.....	80
2.4.4	Future work	81
2.5	Summary.....	83
Chapter 3	Visual acuity in the absence of image motion	84
3.1	Introduction.....	84
3.1.1	Aims.....	86
3.2	Materials and methods	87
3.2.1	Participants	87
3.2.2	Apparatus.....	87
3.2.3	Procedures	93
3.2.4	Paradigm development	95
3.3	Results.....	97
3.3.1	Participants and exclusions	97
3.3.2	Threshold data	97
3.3.3	Tachistoscopic vs constant illumination	100
3.3.4	Effect of orientation.....	100
3.3.5	Effect of age	102
3.4	Discussion	103
3.4.1	Orientation	104
3.4.2	What does this mean for people with nystagmus?	105
3.4.3	Implications for clinical practice	105
3.4.4	Assumptions and potential improvements	106

3.5	Summary.....	108
Chapter 4	Time to see	109
4.1	Introduction.....	109
4.1.1	Aims.....	110
4.2	Materials and methods	111
4.2.1	Participants	111
4.2.2	Apparatus.....	111
4.2.3	Procedures	111
4.2.4	Analysis	113
4.2.5	Paradigm development	115
4.3	Results.....	116
4.3.1	Participants and exclusions	116
4.3.2	Central vs peripheral presentation	116
4.3.3	Horizontal vs vertical presentation	117
4.3.4	Time to fixate vs time to respond.....	118
4.3.5	Horizontal vs vertical fixation and response times in controls.....	121
4.3.6	Effect of age	123
4.3.7	Effect of learning/fatigue.....	124
4.3.8	Instances in which automated analysis failed	124
4.4	Discussion.....	124
4.4.1	Limitations.....	126
4.4.2	Future work	127
4.5	Summary.....	129
Chapter 5	Interaction and timing of voluntary and involuntary saccades	130
5.1	Introduction.....	130
5.1.1	Aims.....	131
5.2	Materials and methods	131
5.2.1	Participants	131

5.2.2	Procedures	131
5.2.3	Analysis	132
5.3	Results.....	136
5.3.1	Participants and exclusions	136
5.3.2	Saccadic overlap.....	137
5.3.3	Changes to waveform metrics	140
5.3.4	Waveform modification prior to target acquisition.....	142
5.3.5	Waveform modification prior to target jumps	143
5.3.6	Effect of target jump timing on targeting saccade latency	143
5.3.7	Instances in which automated analysis failed	148
5.4	Discussion.....	151
5.4.1	Coincidence of quick phases and targeting saccades.....	151
5.4.2	Changes in nystagmus waveform prior to target acquisition	152
5.4.3	Lack of an effect of stimulus onset on saccade timing	152
5.4.4	Implications.....	154
5.4.5	Limitations.....	155
5.5	Summary.....	156
Chapter 6	Preliminary work and future investigations	157
	Preliminary work	157
6.1	Waveform characteristics during visual inattention.....	157
6.1.1	Introduction	157
6.1.2	Materials and methods.....	158
6.1.3	Results	159
6.1.4	Discussion.....	162
	Future investigations.....	163
6.2	Determination of the complete contrast sensitivity function.....	164
6.3	Measurement of parafoveal acuity.....	164
6.4	Partitioning the waveform: assessing temporal effects of nystagmus	165

6.5	Further measures of the ‘slow to see’ phenomenon.....	165
6.5.1	Visual change recognition time	165
6.5.2	Visual search.....	166
6.5.3	Motion change detection.....	167
6.6	Summary.....	168
Chapter 7	Discussion.....	169
7.1	Perception	170
7.2	Oculomotor characteristics	172
7.3	‘Chicken and egg’	172
7.4	Final remarks	173
	References.....	174
Appendix I	Source code for experimental programs	193
	flash.cpp.....	193
	flashtrack_test.m.....	193
	gellermanfellows.m.....	207
	handmarkfoveationperiods.m.....	208
	nystagmus_analyser.m	210
	nystagmus_calc_nafx.m.....	230
	nystagmus_calc_noff.m.....	232
	nystagmus_calibration_live_eyelink.m.....	235
	nystagmus_cycledetection_juhola.m.....	239
	nystagmus_identifycalibrationlocation.m.....	241
	noisechecking.m	243
	oculomotorsuite_beginrecording.m.....	245
	oculomotorsuite_degrees2px.m	245
	oculomotorsuite_drawcross.m	245
	oculomotorsuite_findsaccades_behrens.m.....	246
	oculomotorsuite_findsaccades_dunn.m.....	249

oculomotorsuite_generatecompleteeyetracearray.m	252
oculomotorsuite_lowpassfilter.m.....	252
oculomotorsuite_px2degrees.m	253
oculomotorsuite_removeblinks.m	253
oculomotorsuite_readeyetrace.m	258
oculomotorsuite_receivedatafile.m.....	260
playtone.m	260
skippabledelay.m.....	260
Appendix II Subject information.....	262
II.1 Subjects with nystagmus	262
II.2 Control subjects	266
Appendix III Nystagmus analysis software user manual	268
Appendix IV Lay summary of research: letter to participants	283
Appendix V Patient information sheets and consent forms	286
Appendix VI Ethical applications and approval documents.....	291
Appendix VII Published work	301

List of tables

Table 1.1: Primary, secondary and tertiary actions of the extraocular muscles.	2
Table 2.1: Noise levels recorded in different 'gaze' positions under photopic and scotopic conditions with an EyeLink 1000. All values are in degrees. X and Y refer to horizontal and vertical respectively.....	55
Table 2.2: Offset from expected position (°) for all subjects at all tested locations	73
Table 2.3: Percentage of cycles in a nystagmus recording in which foveations are found with each foveation detection algorithm.....	74
Table 2.4: Percentage of nystagmus waveform identified as foveations by each method.....	75
Table 2.5: Percentage of samples detected by the <i>dynamic threshold method</i> that were also detected by the <i>fixed threshold method</i> at two fixed foveation velocity thresholds	75
Table 3.1: VA (logMAR) obtained for subjects with IIN.....	98
Table 3.2: VA (logMAR) obtained for control subjects.....	98

Table 3.3: Mean and standard errors of VAs (logMAR) shown in Tables 3.1 and 3.2 for all conditions and both groups. Subjects who took part with uncorrected refractive error ≥ 0.50 D (mean sphere) are excluded.....	99
Table 3.4: Mean and standard errors of VAs shown in Tables 3.1 and 3.2 for all conditions and both groups. Subjects who took part with uncorrected refractive error ≥ 0.50 D (mean sphere), and those who did not complete all conditions are excluded.	100
Table 4.1: From response data for which saccade detection was possible, the mean time until execution of the vertical target acquiring saccade and the mean time from saccade termination until subject response. The number of recorded observations for each participant are shown.	119
Table 5.1: List of subjects who participated in the present study, along with the data capture rate, number of analysable target jumps (based on the presence of contiguous data), and number of target jumps that were used in the final analysis	136
Table 5.2: Subject-specific saccadic metrics. Quick phase metrics are not shown for subjects DP and NB, as explained in Section 5.3.7.1.	140

List of figures

Figure 1.1: Diagram showing the extraocular muscles of the right eye. Adapted from Sparks (2002).....	1
Figure 1.2: The main sequence of saccades showing the relationship of both duration and peak velocity to amplitude. Adapted from Bahill, Clark and Stark (1975).....	4
Figure 1.3: The main structures involved in the neural control of saccades. SC, superior colliculus; riMLF, rostral interstitial nucleus of the medial longitudinal fasciculus; NIC, interstitial nucleus of Cajal; III, oculomotor nucleus; IV, trochlear nucleus; PPRF, paramedian pontine reticular formation; VI, abducens nucleus; NPH, nucleus prepositus hypoglossi. Adapted from Sparks (2002).....	5
Figure 1.4: Representation of step signal from a theoretical perfect neural integrator and a leaky neural integrator. Adapted from Leigh and Zee (2006).....	6
Figure 1.5: Physiological instabilities of fixation, showing microsaccades, drifts and OMT (Pritchard 1961).	8
Figure 1.6: A normal OMT waveform from an alert individual measured with a piezoelectric strain gauge. Bursts are underlined (Bojanic, Simpson and Bolger 2001).....	9
Figure 1.7: The components of a nystagmus waveform. Frequency is inferred from cycles per time unit.	13

Figure 1.8: The 12 waveforms found in IN according to Dell’Osso and Daroff (1975). Commonly used acronyms are given in parentheses (R = right; L = left).....	15
Figure 1.9: Schematic representation of baseline oscillation in an IN waveform. Adapted from Pasquariello et al. (2009).....	16
Figure 1.10: The effects of (a) 'effort to see' (attempting to read small letters) and (b) relaxation on nystagmus intensity, both (i) before, and (ii) during each mental state (Abadi and Dickinson 1986).....	25
Figure 1.11: EM trace for a 20 week old infant with IN during (a) waking, (b) and (c) non-paradoxical sleep and (d) paradoxical sleep (Abadi and Dickinson 1986).	26
Figure 1.12: The Skalar IRIS headset and processing unit (Cambridge Research Systems 2007).....	40
Figure 1.13: The Tobii X300 system (Tobii Technology, 2011).....	40
Figure 1.14: The EyeLink 1000 system (SR Research, 2010).....	41
Figure 2.1: Example of foveations detected (red) using the traditional automated method of foveation detection, with foveation velocity threshold set to $6^{\circ}/s$ (subject JS)	45
Figure 2.2: Example of foveations detected (red) using the traditional automated method of foveation detection, with foveation velocity threshold set to $6^{\circ}/s$ (subject DB)	45
Figure 2.3: Visualisation of both the horizontal and vertical components of nystagmus across time might provide new insights into the condition.	47
Figure 2.4: Composite output from nystagmus analysis software, including marked saccades (green), foveations (red), cycle boundaries (black) and subplots showing saccadic main sequence relationships (lower central subplot is three-dimensional).....	48
Figure 2.5: Graphical user interface for nystagmus analysis software	48
Figure 2.6: Graphical user interface for nystagmus calibration software	49
Figure 2.7: An example of a nystagmus EM trace (subject GT) using the Behrens, Mackeben and Schröder-Preikschat (2010) saccade detection algorithm. Detected saccades are shown in green.	52
Figure 2.8: An example of erroneous saccade detection using the method described by Behrens, Mackeben and Schröder-Preikschat (2010) (subject MT). The fuchsia line shows the acceleration trace (divided by 1000 for visibility on the plot). During a detected ‘saccade’, the position line (blue) changes to green. Saccadic acceleration thresholds are indicated as dashed red lines. In this case, the saccadic threshold is sufficiently low that an erroneous saccade is detected before the actual saccade starts. As a result, the true saccade is missed.....	52
Figure 2.9: 'Model eye' used to verify noise levels in eye tracker systems.....	54

Figure 2.10: Figure demonstrating the effect of low-pass filtering on nystagmus waveform data (subject JS). The lower plot shows the same data as above, with a low-pass filter at 90 Hz.	57
Figure 2.11: Example trace showing result of two-point central differentiation to obtain signal velocity and acceleration (subject JS).....	58
Figure 2.12: Example of a nystagmus waveform (subject DK) containing a blink. Note the spikes in the upper trace associated with dropped data at 2400-2500 ms. The lower trace shows the same data, with the blink removed. Red lines in the upper trace show the positional limits used to determine the start and end of a blink.	59
Figure 2.13: Schematic showing the stages of the cycle detection algorithm. Top: horizontal eye position trace (subject LC) with detected cycles marked. Middle: slope function, with zero crossing line shown. Bottom: binary slope function, filtered and repolarised.	60
Figure 2.14: Schematic showing features used by the saccade detection algorithm. The blue line shows the position vector; the green region indicates a detected saccade. The aqua line shows the velocity transform (divided by 100 for visibility). The fuchsia line shows acceleration (divided by 1000). Since this shows a <i>leftward</i> saccade, velocity and acceleration ‘peaks’ are at the bottom of the plot, and troughs are found at the top. The acceleration peak for this saccade is beyond the edge of the plot area.....	62
Figure 2.15: The same EM trace as shown in Figure 2.7, with saccades detected using the newly proposed algorithm. Detected saccades are shown in green.	63
Figure 2.16: A candidate foveation (marked in red) is detected over the boundary between two cycles (dotted line). In this case, the foveation is considered a part of the first cycle, and is not counted as being a part of the second (data from subject GT2).....	64
Figure 2.17: An example of automatically detected foveations in a nystagmus waveform (subject GT2, foveations set to be found in $\geq 50\%$ of cycles). Detected foveations are marked in red.....	65
Figure 2.18: Schematic representation of the locations of on-screen calibration targets.....	66
Figure 2.19: Fixation cross dimensions	66
Figure 2.20: Sony GDM-F520 21” CRT monitor	68
Figure 2.21: Example output from the calibration procedure (subject JT). Slow phases are shown in blue; saccades are shown in green. A blink has been detected and removed at sample #6000. Candidate points to be used for calibration are shown in red.	71
Figure 2.22: Example output from the analysis procedure (same data as Figure 2.21). Unlike the previous figure, red regions now indicate foveations (defined using a velocity threshold of $4^\circ/\text{s}$), and the position trace is now calibrated.....	72

Figure 2.23: Plot showing calculated foveation positions for nine participants, derived from calibrations made using separate recordings. Actual target positions are shown in red. This demonstrates the test-retest repeatability in different angles of gaze. The effect of data capture percentage on the result is also shown (marker opacity).....	73
Figure 2.24: Example (subject DB) of foveations detected (shown in red) using the new algorithm set to detect foveations in 50% of cycles (top); using a fixed foveation velocity threshold of 4°/s (middle); and using a fixed foveation velocity threshold of 10°/s (bottom)	74
Figure 2.25: Custom-made MATLAB software for manual marking of foveation periods. The upper trace is the position trace; the lower trace shows the velocity transform.	76
Figure 2.26: Example of foveations detected (red) using the new method of foveation detection, set to detect a foveation in 50% of nystagmus cycles (subject JS). Compare with Figure 2.1.	79
Figure 2.27: Example of foveations detected (red) using the new method of foveation detection, set to detect a foveation in 50% of nystagmus cycles (subject DB). Compare with Figure 2.2.	80
Figure 2.28: For subjects with IN, each foveation detected over a 10 s period, plotted relative to the mean position of all foveations during this period. This type of analysis may provide a useful method for assessing foveation accuracy of individuals with IN.	83
Figure 3.1: The relationship between retinal image velocity and VA with optotypes (Demer and Amjadi 1993).....	84
Figure 3.2: Combined spectral transmission of flash unit and heat resistant glass.....	88
Figure 3.3: AR-2 relay device, connected to RS-232 cable. Brown wires lead to Metz standard sync cable; black wires lead to a 9V power supply.	89
Figure 3.4: Photograph of the aperture frame illuminated by the flash unit, with a grating mounted inside (tilted 5° up to the left), as viewed by subjects. The bull's-eye targets serving as horizontal and vertical axis references can be seen around the grating edge.....	90
Figure 3.5: Servo-controlled aluminium see-saw and frame for grating mounting and tilting.	90
Figure 3.6: The tilt mechanism in detail, showing servo motor and eight channel USB solenoid relay switch	91
Figure 3.7: Automated occluder and chin/forehead rest	92
Figure 3.8: Microsoft SideWinder game pad	92
Figure 3.9: Laboratory setup for experiment.....	93
Figure 3.10: Schematic to explain the triggering of flash at different waveform loci. Although the absolute position of the waveform in the orbit varies from cycle to cycle, it might be	

possible to step through the waveform in real time and trigger a flash unit at (for example) the loci shown by the arrows.....	96
Figure 3.11: Graphical representation of the mean VA recorded for subjects with < 0.50 D (mean sphere) uncorrected refractive error. Error bars indicate standard error. The number of subjects for each datum is shown in parentheses.	99
Figure 3.12: Data from Table 3.4 represented graphically. Error bars indicate standard error.	101
Figure 3.13: Graph showing the effect of age on the difference in mean thresholds obtained for constant and tachistoscopic stimulus presentation in both nystagmats and control subjects. A positive number indicates a worsening of VA with the flash. Linear regression and confidence intervals are shown.	102
Figure 4.1: Examples of Gabor patches oriented 45° to the left and right.....	112
Figure 4.2: Schematic explanation of the sequence of stimuli presented on-screen for the static task.....	112
Figure 4.3: Schematic explanation of the sequence of stimuli presented on-screen for the saccadic task. Gabor patches were presented in either orientation; only one is shown here for illustrative purposes.....	113
Figure 4.4: EM trace showing horizontal eye position (blue) and vertical eye position (red). Targeting saccades identified in the vertical axis are marked in green. The difficulty faced by automatic saccade detection in the horizontal axis is evident; it is not clear from the EM trace when these target-acquiring saccades took place.....	114
Figure 4.5: The effect of central or peripherally presented gratings on subject response time in subjects with and without IN. Error bars indicate standard error.	117
Figure 4.6: Box plots showing the effect of horizontally or vertically displaced gratings on subject response time in subjects with and without IN. Outliers are displayed as black dots.	118
Figure 4.7: For vertically displaced grating targets, the average time taken for a target-acquiring saccade to be executed. Note that not all target displacements were associated with a detected saccade.....	120
Figure 4.8: For vertically displaced grating targets, the time taken from completion of the target-acquiring saccade until the response was made by the subject. Note that not all target displacements were associated with a detected saccade. Outliers are displayed as black dots.	120

Figure 4.9: For control subjects, the time taken for a target-acquiring saccade to be executed towards horizontally or vertically displaced gratings. Note that not all target displacements were associated with a detected saccade. Outliers are displayed as black dots.....	122
Figure 4.10: For control subjects, the time taken from completion of the target-acquiring saccade until the response was made by the subject for horizontally or vertically displaced gratings. Note that not all target displacements were associated with a detected saccade. Error bars indicate standard error.....	122
Figure 4.11: Scatter plot showing the effect of age on response times to all stimuli in nystagmats and control subjects. Regression lines and 95% confidence intervals (shaded areas) are shown.....	123
Figure 4.12: EM trace showing horizontal eye position (blue) and vertical eye position (red). Targeting saccades identified in the vertical axis are marked in green. Unlike Figure 4.4, this subject has low enough nystagmus amplitude that automated saccade detection may be feasible in the horizontal axis.....	128
Figure 5.1: Schematic explanation of the sequence of stimuli presented on-screen. Note that two magnitudes of target displacement were used; only one is shown here for illustrative purposes.....	132
Figure 5.2: Diagram to illustrate regions of data removed in order to analyse target displacements solely in the vertical axis	133
Figure 5.3: Illustration of a waveform containing multiple saccades in each cycle. Only the saccade with the highest peak velocity in each cycle is chosen to represent the 'quick phase'.	134
Figure 5.4: Example EM trace illustrating how some of the analysis metrics were determined	135
Figure 5.5: Examples of instances in which nystagmus quick phases were <i>not</i> detected as coinciding with vertical saccades, although visible inspection reveals small disturbances around the time that the quick phase would have been expected, as well as a lack of slow phase acceleration and an approximate doubling of slow phase length. The lower figure also shows an apparent change in nystagmus beat direction.	137
Figure 5.6: Schematic of an asymmetric pendular waveform (Dell'Osso and Daroff 1975). 138	
Figure 5.7: An example of target acquisition occurring with a fast drift (marked in green on the red eye trace) and modification of the waveform to asymmetric pendular type.	138
Figure 5.8: Examples of vertical target acquiring saccades occurring mid-slow phase. These occurred only rarely (top, subject NB; middle, subject DP; bottom, subject SW).	139

Figure 5.9: For coincident targeting saccades and quick phases, the relationship between the amplitude of the quick phase and the last quick phase to occur prior to the target jump. Regression line is shown (solid line); the shaded region indicates standard error. The dashed line represents the expected (1:1) relationship if there were no effect.	141
Figure 5.10: For coincident targeting saccades and quick phases, the relationship between the nystagmus cycle length at the time of target acquisition and the length of the last cycle to occur prior to the target jump. Regression line is shown (solid line); the shaded region indicates standard error. The dashed line represents the expected (1:1) relationship if there were no effect.....	142
Figure 5.11: Results from subject GT2 show an obvious modification of the waveform prior to target acquisition. This feature was a common finding in this subject.	143
Figure 5.12: Subject JC exhibits a change to a pendular waveform <i>prior to</i> the target jump, possibly as an adaptation to improve visual function in anticipation of the jump.	143
Figure 5.13: The effect of the timing of target jumps (with respect to the last nystagmus quick phase) on vertical saccade latency for subjects with IN. Regression line is shown; the shaded region indicates standard error.	144
Figure 5.14: The effect of target jump timing during the nystagmus cycle (as a fraction of the total cycle length) on vertical saccade latency for subjects with IN. Regression line is shown; the shaded region indicates standard error.	144
Figure 5.15: For each subject with IN, the relationship between the time during the nystagmus cycle at which the target jump occurred (since the last quick phase) and the latency of the targeting saccade. For each participant, linear regression lines are shown with standard error (shaded region). p values indicate the probability that each regression slope is equal to zero.	145
Figure 5.16: For subjects KL (FMNS) and JC (no nystagmus in primary position), the effect of target jump timing on voluntary saccade latency. Format is identical to Figure 5.15.....	146
Figure 5.17: The same data as shown in Figure 5.17, but with the ordinate based on a <i>prediction</i> of nystagmus cycle length, based on the length of the last complete cycle preceding the target jump.....	147
Figure 5.18: For subjects KL (FMNS) and JC (no nystagmus in primary position), the effect of target jump timing on voluntary saccade latency, where ‘normalised’ cycle length is a prediction based on the length of the last complete cycle to occur prior to the target jump. Format is identical to Figure 5.17.	148
Figure 5.19: Data from subject DP showing cycle boundaries (vertical yellow lines), leading to variable ‘quick phase’ selection for each cycle.....	149

Figure 5.20: Example of a target jump with a non-saccadic target acquisition. The algorithm has instead detected a later erroneous saccade.....	149
Figure 5.21: A subject with an oblique nystagmus axis (JI) exhibits significant vertical and horizontal components. For small target jumps, this makes detection of the target-acquiring saccade difficult.....	150
Figure 5.22: Dampened nystagmus amplitude around the time of the target-acquiring saccade causes incorrect cycle detection, which leads to a quick phase not being identified. Vertical yellow lines indicate cycle boundaries as detected by the algorithm.....	150
Figure 5.23: An initial hypometric vertical saccade causes the algorithm to fail to detect overlap with a nystagmus quick phase.....	151
Figure 5.24: Data from Wang and Dell'Osso (2007), showing horizontal target acquisition time (L_t) against the normalised time within the nystagmus cycle of the target jump ($T_c\%$) for different waveform types. Polynomial regression curves are shown.....	154
Figure 6.1: The effect of inattention on a jerk nystagmus waveform (Reinecke 1997).....	158
Figure 6.2: Nystagmus intensity plotted against time since the start of the recording for each participant. Only 'clean' cycles (i.e. those containing no dropped data) are shown.....	160
Figure 6.3: Quadratic regression models for the null zones of each participant, based on data available from the range of viewing angles recorded during the experiment.....	161
Figure 6.4: Locally weighted polynomial regression models showing change in nystagmus intensity plotted against time for each participant. Changes in intensity due to variation in horizontal gaze angle are controlled for (using the quadratic regression models shown in Figure 6.3). Hence, the ordinate shows the <i>change</i> in nystagmus intensity relative to values predicted by the quadratic regression model at each moment in time.....	162
Figure 6.5: Program for testing visual reaction speed.....	166
Figure 6.6: Screenshot from visual search paradigm.....	167
Figure 6.7: Motion change detection paradigm. The white circle is moving to the right, and will change direction at a random time.....	167

Acronyms

ANAF	automated nystagmus acuity function
CEMAS	Committee for the Classification of Eye Movement Abnormalities and Strabismus
EM	eye movement
FMNS	fusion maldevelopment nystagmus syndrome
IIN	idiopathic infantile nystagmus
IN	infantile nystagmus
NAEF	nystagmus acuity estimator function
NAF	nystagmus acuity function
NAFX	expanded nystagmus acuity function
NOFF	nystagmus optimal fixation function
OKN	optokinetic nystagmus
OMT	ocular microtremor
OPN	omnidirectional pause neuron
PAN	periodic alternating nystagmus
VA	visual acuity
VOR	vestibulo-ocular reflex

A note on CEMAS nomenclature

In 2001, the Committee for the Classification of Eye Movement Abnormalities and Strabismus (CEMAS) produced a document outlining a new nomenclature for disorders of eye movement, bringing much needed structure to a confused array of terms, which previously were subject to multiple definitions in a variety of disciplines (Avallone et al. 2001). The terms used herein relate to those set out in the CEMAS document.

Summary

The purpose of the studies described herein was to better understand the impact of involuntary eye movements on oculomotor control and perception in infantile nystagmus. Therapeutic interventions that result in slowed nystagmus oscillations often fail to elicit significant quantifiable improvements in visual function, despite patients reporting subjective benefits. It is difficult to justify surgical or pharmacological intervention when the only outcome measures are subjective.

Objective quantification of nystagmus eye movements *per se* usually involves time-consuming manual marking of recordings to both calibrate and analyse data. As a result, analyses are rarely (if ever) performed in the clinical setting. Software was therefore developed to automate calibration and assessment.

Psychophysical experiments were undertaken to quantify the spatiotemporal constraints of vision in infantile nystagmus. Visual acuity was measured in the absence of retinal image motion to reveal the maximum improvement to *spatial* vision that might be expected if nystagmus were halted altogether. The results indicate that poor spatial vision underlies infantile nystagmus, even in cases without comorbid pathology.

Gaze acquisition time was compared to stimulus recognition time. The results indicate that infantile nystagmus *does not* increase visual processing time; rather, redeploying gaze takes longer.

An incidental finding revealed a temporal relationship between voluntary saccades and involuntary nystagmus quick phases. Both typically occur together, presumably to maximise efficiency and minimise saccadic suppression.

Clinical tests of gaze acquisition time must now be developed, to be used in conjunction with the software developed here, as objective outcome measures of therapeutic interventions.

Chapter 1 Background

Nystagmus describes a constant, involuntary, oscillation of the eyes. Nystagmus can be invoked physiologically in almost all individuals, yet in its pathological form, it has perceptual consequences that are yet to be fully understood. This chapter provides a general introduction to eye movements (EMs) and an overview of nystagmus as it is currently understood.

1.1 Eye movements

1.1.1 Why do we move our eyes?

Although we refer to eye *movements*, the term does not refer to a translation of the eye, but a rotation of the globes to elicit a change in gaze angle. Rotation of the eyes allows us to shift visual attention rapidly from one object to another with relatively little expenditure of energy (see Section 1.1.3 - *Saccades*). This is important because the human fovea provides extremely detailed vision only over a relatively small visual angle of approximately 2° (Wertheim 1938). As well as shifting our gaze, EMs are used to track moving objects (Section 1.1.6 - *Smooth pursuit*) and to counteract movement of the entire visual field (Section 1.1.4 - *Optokinetic nystagmus*). EMs also serve to stabilise gaze during head movements (Section 1.1.5 - *Vestibulo-ocular reflex*), to prevent visual perceptual fading, and to correct for unintentional drifts of fixation (Section 1.1.7 - *Fixation maintenance movements*).

1.1.2 Neuromuscular control and classification of eye movements

Each eye has six extraocular muscles (see Figure 1.1). Thus, EMs are controlled by twelve muscles, which move the two eyes about one or more of three axes.

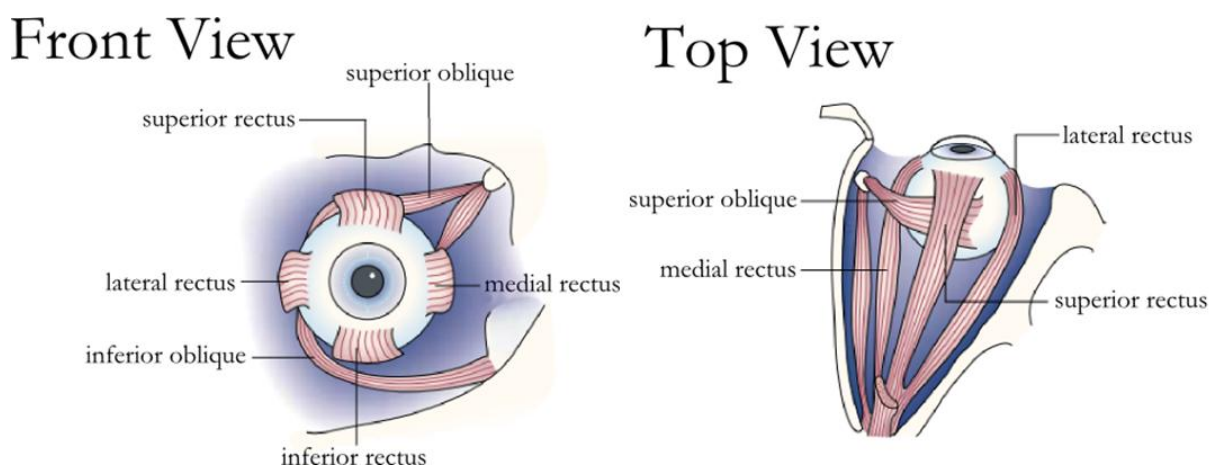


Figure 1.1: Diagram showing the extraocular muscles of the right eye. Adapted from Sparks (2002).

With the exception of the medial and lateral recti (which solely adduct and abduct the eyes), each muscle exerts an influence in three axes (pitch, yaw and roll). Table 1.1 summarises the direction of action of each muscle (Remington 1998).

Table 1.1: Primary, secondary and tertiary actions of the extraocular muscles.

Muscle	Primary action	Secondary action	Tertiary action
Medial rectus	Adduction	None	None
Lateral rectus	Abduction	None	None
Superior rectus	Elevation	Intorsion	Adduction
Inferior rectus	Depression	Extorsion	Adduction
Superior oblique	Intorsion	Depression	Abduction
Inferior oblique	Extorsion	Elevation	Abduction

Four of the extraocular muscles are innervated by the oculomotor nerve, whose origins comprise the midbrain oculomotor nucleus, the caudal central subdivision and the parasympathetic Edinger-Westphal nucleus (May and Corbett 1997). The exceptions are the superior oblique, innervated by the trochlear nerve, and the lateral rectus, innervated by the abducens nerve (Oyster 1999).

Having described the extraocular muscles and their neurological control systems, it is useful to understand the types of EM can be produced. There are seven major classes of EM (Leigh and Zee 2006):

- Saccades
- Optokinetic nystagmus (OKN)
- Vestibulo-ocular reflex (VOR)
- Smooth pursuit
- Fixation maintenance movements
- Nystagmus quick phases (equivalent to saccades)
- Vergence

Each of the types of EM listed above are discussed in the sections that follow. Particular attention is given to the neurology of saccades, which are implicated in Chapters 4 and 5.

1.1.3 Saccades

Saccades are ballistic EMs from one point of fixation to another. They are the fastest type of EM known (Leigh and Zee 2006). On average, humans make three saccades every second. During a saccade, magnocellular pathways of the visual system are suppressed to prevent the perception of a moving retinal image, whilst the parvocellular system remains unsuppressed (Ross, Burr and Morrone 1996; Burr, Morrone and Ross 1994). Saccades may be induced voluntarily to a real or remembered target, or as a reflex.

The majority of saccades made on a day-to-day basis are less than 15° in size (Bahill, Adler and Stark 1975). Those that are larger than 15° tend to occur in two steps; the first step is a hypometric saccade that takes the eye approximately 90% of the way towards the target, followed by another that corrects for the undershoot (Becker and Fuchs 1969). Saccades are extremely rapid, reaching over $800^\circ/\text{s}$ at their fastest (Tovée 1996). There is a latency period, typically of around 200 ms, between stimulus presentation and the saccadic response (Leigh and Zee 2006). Latencies ranging from 100 – 1000 ms have been reported; this is affected by the nature of the stimulus, the urgency and motivation to move the eyes, and the presence of neuropathology (Gilchrist 2011).

1.1.3.1 Saccadic main sequence

The amplitude of a saccade is directly related to both the maximum peak velocity elicited during that movement and its duration; this relationship is known as the *main sequence* (Bahill, Clark and Stark 1975) and is similar for healthy individuals in both adults and infants (Garbutt, Harwood and Harris 2006). Thus, larger amplitude saccades have higher peak velocities and longer durations (Boghen et al. 1974). The main sequence holds true for any saccade; however, a study by Bollen et al. (1993), which measured the main sequence of individuals on two occasions separated by two weeks, found that there can be significant intra-individual variability of the parameters of the main sequence at different times. Figure 1.2 shows typical duration/amplitude and peak velocity/amplitude main sequence relationships.

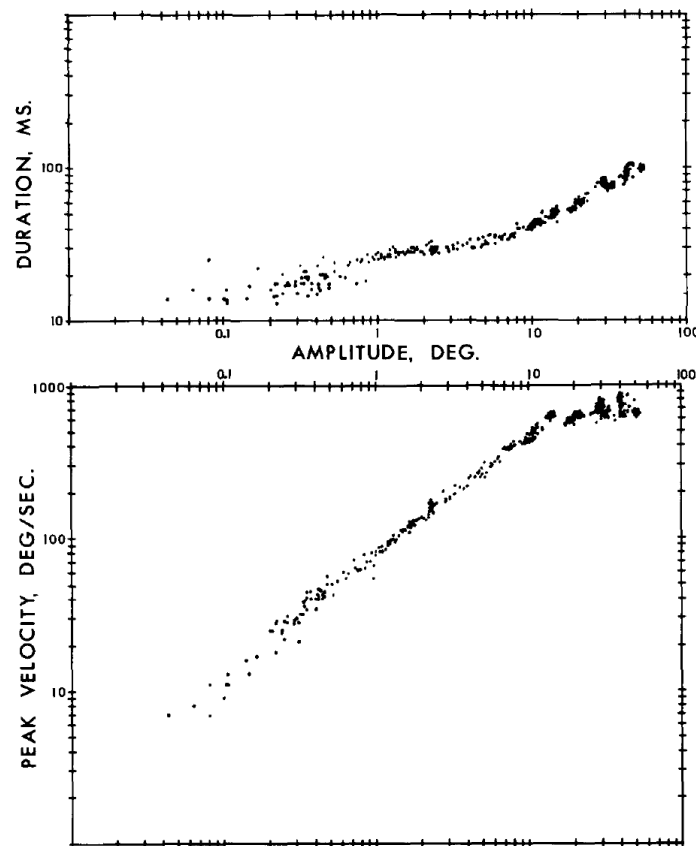


Figure 1.2: The main sequence of saccades showing the relationship of both duration and peak velocity to amplitude. Adapted from Bahill, Clark and Stark (1975).

1.1.3.2 Neurology of saccades

Saccade motor commands are initiated in the cortex (i.e. the superior colliculus and/or frontal eye fields). Many areas of the brain contribute towards the neural control of saccades, either directly or indirectly projecting to the superior colliculus or brainstem gaze centres, including the substantia nigra pars reticula, the posterior parietal cortex and the frontal eye fields (Leigh and Zee 2006), whilst the lateral intraparietal area is involved in deciding in which direction the next saccadic EM should be made (Shadlen and Newsome 2001). For more information about the higher cortical control of saccades, which will not be discussed here, the reader is directed to the comprehensive text, *The Neurology of Eye Movements* (Leigh and Zee 2006).

The frontal eye fields and superior colliculus both have direct projections to the brainstem gaze control nuclei; in the case of a horizontal saccade, this is the paramedian pontine reticular formation (although a direct link is disputed [Keller, McPeck and Salz 2000]). This then projects to the ipsilateral abducens nerve, which in turn projects to the lateral rectus, and, via interneurons, to the contralateral oculomotor nerve which controls the ipsilateral medial rectus. Excitatory burst neurons send a 'pulse' or velocity signal, the length and frequency of which determines the amplitude and duration of the EM (hence defining the

saccadic main sequence). A tonic signal, known as a 'step' or hold signal keeps the eye in the eccentric position determined by the pulse (Sparks 2002). The step signal is generated by the *neural integrator*, which is a complex in the brainstem and cerebellum (Oyster 1999). The neural integrator differs for horizontal and vertical EMs. For horizontal EMs, the primary structures involved are the nucleus prepositus hypoglossi and medial vestibular nucleus (Cannon and Robinson 1987). The interstitial nucleus of Cajal is the primary structure involved in vertical and torsional gaze holding (Crawford, Cadera and Vilis 1991). Figure 1.3 shows the main structures involved in the neural control of saccade generation.

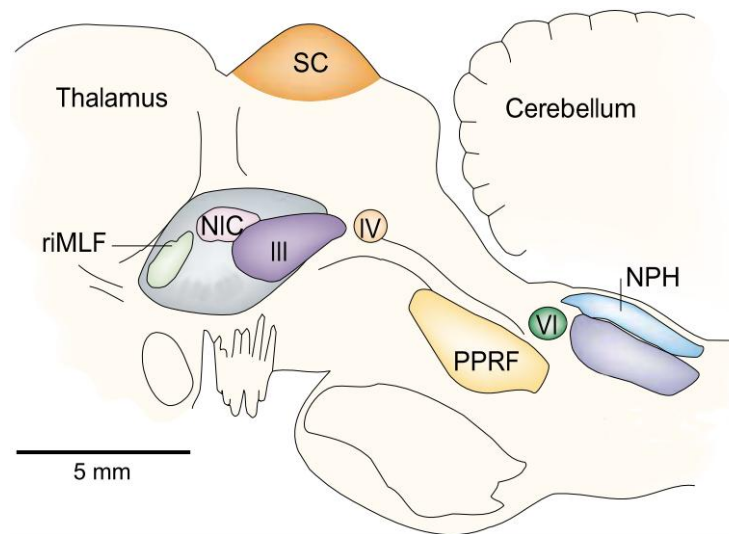


Figure 1.3: The main structures involved in the neural control of saccades. SC, superior colliculus; riMLF, rostral interstitial nucleus of the medial longitudinal fasciculus; NIC, interstitial nucleus of Cajal; III, oculomotor nucleus; IV, trochlear nucleus; PPRF, paramedian pontine reticular formation; VI, abducens nucleus; NPH, nucleus prepositus hypoglossi. Adapted from Sparks (2002).

Ordinarily, the excitatory burst neurons are tonically inhibited by omnidirectional pause neurons (OPNs), located in the raphe interpositus nucleus (Keller 1974; Evinger, Kaneko and Fuchs 1982; Buttner-Ennever et al. 1988; Hittinger and Horn 2012). Prior to saccade initiation, the OPNs are inhibited, suddenly releasing the inhibition of excitatory burst neurons, thus providing a 'kick-start' (known as *post-inhibitory rebound*) to the saccade. This 'burst' is what affords saccades their great speed. OPN activity resumes shortly after the saccade is complete (Leigh and Zee 2006). Specifically, post-inhibitory rebound is the result of a rapid increase in discharge from the membrane of a burst neuron following a period of hyperpolarisation. Ion channels within the burst neurons facilitate this discharge (Shaikh et al. 2008).

In order for a system to compensate for inaccuracy, feedback is required. *Proprioception* is the brain's perception of the position of parts of the body relative to one another (Warren,

Yeziarski and Capra 1997). For the calculation of accurate EMs, knowledge of the position of the eye in the orbit and that of the intended visual target are required. When a voluntary EM is made, a copy of the motor command is created to update ocular proprioception. This signal is known as *efferece copy*. Along with proprioception and visual input, efferece copy provides feedback for the visual system to calculate the magnitude of signals, such as the saccadic pulse and step signals (Leigh and Zee 2006).

1.1.3.3 The 'leaky' neural integrator

In order for the eyes to be held in an eccentric position, the neural integrator must produce a constant step signal, the size of which is related to the eccentricity of the eye position. Without it, the eyes drift back to the primary position. A 'perfect' neural integrator would hold the eyes in the intended eccentric position indefinitely. However, normal individuals will exhibit drifts in the absence of visual feedback (Becker and Klein 1973). This is due to decay of the inconstant step signal – described as 'leakiness' of the neural integrator. Figure 1.4 shows the difference between these signal types. The presence of drugs or disease will increase neural integrator leak, causing more regular drifts. This forms the basis of the roadside nystagmus sobriety test, a controversial technique used by police in some areas of the United States to assess intoxication (Good and Augsburger 1986).

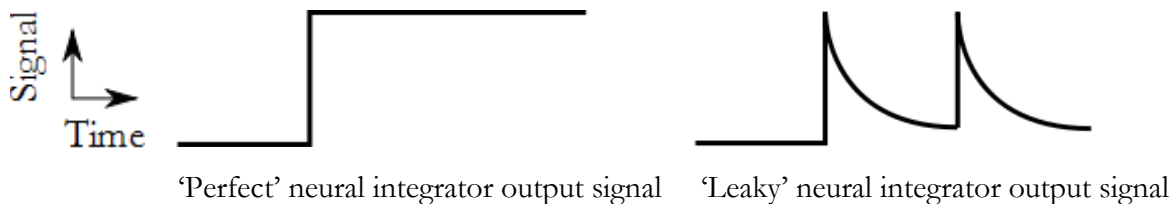


Figure 1.4: Representation of step signal from a theoretical perfect neural integrator and a leaky neural integrator. Adapted from Leigh and Zee (2006).

As shown in Figure 1.4, a leaky neural integrator results in periodic step signals. The result of this is that the eye repeatedly switches between drifts towards the primary position and saccades towards the intended gaze angle. This is one form of nystagmus.

1.1.4 Optokinetic nystagmus

OKN is a compensatory EM and a normal response to minimise the retinal slip provoked by a large moving visual stimulus or the entire visual field. If the slow movement causes the eyes to reach maximum rotational eccentricity, a jerk movement occurs in the opposite direction, in order to re-fixate the background and continue holding the image of the visual field steady on the retina. This jerk movement is known as the OKN *quick phase*, whilst the smooth drift is called the *slow phase*. An oft-cited example of OKN is that of watching the countryside pass from the window of a moving train; in order to achieve a clear image, it is necessary to reduce

image motion by tracking one part of the scene. It is inevitable that at some point the tracked portion of the image passes out of view, due to the eyes reaching maximum rotation; at this point, gaze jerks to a point further back in the scene. Although relying on a similar mechanism, OKN is not the same as smooth pursuit. Indeed, during smooth pursuit, OKN is suppressed to allow tracking of small objects moving against the visual background (Leigh and Zee 2006).

1.1.5 Vestibulo-ocular reflex

VOR is another compensatory EM with a similar function to OKN, but instead of being driven by visual feedback, this EM is produced by the movement of fluid in the semi-circular canals of the inner ear in response to head movements. This fluid bends the kinocilia (small hair-like projections), which cause the ampullae to send a signal to the vestibulocochlear nerve, causing an EM in the opposite direction to the head movement. VOR *nystagmus* describes the jerk EM that occurs when the eye has reached maximum rotation (as would occur during a large rotation of the body). Like OKN, this rapid reset EM is in the opposite direction to the slow phase of movement and non-pathological.

VOR nystagmus can also be induced by irrigating the external meatus (Barker and Barasi 1999). The difference in temperature between liquid and body creates a convection current in the horizontal semi-circular canal, stimulating the kinocilia and resulting in VOR nystagmus. This is known as *caloric reflex testing*, and is used to investigate vestibular function.

1.1.6 Smooth pursuit

Smooth pursuit describes foveal tracking of moving objects. OKN is suppressed during smooth pursuit to prevent retinal slip of the background driving the eyes in the opposite direction to the moving target (Leigh and Zee 2006). The smooth pursuit system uses predictive mechanisms to update its velocity and direction based on where a target is expected to move (Barnes, Schmid and Jarrett 2002). In adulthood, the ability to maintain steady smooth pursuit declines with age (Leigh and Zee 2006).

Interestingly, during smooth pursuit, sensitivity to briefly flashed high resolution or coloured stimuli increases, suggesting that pursuit causes a boost in the konio- and parvocellular systems (Schütz et al. 2008). Furthermore, perception of time is compressed during smooth pursuit (the ability to make judgements of the duration of visual stimuli is impaired, with stimuli seen during pursuit appearing to be briefer in duration than during steady fixation [Schütz and Morrone 2010]).

1.1.7 Fixation maintenance movements

The eyes are never completely stable. In normal subjects, there exist three physiological instabilities of fixation:

- Microsaccades
- Ocular microtremor (OMT)
- Drifts

Figure 1.5 represents a 0.05 mm patch of fovea with arbitrary examples of the above EM directions and amplitudes superposed.

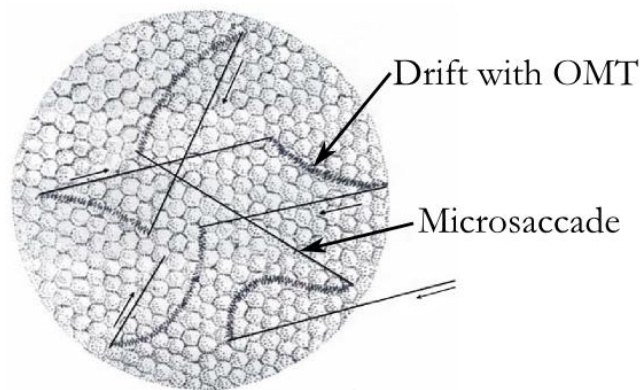


Figure 1.5: Physiological instabilities of fixation, showing microsaccades, drifts and OMT (Pritchard 1961).

Each of the fixation-maintaining EMs listed above are discussed in the sections that follow.

1.1.7.1 Microsaccades

Microsaccades, as the name suggests, are very small EMs which lie on a continuum with normal saccades. The movements have amplitudes of 1-30' arc, and occur involuntarily. Frequencies between 0.2 and 3.8 Hz have been reported (Martinez-Conde et al. 2009). Aside from being smaller in amplitude, they are believed to be physiologically identical to saccades, and even follow the main sequence (Zuber and Stark 1965). Functionally, they serve to prevent conscious visual perception disappearing during fixation due to neural adaptation (i.e. the *Troxler effect*) (Martinez-Conde, Macknik and Hubel 2004). Microsaccade frequency may be reduced during times of high visual demand to increase accuracy in tasks such as firing a rifle or threading a needle (Winterson and Collewijn 1976). It has been shown that 32.1% of microsaccades correct fixation towards the preferred retinal location of fixation (Møller, Laursen and Sjølie 2006).

1.1.7.2 Ocular microtremor

OMT is a high frequency (30-150 Hz), low amplitude (about 6" arc) oscillation of the eyes found in normal individuals during fixation. It is unclear whether OMT contributes in any useful way to vision (Spauschus et al. 1999; Martinez-Conde, Macknik and Hubel 2004). Whilst this motion is constant, there are distinct bursts of OMT that occur intermittently with a greater amplitude than the background OMT, and are almost sinusoidal in waveform (Bolger et al. 2001) (see Figure 1.6).

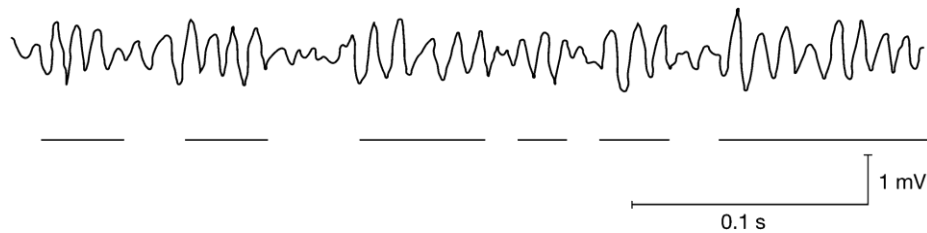


Figure 1.6: A normal OMT waveform from an alert individual measured with a piezoelectric strain gauge. Bursts are underlined (Bojanic, Simpson and Bolger 2001).

OMT is directly correlated with brainstem activity – both its pattern and frequency change with consciousness, and peak frequency reduces with increasing levels of anaesthesia (Coakley and Thomas 1977; Bojanic, Simpson and Bolger 2001).

1.1.7.3 Drifts

Originally believed to be random movements due to instabilities of the oculomotor system (Cornsweet 1956), drifts are slow EMs that are now considered to represent a fixation compensation mechanism. Their corrective nature is not as great as that of microsaccades, however a greater percentage of drifts correct the eye position towards rather than away from the preferred retinal location of fixation (St Cyr and Fender 1969; Møller, Laursen and Sjølie 2006). The amplitude is generally < 5', and the frequency is usually 2-5 Hz (Barlow 1952).

1.1.8 Vergence

With the exception of OMT, all of the aforementioned EMs are usually conjugate (both eyes move together, with approximately the same amplitude and direction). *Vergence* describes a disjunctive binocular EM which serves to either reduce the horizontal angle between the visual axes (convergence) or increase it (divergence). Vergence EMs are usually used to change the distance at which an individual is viewing; as such, they are accompanied by a change in ciliary muscle tonus (accommodation) and pupil size. The relationship between vergence, accommodation and pupil size is known as the 'near triad', and is neurologically hard-wired (Millodot 2004; Rowe 1997).

1.2 Nystagmus

Nystagmus describes a constant, involuntary, oscillation of the eyes. This can occur for a multitude of reasons, both pathological and physiological. The prevalence of pathological nystagmus is estimated to be around 24 in 10,000 (0.24%) in the general population (Sarvananthan et al. 2009). However, a more recent study of preschool children identified nine out of 2546 as having pathological nystagmus of some form, i.e. higher a prevalence of 0.35% (Repka et al. 2012).

As many as 45 types of nystagmus have been reported in the literature (Dell'Osso 1989). However, many of these represent non-nystagmoid *saccadic oscillations*, synonyms or speculative forms that may never have existed at all (Fishman 2006). True nystagmus can be divided into three major categories: physiological, acquired, and early-onset. Each of these categories are briefly described and discussed in the sections that follow.

1.2.1 Physiological nystagmus

As the name suggests, physiological nystagmus describes nystagmus seen in normal, healthy individuals. Three common physiological forms of nystagmus are OKN, VOR nystagmus and end-point nystagmus. OKN and VOR nystagmus have been discussed in Sections 1.1.4 and 1.1.5 respectively.

End-point nystagmus can occur when attempting to look to the far extremes of gaze. Many individuals will exhibit drifts towards the primary position, followed by a jerk movement back to the intended eye position. This *end-point nystagmus* is believed to occur as the result of a 'leaky' neural integrator (Abel, Dell'Osso and Daroff 1978; Abadi and Scallan 2001) (see Section 1.1.3.3), and may occur in as much as half the population. Although this form of nystagmus is an unremarkable clinical finding, end-point nystagmus that is sustained after returning to the primary position is known as *gaze evoked nystagmus*, and is indicative of pathology (Leigh and Zee 2006).

1.2.2 Acquired nystagmus

Pathological nystagmus may develop at any point in life as a result of disease or injury, often to the vestibular or central nervous systems. The most common causes are multiple sclerosis and stroke (Choudhuri, Sarvananthan and Gottlob 2007). The many forms of acquired nystagmus are beyond the scope of this thesis, but the reader is directed to Leigh and Zee (2006) for further information.

1.2.3 Early-onset nystagmus

Early-onset nystagmus describes any form of nystagmus that presents within the first few months of life, unless precipitated by a condition causing acquired nystagmus within that time. The three most common forms are fusion maldevelopment nystagmus syndrome (FMNS), spasmus nutans syndrome, and infantile nystagmus (IN). Early-onset nystagmus is usually primarily horizontal in direction, although vertical and/or torsional movement can also be exhibited, either as a major or secondary component (Abadi and Bjerre 2002). The first two of these conditions are described briefly below, whereas IN is considered in much greater detail in Section 1.3.

1.2.3.1 Fusion maldevelopment nystagmus syndrome

FMNS is a horizontal jerk nystagmus¹ that only occurs when binocularity is disrupted. The quick phase always beats towards the fixating eye (Leigh and Zee 2006). Reduced binocular function precipitates FMNS (Avallone et al. 2001); amblyopia and strabismus often occur in conjunction with the condition (Gottlob 2000). FMNS has been estimated to have a clinical prevalence of 0.6 in 10,000 in Leicestershire (Sarvananthan et al. 2009), yet the true prevalence may be much higher; a recent study of children with hyperopic anisometropia using detailed EM recordings found evidence of FMNS (often transient and subclinical) in 88% of those with no stereoacuity (Birch, Subramanian and Weakley 2013). There are two forms of FMNS: pure latent nystagmus (nystagmus is present only when one eye is occluded) and manifest latent nystagmus (nystagmus is always present but worsens on occlusion).

1.2.3.2 Spasmus nutans syndrome

Spasmus nutans syndrome is a rare disorder, causing (in combination): a high frequency, low amplitude nystagmus of a disconjugate nature; irregular head nodding; and an abnormal head posture. Its onset is usually within the first year of life and the condition ceases spontaneously, usually within two years of onset, although it has been known to persist for over eight years. However, a low-amplitude nystagmus (not detectable clinically) may persist until at least five to twelve years of age, when it spontaneously resolves (Gottlob, Wizov and Reinecke 1995). The pathogenesis of spasmus nutans syndrome is unknown (Leigh and Zee 2006).

¹ See Section 1.3.1 for an explanation of *jerk*.

1.3 Infantile nystagmus

IN (also known as *infantile nystagmus syndrome* or [formerly] *congenital nystagmus*) almost always develops within the first six months of life. Gottlob et al. (1990) estimate the average age of onset to be 1.9 months. One report has demonstrated a lack of any detectable EM abnormalities soon after birth in an infant that later developed IN (Gottlob 1997). There have been reports in the literature of IN-like nystagmus developing later in life (in the absence of pathology or neurotrauma) (Gresty et al. 1991), but such cases are rare. Abel (2006) suggests that these reports are probably the result of non-symptomatic nystagmus remaining undetected as a result of inadequate eye care facilities.

IN often occurs in conjunction with pathology of the visual system such as albinism, achromatopsia and infantile cataracts (see Leigh and Zee [2006] for a complete list of associated conditions). IN can also occur seemingly in isolation, in which case it is termed *idiopathic infantile nystagmus* (IIN). Although frequently associated with some form of visual deprivation, the extent of a causal relationship is still unknown. Indeed, it is unclear whether or not rectifying visual problems promptly can prevent the condition developing. For example, over 40% of children receiving operations for infantile cataracts have been shown to develop IN postoperatively, regardless of when the surgery is performed (Young, Heidary and VanderVeen 2011; Young, Heidary and Vanderveen 2012). IN is significantly more common in white Europeans than the Asian population, and, based on a large scale study of the population of Leicestershire, the overall prevalence of IN was estimated at 14 in 10,000 (Sarvananthan et al. 2009).

IN has been reported in children born to mothers exposed to benzodiazepines, opiates and opiate substitutes during pregnancy (Gupta et al. 2009; Mulvihill et al. 2007; Tinelli et al. 2013; McGlone et al. 2013). However, many of the children reported in these studies had other congenital visual system pathologies (such as optic nerve hypoplasia or delayed visual maturation), yet some presented with apparent IIN.

It is possible (although rare) for IN to appear only transiently in infancy, usually beginning and regressing in the first year of life (Good, Hou and Carden 2003). The authors of this study point out that not all forms of regressing nystagmus should be diagnosed as spasmus nutans syndrome (see Section 1.2.3.2). The mechanism for regression in these cases is unknown, but may ultimately provide valuable clues as to whether and how early intervention might impact on IN.

Visual acuity (VA) is usually reduced in individuals with IN, with the magnitude of the reduction being related to the underlying pathology (typically an average of 0.67 logMAR in albinos and 0.55 logMAR in patients with a comorbid ocular pathology). However, even in cases of IIN, VA is typically moderately reduced to around 0.35 logMAR (Abadi and Bjerre 2002). The reduction of VA in cases of IN with no associated visual pathology begs the question as to whether nystagmus *per se* is responsible for poor VA, or whether an underlying diagnosis remains hidden in these patients. It is worth noting that, whilst there is *usually* a moderate reduction in visual function with IIN, cases have been reported with VA better than -0.10 logMAR (Abadi and Bjerre 2002).

1.3.1 Waveforms of infantile nystagmus

IN can be characterised by its *waveform*, representing eye position over time, which depicts the frequency, amplitude and pattern of the oscillations. Nystagmus *intensity* describes the amplitude multiplied by the frequency, and is often used as a quantitative metric in the literature. Figure 1.7 shows the clinically significant characteristics of a typical nystagmus waveform. Note that, in horizontal EM traces, an upward movement conventionally indicates a rightwards movement of the eye.

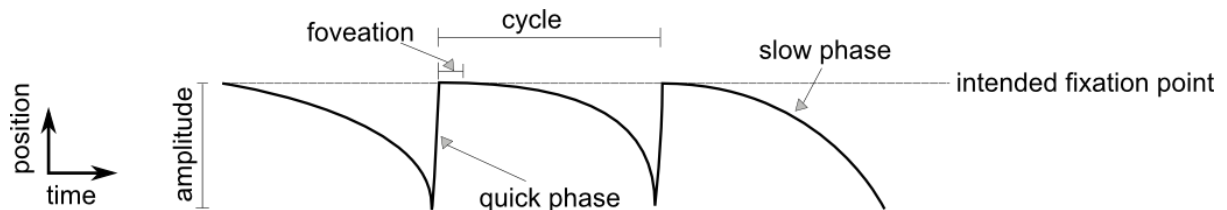


Figure 1.7: The components of a nystagmus waveform. Frequency is inferred from cycles per time unit.

By definition, *foveations* in a nystagmus waveform are regular reductions in velocity during which the fovea is directed towards the point of regard. The actual parameters that define the start and end of a foveation period are somewhat ambiguous; the exact definition (and whether it should be defined at all) remains a subject of debate. Westheimer and McKee (1975) found that VA in normally sighted individuals is not degraded by retinal image motion less than 2.5°/s, whilst Barnes and Smith (1981) identified a significant reduction in VA when viewing visual targets moving at 3-4°/s. A study by Chung and Bedell (1996), in which nystagmoid image motion was simulated in normally sighted individuals, found that VA was significantly degraded when retinal image velocity exceeded 3°/s for simulated foveation periods of 40-100 ms; whereas when the duration of the simulated foveation was reduced to 20 ms, 5°/s was the critical velocity at which VA worsened (as compared to nystagmoid motion of a lower velocity). If one were to assume that this is also the case in nystagmats,

then this velocity criterion might reasonably be used to define foveation periods. Abadi and Worfolk (1989) arbitrarily defined foveation as ocular velocity of less than $10^\circ/\text{s}$ in a study comparing VA to foveation duration. Many publications since 1992 have settled on a threshold of $4^\circ/\text{s}$ to define foveation periods (Dell'Osso et al. 1992a; Cesarelli et al. 2000; Bifulco et al. 2003). In addition, the definition of 'foveation' often includes a positional constraint, by which successive foveations must lie (for example) within $\pm 0.5^\circ$ of one another (Dell'Osso and Jacobs 2002).

Such variability in the definition of *foveation* can cause confusion when directly comparing the results of interventional studies. A variety of methods for quantifying nystagmus have been defined; these are described in detail in Section 1.3.8.5. However, these methods all rely on setting absolute velocity thresholds in order to determine foveation durations. As will be seen in Chapter 2, this 'one size fits all' approach may not be appropriate in all cases.

The three major types of IN waveform are pendular (three subtypes), jerk (eight subtypes), and dual jerk. In Figure 1.7, the waveform shows both quick phases and slow phases. This indicates a *jerk* type movement. A nystagmus quick phase is generally assumed to be equivalent to, and generated by the same neural circuitry as, a saccade (Ron, Robinson and Skavenski 1972; Garbutt, Harwood and Harris 2001), whilst a slow phase indicates a drift from fixation. Note that IN slow phases always accelerate; the presence of accelerating slow phases is considered diagnostic of the condition (Abadi and Bjerre 2002). Pendular waveforms have no quick phases, but may be asymmetrical or contain foveating saccades superposed on the pendular waveform (Dell'Osso and Daroff 1975).

Figure 1.8 shows the 12 'classical' waveforms of IN as described by Dell'Osso and Daroff (1975). Many nystagmats will exhibit multiple waveforms, with different types being elicited at different times, or by varying gaze angle.

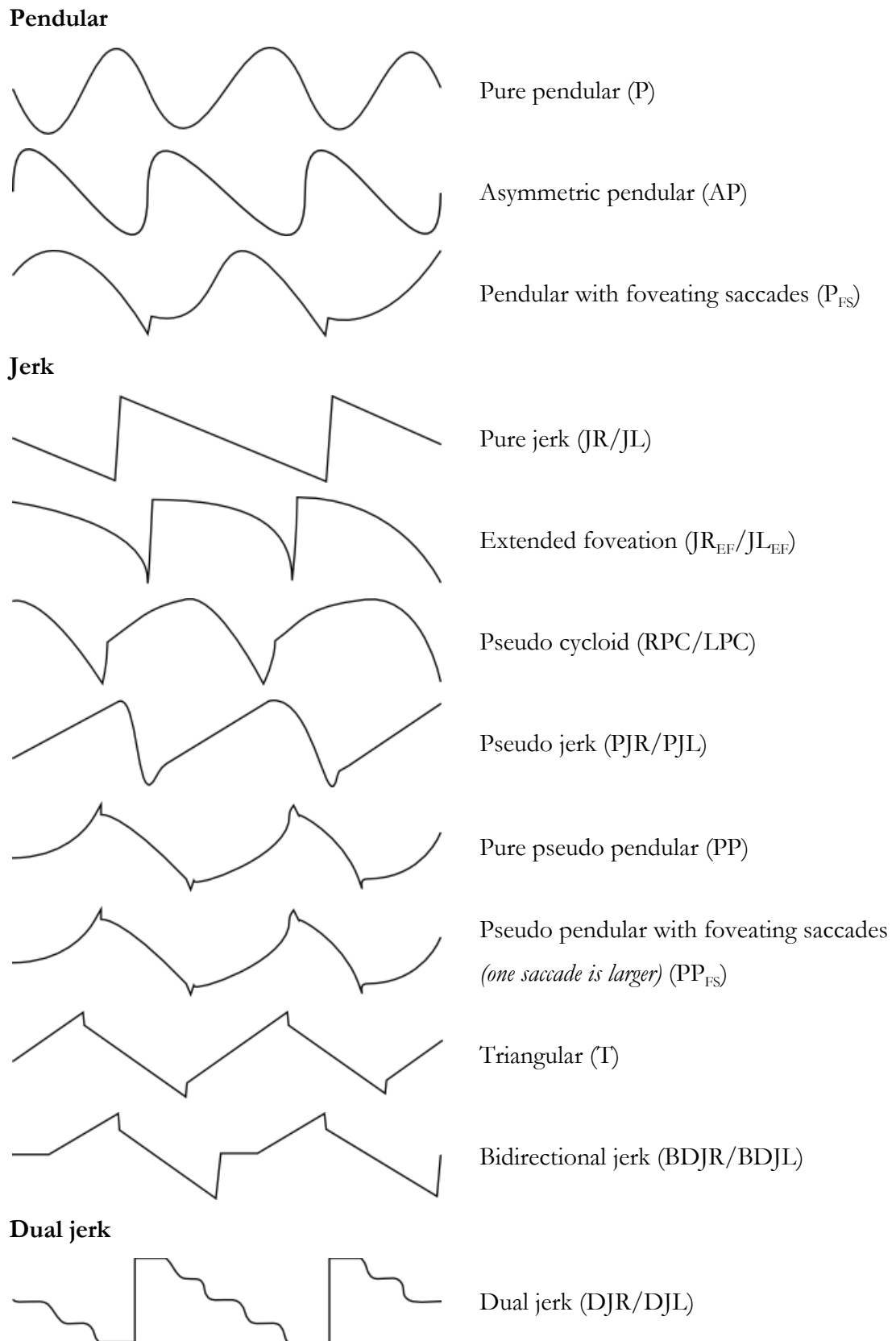


Figure 1.8: The 12 waveforms found in IN according to Dell'Osso and Daroff (1975). Commonly used acronyms are given in parentheses (R = right; L = left).

The parameters of IN waveforms vary enormously between individuals; frequencies have been shown ranging from 0.5-8 Hz (the mode is 2-3 Hz), whilst amplitudes can vary from

0.3-15.7° (typically 6-8°) (Abadi and Bjerre 2002). The average eye velocity throughout the nystagmus waveform is 14°/s (Bedell 2000), whilst the peak velocity of the slow phase has been shown to vary from 20-180°/s (Abadi and Worfolk 1989).

1.3.2 Baseline oscillation

The accuracy of beat-to-beat foveation position is affected by the presence of a baseline oscillation which has a low frequency ranging from 0.1-0.7 Hz and an amplitude ranging from 0.39-4.17° (Bifulco et al. 2003; Pasquariello et al. 2009). Baseline oscillation amplitude is positively correlated with both nystagmus amplitude and frequency (Pasquariello et al. 2009).

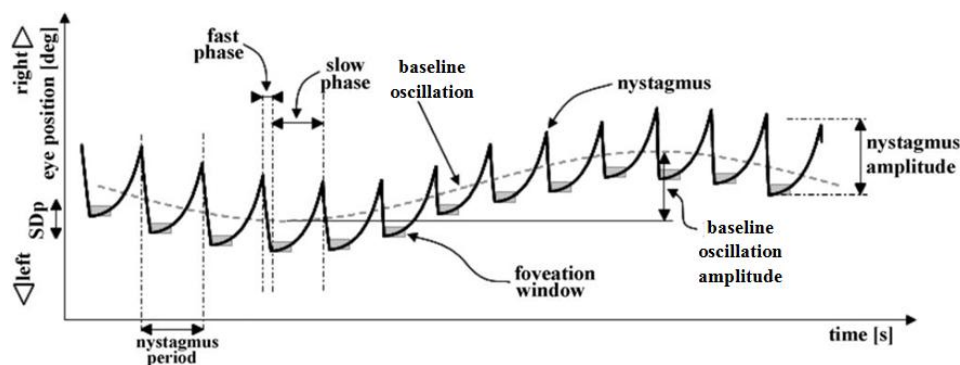


Figure 1.9: Schematic representation of baseline oscillation in an IN waveform. Adapted from Pasquariello et al. (2009).

1.3.3 Head shaking

It is estimated that 27% of subjects with IN exhibit concurrent oscillations of the head. These may not occur all the time, are known to increase in intensity with ‘effort to see’, and can be voluntarily suppressed by the patient (Khanna and Dell’Osso 2006). The direction and speed of head shaking does not appear to counteract the oscillations of the eyes, and therefore is unlikely to represent a compensatory mechanism (Carl et al. 1985). Perception of motion smear is slightly attenuated during motion of the head (Tong, Patel and Bedell 2006); it has therefore been suggested that head shaking might be a mechanism used to reduce perception of oscillopsia (see Section 1.3.9.1). Head shaking has also been attributed to the same neural signals that drive nystagmus quick phases (Khanna and Dell’Osso 2006).

1.3.4 Visual and oculomotor development in infantile nystagmus

The rate of development of VA in IN has been shown to be similar to that of normally sighted infants; i.e. despite having a relatively reduced VA both at the time of diagnosis and visual maturity, the *rate* of visual development progresses as normal (Weiss and Kelly 2007; Fu et al. 2011).

The term *infantile* nystagmus was first proposed in 1988 (Reinecke, Guo and Goldstein) due to the observed inaccuracy of the term *congenital* nystagmus. Of the 35 cases studied in their report, only three were noted to have had nystagmus in the first two weeks of life. Nystagmus typically starts between one and eight months of age, and often begins with a large-amplitude triangular waveform (without foveation periods). The waveform typically shifts to a pendular type before 1½ years of age (Reinecke, Guo and Goldstein 1988). One case study obtained longitudinal EM recordings from an infant at risk of developing IN. Square wave jerks were observed at seven weeks of age, followed by pendular nystagmus at eight weeks, and jerk at 10 weeks. The waveform returned to a pendular type at 14 weeks (Gottlob 1997). Foveation periods usually first develop at around 35 months of age, and the length of time taken for this final transition to take place is negatively correlated with the final VA later in life (Felius and Muhanna 2013). However, the 56 children documented in this study came from a total of 105 with IN; only these 53% exhibited a distinct waveform evolution from pendular to jerk type (Joost Felius, personal communication 2013). As yet, it is not known whether this correlation indicates that delayed waveform evolution leads to poor VA, or if poor underlying VA leads to delayed waveform evolution.

1.3.5 Pathogenesis

As yet, there is no consensus on the exact cause of IN (Gottlob and Proudlock 2014), although the strong association between congenital visual pathology and IN suggests that visual deprivation plays a role in its development. However, the types of pathologies observed are hugely variable, and further to this, in IIN there is no appreciable pathology evident (at least with current diagnostic techniques) besides the nystagmus itself.

Many theories about the aetiology of IN have been suggested; these are outlined below.

1.3.5.1 Excessive neural integrator gain

Optican and Zee (1984) suggested that velocity feedback to the neural integrator is somehow reversed in IN, leading to excessive gain. This in turn could lead to accelerating drifting EMs, which could account for many of the waveforms seen in IN. The reason that this theory has not been widely accepted is due to the fact that IN often occurs in conjunction with a physical ocular defect. It seems unlikely that the common presence of comorbid ocular pathology is purely coincidental (Casteels et al. 1992).

1.3.5.2 Loss of smooth pursuit damping

Jacobs and Dell'Osso (2004) suggested IN could be caused by a loss of damping of velocity oscillations present normally in the smooth pursuit system. An oculomotor system model

incorporating these velocity oscillations was originally proposed by Robinson, Gordon and Gordon (1986), who noted that smooth pursuit velocity oscillated with a frequency around 3.96 Hz when tracking unpredictable target motion. Jacobs and Dell'Osso engineered a neurocybernetic model of an oculomotor system with IN by implicating a failure of the system to calibrate the gain in this underlying oscillation. Their model is able to account for the classical *pendular* IN waveforms (see Figure 1.8), but cannot explain jerk waveforms. They suggest that the lack of gain calibration could result from an afferent visual pathway defect, which would explain why comorbid pathologies of the visual system often exist with IN.

1.3.5.3 Abnormal saccade termination

Broomhead et al. (2000) were able to create models of IN waveforms using abnormal saccade termination as the underlying factor, suggesting that the oscillations are caused by an inappropriate 'motor error'; the signal determining how far the eyes must move to arrive at a given location. As explained in Section 1.1.3.2, OPNs gate the activity of saccadic burst neurons, which are believed to be inherently unstable due to having a high gain. This could lead to saccadic oscillations if the activity of the OPNs is downregulated. Indeed, many forms of saccadic oscillations such as ocular flutter, opsoclonus and psychogenic flutter are hypothesised to be the result of such a downregulation of OPNs (Ramat et al. 2005; Leigh and Kennard 2004). Moreover, Broomhead et al. noted that modifying the parameters of burst cells in a neurocybernetic model (specifically, the manner in which burst cells cease their activity) results in the generation of many of the waveforms seen in IN.

1.3.5.4 Adaptation to reduced visual input

Monkeys reared with both eyelids sutured and the tarsal plates removed (surmised to allow retention of form perception) develop FMNS after 25-40 days of life. After 55 days, pendular nystagmus developed. This did not occur if the tarsal plates remained intact (supposedly, this procedure eliminated form perception). Monkeys raised in a stroboscopic environment also develop pendular nystagmus (Tusa et al. 2002). This, along with the fact that in humans there is often a visual pathology, suggests that nystagmus is a response of the oculomotor system to poor (but not absent) vision. Following this line of reasoning, a model has been proposed, which postulates that IN develops as a result of reduced contrast sensitivity at high spatial frequencies (Harris and Berry 2006). This model suggests that slow phases move the image across the retina to enhance contrast perception, whilst quick phases serve to prevent the image drifting too far from the photoreceptor-dense fovea.

In the author's opinion, the theory that IN results from reduced visual input seems the most plausible, since it does not rely on abnormal neural development to explain the oscillations of IN. It seems unlikely that all the pathologies known to accompany IN would share a common neurological deficit. However, the existence of IIN does present a problem: under this theory, in these individuals there either exists an undiagnosed pathology, or IN development must be linked to a mistiming of sensory/oculomotor development. More recent theories (see below) may also be useful in fully understanding *how* the oscillations arise.

1.3.5.5 Axonal miswiring

Huang et al. (2006) reported the potential application of a new animal model for IN: achiasmic zebrafish. These fish show similar waveforms to those found in humans (Huang et al. 2011). A strain of achiasmic mutant Belgian sheepdogs have also been found to have IN (Williams, Garraghty and Goldowitz 1991). This correlation between axonal misrouting in animals and IN has led to speculation that axonal miswiring is to blame for IN in humans (Huber-Reggi et al. 2012). Whilst axonal miswiring is certainly present in humans with albinism, this view fails to address the lack of a pathophysiological mechanism for axonal miswiring in the many other visual disorders associated with IN, such as congenital cataracts and achromatopsia.

1.3.5.6 Reversed optokinetic feedback

Recently, Chen et al. (Chen et al. 2014) suggested that the accelerating slow phases of IN could be the result of reversed optokinetic gain, such that the usual negative feedback that stabilises the retinal image is instead positive. They demonstrated that IN-like eye oscillations can be produced in normally-sighted individuals using a 'reversed' gaze contingent visual paradigm that simulates this situation. Unlike most gaze contingent studies, in which negative feedback from an eye tracker is used to stabilise an image on the retina, feedback was reversed so that deviation of the eyes from a fixation target caused the image to move in the *same* direction. This resulted in participants exhibiting accelerating 'slow phases', accompanied by quick phases that reoriented the gaze. Furthermore, their EM data show waveforms with a striking similarity to the classical waveforms '*jerk with extended foveation*' and '*pseudo pendular*'. The authors admit that this theory does not account for the presence of nystagmus in the dark (Shawkat, Harris and Taylor 2001), in which there is no specific 'need' to reorient gaze and hence produce quick phases. Nonetheless, they point out that in goldfish with artificially induced nystagmus, long periods of nystagmus in the light resulted in nystagmus being present in the dark, perhaps as a learned 'habit' (Easter and Schmidt 1977). The same mechanism may explain the presence of IN in the dark in humans. Chen et al. (Chen et al.

2014) relate their theory to Huang et al. (2006)'s theory of axonal miswiring (see Section 1.3.5.5 above), suggesting this as a mechanism by which the positive feedback loop might have developed. As discussed above, this theory fails to address a pathophysiological mechanism for the development of the condition in any comorbid ocular conditions other than albinism. Nonetheless, Chen et al. (Chen et al. 2014)'s argument that waveforms might arise from reversed optokinetic feedback remains highly convincing.

Although not mentioned in their paper, it seems feasible that reversed optokinetic feedback might also provide a means for explaining the presence of null zones in IN (see Section 1.3.8.1). The 'null point' of a system with positive feedback must exist at a specific location, which might represent the centre of the null zone for any given individual. It would be interesting to perform simulations in normally-sighted individuals with feedback null points at various gaze angles.

Another recent theory has proposed a similar idea, also implicating positive optokinetic feedback in the generation of IN (Brodsky and Dell'Osso 2014). However, Brodsky and Dell'Osso suggest that rather than being caused by axonal miswiring, the feedback loop might result from an inability to suppress OKN during smooth pursuit. They surmise that effort to fixate (or pursue) a target is counteracted by optokinetic signals in the opposite direction, leading to accelerating slow phases. Their theory implicates an immature cortical pursuit system, which normally replaces the phylogenically older subcortical optokinetic system at around two months of age (Braddick, Atkinson and Wattam-Bell 2003). According to Brodsky and Dell'Osso, in individuals with IN, the subcortical pursuit system continues to function after this time due to delayed or deranged maturation of the cortical pursuit pathways.

The possibility that IN arises from reversed optokinetic feedback (whatever the underlying mechanism) seems, to this author, to be genuinely plausible. In conjunction with Harris and Berry (2006)'s suggestion that IN is a developmental adaptation to reduced visual input, we may now be coming close to arriving at a full explanation for this fascinating condition.

1.3.6 Periodic alternating nystagmus

Periodic alternating nystagmus (PAN) describes a type of nystagmus waveform found in both infantile and acquired nystagmus, containing regular reversals in the beat (quick phase) direction, between which there may be a quiescent phase when nystagmus amplitude is reduced (Shallo-Hoffmann, Faldon and Tusa 1999). It has been known for some time that the periodicities of the reversals vary between individuals (Baloh, Honrubia and Konrad 1976). In

a more recent study, PAN was found in seven out of 18 patients with IN, simply by recording for a longer period than usual (up to eight minutes); PAN periods of up to five minutes were identified (Shallo-Hoffmann, Faldon and Tusa 1999). In a study of treatment methods for PAN, 9% of patients seen were previously diagnosed with IN, but not PAN (Gradstein et al. 1997), suggesting that PAN is relatively under-diagnosed in the wider population due to testing times being too short.

Although PAN usually has a regular periodicity, some patients will show an irregular pattern of beat reversal. This is known specifically as *aperiodic alternating nystagmus* (Hertle, Reznick and Yang 2009). Interestingly, a recent report in the literature detailed a patient for whom caloric stimulation (see Section 1.1.5) induced PAN (Taki et al. 2014). The authors conclude that it is most likely that the patient (a 75 year old male) had a latent lesion of some sort.

1.3.7 Idiopathic infantile nystagmus

IIN can only be diagnosed by exclusion, i.e. after all other possible causes of, and associations with, nystagmus are ruled out². This includes the acquired forms, which may also occur in infancy. Thirty per cent of people with IN have IIN (Lorenz and Gampe 2001). Although it is possible that nystagmus is the primary defect in IIN, it remains possible that some other pathology of the visual pathway remains undiagnosed. Significant refractive error (especially myopia) is more common in individuals with IIN, perhaps indicating poor emmetropisation (Sampath and Bedell 2002). High ametropia associated with IN in the absence of other ocular pathology is still classified as IIN. In a recent study, 15 patients with an existing diagnosis of IIN underwent extensive medical testing to identify comorbid pathologies. The study resulted in 13 of these subjects receiving an additional diagnosis, thus removing their *idiopathic* label (Holmström et al. 2013). However, subjects for this study were recruited from a low vision centre. Since this would represent individuals with particularly poor VA (a feature that is less common in IIN), it is perhaps unsurprising that so many participants were found to have an underlying pathology. Therefore, the results of this study may not necessarily represent the true prevalence of undiagnosed pathology in all individuals with IIN.

If one is to assume that there *is* an undiagnosed pathology underlying IIN, then hope lies in the possibility that emerging clinical technologies will elucidate the exact nature of the

² Since the term *idiopathic* refers to a condition with an unknown cause, one might consider that *idiopathic infantile nystagmus* ought to refer to *all* forms of IN. Despite the fact that sensory defects have not been proven to *cause* IN, only IIN is referred to as being ‘idiopathic’. Brodsky and Dell’Osso (2014) have recently proposed the phrase *isolated IN* as a more appropriate term for this group of patients.

problem(s). If this is the case, then IIN may be considered a highly sensitive indicator of visual pathology.

Genetic work has identified a restriction in expression of the *four point one ezrin, radixin, moesin domain containing 7* (FRMD7) gene in many individuals with X-linked IIN (Tarpey et al. 2006). As of 2007, 28 mutations of this gene had been documented in nystagmus (Self and Lotery 2007). Since then, further mutations have been discovered in Chinese and Indian families (Xiao et al. 2012; Li et al. 2012; Radhakrishna et al. 2012; Liu et al. 2013). FRMD7 is expressed mostly in the foetal brainstem, suggesting a possible involvement of the gene in gaze stability (Pu et al. 2011). These mutations account for approximately 40-50% of X-linked cases of IIN, and 3-5% of isolated cases (Jay Self, personal communication 2014). Individuals with the mutation have been shown to express different phenotypical characteristics to those without it; for example, nystagmus amplitude tends to vary more with gaze angle in FRMD7-related IIN, whereas anomalous head postures are more prevalent *without* FRMD7 mutations (Thomas et al. 2008). In addition, individuals with FRMD7-related IIN are more likely to express pendular waveforms with higher frequencies than individuals with comorbid albinism (Kumar et al. 2011a). All of these variations suggest that FRMD7 mutations represent a unique subclass of nystagmus, or a subtle afferent visual system pathology.

For many years, no such afferent visual system defect was detectable in FRMD7-related IIN (Proudlock and Gottlob 2011). In 2009, foveal imaging was successfully accomplished using optical coherence tomography in individuals with IIN (a difficult undertaking, considering the presence of incessant ocular oscillations). In total, 19 patients with IIN were imaged with a 95% success rate in image acquisition. These images exhibited the presence of normal *gross* foveal morphology in IIN (Cronin et al. 2009). More recently however, ultra-high resolution optical coherence tomography was used to study the retinas of individuals with FRMD7-related IIN in more detail (Thomas et al. 2014). Foveal pits were shown to be significantly shallower, and there were significant changes to the structure of the optic nerve head. It is unclear whether these changes are a primary deficit, or the result of abnormal ocular development in the presence of nystagmus. However, if Thomas et al.'s recent finding *does* represent a primary defect, it has the potential to result in the removal of the 'idiopathic' label from many individuals with IIN.

Research into the genetics of IIN continues to progress at a rapid pace. Most recently, mutations in the PAX6 gene have been demonstrated in a multi-generational British family with a history of IIN (Thomas et al. 2013).

In a sample of 139 individuals with IIN, the average clinical VA was 0.35 logMAR (Abadi and Bjerre 2002), which is clearly much lower than the VA of normally sighted individuals (usually $-0.14 - 0.00$ logMAR [Elliot 2003]). There are three possible explanations for the reduced VA in adults with IIN:

1. An undetected pathology of the visual system exists
2. Motion blur inherent from the EMs degrades visual performance
3. A form of amblyopia has developed as a result of visual deprivation during the critical period of visual development

Each of the possible causes above are discussed in the sections that follow.

1.3.7.1 Undetected pathology?

Since, by definition, IIN describes the absence of any other known pathology, if a common cause were to be discovered for this group of patients, IIN would no longer exist as a diagnosis.

1.3.7.2 Motion blur?

One previous study has examined the effects of nystagmoid image motion on the vision of normal subjects, and found a decline in VA at velocities above $3^\circ/\text{s}$ (Chung and Bedell 1995). It has been suggested that the presence of motion smear during nystagmus slow phases might contribute to the poor VA observed in patients with IN (Chung 2012). Chung, LaFrance and Bedell (2011) found that normal subjects presented with an image moving in a nystagmoid fashion have improved VA when the image is shown during the simulated foveations but hidden for the remainder of the slow phases. One might therefore expect VA to be similarly degraded by motion blur during the entire slow phase in individuals with IN. Chapter 3 of this thesis explicitly deals with this issue, the results of which indicate that motion blur does *not* actively impact on the VA of adults with IN (Dunn et al. 2014).

1.3.7.3 Amblyopia?

It seems possible that visual deprivation during the critical period of visual development (i.e. amblyopia) could be responsible for reduced visual function in adults with IIN. Felius and Muhanna (2013) found that VA in children with IN negatively correlates with the amount of time spent during visual development with a pendular nystagmus waveform. This suggests that slow evolution of the nystagmus waveform leads to the development of poor VA (due to deprivation). However, the authors admit that the inverse might also be true: that poor VA could lead to slow evolution of the nystagmus waveform.

VA has been shown to be significantly worsened in IN in the presence of visual crowding, an effect that is usually suggestive of amblyopia (Chung and Bedell 1995; Huurneman and Boonstra 2013).

Normally sighted individuals, presented with an image moving in a similar fashion to horizontal jerk nystagmus (through the use of a galvanometer-mounted mirror), have been shown to have higher contrast sensitivity than most individuals with IIN. This suggests that there is a true visual impairment in IIN, beyond motion blur from the EMs. However, it is worth noting that this study only involved four subjects with IN, who were compared to three controls (Bedell 2006).

1.3.8 Motor control in infantile nystagmus

Despite the constant oscillations of the eyes, individuals with IN are able to perform oculomotor functions such as smooth pursuit and VOR, simply with the nystagmus waveform superposed (Dell'Osso et al. 1992b; Dell'Osso et al. 1992c; Yee et al. 1981). The positional variability of foveations in IIN has been shown to be very low (i.e. 'fixation' is relatively accurate, when non-foveating periods of the waveform are ignored). In a study of one individual, the standard deviation of horizontal foveation position whilst viewing a static target was 12.82' (Dell'Osso et al. 1992a). It is worth noting that, with the exception of Yee et al. (1981), each of the studies listed above derived their conclusions from data obtained from a single subject; the study author (Dell'Osso et al. 1992a; Dell'Osso et al. 1992b; Dell'Osso et al. 1992c).

Horizontal OKN does *not* appear to function normally in individuals with IN. In a study of 46 patients, gain was reduced in all measurable participants, and OKN after-nystagmus³ was absent in all subjects (Yee, Baloh and Honrubia 1980).

Nystagmus intensity in an individual with IN is not constant. Intensity can be influenced by gaze position, vergence, psychological state and consciousness. Further detail is given in the sections that follow.

1.3.8.1 Null zone

The intensity of IN varies with gaze angle. The position(s) of gaze in which nystagmus intensity is least is known as the *null zone* (Abadi and Whittle 1991). A large-scale study (224 subjects with IN) by Abadi and Bjerre (2002) found that 73% of participants had a null zone

³ OKN *after-nystagmus* is a sustained, decelerating nystagmus that occurs in normally-sighted individuals when lights are extinguished during OKN.

within 10° of the primary position. Sixty-nine per cent of subjects exhibited an abnormal head posture to facilitate this. When the null zone was $\geq 20^\circ$ from the primary position, *all* nystagmats exhibited an abnormal head posture. The null zone changes its position during smooth pursuit, shifting in the opposite direction to that of the pursuit (Kurzan and Buttner 1989).

1.3.8.2 Convergence

In many individuals with IN, convergence reduces nystagmus intensity in a similar way to a null zone of gaze (Dickinson 1986; Gradstein et al. 1998). In Abadi and Bjerre's (2002) study, 44% of subjects exhibited a significant reduction in nystagmus intensity at 33 cm compared to fixation at 6 m. This dampening has been shown to be solely due to a reduction in the angle between the eyes (as opposed to accommodation), and even occurs with asymmetric convergence in which one eye adducts whilst the other views a target (Dickinson 1986).

1.3.8.3 Psychological factors

The intensity of nystagmus in IN is related to a patient's state of attention and fatigue (Abadi and Dickinson 1986) (see Figure 1.10 for examples).

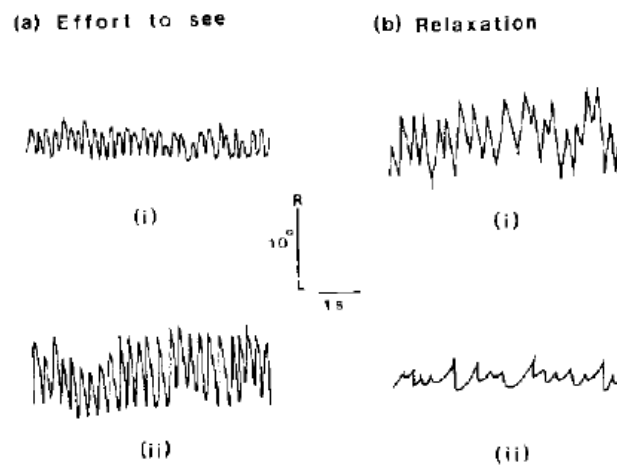


Figure 1.10: The effects of (a) 'effort to see' (attempting to read small letters) and (b) relaxation on nystagmus intensity, both (i) before, and (ii) during each mental state (Abadi and Dickinson 1986).

Task-induced stress increases the amplitude and frequency of nystagmus (Cham, Anderson and Abel 2008b; Jones et al. 2013). Tkalcevic and Abel (2005) suggested that nystagmus intensity is worsened not by visual demand *per se*, but by visual demand in which the outcome of the task is of importance to the individual, i.e. the individual has to *want* to see well, so this may be better described as visual 'effort'. Wiggins et al. (2007) found that increasing visual demand in the absence of stress (by increasing spatial frequency of a target) actually served to *reduce* nystagmus intensity. These results show the variety of factors that can influence

nystagmus intensity, i.e. that psychological stress and visual demand/effort can have opposing effects.

1.3.8.4 Sleep

The characteristics of paradoxical sleep⁴ in individuals with IN have only been investigated in a handful of studies (Arkin, Weitzman and Hasteley 1966; Arkin, Lutzky and Toth 1972; Abadi and Dickinson 1986). Figure 1.11 shows an EM trace for an infant with IN in varying states of consciousness. Note the apparent absence of nystagmus during a non-paradoxical sleep phase, and the superposition of nystagmus upon rapid eye movements during paradoxical sleep. Amplitude is not shown, as calibration was not possible (Abadi and Dickinson 1986).

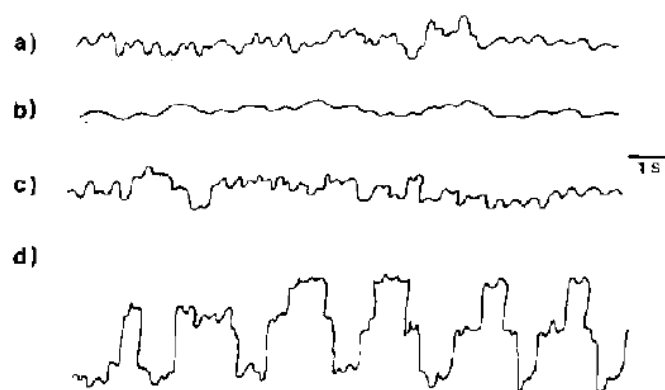


Figure 1.11: EM trace for a 20 week old infant with IN during (a) waking, (b) and (c) non-paradoxical sleep and (d) paradoxical sleep (Abadi and Dickinson 1986).

1.3.8.5 Quantification of motor characteristics of infantile nystagmus

In an attempt to provide a quantifiable measure of nystagmus that takes into account intensity and foveation quality, a battery of quantitative measures have been devised. These measures, it is believed, provide a tangible way of tracking changes in nystagmus function when normal measures of VA fail to find a difference (see Section 1.3.11). They essentially attempt to provide an outcome measure by collapsing various waveform characteristics into a single number. The first such method to be developed was the *nystagmus acuity function* (NAF), an algorithm that uses the velocity and duration of foveation periods detected in an EM trace as a representation of foveation ‘quality’. The values obtained correlate well with VA *between* individuals (Sheth et al. 1995).

⁴ *Paradoxical* sleep is the period of sleep during which dreams are most likely to occur (Manni 2005), and is also known as *rapid eye movement* sleep. To avoid inevitable confusion in a report concerning eye movements, the term *paradoxical* is used here.

The *nystagmus acuity estimator function* (NAEF) built upon NAF by taking into account the variability of foveation position (Cesarelli et al. 2000). NAF and NAEF calculation depend on the nystagmat being capable of maintaining EM velocities $\leq 4^\circ/\text{s}$ during their foveation periods, as well as having a foveation accuracy of $\pm 0.5^\circ$. To address these limitations, the function was further improved upon by the so-called *expanded nystagmus acuity function* (NAFX), which allows for calculation of NAF using a range of position and velocity thresholds to define ‘foveation’ (Dell’Osso and Jacobs 2002). A coefficient to the algorithm (τ) is retrieved from a table based on the foveation criteria (position and velocity thresholds) used. The criteria used for any individual are adjusted by the clinician within certain limits (position variability can range from $\pm 0.5^\circ$ to $\pm 6^\circ$; velocity threshold can vary from $4^\circ/\text{s}$ to $10^\circ/\text{s}$). Due to the complexity of the calculation of NAFX, it is usually performed using a software package, *OMTools* (see Section 2.1.4 for more detail).

More recently, a new measure was developed – the *automated nystagmus acuity function* (ANAF). ANAF was devised in order to perform NAFX measurement more quickly and easily. It assumes that acuity function is proportional to the inverse of the root of the distance of the image eccentric from the fovea (Tai et al. 2011)⁵. ANAF does not require identification of foveations (relying solely on eye position and velocity), and has been shown to correlate reliably with NAFX, without the need for manual intervention (Yao, Tai and Yin 2014).

Finally, the *nystagmus optimal fixation function* (NOFF) is designed for use with children (Feliuss et al. 2011). Due to difficulties in capturing a child’s attention during EM recording, the NOFF must be able to deal with noisy data. In order to find the *best* data for analysis, the 4 s segment with the most samples that satisfy foveation criteria is found (samples with eye velocity $\leq 6^\circ/\text{s}$ within a $\pm 0.5^\circ$ position window). This assumes that there is at least one 4 s period of ‘clean’ fixation in the recording. Having found the best segment, the percentage of samples in that segment that satisfy the foveation criteria are determined (this is the ‘foveation fraction’). NOFF is calculated using Equation 1.1.

$$NOFF = \log\left(\frac{\textit{foveation fraction}}{1 - \textit{foveation fraction}}\right) \quad \text{Equation 1.1}$$

Whilst this method may successfully reject non-fixating EM data (by ignoring high velocity saccadic data), there is a possibility that it might underestimate the severity of nystagmus. For example, in a patient with PAN, it might identify a quiescent period as the ‘best’ segment.

⁵ ANAF makes the assumption that the relationship between retinal eccentricity and VA exhibited in normally sighted individuals holds true in nystagmats. This has never been tested.

MATLAB code for automatically calculating NOFF was recently released publicly, and is available in Appendix I – *nystagmus_calc_noff.m*.

It is important to note that each of the nystagmus waveform quantification functions reported here are designed to act as *predictors* of VA, and are predicated on their relationship with VA when plotted *between* individuals. Despite the large number of functions available to the clinician, one study in which 10 adults with IN had a range of nystagmus functions calculated from EM recordings (including NAF, NAEF and NAFX) in fact found that average eye velocity was a better predictor of VA than any of the other, more complex, functions used (Theodorou 2006). Furthermore, recent work has shown that changes in nystagmus parameters elicited by stress or viewing in the null zone do not reliably change the VA of individual subjects (Erichsen et al. 2013; Wiggins 2008; Jones et al. 2013). As such, it appears that these functions cannot predict the change in VA that an individual might experience when their own waveform parameters are changed, i.e. nystagmus functions may only be useful for predicting VA when applied *between* individuals.

1.3.9 Visual perception in infantile nystagmus

1.3.9.1 Oscillopsia and its absence in infantile nystagmus

Oscillopsia is the perceptual experience of the visual scene oscillating back and forth (Brickner 1936). Acquired nystagmus often causes oscillopsia (Lee and Brazis 2006). However, despite experiencing similar retinal image motion, individuals with IN very rarely describe such symptoms (Leigh et al. 1988). The reason for this is unclear, but several theories exist:

1. Image motion is cancelled out by efference copy of extra-retinal signals.
2. Vision is sampled during foveation periods, and these ‘snapshots’ are interpolated.
3. Oscillopsia is not noticed because the motion detection threshold is elevated.
4. A combination of the above is responsible for the lack of oscillopsia.

The first hypothesis suggests that perceptual stability is achieved by efference copy of the EMs effectively cancelling out the perception of motion (Bedell and Bollenbacher 1996; Bedell 2000). This is the most widely accepted theory, and is corroborated by the fact that stabilising an image on the retina of an individual with IN causes oscillopsia (Leigh et al. 1988).

The second hypothesis postulates that vision is suppressed during non-foveating periods of the nystagmus waveform, and that the visual experience is derived from interpolation of the

snapshots achieved during foveations. This is deemed to be unlikely, since images stabilised on the retina, afterimages of bright flashes and migraine auras are all occasionally perceived as moving in individuals with IN (Dell’Osso 2011).

The third hypothesis also seems unlikely; although the threshold for motion sensitivity is usually increased in IN (Eggert, Straube and Schroeder 1997), this threshold is still much lower than the speed of the slow phases of nystagmus (Dell’Osso 2011). For more detail, see Section 1.3.9.4.

In 1989, a Korean study showed that four nystagmats were just as likely to perceive a 0.8° or 10° flash of light during all phases of their nystagmus (Jin, Goldstein, and Reinecke). A subsequent study found that nystagmats are able to correctly localise a 2 ms point flash of light at all points along the nystagmus waveform (Goldstein, Gottlob and Fendick 1992). Bedell and Currie (1993) went on to estimate that extra-retinal signals are available for around 75% of the eye position changes in IN, which could be used to cancel out the oscillopsia experienced due to image motion. This was achieved by having subjects point in the direction of a flash of light produced at different phases of the nystagmus waveform. These studies suggest that visual perception is constant throughout the waveform, and are put forth as evidence against the visual sampling hypothesis⁶.

Waugh and Bedell (1992) reported that the temporal contrast sensitivity function of individuals with IIN is essentially normal. At a rate of 0.5 Hz, nystagmats were shown to have a higher sensitivity to full field flicker than controls, whereas at faster rates of flicker, sensitivity was significantly reduced compared to controls. At even higher rates of flicker, the sensitivity of controls and nystagmats converged⁷. They concluded that the lack of a reduction in luminance modulation sensitivity (as compared to controls) suggests that visual information is processed continuously throughout the nystagmus waveform.

Further evidence against the visual sampling hypothesis was provided by Woo and Bedell (2006). In an investigation determining the efficacy of the *rapid serial visual presentation* technique on reading speeds, words could be read with 47-65% accuracy (depending on word length) during non-foveating periods of the waveform.

⁶ The author of this thesis argues that any suppression, were it present, might be broken through by complex features such as a salient flash of light.

⁷ As with the above studies, the present author notes that a breaking of suppression could explain the data: full field flicker at ~ 0.5 Hz may be sufficient to break through retinal suppression, whereas at higher frequencies, the luminance modulation may not have been sufficiently salient to break through suppression; hence, the controls showed a greater sensitivity. At the highest frequencies, both nystagmats and controls may have detected flicker equally poorly.

1.3.9.2 Inducing oscillopsia in infantile nystagmus

There are situations in which oscillopsia can be induced in individuals with IN; for example, in response to a flash afterimage in the dark, or through electronic image stabilisation (Leigh et al. 1988). Interestingly, in Leigh et al. (1988)'s study, one individual who experienced oscillopsia in response to electronic image stabilisation was able to voluntarily suppress the oscillopsia. The fact that individuals with IN are able to experience oscillopsia on occasions indicates that, at least at those times, visual suppression is *not* taking place.

Dell'Osso, Daroff and Tomsak (2001) reported a migraineur with IN who experienced a migraine aura as oscillating horizontally. The oscillopsia was of a similar nature to that experienced by the subject during retinal image stabilisation. It is worth noting that no torsional oscillopsia was perceived, albeit a small component of the subject's nystagmus waveform. The authors suggested that the migraine aura effectively acted in the same way as a stabilised retinal image.

Oscillopsia can also be induced in IN by inattention. Cham, Anderson and Abel (2008a) found that some individuals with IN perceived a background as moving when fixating a stationary LED, which itself appeared stable. Oscillopsia has also been known to occur following visual maturity in individuals with IN due to other failures of the visual/oculomotor systems, such as degenerations of the retina and decompensating heterophoria. Treatment of the underlying problem usually halts the oscillopsia (Reinecke et al. 2001).

1.3.9.3 The 'slow to see' phenomenon

Hertle et al. (2002) found that nystagmats take significantly longer than controls to recognise the orientation of small static and moving 'E' optotypes. However, meridional amblyopia⁸ was not taken into consideration in this study, so it is possible that the nature of the experiment (recognition of optotype orientation) may have led to an erroneous result.

Wang and Dell'Osso (2007) concluded that the time taken for individuals with IN to make a saccade to a new target varies depending on the time within the waveform at which the new target is presented. If the new target appears around the same time as a saccadic quick phase, the voluntary saccade is slightly delayed. Whilst this paper shows an inherent delay in saccade generation, it does not distinguish whether the delay is due to an impairment of perception during some portion of the waveform, or the interplay of voluntary saccades and nystagmus

⁸ *Meridional amblyopia* describes a deficit in orientation-specific cells of the visual cortex due to reduced orientation exposure during visual development (Mitchell et al. 1973).

quick phases. Furthermore, their conclusion is based on the use of polynomial regression models in a limited dataset of saccade latencies. For further discussion of this paper, see Section 5.4.3.1.

In more recent studies, children with IN have demonstrated increased latencies to fixate on novel cartoon and high contrast stimuli presented in the corner of a monitor as compared to controls (Pel et al. 2011; Pel et al. 2013). In a similar manner to the above experiment, it is not clear from these results whether the delay is in the time to perceive the change, or if it is due to difficulties in quickly executing the saccadic EM to fixate the target.

Further evidence for the ‘slow to see’ phenomenon was presented by Jones et al. (2013). They found that increased nystagmus intensity induced by stress increased the time taken to respond to a visual stimulus, despite not significantly affecting VA.

The evidence above indicates that visual function in IN is somehow slowed, due to difficulties in acquiring fixation, slow visual processing or a combination of both. The work presented in Chapter 4 aims to clarify this.

1.3.9.4 Motion perception

Individuals with IN have elevated thresholds for detecting the direction of motion of gratings in the periphery and (for slow motion) at the fovea, but have similar thresholds to normally sighted individuals for motion $> 1^\circ/s$ at the fovea (Lappin et al. 2009). The perception of motion appears to be more reduced for objects than perceived self-motion (the latter was induced by a large field OKN stimulus) (Eggert, Straube and Schroeder 1997). The motion aftereffect has a shorter duration in IN, and nystagmats have reduced perception of motion and motion smear in the opposite direction to their slow phase movements; a phenomenon also exhibited during smooth pursuit in normally-sighted individuals (Bedell and Tong 2009; Shallo-Hoffmann et al. 1998).

1.3.9.5 Meridional amblyopia

Individuals with horizontal IN typically have worse VA for vertically oriented gratings than horizontal gratings (Abadi and Sandikcioglu 1975; Jones 2011; Loshin and Browning 1983; Bedell and Loshin 1991). It has been postulated that the nearly constant image motion in nystagmus causes a meridional amblyopia to develop⁹. An experiment in which gratings were

⁹ A recent review indicates that the sensitive period for meridional amblyopia development is somewhere between six months and five years of age, although the end point of amblyopia development is unclear and probably idiosyncratic (Harvey 2009).

briefly presented (in order to eliminate retinal image motion) showed three individuals with horizontal IN to have a greater sensitivity to horizontally aligned gratings than vertical ones; the reverse was true for one subject with primarily vertical nystagmus (Abadi and King-Smith 1979). However, the subjects also had astigmatism; a condition which itself can induce meridional amblyopia. It is claimed that, in this study, all except one of the subjects had developed astigmatism after the age of nine years. This is significant, as it is beyond the plastic period during which amblyopia would be likely to develop.

Meridional amblyopia can also develop in response to uncorrected astigmatism (Harvey 2009). The incidence of corneal with-the-rule astigmatism is much higher than normal in IN, possibly due to long-term interaction between the cornea and eyelids in horizontal IN (Dickinson and Abadi 1984). In Abadi and Bjerre's study (2002), 57% of nystagmats had astigmatism exceeding 2.00 DC. The level of astigmatism in IIN and IN associated with albinism is inversely correlated with corrected VA (Bedell and Loshin 1991). A recent retrospective study found a high prevalence of astigmatism (usually with-the-rule) in 488 patients with IIN, with a tendency for this to increase with age (Fresina et al. 2013).

1.3.10 Treatments for infantile nystagmus

IN is a lifelong condition: no 'cure' has yet been discovered. However, there are a large number of treatments that have been shown to be effective in modifying waveforms or correcting abnormal head posture. Some of these treatments have demonstrated modest improvements in visual function. However, these changes are rarely significant in large studies. Treatments previously reported in the literature are outlined below.

1.3.10.1 Prism therapy

The fact that many nystagmats have a convergent null zone led to the suggestion that prescribing base out prism (to drive convergence) could improve visual function. A study by Dickinson (1986) found no improvement in the contrast sensitivity function with this method, yet nystagmus intensity was reduced. Rarely, the null zone is in the divergent position, in which case base in prism has been shown to be useful for reducing nystagmus intensity (Stahl, Plant and Leigh 2002). A study by Dell'Osso (2002) found an improvement in VA of two Snellen lines in a single subject when prisms were used both to drive convergence and to place the eyes into a null zone of gaze. As ever when prescribing prism, care must be taken to balance the refractive and prismatic prescriptions with respect to the *accommodative*

convergence: accommodation ratio (Dell’Osso 2002). Accommodative convergence¹⁰ has been shown to have no effect on nystagmus, hence spherical manipulation of spectacle prescriptions does not improve nystagmus characteristics (Dickinson 1986).

1.3.10.2 Botox

Retrobulbar injections of clostridium botulinum A exotoxin (*Botox*) are occasionally used as a therapy for oscillopsia reduction in acquired nystagmus. The toxin causes a temporary extraocular muscle paralysis, with oscillopsia reduction lasting for 5-13 weeks (Helveston and Pogrebniak 1988). Although oscillopsia is typically absent in IN, Botox injections have been shown to reduce nystagmus amplitude and improve VA in some subjects (Carruthers 1995; Hernández-García and Gómez-De-Liaño-Sánchez 2012). Despite low complication rates, due to the short duration of the effects, repeated injections are necessary to maintain therapeutic efficacy. In addition, paralysis of the extraocular muscles restricts patients’ ability to execute normal EMs.

1.3.10.3 Surgical procedures

Several surgical procedures have been advocated for IN. Those currently in use are listed below.

Anderson-Kestenbaum surgery

In 1953, Kestenbaum devised a surgery intended to move the null zone towards the primary position, thus reducing any abnormal head posture present. This procedure involves a recession of the rectus muscles with action in the direction of the face turn, and resection of the antagonists. A form of this procedure is still used today and is effective at reducing abnormal head postures (Lee 2002).

Artificial divergence

Using a similar principle to base out prisms (see Section 1.3.10.1), performing resections in both lateral recti induces a latent exophoria which is overcome by employing fusional convergence (in patients with sufficient fusional reserves). This serves to reduce nystagmus intensity. In a surgical study by Zubcov et al. (1993), three out of six patients undergoing artificial divergence surgery experienced a measurable improvement in VA. Five patients underwent combined Anderson-Kestenbaum and artificial divergence surgery, four of whom gained two or more lines of Snellen VA.

¹⁰ *Accommodative* convergence refers to convergence induced in response to an accommodative stimulus, as part of the near vision triad (lens accommodation, convergence and pupil constriction).

Recession of all horizontal recti

Recessing all four horizontal recti can reduce nystagmus intensity, and has been suggested as an easier-to-perform alternative to Anderson-Kestenbaum surgery, with an improvement of VA shown in seven out of 12 patients (average change -0.12 logMAR [Atilla, Erkam and Işıkçelik 1999]). In an early study of 10 subjects with IN undergoing this procedure, eight exhibited a reduction in nystagmus amplitude with a concordant average VA improvement of one line (Helveston, Ellis and Plager 1991). Another found an improvement of binocular VA in 19 out of 42 (45.2%) individuals undergoing the procedure (average change -0.08 logMAR [Alió et al. 2003]). A later study by Boyle, Dawson and Lee (2006) found similarly small improvements in VA; of 18 patients studied, 50% gained one line of VA, one was left with reduced VA, and the rest did not exhibit a measurable change in VA. The study authors concluded that the procedure provides limited, if any, measurable benefit. This was refuted by Hertle and Dell’Osso (2007), who claimed that Boyle, Dawson and Lee’s study was flawed, due to the lack of a ‘visually appropriate’ outcome measure and poor diagnostic classification/inclusion criteria.

Tenotomy and reattachment

The *anterior tenotomy* procedure, which involves severing the horizontal recti followed by reattachment at the original site, was first proposed in 1998 (Dell’Osso), and pioneered in 1999 (Dell’Osso et al.) on an achiasmatic mutant Belgian sheepdog with EMs resembling IN. The procedure was later performed on 10 human subjects with no adverse events, leading to increased foveation periods in nine subjects, and improved visual function in these same nine subjects as quantified by questionnaires. However, despite this subjective improvement, clinically measured VA only improved in five subjects. The average change in VA was an improvement of only 2.5 letters on an ETDRS chart (Hertle et al. 2003). Further research confirmed that the operation can reduce nystagmus intensity over a broad range of gaze angles, but did not find any improvement in the accuracy of smooth pursuit. Whilst the study claims that the procedure can improve VA, this is derived from NAFX recordings rather than actual VA measurement (Wang et al. 2012).

Combination surgery

Given the number of approaches available, surgeons have recently been implementing combinations and modifications of the above procedures, with generally positive outcomes in nystagmus intensity, and occasionally positive changes in VA. A study by Bishop (2011) found a reduction in nystagmus intensity in four out of five subjects, with an improvement in clinical VA in five eyes (although this was less than one Snellen line in two of these), and no

change in VA in the other five eyes. On the other hand, Kumar et al. (2011b) found a more convincing VA change in 28 patients, with an average improvement of 0.09 logMAR postoperatively. Nonetheless, this only represents an improvement of less than one line on a standardised letter chart.

1.3.10.4 Biofeedback

Auditory biofeedback, derived from live EM recordings, provide nystagmats with direct feedback from their EMs, and with practice, patients can learn to consciously reduce their nystagmus intensity (Mezawa, Ishikawa and Ukai 1990). After six half-hour sessions of auditory biofeedback, a study by Sharma et al. (2000) found nystagmus amplitude was reduced by 51% and intensity reduced by 60%, but with only a *subjective* improvement in quality of vision (i.e. VA was not improved). However, Abadi, Carden and Simpson (1980) found VA improvements between 0.13 and 0.32 logMAR. These improvements are generally not sustained following discontinuation of the therapy (Sharma et al. 2000), but in a study by Ciuffreda, Goldrich and Neary (1982), one subject was able to reduce their nystagmus EMs to 50% of the pre-training level on demand, without biofeedback.

1.3.10.5 Contact lenses

Contact lenses provide superior refractive correction over conventional spectacle lenses for nystagmats due to the reduction in peripheral lens aberrations and lack of induced prismatic effect that would be experienced as the eye moves away from the primary position with spectacles. Indeed, Allen and Davies (1983) found an increase in VA of at least one Snellen line in seven out of eight nystagmats using contact lenses compared to when wearing spectacles, and this was confirmed by Biousse et al. (2004). Contact lenses also appear to dampen nystagmus EMs in IN, but this effect is not present when the eye is anaesthetised (Dell'Osso et al. 1988). This interesting finding suggests that the presence of the lens touching the eye – rather than the optical effects of the lens – serve to reduce the movement, which implies that nystagmus intensity is partially governed by signals from nerves in this region. Dell'Osso, Leigh and Daroff (1991) went on to show that cutaneous stimulation of the ophthalmic division of the trigeminal nerve can cause a reduction of nystagmus intensity, using gentle touches, vibrations, pressing and rubbing of the forehead and upper eyelids.

1.3.10.6 Acupuncture

Ishikawa, Ozawa and Fujiyama (1987), have shown that acupuncture reduced IN intensity in nine out of 16 subjects tested. Blekher et al. (1998) later showed that insertion of two acupuncture needles in the sternocleidomastoid muscles of the neck caused a significant

increase in foveation durations in four out of six patients, which was observed five minutes following the end of treatment. In this experiment, one subject who was particularly responsive to the treatment later had a sham treatment administered, which caused exacerbation of his nystagmus. In this instance, foveation periods reduced at the times when the needle guide tubes were tapped, in contrast to an observed increase in foveation time during genuine acupuncture treatment.

1.3.10.7 Intermittent photic stimulation

First proposed by Mallett (1983), intermittent photic stimulation involves patients viewing visual targets that are retro-illuminated by a red light flashing at 4 Hz. They must identify the stimuli whilst attempting to consciously keep the afterimages as still as possible. It was claimed that training using the device could lead to long-term improvements in VA (Mallett 1983), but the treatment was shown to be no more effective than a placebo in a randomised double-masked clinical trial (Evans, Jordahl-Moroz and Nabee 1998).

1.3.10.8 Pharmacological treatments

Many medicines are known to reduce the intensity of nystagmus. In 2002, a list of fourteen treatments reported to improve the condition was published (Stahl, Plant, and Leigh). Of these, four have been shown to effectively dampen nystagmus intensity in IN (memantine, gabapentin, cannabis and baclofen). Memantine (20-24 mg) and gabapentin (up to 2400 mg) both reduce nystagmus intensity and improve VA in IN (memantine, 0.15 logMAR; gabapentin, 0.09 logMAR; placebo, 0.04 logMAR), and are the only treatments to have been validated in a controlled, double-masked randomised trial (Sarvananthan et al. 2006; Shery et al. 2006; McLean et al. 2007). One case report of a subject with IIN showed that smoking cannabis reduced nystagmus intensity by 30% in the primary position of gaze, and improved clinical VA by 2-3 logMAR lines (Pradeep et al. 2008). Baclofen is often used in patients with PAN, as it is known to reduce nystagmus amplitude, improve VA and alleviate abnormal head posture (Solomon, Shepard and Mishra 2002; Comer, Dawson and Lee 2006).

Dexedrine, a stimulant used to treat attention deficit hyperactivity disorder, has been shown to increase foveation duration, improve stereopsis, reduce exotropia magnitude, and improve VA in a patient with IN associated with rod-cone dystrophy (Hertle et al. 2001).

A recent study demonstrated that brinzolamide, applied as topical eye drops, caused an improvement in NAFX in a patient with IN, providing hope for non-systemic approaches to nystagmus pharmaceuticals (Dell'Osso et al. 2011).

The mechanisms of the above medications are currently unknown, although their mode of action is suspected to be through sedation rather than specifically reducing the EMs (Abel 2006). For a detailed account of the pharmacological treatments available for IN, the reader is directed to McLean and Gottlob (2009) and Strupp et al. (2011).

1.3.11 Appropriate measures of visual function

Section 1.3.10 lists many treatments that have been shown to reduce nystagmus intensity. Some have also been shown to improve VA; however, these improvements are often very minor, and the actual effect of reducing nystagmus intensity on visual function is not yet known. A 1999 study of VA measurements in a large optometric practice concluded that a change of 0.15 logMAR must be present before being considered significant (Siderov and Tiu 1999). The fact that the studies listed in Section 1.3.10 either used very few subjects or showed VA improvements rarely exceeding two lines (0.20 logMAR) suggests that their effects on VA are, at best, minimal.

Despite the significant reduction in intensity induced by convergence in IN, VA does not significantly improve (Hanson et al. 2006; Ukwade and Bedell 1992; Gradstein et al. 1998; Dickinson 1986). The increase in intensity brought on by stress also has no significant adverse effect on VA; however, it *does* significantly increase the time that subjects take to respond to a visual stimulus (Jones et al. 2008; Jones 2011). Anecdotal evidence suggests that nystagmats often complain of worsened vision in stressful situations and improved vision during near work (Wiggins 2008). Clearly, clinical VA is not a complete or consistent measure of visual performance in IN. Therefore, it seems reasonable that temporal aspects of vision and a more complete analysis of the contrast sensitivity function ought to be taken into consideration as well.

The nystagmus quantification functions described in Section 1.3.8.5 (NAF, NAEF, NAFX and NOFF) are justified by the fact that their values correlate with VAs of patients with IN. However, these correlations only hold *between subjects*, and improvement in a nystagmus function within a single individual have been shown not to correlate with VA (Wiggins 2007; Erichsen et al. 2013). This fact alone suggests that the relationship between VA and motor characteristics may have been misinterpreted: perhaps it is not a poor waveform that leads to poor VA, but poor VA that leads to adoption of a ‘sloppy’ waveform.

Recognising the inadequacies of VA and the nystagmus quantification functions in predicting visual performance, alternative tests of visual function have been proposed which look specifically at the temporal aspects of the condition. These are outlined below.

1.3.11.1 Restricted viewing time

Yang et al. (2005) proposed the use of optotypes with a restricted viewing time (550 ms was used) to quantify visual function in IN. They found that time-restricted VA is significantly reduced when viewing out of the null zone as compared to non-time-restricted VA.

A 2012 study on surgical interventions in IN (ElKamshoushy et al. 2012) used a similar outcome measure to Yang et al.'s 2005 study. To validate surgical methods, they presented three tumbling Es for 100 ms each. If subjects could correctly identify the orientation of at least two of the optotypes, the test ended. If not, new tumbling E optotypes were presented for 200 ms each. This process continued, with presentation time increasing by 100 ms each time, until at least two optotypes were correctly identified.

1.3.11.2 Moving optotypes

The outcome measure in the study of ElKamshoushy et al. (2012) study was based on a similar test performed by Hertle et al. (2002). Recognising that the 'slow to see' phenomenon in IN also impinges on the time taken to acquire moving targets, Hertle et al. presented single *moving tumbling Es* and measured the time taken to respond to the orientation of the optotype at various spatial frequencies (0.60 – 1.04 logMAR) and speeds of movement (10 – 30°/s). The study concluded that this might be a useful test of visual function in IN.

1.4 Eye movement recording

Many systems exist that record human EMs. The perfect EM recording system would:

- produce data with a high spatial and temporal resolution and no noise
- provide data that remain linear across the entire calibration range
- be easy to set up and calibrate
- be comfortable to use for an extended period of time
- distinguish between head and EMs without head restraint
- be able to distinguish ocular rotation from lateral translation
- not interfere with normal behaviour
- be able to detect the full range of ocular rotation ($\sim\pm 50^\circ$ horizontally/vertically and $\sim\pm 20^\circ$ of torsion [Collewijn 1999]).

Of course, no such system exists. The three most common methods of EM recording are the scleral search coil, electro-oculography and photo-oculography (Eggert 2007). These devices are described in the following paragraphs.

1.4.1 Scleral search coil

The scleral search coil is often considered the gold standard in EM measurement (Irving et al. 2003). It uses a copper wire embedded in a silicon scleral contact lens, in which changes in current are induced by a magnetic field around the subject's head in order to calculate its angle, and thus eye position. It is highly accurate, detecting EMs with amplitudes of 5-10" arc and having a temporal resolution of 1000 Hz, but this level of accuracy is only maintained over a range of $\pm 5^\circ$ (Robinson 1963; Duchowski 2007). However, by its very nature, it is uncomfortable to wear, even in the anaesthetised eye, and is therefore unsuitable for use for periods longer than 30 minutes (van der Geest and Frens 2002). It does not cause any significant impairment of visual function (Murphy et al. 2001), but may affect the intensity of nystagmus if used in these subjects (see Section 1.3.10.5).

1.4.2 Electro-oculography

There is a potential difference (voltage) between the front and back of the eye, ranging from 15 to 200 μV (Duchowski 2007). This is known as the *corneoretinal potential*. An electro-oculography system for measuring horizontal EMs uses electrodes placed at the outer canthi which detect changes in voltage when the eye moves. The voltage is amplified, compared to a reference electrode (usually placed on the forehead), and recorded. With a high enough sampling rate, the amplitude of saccades can be accurately measured (Stern, Ray and Quigley 2001). Unfortunately, the voltage dipole of the eye is not located at the centre of rotation, and the corneoretinal potential fluctuates due to photoreceptor activity (i.e. a change in luminance at the retina will alter output), so electro-oculography data provide a potentially inaccurate measure of eye position (Berg and Scherg 1991; Collewijn 1999). However, electro-oculography does have useful applications, as the eyelids do not need to be open and other electrophysiological data, for example from electroencephalography, can be processed in parallel.

1.4.3 Photo-oculography

A wide range of eye tracking systems use reflections from the limbus, pupil margin, or the ocular Purkinje images to calculate eye position. A few examples of these are given in the sections that follow.

1.4.3.1 Skalar IRIS System

The IRIS system was devised by Reulen et al. (1988), and comprises head-mounted photo-oculography systems that track the position of the limbus and a separate processing unit. The IRIS uses infrared light for tracking. Nasal and temporal detectors for each eye detect changes

in the amount of infrared light reflected, which is converted into a voltage by a phototransistor. By comparing the nasal and temporal voltages, the position of each eye is calculated individually (Cambridge Research Systems 2007) (see Figure 1.12).



Figure 1.12: The Skalar IRIS headset and processing unit (Cambridge Research Systems 2007).

For horizontal eye tracking, the IRIS system provides accurate data to up to $\pm 25^\circ$ eccentricity, with a sampling frequency of 1000 Hz (Reulen et al. 1988) and an optimal resolution of $2'$ arc (Cambridge Research Systems 2007). One major disadvantage of the IRIS system is that it is uniaxial; it cannot measure both horizontal and vertical eye position concurrently.

1.4.3.2 Tobii X300

The Tobii X300 is an infrared-based photo-oculography system that uses a combination of visible features (including the pupil margin and Purkinje images) and can track the eyes with the head free (see Figure 1.13). It measures binocularly at 300 Hz, with a maximum spatial resolution of $\pm 0.5^\circ$. In addition to being capable of tracking horizontal and vertical gaze together, one major advantage over the IRIS system is its reduced setup time and minimal intrusion into normal activity (i.e. nothing touches the eyes or head). Freedom of head movement is reported as being within a volume of $37 \times 17 \times 30$ cm (horizontal \times vertical \times depth), and maximum gaze eccentricity is reported as $\pm 35^\circ$ (Tobii Technology 2011) (see Figure 1.13). The Tobii X300 tracks the pupil border rather than the limbus. Whilst this has become somewhat of a standard in modern eye tracking systems, this can reduce tracking performance in individuals with iris transillumination, such as in ocular albinism (Sjödell, Sjöström and Abrahamsson 1996).



Figure 1.13: The Tobii X300 system (Tobii Technology, 2011).

1.4.3.3 EyeLink 1000

The EyeLink 1000 is another example of an infrared photo-oculographic system (see Figure 1.14). Like the Tobii X300, it does not require the head to be restrained; however, the manufacturer recommends the use of a chin rest when spatial resolution is important (SR Research, 2010). The EyeLink 1000 has a monocular sampling rate of 1000 Hz (500 Hz binocularly), a spatial resolution of $\pm 0.1^\circ$, and can track gaze angles up to $\pm 32^\circ$ horizontally and $\pm 25^\circ$ vertically. Without the head supported, a range of head movement of $25 \times 25 \times 10$ cm (horizontal \times vertical \times depth) is permissible (SR Research 2010). The EyeLink 1000 uses a high-precision calibration method originally described by Stampe (1993). Like the Tobii X300, the EyeLink 1000 uses the border between the pupil and iris for eye tracking (in addition to the Purkinje images), so use in ocular albinism is contraindicated.



Figure 1.14: The EyeLink 1000 system (SR Research, 2010).

1.5 Summary

The preceding chapter provides a synopsis of the literature relating to the control of EMs as well as the characteristics of nystagmus and its perceptual consequences as they are presently understood. Chapter 2 details the development of software which allows for speedy calibration and analysis of nystagmus EM traces. This software is utilised in the analysis of later chapters (4-6), which deal with understanding the spatial and temporal constraints of vision in IN.

Chapter 3 details a study in which VA was measured using targets illuminated by brief flashes of light. This experiment elucidates the limitations to VA improvements that ought to be achievable in adults with IN by slowing their EMs, in an attempt to understand why so many of the treatments for IN (listed in Section 1.3.10) fail to elicit significant improvements in VA. The results indicate that VA is fundamentally limited in IN, perhaps due to amblyopia or undetected pathology. Nonetheless, the problem still remains that these treatments often produce significant *subjective* improvements to vision, as recorded by visual function questionnaires.

In Chapter 4, *temporal* aspects of vision in IN are investigated. The time taken to recognise visual targets was measured in individuals with IN and in control subjects. Specifically, comparisons were made between the time taken to respond to centrally and peripherally presented targets. Those stimuli presented in the periphery require a targeting EM (i.e. saccade) to be made in order to view the stimulus before it can be recognised. Perhaps unsurprisingly, individuals with IN took longer to direct their gaze towards the targets. Interestingly though, after the targeting EM had been completed, those with IN took no longer than controls to recognise and respond to target orientation. This is significant, as it suggests that visual processing in IN is not slow; i.e. the reason that nystagmats are ‘slow to see’ appears to be entirely due to difficulties in deploying gaze as quickly as normally-sighted individuals.

Finally, Chapter 5 looks at the *timing* of voluntary EMs in IN, as the result of a fortuitous finding made during the analysis of the results of Chapter 4. A strict relationship was discovered between the time at which voluntary EMs are initiated and nystagmus quick phases. In most cases, the two EM types were combined into unified movements, and perhaps more interestingly, quick phase timing appeared to be modified in order to accommodate the voluntary movement, rather than vice versa.

This thesis is concluded in Chapters 6 and 7, which present ideas for future work and a discussion of the work as a whole, respectively. Whilst the studies presented here provide new insights into perception and oculomotor control in IN, the results make clear that new techniques must now be developed to quantify the perceptual experience of IN in the clinic. Waveform quantifying measures such as NOFF and NAFX (see Section 1.3.8.5) are currently predicated on an assumed relationship between waveform characteristics and VA, which now appears unlikely to hold *within* individuals.

Chapter 2 Automated waveform analysis

2.1 Introduction

Much of the literature surrounding nystagmus involves eye tracking technology at some level. In order to understand the relationship between EMs and perception, it is necessary to record and analyse EMs. The present chapter explains the challenges faced when using eye tracking technology in nystagmus research, and describes the design, evaluation and application of a novel software suite for calibration and automated analysis of IN waveform data.

2.1.1 The problem with calibration

The standard calibration methods for many photo-oculographic eye tracking systems (see Section 1.4.3) require the subject to look directly at visual targets displayed sequentially at known locations. Typically, the system waits until the eye is almost stable before recording the eye position for each calibration point. In most individuals with nystagmus, the eyes are never stable enough to be automatically accepted as fixations. Although it is usually possible to manually override the system (i.e. to force acceptance of eye position regardless of on-going movement), doing so introduces a potential calibration inaccuracy, since the gaze could be at any point along the nystagmus waveform at the time of manual override.

Such inaccuracies may be tolerable for many research studies. However, in order to guarantee high precision in nystagmus waveform analysis, it is necessary to ensure that only the visual axis (i.e. eye position during foveation) is used for calibration.

In IN, the fovea is far more likely to be directed towards the object of regard during a foveation period (Feliuss et al. 2011). In principle, these foveation periods therefore provide a reliable means for calibrating an eye tracking system. Foveations, as described in Section 1.3.1, are a loosely defined phenomenon relating to the slowest portion of a nystagmus waveform, in which it is assumed that the majority of useful visual input is gathered. Whilst there has been much debate about the absolute velocity threshold that should be used to define a foveation period, such thresholds are meaningless in the absence of accurate calibration data. There is no way of knowing what constitutes a velocity threshold of, say, $4^\circ/\text{s}$, unless one already knows what constitutes a degree of movement. This presents something of a ‘catch 22’: one cannot calibrate an eye tracking system without finding foveations, whereas foveations cannot be found unless the system is already calibrated.

In a study by Hertle et al. (2012), nystagmus EM traces were calibrated by assuming that the eye position(s) immediately following saccades represent foveations. Whilst this approach is

suitable for many nystagmus waveforms, in those containing multiple quick phases it would not be clear which gaze angle represents the true ‘foveation’ position¹¹.

It may be possible to solve the problem by pre-calibrating an eye tracker to a subject *without* nystagmus prior to data collection, or to use an approximate calibration from points obtained through the ‘manual override’ method described above. This would provide an estimate on which to base an absolute foveation velocity threshold. Both of these solutions would provide an approximation to the ‘true’ foveation periods, but neither could be considered accurate. As a result, eye tracker calibration has, up until now, been a laborious process, requiring a skilled observer to manually mark candidate foveations based on knowledge and experience of IN waveforms. This time-consuming task is usually performed after the recording session is complete. A method of speeding up this process would make it feasible to calibrate an eye tracker *prior* to a recording session, which in turn opens the possibility for new experimental paradigms, such as gaze-contingent presentation of stimuli.

In addition to providing a useful research tool, an automatic calibration method for use in IN would provide a means for nystagmats to interact with the growing number of gaze-based consumer technologies that are emerging on mobile devices and computers.

This chapter details the development of a software suite for the automated calibration and analysis of nystagmus waveforms. Previous solutions have applied a ‘one size fits all’ foveation definition. The novel approach proposed here is to view foveations as simply the ‘slowest’ periods of the nystagmus waveform (regardless of the overall intensity), such that a given proportion of the nystagmus cycles present in a recording contain a detected foveation. As a result, foveation ‘quality’ using this new method may be gauged by the *velocity* of foveation, rather than *duration*.

2.1.2 Foveations are not the same in all individuals

One of the problems with the way that foveation is currently defined (apart from being impossible to calculate prior to calibration) is that the same criterion is applied to all participants in a single study. Figure 2.1 shows an example of a recording from a subject with high-intensity nystagmus (subject JS, mean intensity = 35.4°/s). Using a traditional method of foveation detection with a *foveation velocity threshold* of 6°/s, only four foveations are found in the entire recording. At the (more commonly used) 4°/s threshold, no foveations are found at all.

¹¹ This approach was originally taken in an early incarnation of the algorithm presented in this chapter. It was successful at detecting foveations in most waveforms, but only if each cycle contained a single saccade.

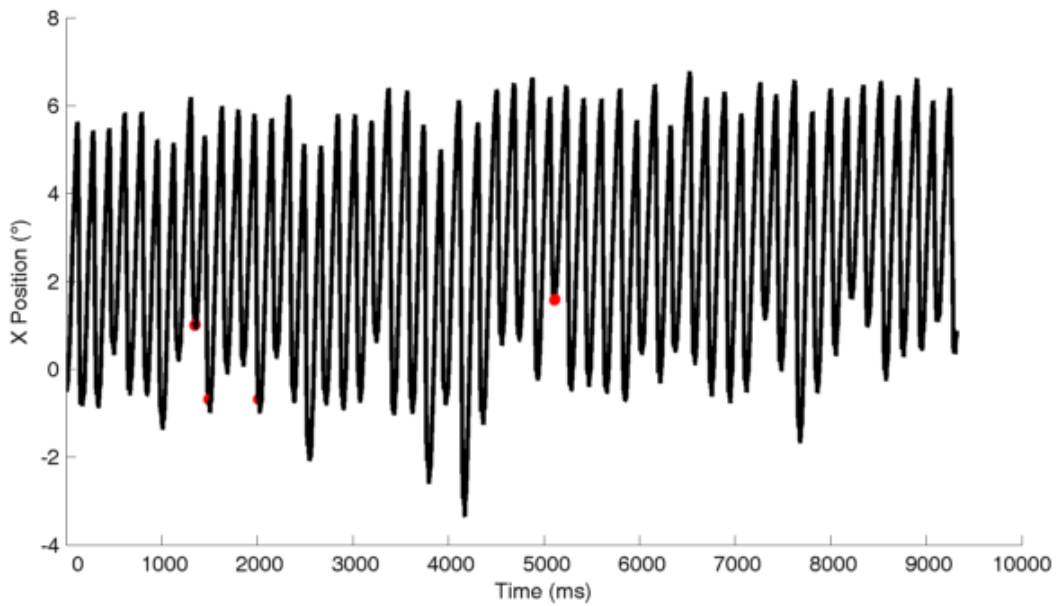


Figure 2.1: Example of foveations detected (**red**) using the traditional automated method of foveation detection, with foveation velocity threshold set to $6^\circ/\text{s}$ (subject JS)

Figure 2.2 shows another subject (DB, intensity = $3.4^\circ/\text{s}$), with foveations detected at the same *foveation velocity threshold* as that shown in Figure 2.1.

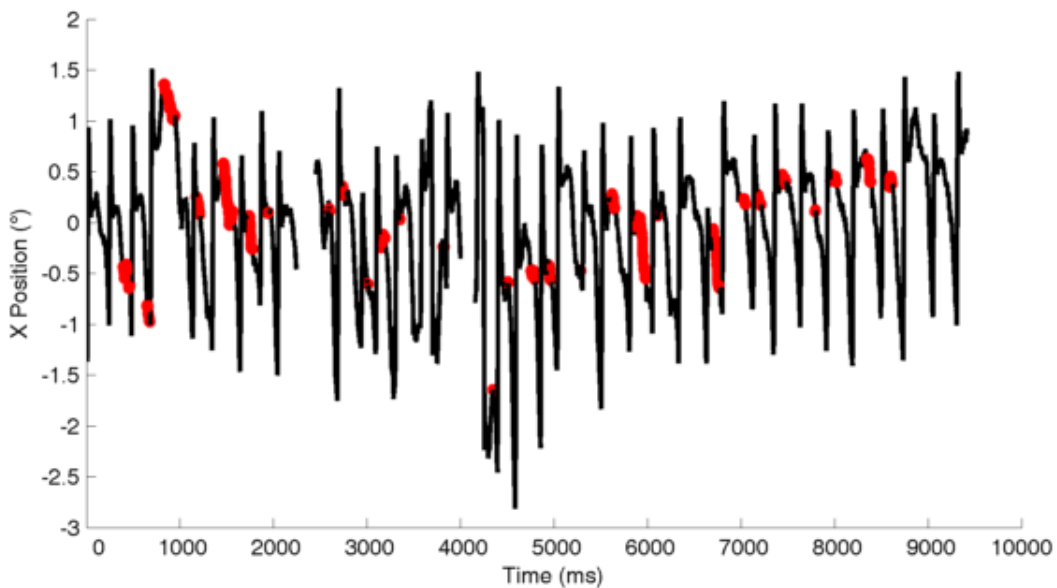


Figure 2.2: Example of foveations detected (**red**) using the traditional automated method of foveation detection, with foveation velocity threshold set to $6^\circ/\text{s}$ (subject DB)

Note that far more foveations are detected for subject DB. Clearly, foveation cannot be defined by a ‘one size fits all’ criterion. Chung and Bedell (1996) suggested that *foveation velocity threshold* ought to be different for each individual, set in relation to the duration of foveations. The approach set out in this chapter provides an automated method of achieving this end.

2.1.3 Complete waveform analysis

The software described in the present chapter separates the various components of the nystagmus waveform. As a result, it is capable of performing detailed analyses on each of these components. Once a calibration has been performed, an accurate analysis of nystagmus can take place. An example of the graphical output from the software can be seen in Figure 2.4. The software was programmed to output the following metrics:

- Axis of nystagmus
- Number of blinks detected
- Final saccadic and foveation velocity thresholds used (alternatively, these can be set to absolute values by the user for use with pre-calibrated data)
- Number of back-to-back saccades
- NAFX (see below)
- NOFF (see below)
- Whether or not the majority of slow phases are accelerating (i.e. whether the recording is likely to represent *infantile* nystagmus)
- For each cycle:
 - Nystagmus frequency
 - Nystagmus amplitude
 - Nystagmus intensity
- For each foveation:
 - Foveation duration
 - Foveation position
 - Foveation velocity
- For each saccade:
 - Saccade duration
 - Saccade direction
 - Saccade peak velocity
 - Saccade mean velocity
 - Saccade amplitude
- For each slow phase:
 - Slow phase duration
 - Slow phase peak velocity
 - Slow phase mean velocity

Using the latest algorithms (Jacobs and Dell’Osso 2009), NAFX (see Section 1.3.8.5) can only be calculated for a limited range of ‘foveation’ definitions (absolute maximum values for velocity and positional drift). Since foveation velocity is calculated dynamically by the software presented in this chapter, it is very unlikely that the calculated value will equate exactly with a value specified on the NAFX ‘tau surface’. In these situations, the nearest available values (from the published tau surface) are used for NAFX calculation. However, if desired, the present software can be forced to use specific velocity and position limits to define foveation, in order to calculate NAFX in the classic way. Code for this function was adapted from that written by Jonathan Jacobs and can be found in Appendix I – *nystagmus_calc_nafx.m*.

The software also calculates NOFF (see Section 1.3.8.5): a sub-function was written which calculates NOFF in the manner described in Felius et al. (2011). The author is grateful to Joost Felius for guidance and verification of the code, which was recently released publicly and can be found in Appendix I – *nystagmus_calc_noff.m*. This calculation is performed on a single four second window of EM data, which is determined by seeking through the entire EM trace for the period of clean data with the lowest mean velocity.

The software described in this chapter is capable of producing three-dimensional visualisations of nystagmus waveforms (i.e. including time as the third dimension; see Figure 2.3), as well as plots showing the saccadic main sequence relationships (*duration : amplitude*, *duration : peak velocity* and [*peak velocity × duration*] : *amplitude*). An example of the visual output from the software is shown in Figure 2.4.

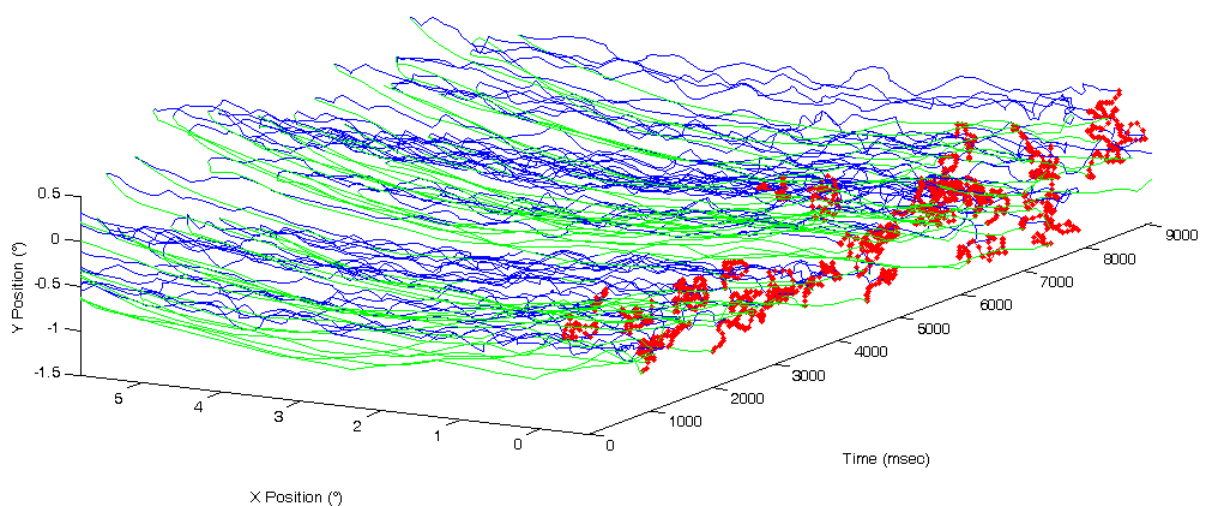


Figure 2.3: Visualisation of both the horizontal and vertical components of nystagmus across time might provide new insights into the condition.

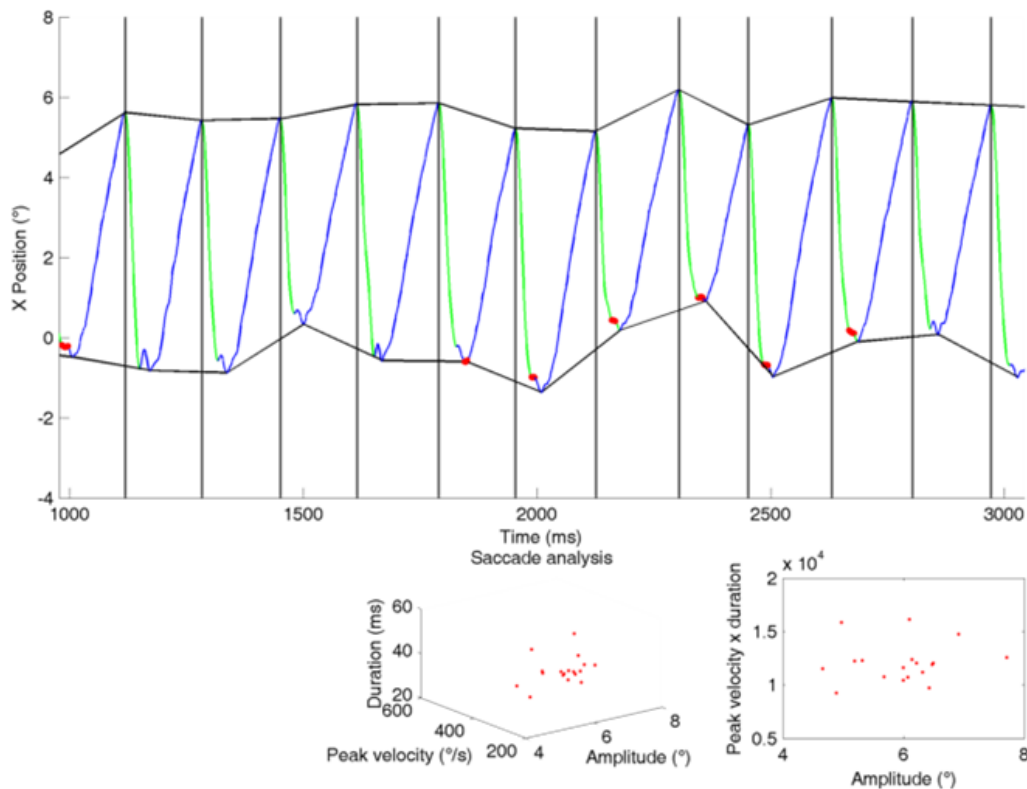


Figure 2.4: Composite output from nystagmus analysis software, including marked saccades (green), foveations (red), cycle boundaries (black) and subplots showing saccadic main sequence relationships (lower central subplot is three-dimensional).

A ‘front-end’ graphical user interface was also created for the software, which allows the algorithms to be used by clinicians and researchers without any knowledge of MATLAB programming. The graphical user interfaces for analysis and calibration are shown in Figures 2.5 and 2.6. The source code for the software can be found in Appendix I – *nystagmus_analyser.m*, and the software package’s user manual can be found in Appendix III.

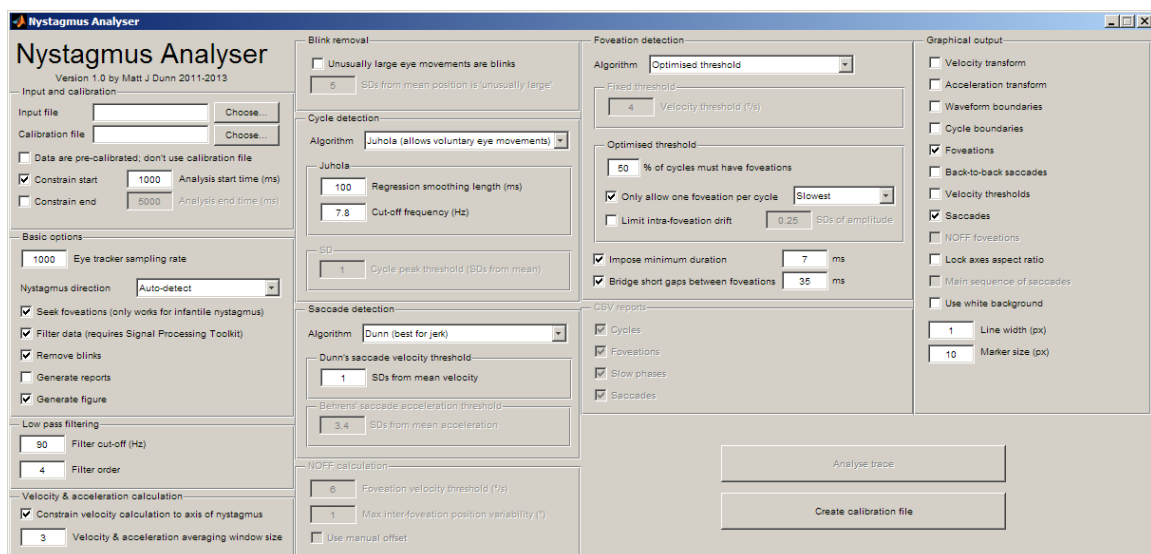


Figure 2.5: Graphical user interface for nystagmus analysis software

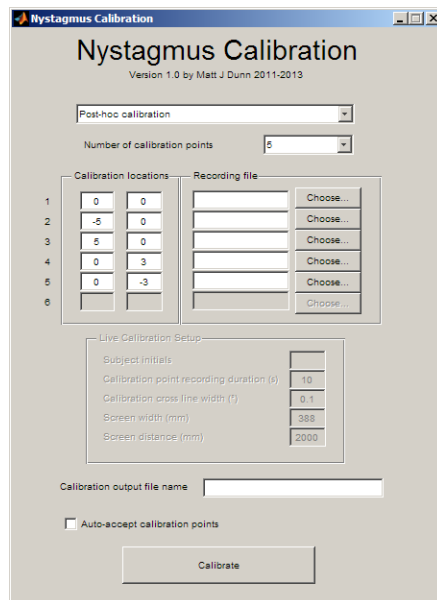


Figure 2.6: Graphical user interface for nystagmus calibration software

These additional features and analyses provide the basis for data analysis in subsequent chapters of this thesis. Since almost all of the data analyses are automated and performed rapidly, there is potential for incorporation of this software into clinical instruments.

2.1.4 Waveform analysis: existing solutions

Algorithms for automated analysis of nystagmus have been described before (Banks and Wall 1989; Radinsky and Galiana 2004; Engelken and Stevens 1990; Juhola 1988; Janczewski et al. 1996). However, these algorithms are designed for use in physiological nystagmus (not early-onset). Of course, for these solutions, calibration can be performed *prior* to the nystagmus induction, hence the issue of how to calibrate the system in the presence of nystagmus does not exist. Moreover, these solutions do not detect foveation periods and cannot deal with complex waveforms, such as those containing multiple saccades.

OMtools is a suite of tools, written by Jonathan Jacobs and Louis Dell’Osso for the analysis of nystagmus EM data, which also provides a calibration function. However, this is a manual method that requires the user to select a *single* calibration point for each target location. Additionally, the software described in this chapter provides the option to manually override calibration to a single point (see Section 2.2.2.11, point 3), but this is considered a last resort, only to be used if foveation detection cannot be performed automatically. *OMtools* does not perform detailed analysis of the components of the waveform as the newly proposed software does. However, it does report some interim statistics relating to NAFX:

- Mean foveation time per cycle

- Mean foveation time per second
- NAFX, taking into account the position limit only (i.e. ignoring the velocity criterion)

NAFX calculation using OMtools requires the user to manually select parts of the nystagmus waveform, whereas the new software performs this calculation automatically.

2.1.5 Existing methods for automated saccade detection

In order to split a nystagmus waveform into its component parts, it is necessary to apply a saccade detection algorithm to detect quick phases. Many saccade detection algorithms rely on having a pre-calibrated position signal. For the present application, this was impossible since saccade detection forms an intrinsic part of the calibration procedure. As a result, a novel saccade detection algorithm had to be developed. Examples of existing saccade detection algorithms are given below.

2.1.5.1 Behrens, Mackeben and Schröder-Preikschat's method

Recently, Behrens, Mackeben and Schröder-Preikschat (2010) detailed an algorithm for automatic saccade detection. This method looks at the acceleration transform of the eye position data and uses relative acceleration (rather than absolute) to detect saccades. The advantage of using such a threshold is that the method can be used with uncalibrated data.

In Behrens, Mackeben and Schröder-Preikschat's method, the acceleration threshold is dynamically calculated for any given moment based on the velocities present in the preceding 200 ms of the recording. Although not a requirement for the present study, this provides the obvious advantage that it is transferable for use on *live* EM data and adapts to the magnitude of the underlying signal.

The algorithm works in the following way (see also Figure 2.8 which shows some of the components described here graphically):

1. For any given sample, the mean and standard deviation acceleration of the preceding 200 ms is calculated. The *saccadic acceleration threshold* is set to the mean value plus 3.4 standard deviations (this value was chosen by the authors empirically).
2. If ocular acceleration exceeds the *saccadic acceleration threshold* at any time, the start of a saccade is noted.
3. Once a saccade has begun, the *saccadic acceleration threshold* is held constant.
4. The acceleration transform is monitored to find the time at which the acceleration again drops below the (now fixed) *saccadic acceleration threshold*.

5. Once the acceleration has dropped, the position trace is monitored to find when it ceases to be a monotonic function (i.e. when the eye stops moving or reverses direction).
6. When step 5 has been satisfied, the acceleration transform is monitored to find the first time at which acceleration is above the *negative saccadic acceleration threshold*. In a normal biphasic saccade, the acceleration transform displays both an acceleration peak and a deceleration trough. The saccade must therefore have passed its deceleration ‘trough’ for this criterion to be satisfied.
7. The end of the saccade is declared. The total length of the saccade is now calculated. If this is found to be less than 100 ms, the whole saccade is rejected and considered to be an artefact.
8. Following the end of a saccade, the *saccadic acceleration threshold* value is steadily increased until 200 ms have passed without a saccade, at which point it is recalculated as in step 1. The *saccadic acceleration threshold* continues to be steadily increased until it exceeds the dynamically calculated value.

In order to test the efficacy of this method, it was converted into MATLAB code (The MathWorks, Natick MA) and incorporated into the software for the current project. The code can be found in Appendix I – *oculomotorsuite_findsaccades_behrens.m*.

Because Behrens, Mackeben and Schröder-Preikschat’s method sets the *saccadic acceleration threshold* based on the preceding 200 ms of data, it is significantly affected by recent EM activity. For example, if several rapid EMs occur in succession, the average acceleration in the EM trace will increase, inducing a higher *saccadic acceleration threshold*, and potentially leading to genuine saccades being missed. The algorithm attempts to avoid this problem by only calculating the *saccadic acceleration threshold* 200 ms after the previous saccade, but unless there is a quiescent period lasting at least 200 ms, then such a recalculation can never take place. In most applications this problem never presents, since there need only be a brief period of time without saccades for the algorithm to recalibrate its *saccadic acceleration threshold*. In the complex waveforms of IN however, such a situation often arises, leading to erroneous saccade detection. An example is given in Figure 2.7, in which Behrens, Mackeben and Schröder-Preikschat’s method is applied to two seconds of EM data during attempted fixation from subject GT, whose complex waveform contains two large saccades per cycle.

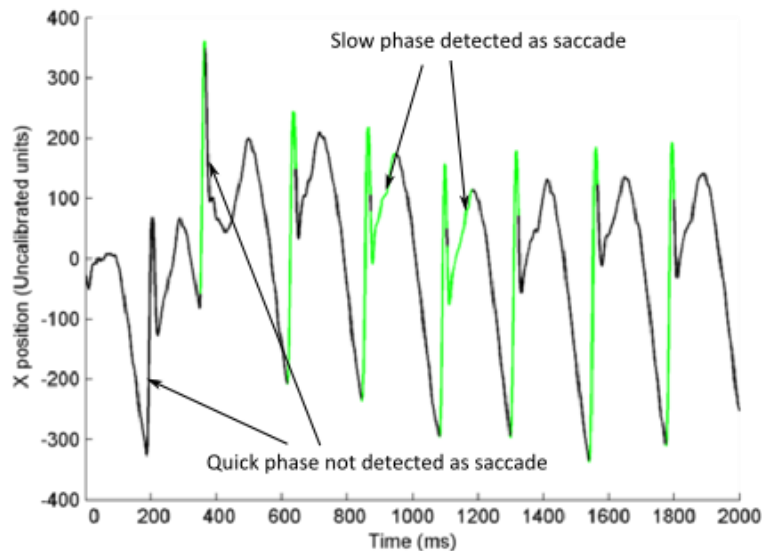


Figure 2.7: An example of a nystagmus EM trace (subject GT) using the Behrens, Mackeben and Schröder-Preikschat (2010) saccade detection algorithm. Detected saccades are shown in green.

Figure 2.7 clearly shows erroneous saccade detection in the form of both false positives and false negatives. The schematic shown in Figure 2.8 illustrates how erroneous saccade detection can arise. The blue/green line shows a single saccadic EM to the left following a right-drifting nystagmus slow phase. The green regions of the line indicate the times identified as a saccade. Notice that a ‘saccade’ is marked as beginning during the slow phase of the waveform. This is because the *saccadic acceleration threshold* (dashed red lines) was sufficiently low to detect a small fluctuation in acceleration (fuchsia line) during the slow phase. The *saccadic acceleration threshold* is stuck at this level because it cannot adjust until 200 ms have passed since the last saccade. Nystagmus EM data contain frequent saccades, so this filter often gets ‘stuck’ at one threshold. The erroneous saccade in this example is determined as ending during the *actual* saccade, and another ‘saccade’ is detected as starting shortly thereafter.

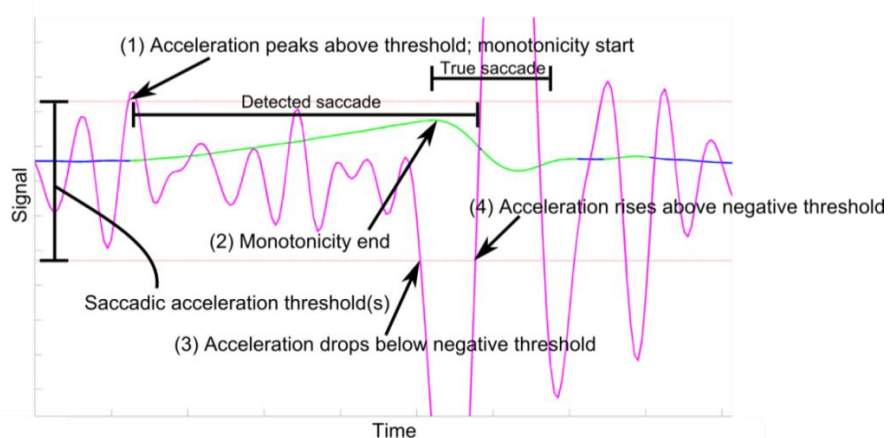


Figure 2.8: An example of erroneous saccade detection using the method described by Behrens, Mackeben and Schröder-Preikschat (2010) (subject MT). The fuchsia line shows the

acceleration trace (divided by 1000 for visibility on the plot). During a detected ‘saccade’, the position line (blue) changes to green. Saccadic acceleration thresholds are indicated as dashed red lines. In this case, the saccadic threshold is sufficiently low that an erroneous saccade is detected before the actual saccade starts. As a result, the true saccade is missed.

2.1.5.2 Pander et al.’s method

Another method for saccade detection, specifically for use in nystagmus EM trace data was described in 2012 (Pander et al.). This method simply detects the times of the *peak velocity* of saccades, using the following steps:

1. EM trace position data are filtered to remove noise.
2. Velocity is calculated through differentiation of position data.
3. Velocity spikes are detected using a peak detection function that looks for local maxima and minima fluctuations in a vector. These spikes, which coincide with the peak velocities in the EM trace, are marked as saccades.

2.1.5.3 Wyatt’s method

Since the above method only detects the *peak velocity* of saccades, it is not suitable for use in complex saccade metric analysis. Such a method, whilst effective at determining the approximate time of a saccade, cannot determine saccade duration, amplitude or overall velocity, since it does not determine the start or end times of each saccade. Another method (Wyatt 1998) detects saccades in a similar way, but uses the third derivative of the position vector (the ‘jerk’ transform), rather than the first or second (velocity/acceleration). Wyatt’s method determines the beginning of the saccade using the jerk transform, but saccade termination is less clear. Depending on the EM trace examined, saccade termination is determined using either the jerk or acceleration transform (second transformation of position vector), this being decided by the user. A semi-automated approach such as this is obviously less preferable than a fully-automated one.

2.1.6 Aims

As described above, the present study aimed to design an automated method of calibrating an eye tracker in the presence of IN. A series of algorithms that automatically parse the waveform into its component parts were designed, enabling rapid, detailed analysis of clinical data. As explained above, existing saccadic detection algorithms are unsuitable for use in (uncalibrated) nystagmus data. Therefore, a novel saccade detection algorithm was also designed.

The calibration method was subsequently verified by cross-checking the results obtained by the same algorithm in separate recordings, and by comparing its results to those obtained by existing methods.

2.2 Materials and methods

2.2.1 Eye tracking apparatus

Due to the relatively simple set-up, high sampling rate and the ability to program the device using both the C and MATLAB programming languages, the EyeLink 1000 (see Section 1.4.3.3) was chosen for EM recording in the studies documented in this thesis.

2.2.1.1 Noise confirmation

In order to confirm the level of noise produced by the EyeLink 1000, a device designed to imitate the human eye was calibrated and recorded in a range of stationary positions. A variety of solutions can be used for this purpose, including circles of paper and computerised images (Cavegn, Rensbergen and d'Ydewalle 1993). For the present study, the 'model eye' comprised an artificial pupil covered by a rigid gas permeable contact lens (Quasar, 7.3 mm back optic zone radius, 9.2 mm diameter, -3.00 DS power), mounted on a device that could be rotated to any angle in each of three axes. The contact lens was included to provide a suitable 'corneal' reflection for the eye tracker to detect. The device is shown in Figure 2.9.

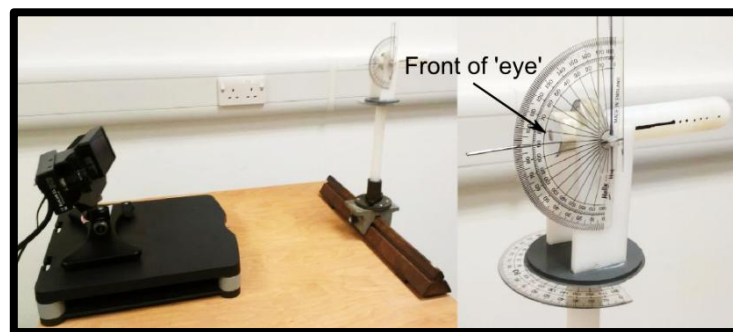


Figure 2.9: 'Model eye' used to verify noise levels in eye tracker systems

The device was calibrated to a monitor situated 2 m away, with the eye tracker 53 cm away (this mimicked the setup used in the experiments presented in this thesis, and was performed in the same lab). The EyeLink 1000's 35 mm camera was used, and infrared illumination from the eye tracker was set to 75%. A nine point calibration was performed over an area of $9.8 \times 7.0^\circ$ (horizontal \times vertical), in which the eye was carefully aligned in the direction of each target using protractors attached to the device. Following calibration, 10 second recordings were made with the model eye at each of five 'gaze' positions: central, 3° right, 3° left, 3° up and 3° down. The procedure was performed under both photopic and scotopic conditions

(identical lighting conditions to those under which the experiments described in this thesis were performed). The ‘eye’ was recalibrated for each lighting condition. The range and standard deviations of the noise (variation in reported gaze position) for both the horizontal and vertical axes, in each of the five positions, under both lighting condition are reported in Table 2.1.

Table 2.1: Noise levels recorded in different ‘gaze’ positions under photopic and scotopic conditions with an EyeLink 1000. All values are in degrees. X and Y refer to horizontal and vertical respectively.

Position	Photopic				Scotopic			
	X range	X SD	Y range	Y SD	X range	X SD	Y range	Y SD
Central	0.0475	0.0063	0.0753	0.0084	0.0365	0.0049	0.0463	0.0060
3° right	0.0526	0.0075	0.0492	0.0071	0.0433	0.0056	0.0469	0.0063
3° left	0.0554	0.0062	0.1401	0.0105	0.0570	0.0086	0.0463	0.0064
3° up	0.0475	0.0058	0.0710	0.0098	0.0428	0.0056	0.0583	0.0079
3° down	0.0550	0.0079	0.0659	0.0087	0.0643	0.0103	0.0335	0.0047
Average	0.0516	0.0067	0.0803	0.0089	0.0488	0.0070	0.0463	0.0063

These results show that the EyeLink 1000 provides eye position signals that are accurate to $< 0.1^\circ$ under varying illumination levels when used with an artificial eye. Note that these data do not take into account human factors such as head and body shifts. Nonetheless, such a high level of precision from the eye tracker itself is a desirable starting point for the studies that follow in this thesis.

Code written to perform the noise confirmation is presented in Appendix I – *noisechecking.m*.

2.2.2 Software design

The following section explains the various sub-functions performed by the software created for the calibration and analysis of nystagmus data. Many of the processes described here are used in the analysis of EM data in later chapters. Some of the processes are optional (for example, low-pass filtering of the data). All aspects of the software are described, since they form the basis of a package designed for general use in nystagmus research.

2.2.2.1 General design

As described in Section 1.3.1, IN waveforms contain quick and slow phases, with foveations occurring at some point during each slow phase. In order to find the *slowest* period of each nystagmus cycle, it is necessary to perform the following steps:

1. Split the nystagmus waveform into cycles
2. Distinguish saccades from slow phases
3. Find the slowest part of each slow phase

Software to perform these tasks was written in the MATLAB programming language (The MathWorks, Natick MA), and the source code can be found in Appendix I – *nystagmus_analysers.m*. In order to maximise flexibility of data input, the program was written to be capable of processing data directly from EyeLink data files, as well as from comma-separated value (CSV) files¹². The program can receive up to two eye position vectors¹³ as input – one for each of the (horizontal and vertical) axes. For compatibility with older eye tracking systems, the software is also capable of processing data recorded along a single axis.

2.2.2.2 Low-pass filtering

After reading in an EM trace data file, the software filters the data using a 4th order Butterworth filter¹⁴ (see Appendix I – *oculomotorsuite_lowpassfilter.m*). This smooths out noise in the signal which might otherwise be amplified when calculating velocity and acceleration (see Section 2.2.2.4). Filter cut-off frequency is set to 90 Hz by default, but can be specified by the user, since there is much variability in the exact level of filtering used in the EM literature. For an example of a recent publication using a 90 Hz Butterworth filter, see Shaikh et al. (2010). It is worth pointing out that over-zealous filtering could effectively dampen the nystagmus oscillation signal, and so should be applied with caution. Figure 2.10 demonstrates the effect

¹² CSV files are the universal standard for digital storage of numerical arrays. As such, all eye trackers with a digital output should be capable of producing data in this format.

¹³ In computer programming, a *vector* is a one-dimensional array.

¹⁴ A Butterworth filter is a low-pass filter with a relatively flat frequency response in the passband (Butterworth 1930).

of low-pass filtering on nystagmus EM data. Note the (relatively mild) smoothing of the position vector in the filtered data.

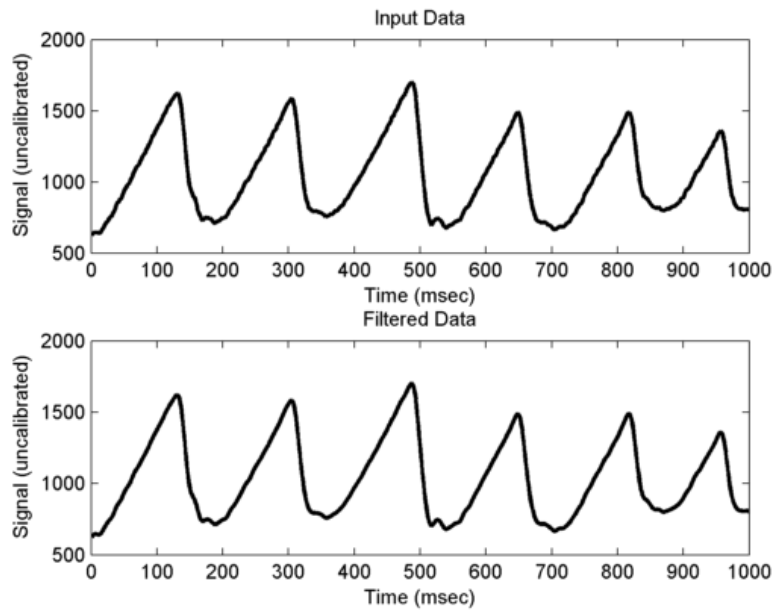


Figure 2.10: Figure demonstrating the effect of low-pass filtering on nystagmus waveform data (subject JS). The lower plot shows the same data as above, with a low-pass filter at 90 Hz.

2.2.2.3 Nystagmus axis detection

If not specified by the user, the program automatically detects the primary axis of nystagmus¹⁵. This is determined as the axis with the highest standard deviation of the position vector. Photo-oculographic eye trackers are unable to assess torsional movement of the eyes. However, it *is* possible to determine whether the nystagmus is principally horizontal or vertical. Recordings should be made during attempted fixation. Since no voluntary EMs are expected during the recording, the position channel with the greatest standard deviation can be assumed to be the primary axis of nystagmus.

2.2.2.4 Calculation of velocity and acceleration

Following nystagmus axis detection, the velocity and acceleration for each axis are obtained by second and third order differentiation of the eye position signals using a two-point central difference algorithm (see Appendix I – *oculomotorsuite_datadifferentiator.m*). The EyeLink 1000 data output contains its own self-calculated velocity trace, but by calculating the values from scratch, the program described here can be run in the same way on data collected with a

¹⁵ As is traditional in nystagmus research, this is defined either as ‘horizontal’ or ‘vertical’. However, since some individuals actually have nystagmus that oscillates obliquely, it may be wise in future work to determine the nystagmus axis geometrically. This would involve an extra processing step to convert the ‘X’ and ‘Y’ data from the eye tracker to geometric vectors.

variety of systems. In addition, using a conservative two-point central difference algorithm¹⁶ (rather than the 19-point algorithm employed by the EyeLink 1000) reduces the frequency limitations imposed by the filter (Bahill, Kallman and Lieberman 1982). The resulting velocity and acceleration traces from these calculations are shown for a 1 s segment of nystagmus data in Figure 2.11.

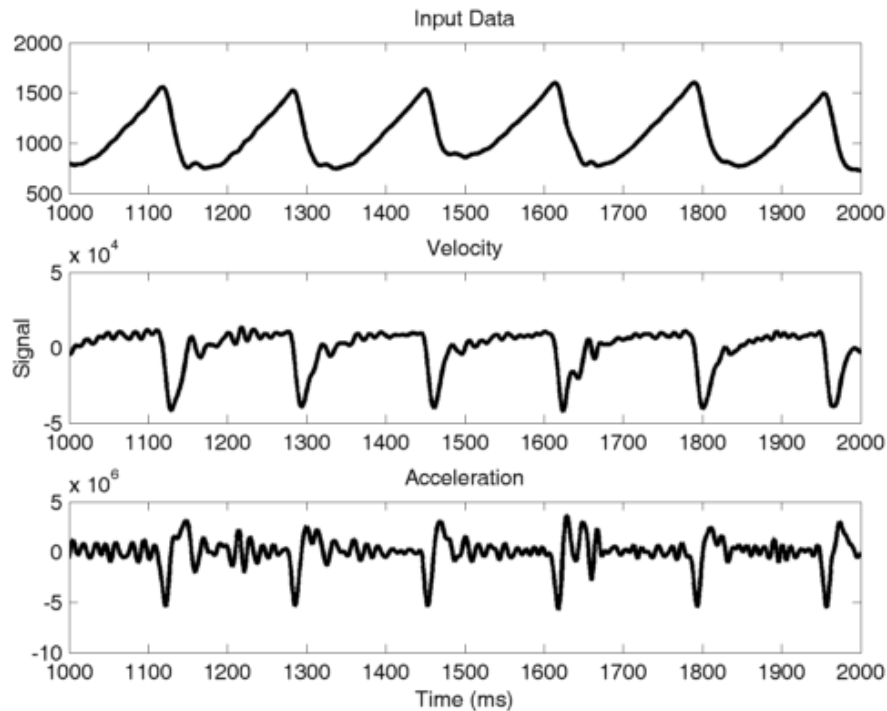


Figure 2.11: Example trace showing result of two-point central differentiation to obtain signal velocity and acceleration (subject JS)

Optionally, *total* velocity can be calculated based on the change in eye position signal as a Euclidian norm of the combined horizontal and vertical axes. By the same method, total acceleration is calculated by differentiation of the velocity signal. From a research standpoint, the inclusion of this option affords greater flexibility by providing more ways in which EM traces can be analysed.

2.2.2.5 Blink removal

Next, the data are stepped through to find and remove blinks. In many individuals, the presence of Bell's phenomenon causes unwanted EMs during blinks (Jones 2001). Whilst these EMs are not artefacts of the recording method, they are unhelpful for the purpose of nystagmus analysis and are therefore removed. A separate function (*oculomotorsuite_removeblinks.m*; see Appendix I) was written to achieve this aim. The function

¹⁶ A central difference algorithm determines the differential of the data preceding and following the datum being examined.

first identifies dropped data. Any EM trace data (position, velocity and acceleration) that are contiguous with dropped data are checked to see if they lie within three standard deviations of the median values for the entire recording. The value of *three* standard deviations was chosen empirically; for the EyeLink 1000, this value effectively rejects blinks without eliminating useful data. However, this value might vary for other eye trackers, so the option to adjust this value is provided to the user in the complete software package. Data that lie outside of these limits (whether in the position, velocity or acceleration channel) are removed from the recording. Figure 2.12 shows an example of an EM trace containing a blink, and the result of running the blink removal function on the trace.

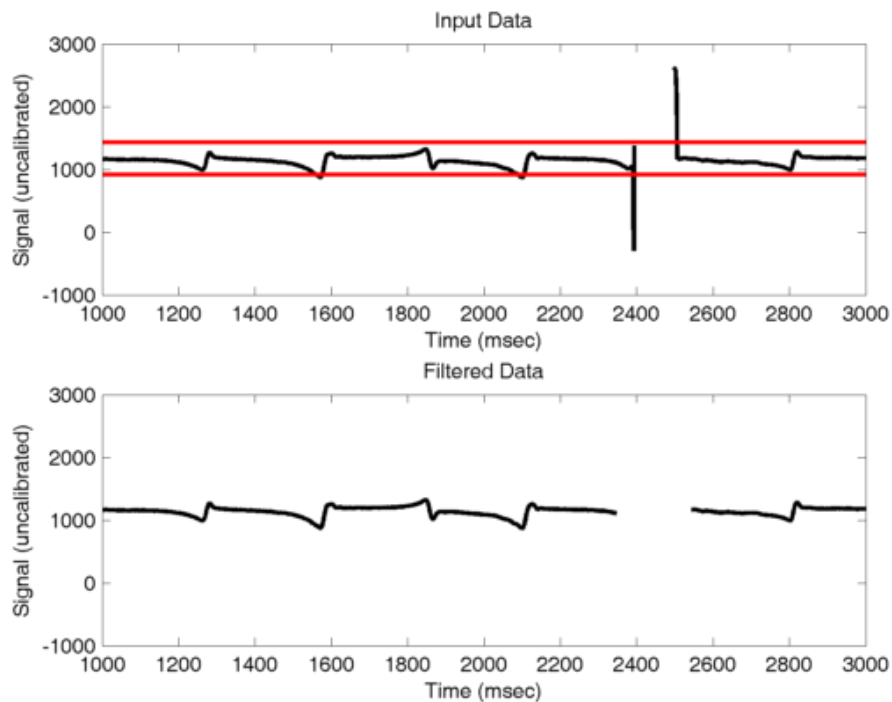


Figure 2.12: Example of a nystagmus waveform (subject DK) containing a blink. Note the spikes in the upper trace associated with dropped data at 2400-2500 ms. The lower trace shows the same data, with the blink removed. Red lines in the upper trace show the positional limits used to determine the start and end of a blink.

At this step another option is provided, depending on the type of system used to collect the data. Some eye tracker systems (such as electro-oculography and infrared limbal trackers) do not ‘drop’ data during a blink. Instead, the position channel simply spikes. To accommodate for this, the blink removal function can be set to throw away these large fluctuations. One potential problem with this could arise if there are *no* blinks in the entire recording. In this event, the standard deviation of the eye position signal will be relatively small, leading to non-blink data being considered a blink. In other words, if this additional blink removal feature is active, the data must contain at least one blink, or erroneous blink detection will result. For data collected with the EyeLink 1000 (all data presented in this thesis), the option was not

required, because the system always drops data when the eye is occluded by the lid during a blink.

2.2.2.6 Cycle detection

The waveform is next split into cycles, through the use of a method first described by Pasquariello et. al (2010), which in turn was based on a method by Juhola (1988). For each sample in the recording, the least squares regression slope of the preceding 100 ms of data is found. The result is a vector that oscillates at the same frequency as the nystagmus waveform. The values of this vector are converted to +1 or -1, depending on whether each value is positive or negative. The resulting binary vector gives an approximation of the cycle lengths. This vector is smoothed using a moving average filter with a 7.8 Hz cut-off frequency (thus preventing any slope reversals with duration < 130 ms). The resulting vector is repolarised to +1 or -1.

By searching between each sign change of the binary slope function, the local maxima and minima of the input signal (i.e. the position vector) are found. The difference between these can later be used to calculate waveform amplitude. Cycle boundaries are marked at the times of all the maxima in the waveform. Figure 2.13 shows diagrammatically the processes involved in cycle detection.

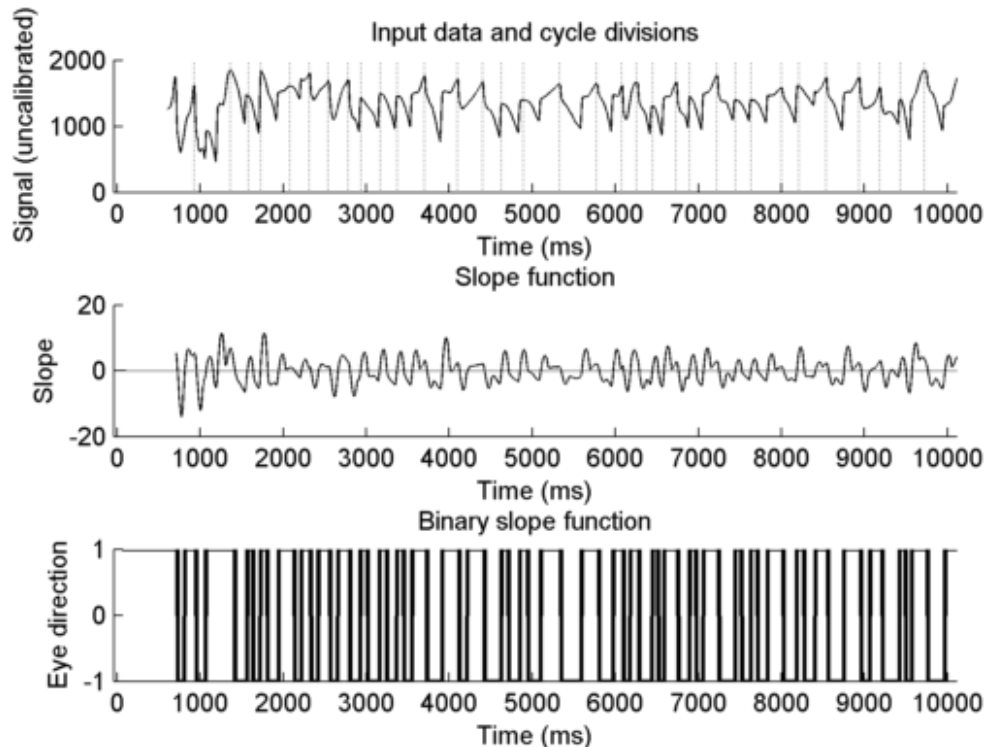


Figure 2.13: Schematic showing the stages of the cycle detection algorithm. Top: horizontal eye position trace (subject LC) with detected cycles marked. Middle: slope function, with zero crossing line shown. Bottom: binary slope function, filtered and repolarised.

Code to achieve this function is shown in Appendix I – *nystagmus_cycledetection_juhola.m*.

2.2.2.7 Saccade detection

In order to overcome the problems presented by the saccadic detection algorithms outlined in Section 2.1.5, an alternative algorithm was designed. This solution combines the principles of the two methods described in Section 2.1.5, first seeking velocity spikes in the EM trace (as in Pander et al. [2012]), and then proceeding to test them against an acceleration threshold (as in Behrens, Mackeben and Schröder-Preikschat [2010]). Unlike Behrens, Mackeben and Schröder-Preikschat's method, the saccade threshold is fixed, being calculated as a function of the standard deviation of the range of velocities present in the *entire* recording.

The exact protocol is outlined below. MATLAB code for the algorithm can be found in Appendix I – *oculomotorsuite_findsaccades_dunn.m*.

1. The mean and standard deviations of the velocity and acceleration vectors (for the entire recording session, and for each axis individually) are found.
2. *Saccadic velocity threshold* is set to the mean velocity plus one standard deviation¹⁷ (as determined in step 1).
3. Peaks and troughs in the velocity traces are found through the use of an open source function called 'peakdet' (Billauer 2012) – this function looks for changes in maxima and minima that exceed a given value, δ ¹⁸. For the purposes of this algorithm, δ was set to the standard deviation of all the velocities present in the recording, as determined in step 1. These peaks and troughs indicate the times of the peak velocities of candidate saccades.
4. Any candidate saccades with peak velocities below the *saccadic velocity threshold* are discarded. This serves as an artefact rejection mechanism. All other saccades are accepted as being genuine.

Having identified the time of each saccade's peak velocity, the start and end times of each saccade are determined as follows:

5. The acceleration transform is stepped through to find peaks and troughs using the *peakdet* function described in step 3. These acceleration spikes indicate the times of

¹⁷ As with the blink removal threshold, this value was chosen empirically since it provided reliable saccade detection in a range of EM traces. The value can optionally be adjusted by the user.

¹⁸ One approach to finding peaks and troughs in a signal is to differentiate it and identify the times at which this transformation equals zero. Whilst this approach works in theory, a noisy signal often produces zero crossings which do not truly represent the local maxima and minima. The *peakdet* function overcomes this problem by introducing the δ term.

- maximum acceleration and deceleration – for a typical biphasic saccade, the acceleration transform will display a shape similar to that in Figure 2.8.
6. Having found the acceleration spikes associated with the saccade, the position vector of the EM trace is stepped through to find the beginning and end of monotonicity. Starting from the time of the velocity spike, each sample of the position vector is compared to its neighbour to find the first and last times at which the eye is not moving in the same direction (i.e. a *strict* monotonic function is sought).
 7. The saccade bounds are determined by the most proximal samples (to the velocity spike) that satisfy both the acceleration criteria (the peak or trough detected in step 5) and lie outside of the monotonic position function (as found in step 6).

Figure 2.14 shows the cardinal features used by the saccadic detection algorithm in determining the start and end of a saccade.

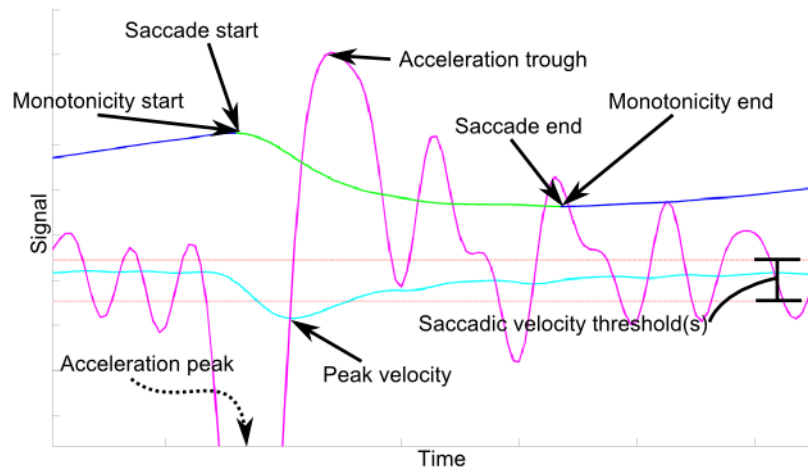


Figure 2.14: Schematic showing features used by the saccade detection algorithm. The **blue** line shows the position vector; the **green** region indicates a detected saccade. The **aqua** line shows the velocity transform (divided by 100 for visibility). The **fuchsia** line shows acceleration (divided by 1000). Since this shows a *leftward* saccade, velocity and acceleration ‘peaks’ are at the bottom of the plot, and troughs are found at the top. The acceleration peak for this saccade is beyond the edge of the plot area.

Figure 2.15 shows the same EM trace data as were shown in Figure 2.7, but with the new algorithm proposed above applied to detect saccades, rather than the *Behrens, Mackeben and Schröder-Preikschat* method.

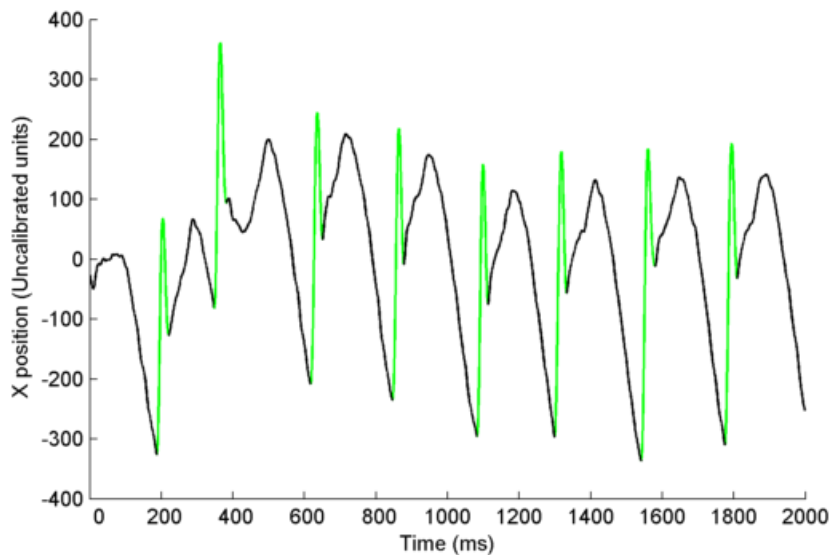


Figure 2.15: The same EM trace as shown in Figure 2.7, with saccades detected using the newly proposed algorithm. Detected saccades are shown in green.

2.2.2.8 Slow phase detection

Having detected saccades in the EM trace, slow phases are simply considered to be any times when a saccade is *not* occurring.

2.2.2.9 Foveation detection

In order to perform a calibration, an eye tracker requires position data relating to the subject's foveation location for each calibration point. For the purposes of calibration, it is not necessary to determine a foveation period in *every* cycle. Since there is the possibility that noise or unexpected EMs might exist in the data, the present algorithm is set to detect foveations in approximately 50% of nystagmus cycles. This ensures that only the *best* foveations are used for calibration, and reduces the chance of data from cycles containing contaminated data (such as non-nystagmus saccades) being used.

This method of foveation detection is directly opposed to conventional methods. Rather than the examiner specifying a specific *foveation velocity threshold*, the threshold is dynamically adjusted until it is able to find foveations in 50% of cycles. Calibration location is determined as the mean position of all foveation data found by this method. Note that this approach will naturally lead to the detection of very *brief* foveation periods. Since *foveation velocity threshold* is set as low as possible, detected 'foveations' will be very short. Whilst foveation quality has typically been measured by foveation *duration*, using the new method, an individual with high foveation 'quality' will be one who has a low *foveation velocity threshold*.

Once data are calibrated in this way, the software can be re-run using either the new method (which returns *foveation velocity threshold* as a result), or in the traditional way (by specifying a velocity threshold), which returns the *mean foveation duration* and *number of foveations detected*.

For calibration purposes, candidate foveations are identified in the following manner:

1. Having determined the slow phases of the waveform, any velocities in the dataset that are lower than one standard deviation below the mean velocity of these periods are marked as candidate foveations. These periods must exceed 7 ms. Adjacent candidates separated by no more than 35 ms are joined (whilst arbitrary, both of these temporal criteria have been used before [Dell’Osso and Jacobs 2002; Felius et al. 2011]).
2. Based on the cycle boundaries (detected previously), the number of cycles containing a candidate foveation are identified. Candidate foveations that straddle cycle boundaries are retained in their entirety but treated as if they were entirely contained within the first of the two cycles (see Figure 2.16).

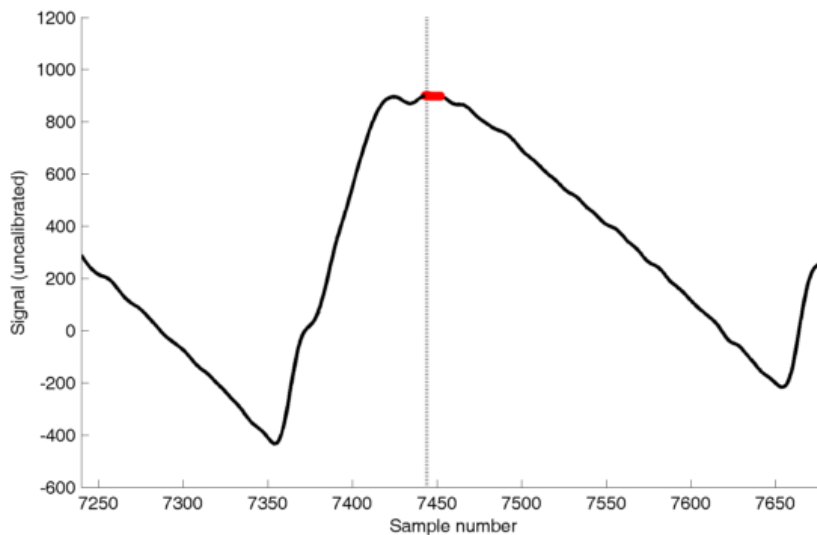


Figure 2.16: A candidate foveation (marked in red) is detected over the boundary between two cycles (dotted line). In this case, the foveation is considered a part of the first cycle, and is not counted as being a part of the second (data from subject GT₂).

3. If more than 50% of the cycles contain candidate foveations, the *foveation velocity threshold* is next reduced by 10%. This is repeated until less than 50% of the cycles have candidate foveations. At this point, *foveation velocity threshold* is increased again by 10%. Through this method, just over half of the cycles in the recording will have candidate foveations found. An example is shown in Figure 2.17.

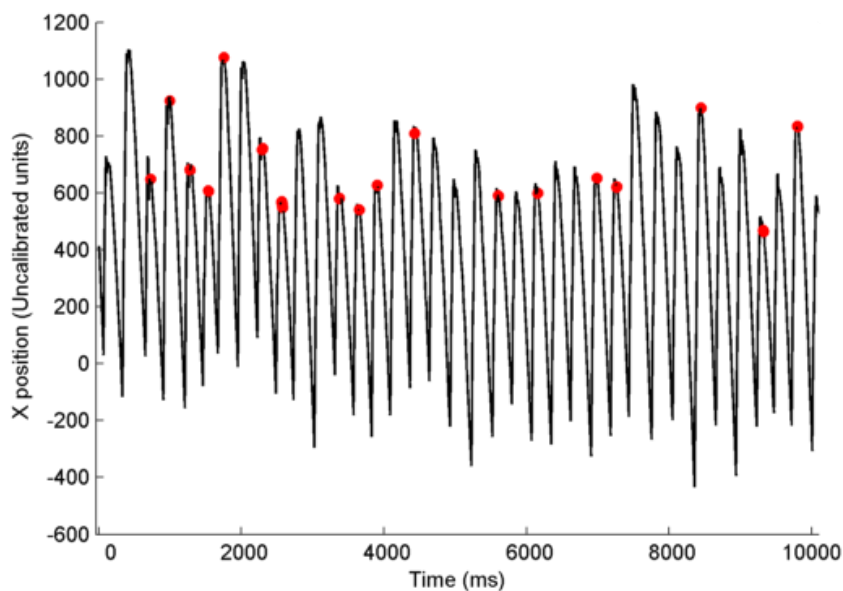


Figure 2.17: An example of automatically detected foveations in a nystagmus waveform (subject GT2, foveations set to be found in $\geq 50\%$ of cycles). Detected foveations are marked in red.

If more than one candidate is identified within any given cycle, the foveation with the lowest mean velocity is chosen. If the algorithm is unable to find a velocity threshold within 100 iterations, the program reports a failure (see Section 2.2.2.11). In the author's experience, this only happens if the '50%' threshold is changed to a very high value (such as 95%) or if there are lots of missing data in the recording.

2.2.2.10 Calibration

In order to have enough information to correctly scale an EM trace in two dimensions, it is necessary to calibrate to multiple known locations in space. Any number of locations can be used, depending on the level of accuracy required. For the results presented here, a five-point calibration was used, as represented in Figure 2.18. Each target comprised a simple black cross subtending $0.3 \times 0.3^\circ$ on a mid-grey background (see Figure 2.19). These targets were presented sequentially at -5° and $+5^\circ$ horizontally, and -3° and $+3^\circ$ vertically (relative to the centre of the screen). Each target was displayed for 10 seconds, and subjects were encouraged to maintain 'fixation' on the targets. Only the last nine seconds of each fixation point presentation were used for calibration, in order to give subjects ample time to take up fixation.

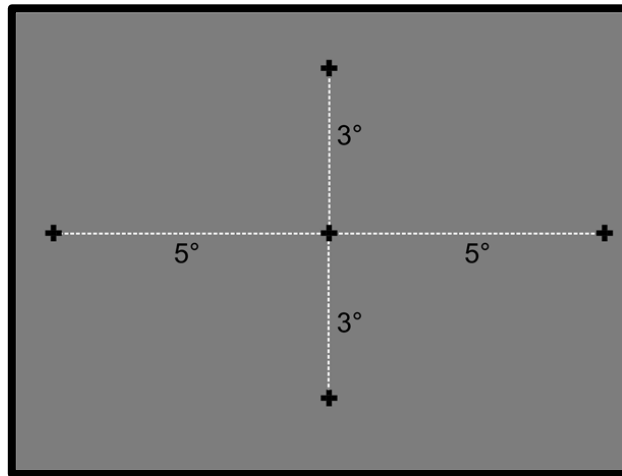


Figure 2.18: Schematic representation of the locations of on-screen calibration targets

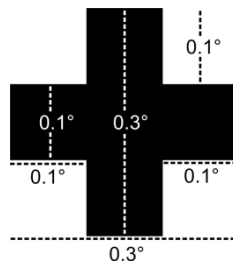


Figure 2.19: Fixation cross dimensions

Calibrating an eye tracker with one eye occluded reduces the chance of strabismus affecting the calibration. Calibration was therefore performed monocularly, using the subject's dominant eye where applicable (in the case of equidominance, the right eye was calibrated by default). Source code for the calibration display program can be found in Appendix I – *nystagmus_calibration_live_eyelink.m*.

Transformation matrices

From all of the 'foveation' data obtained for each calibration location, the median position co-ordinates during all foveation periods are calculated, resulting in a single co-ordinate pair for each calibration location. A two-dimensional polynomial regression is then calculated from these co-ordinate pairs and the known 'true' co-ordinates of the calibration targets (in degrees). This calculation includes a cross-talk term to account for rotation of the calibration field. The regression coefficients are then saved to a calibration file, which is made available for calibration of all subsequent recordings.

In order to calibrate incoming data from the eye tracker, a transformation matrix is applied to each of the horizontal and vertical axes separately, using the coefficients stored in the calibration file.

The author would like to make clear that code to calculate polynomial regression coefficients and the corresponding correction of incoming data through the use of transformation matrices (i.e. that described in the previous two paragraphs) was conceived and written by Chris Harris of the Centre for Robotics and Neural Systems, Plymouth University.

Note that since each calibration target location is analysed separately, changes in waveform intensity and type at different gaze angles are accounted for.

2.2.2.11 Visual confirmation and failsafes

The calibration program provides the option to visually inspect and confirm the detected foveation periods before accepting their median position as a calibration point. In case the foveation detector algorithm fails, or the user simply doesn't agree with the automatically-detected foveations, a few options are available:

1. The user may request a re-recording of the calibration point. This is automatically recommended by the software if there is very poor data capture (less than 1 s of recording).
2. For some pendular waveforms, it may be desirable to calibrate to one 'side' of the waveform oscillation (which side cannot be determined solely by analysing the EM trace; a visual inspection of the patient is required). The program can be forced to calibrate to the mean of either the peaks or troughs of the waveform, as found during cycle detection.
3. A manual override option is available, which allows the user to select a point in the waveform plot to use as the calibration point.
4. The user can choose to calibrate to the mean of the *entire* recording. This option is not generally recommended, but may be useful in some situations, such as ambiguous waveforms or for those with very little data capture.

2.2.3 Participants and procedures

Thanks to the many years of nystagmus research carried out at Cardiff University School of Optometry and Vision Sciences, a cohort of volunteers with nystagmus has been established who are willing to lend their time as participants in research studies. Subjects are typically recruited by advertisement through *Nystagmus Network*, a UK-based charity and the first nystagmus support group in the world (Sanders 2006). At the time of writing, the active list contains 74 subjects with early-onset nystagmus, 30 of whom have a confirmed diagnosis of IIN, five of whom have FMNS, 18 for whom diagnosis is unknown, and a further 21 who

have albinism, achromatopsia or congenital optic atrophy. Cohort members are recruited for research studies via email, telephone and mail.

Twenty-four individuals with early-onset nystagmus were recruited from the *Cardiff Research Unit* for Nystagmus cohort. Subjects were seated in a room lit at $\sim 1.78 \log \text{ cd/m}^2$, 2 m from a Sony GDM-F520 21" CRT monitor (see Section 2.2.4). The chin and head were supported by a rest. Subjects wore their habitual refractive correction (if any), and the non-dominant eye was patched. Calibration was performed in the manner described above. The first 1 s from each recording was removed from the analysis, to give subjects chance to take up fixation.

2.2.3.1 Inclusion / exclusion criteria

EM recordings were made to ensure that participants had IN (as opposed to any other oculomotor instability). Accelerating slow phases were an essential criterion for diagnosis. In addition, any subjects whose data quality was not sufficient for analysis (due to dropped samples) were excluded post-hoc.

2.2.4 Display equipment

Visual stimuli were presented on a Sony GDM-F520 21" CRT monitor (see Figure 2.20). This monitor has an optimum resolution of 1024×1024 pixels and a refresh rate of 85 Hz (National Information Display Laboratory 2001).



Figure 2.20: Sony GDM-F520 21" CRT monitor

2.2.5 Ethics

Ethical approval for this, and all subsequent studies, was granted by the Human Science Research Ethics Committee, School of Optometry and Vision Sciences, Cardiff University. Subjects gave informed consent to the studies according to the Declaration of Helsinki (World Medical Association 2008). The patient information leaflet and consent form can be found in Appendix III, and the ethical application and acceptance documents can be found in Appendix VI.

2.2.6 Validation

Testing the usefulness of any new algorithm requires a validation method. Note that the purpose of the newly-proposed foveation detection algorithm is to find optimum waveform locations for the calibration of an eye tracker. Whilst these locations ought to coincide with foveations, due to the nature of the algorithm (i.e. that it only chooses data in a fixed percentage of nystagmus cycles), the waveform loci chosen by the algorithm will not represent *every* ‘foveation’ period. Similarly, since the algorithm optimises the *foveation velocity threshold* to find the ‘tightest’ possible criteria, it is very unlikely that the ‘foveations’ detected by the new algorithm will last as long as those found by traditional methods. As a result, direct comparison with existing methods is difficult. However, most importantly, the new method ought to identify periods of the waveform that *overlap* (in time) with those found by the existing methods. An alternative approach is to test the results of the calibration algorithm against itself in a separate recording. Naturally, this involves some level of recursive logic. Validation of the new algorithm therefore involved a combination of self-validation and comparison with existing methods.

The foveation detection algorithm was evaluated by three methods:

1. Self-validation

Nine of the subjects underwent a ‘verification’ procedure immediately following calibration¹⁹, in which targets were presented at the same locations as the calibration points for ten seconds each. The same algorithm was applied to these validation recordings, in order to assess whether similar results were obtained in repeated recordings.

2. Comparison with existing methods

- a. Foveations detected by the new method were compared to those obtained by an established automated method (any periods in which velocity is below 4°/s for at least 7 ms; joining any foveations that are separated by a gap of 35 ms or less, with intra-foveation drift no greater than 1° [Dell’Osso and Jacobs 2002]). In order to understand the effect of the *foveation velocity threshold* on the data obtained, this method was repeated at both the 4°/s velocity threshold and the more liberal, occasionally used 10°/s threshold (Abadi and Worfolk 1989). Note that this comparison was only possible *after* calibration of the

¹⁹ Not all participants took part in this verification procedure, as it was added to the experimental protocol at a late stage.

data, since the ‘established’ method can only be used in the presence of calibrated data.

- b. Foveations detected by the new method were compared to manually marked periods by an expert in eye tracking methodology.

Method 1 assesses the repeatability of the algorithm. However, it is impossible to know whether any inaccuracies highlighted by this analysis relate to the algorithm itself or the subjects’ inability to repeatedly fixate accurately.

Validation method 2.a requires a pre-calibrated EM trace in order to determine the 4°/s threshold; hence it is itself influenced by the initial calibration performed. As discussed in Section 2.1.1, this is one of the major reasons that the new algorithm was developed.

For validation method 2.b, the outcome of the foveation detection algorithm was compared to manually marked foveation periods by an expert in eye-tracking methodology. To eliminate bias, the manual marking was performed not by the author, but by a colleague with no prior knowledge of how the algorithm worked. Since this is the only existing method that can be used in the absence of a pre-calibrated waveform, it arguably represents the best validation method for the new algorithm.

Statistical analysis was performed in the R Environment for Statistical Computing (R Core Team 2012).

2.3 Results

2.3.1 Participants and exclusions

Recordings were attempted in 24 subjects with early-onset nystagmus. Eighteen of these were successfully calibrated (the remainder could not be tracked by the EyeLink 1000, due to either iris transillumination or hardware malfunction). Subjects who took part also contributed to other studies during the same day. General information and biometrics for each subject can be found in Appendix II. The subjects who took part in this study were:

- DB, DK, DP, DT, GT, GT2, IG, JC, JS, JT, JX, KF, KL, LC, LL, MT, NB and SW

Of these subjects, five were excluded:

- One (IG) was excluded due to being unable to see the fixation cross clearly. The total cross size was increased to 1.5° (a five-fold increase), but the subject still reported that he was unable to clearly see the target.

- One (JC) was excluded due to having nystagmus that was only present in right-gaze (there was no nystagmus to analyse in other positions of gaze).
- Three (KF, KL and LL) were excluded due to having FMNS. Foveations are a hallmark feature of IN only, so calibration by foveation detection would not be possible in FMNS.

2.3.2 Software output

Figure 2.21 shows an example of output from the calibration procedure using the software. Note that ‘candidate calibration points’ identified by this procedure indicate the waveform locations *most likely* to represent the visual axis, but don’t necessarily represent *every* foveation period (since only the ‘best’ 50% of foveations were used).

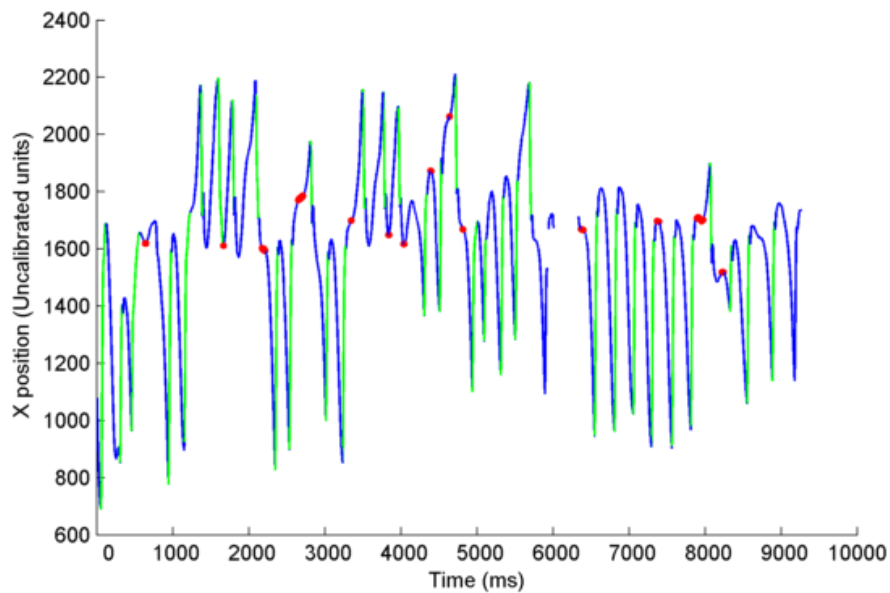


Figure 2.21: Example output from the calibration procedure (subject JT). Slow phases are shown in **blue**; saccades are shown in **green**. A blink has been detected and removed at sample #6000. Candidate points to be used for calibration are shown in **red**.

Once a calibration file has been generated, the software can be run again with a predefined (fixed) *foveation velocity threshold*, as is traditionally used in IN research. Figure 2.22 shows the same data as Figure 2.21, but these are now calibrated (note the ordinate). For Figure 2.22, the foveation velocity threshold was set to $4^\circ/\text{s}$.

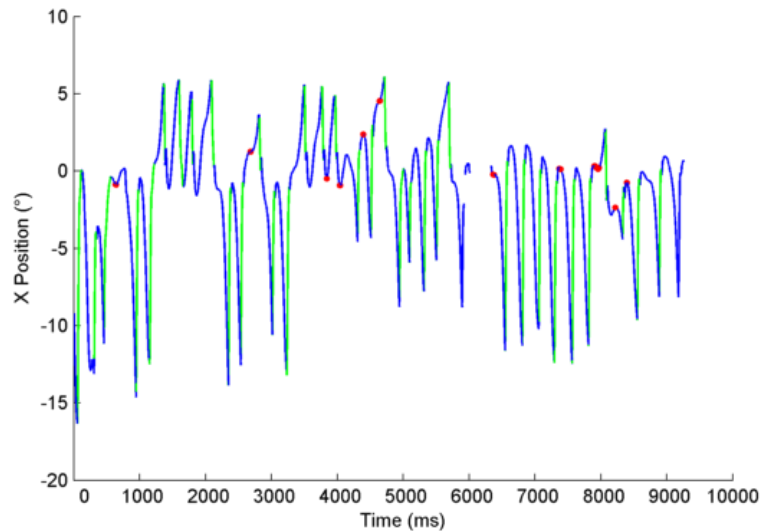


Figure 2.22: Example output from the analysis procedure (same data as Figure 2.21). Unlike the previous figure, red regions now indicate foveations (defined using a velocity threshold of $4^{\circ}/s$), and the position trace is now calibrated.

The analysis output for the data shown in Figure 2.22 are shown below.

Subject has horizontal nystagmus
6 blinks were detected and removed...
3.76% of the data were dropped

*** WAVEFORM ANALYSIS ***

29 cycles were detected (28 of these were free from blinks)
Frequency = 3.9Hz (SD = 1.2Hz)
Amplitude = 9.9° (SD = 4.1°)
Intensity = $35.2^{\circ}/s$ (SD = $13.7^{\circ}/s$)

*** FOVEATION ANALYSIS ***

11 foveations were detected
Foveation duration = 19.4ms (SD = 20.2ms)
Foveation velocity threshold (fixed) is $4.0^{\circ}/s$
Foveation position = $(0.3^{\circ}, 3.1^{\circ}) \pm (3.5^{\circ}, 0.7^{\circ})$ (SD = $[1.9^{\circ}, 0.4^{\circ}]$)
Foveation velocity = $2.2^{\circ}/s$ (SD = $1.0^{\circ}/s$)
NAFX = 0.12 , using a velocity limit of $4.0^{\circ}/s$, position limit of 3.5° and tau value of 33.00ms
NOFF = -2.78 , using a velocity limit of $6.0^{\circ}/s$ and position limit of 1.0°

*** SACCADIC ANALYSIS ***

35 saccades were detected
Saccade duration = 35.9ms (SD = 18.4ms)
0 saccades had no intersaccadic interval
Saccade velocity threshold is $211.38^{\circ}/s$
Dominant saccade direction is right: 24 right saccades and 11 left saccades were detected
Saccade peak velocity = $538.5^{\circ}/s$ (SD = 164.0°)
Saccade mean velocity = $243.3^{\circ}/s$ (SD = 75.9°)
Saccade amplitude = 8.5° (SD = 3.5°)

*** SLOW PHASE ANALYSIS ***

Slow phases appear to be accelerating
Slow phase peak velocity = $146.7^{\circ}/s$ (SD = 74.4°)
Slow phase mean velocity = $51.7^{\circ}/s$ (SD = 18.6°)

2.3.3 Verification

2.3.3.1 Self-validation

As described in Section 2.2.6, following the calibration procedure, nine participants had a ‘verification’ recording made. This involved looking in the same locations as those that were used for calibration, for 10 seconds at each location. Using the calibration files generated by the *initial* calibration procedure, the mean foveation position for each of these target locations in the *new* recording were calculated. Figure 2.23 shows the calculated gaze angles for each of the target positions in the verification recording. This illustrates the test-retest repeatability of the calibration procedure.

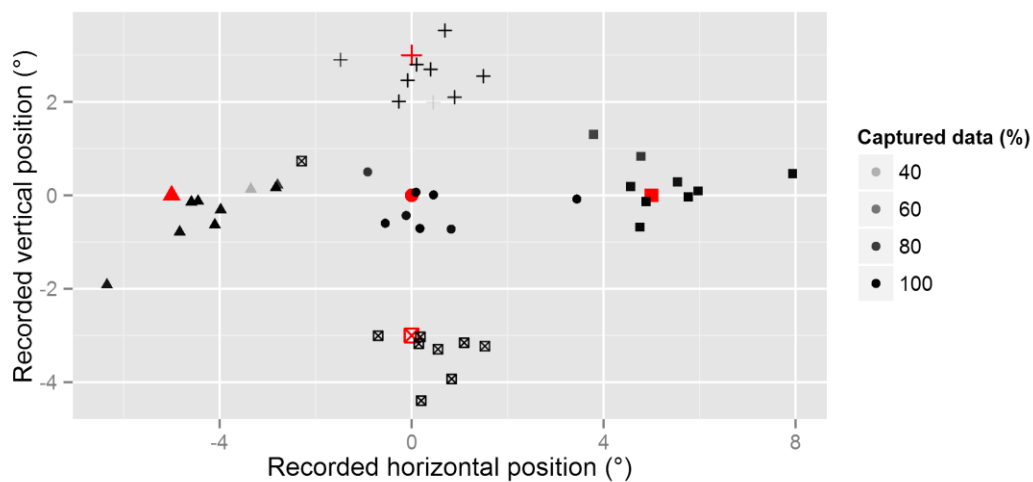


Figure 2.23: Plot showing calculated foveation positions for nine participants, derived from calibrations made using separate recordings. Actual target positions are shown in red. This demonstrates the test-retest repeatability in different angles of gaze. The effect of data capture percentage on the result is also shown (marker opacity).

For each datum in Figure 2.23, the offset from the true target position was calculated. The mean and standard deviation of the offset values for all participants are summarised in Table 2.2. Note that this shows the offset from each expected target position, rather than the variability of foveations detected *within* each recording.

Table 2.2: Offset from expected position (°) for all subjects at all tested locations

	Mean	Standard deviation
Horizontal axis	±0.86	±0.79
Vertical axis	±0.53	±0.65

2.3.3.2 Comparison with existing methods

Comparison with an automated method

EM recordings from 13 individuals with IN were analysed using both the foveation detection algorithm described in the present chapter (referred to here as the *dynamic threshold method*), and the automated method described in Section 2.2.6 (point 2.a), hereafter referred to as the *fixed threshold method*. Figure 2.24 gives a cursory glance at the comparisons being made; each of the plots in this figure represent the foveations as detected by a different method.

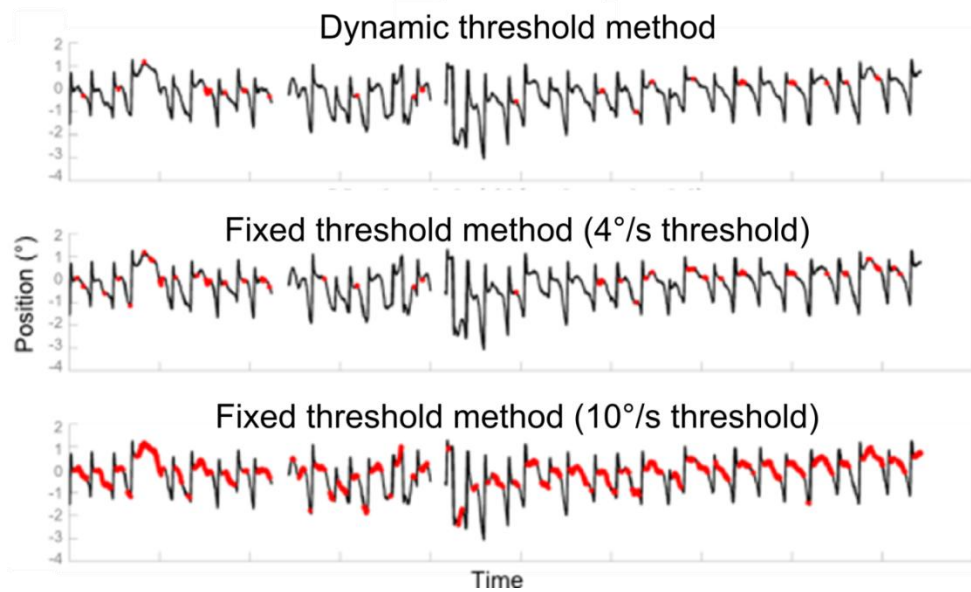


Figure 2.24: Example (subject DB) of foveations detected (shown in red) using the new algorithm set to detect foveations in 50% of cycles (top); using a fixed foveation velocity threshold of $4^{\circ}/s$ (middle); and using a fixed foveation velocity threshold of $10^{\circ}/s$ (bottom)

Since the *dynamic threshold method* explicitly searches for a foveation velocity threshold that will satisfy foveations in just over 50% of nystagmus cycles, comparisons made here are between those nystagmus cycles in which foveations were detected using *both* methods.

Number of foveations detected

Sixty-five recordings were analysed (five for each participant). The average percentage of cycles in which foveations were detected for each method are shown in Table 2.3.

Table 2.3: Percentage of cycles in a nystagmus recording in which foveations are found with each foveation detection algorithm

	Mean	Standard deviation
Dynamic threshold method	52.3%	4.0%
Fixed threshold method ($4^{\circ}/s$ threshold)	61.6%	35.4%
Fixed threshold method ($10^{\circ}/s$ threshold)	87.9%	26.1%

The mean value for the *dynamic threshold method* is easily explained, since the algorithm by *definition* is constrained to find foveations in just over 50% of cycles.

Of the 65 recordings analysed, seven recordings did not contain any cycles at all with detected foveations with the *fixed threshold method* using the 4°/s velocity threshold, whereas, at 10°/s, foveations were found in every recording.

Precision

Since eye position changes throughout the nystagmus waveform, the *duration* of detected foveations indicates the precision that can be obtained when using them as a calibration reference point. Put another way, if a ‘foveation’ lasts for the majority of the waveform, then it cannot be used as a precise indicator of the subject’s intended fixation point for calibration purposes. The duration of foveations detected by each method (expressed as a percentage of the entire waveform) are shown in Table 2.4.

Table 2.4: Percentage of nystagmus waveform identified as foveations by each method

	Mean	Standard deviation
Dynamic threshold method	3.9%	2.2%
Fixed threshold method (4°/s threshold)	15.3%	18.2%
Fixed threshold method (10°/s threshold)	33.0%	24.4%

The results in Table 2.4 indicate that the *dynamic threshold method* detected far shorter durations of nystagmus waveforms as foveations than the *fixed threshold method* did at either of the thresholds tested here. As explained above, this suggests that the *dynamic threshold method* is a more precise indicator of intended gaze angle.

Agreement of methods

The agreement between the two methods was calculated by finding the percentage of samples that were found by the *dynamic threshold method* that were also found by the *fixed threshold method* at two fixed threshold levels. The results are shown in Table 2.5.

Table 2.5: Percentage of samples detected by the *dynamic threshold method* that were also detected by the *fixed threshold method* at two fixed foveation velocity thresholds

	Mean	Standard deviation
4°/s threshold	89.5%	20.4%
10°/s threshold	94.4%	13.8%

The results in Table 2.5 show that the *dynamic threshold method* detected similar regions of nystagmus waveforms to the *fixed threshold method*, even at the 4°/s threshold. Since the 4°/s threshold method found foveations in approximately 15.3% of the data (see Table 2.4), this indicates that 89.5% of the foveation data found by the *dynamic threshold method* lay within the same 15.3% of the data identified by the 4° *fixed threshold method*.

Comparison with a manual method

In order to test the agreement of the new method with manual determination of foveation periods, one recording from each participant was manually marked by an individual who was experienced in EM analysis, but who had no prior knowledge of how the new algorithm worked. For each participant, one uncalibrated EM recording of the subject viewing in the primary position for 9 s was analysed by the experienced observer using custom-made software in the MATLAB environment (see Figure 2.25; code available in Appendix I – *handmarkfoveationperiods.m*). The software provided a view of both the position and velocity traces, which could be rotated and viewed in three dimensions. This meant that the user had exactly the same information available to them as the automated method. The user was instructed to use the position and velocity traces to identify foveation periods. The software was briefly demonstrated to the user with a separate EM trace, after which the author did not interact with the user until manual marking was complete.

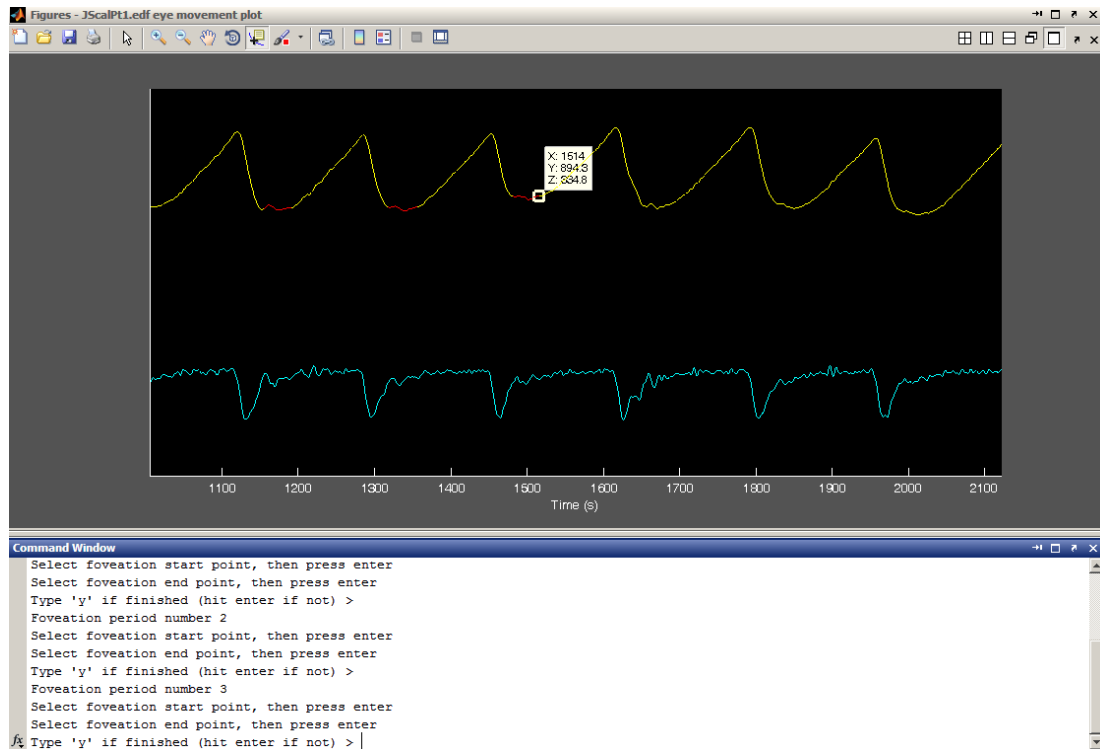


Figure 2.25: Custom-made MATLAB software for manual marking of foveation periods. The upper trace is the position trace; the lower trace shows the velocity transform.

As before, since the *dynamic threshold method* explicitly searches for a foveation velocity threshold that will satisfy foveations in just over 50% of nystagmus cycles, comparisons made here are between those cycles for which a foveation was found using both the manual marking method *and* the *dynamic threshold method*.

Precision

The foveation periods that were manually marked occupied an average of 31.4% of the waveform (standard deviation = 15.3%). This is contrasted with the automated method, which, by design, identified foveations of as brief duration as possible. For the same data, the automated method found foveations occupying 4.1% (standard deviation = 1.8%).

Agreement of methods

Eighty per cent of the samples detected by the automated method were also detected by manual marking (standard deviation = 18%).

2.4 Discussion

The following section discusses the accuracy of the new foveation and saccade detection algorithms as well as the waveform analysis software as a whole, and outlines some of the limitations and possible avenues for future improvements to the package.

2.4.1 Verification

2.4.1.1 Self-validation

Self-validation of the foveation detection algorithm allows us to check the repeatability of the algorithm on separate recordings. The results in Section 2.3.3.1 indicate that, on repeated testing (of different recordings from the same subject), similar foveation positions are obtained, to within one visual degree. Since foveations have (historically) been defined with a positional error window of 1° (Dell’Osso and Jacobs 2002), this seems a reasonable result. In addition, the low frequency baseline oscillation known to exist in nystagmus waveforms (see Section 1.3.2) has an average amplitude of 1.31°; fixation accuracy cannot therefore be expected to be much better than this (Bifulco et al. 2003). Of course, regarding the error that *has* been found, as with any calibration method, there is no way of knowing how much is due to poor algorithm design or to real ‘fixation’ inaccuracies of the participants.

2.4.1.2 Comparison with existing methods

Before embarking on a direct comparison between the novel and existing methods of foveation detection, it is worth remembering that their aims are different: the new (*dynamic threshold*) method seeks to identify the *very best* portions of the nystagmus waveform to use for calibration, whereas the *fixed threshold method* applies a fixed velocity threshold to test *how much* of the waveform satisfies the criterion.

Comparison with an automated method

The algorithm proposed in this chapter is the first and only automated method of foveation detection that does not rely on a pre-calibrated EM trace. It is important to note that the analysis of the data using the *fixed threshold method* was predicated on a calibration using the *dynamic threshold method*, so there is some recursive logic involved in the interpretation of these data.

Section 2.3.3.2 indicates that the *dynamic threshold method* (i.e. the newly proposed method) provides a much more precise estimation of foveation position than the *fixed threshold method*. A more tightly defined foveation naturally lends itself to a more precise calibration. This confirms that the new method achieves its aim: it is highly selective and identifies a very precise portion of the nystagmus waveform to use for calibration.

The *fixed threshold method*, regardless of whether the foveation velocity threshold is set to 4 or 10°/s, identifies a very variable number of cycles as containing foveations. This is to be expected, since nystagmus waveforms are by their nature variable. The fact that the *dynamic threshold method* finds foveations in just over 50% of cycles is unsurprising since that is what it is programmed to achieve. An alternative approach that might find foveations in *every* cycle is suggested in Section 2.4.4.3. Of course, one could simply increase the program's threshold from 50% all the way up to 100%, but this increases the chances of the velocity threshold being affected by contaminated data, such as blinks or voluntary (non-nystagmus) EMs. Again, the solution offered in Section 2.4.4.3 might overcome this problem.

Finally, notwithstanding the above consideration, the agreement between methods is very strong. Whilst the *fixed threshold method* consistently finds foveation periods that last much longer than the *dynamic threshold method*, at both the 4 and 10°/s velocity thresholds, the *fixed threshold method* agrees with over 85% of the candidate foveation samples chosen by the *dynamic threshold method*.

The results in Table 2.5 show that the *dynamic threshold method* detected similar regions of nystagmus waveforms to the *fixed threshold method*, even at the 4°/s threshold. Since the 4°/s threshold method found foveations in approximately 15.3% of the data (see Table 2.4), this indicates that 89.5% of the foveation data found by the *dynamic threshold method* lay within the same 15.3% of the data identified by the 4° *fixed threshold method*.

Comparison with a manual method

Whether or not manual foveation detection can be considered the ‘gold standard’ is debatable, since it relies on the skill and pattern recognition ability of the observer. Nonetheless, this is the method that has been traditionally used to *calibrate* a nystagmus EM trace. A large proportion (80%) of the samples detected by the new automated method were also detected manually, indicating a good level of agreement with the new method.

2.4.2 Redefinition of ‘foveation’

Foveations have typically been defined as the times in a nystagmus waveform at which the fovea is near the point of regard, which also happen to be the times at which eye velocity is lowest. The new method, which is used for calibration, does not require pre-calibrated data to find the foveations in the waveform. In other words, the algorithm does not impose any constraints on position, and is only concerned with *relative* velocity. Therefore, it is suitable for use in *any* subject with a waveform containing foveation periods. The *fixed threshold method* requires prior agreement on a fixed *foveation velocity threshold* which may not be suitable for all subjects. Compare Figures 2.1 and 2.2 with Figures 2.26 and 2.27 below, which show the same data analysed using the *dynamic threshold method*, set to detect foveations in 50% of the nystagmus cycles.

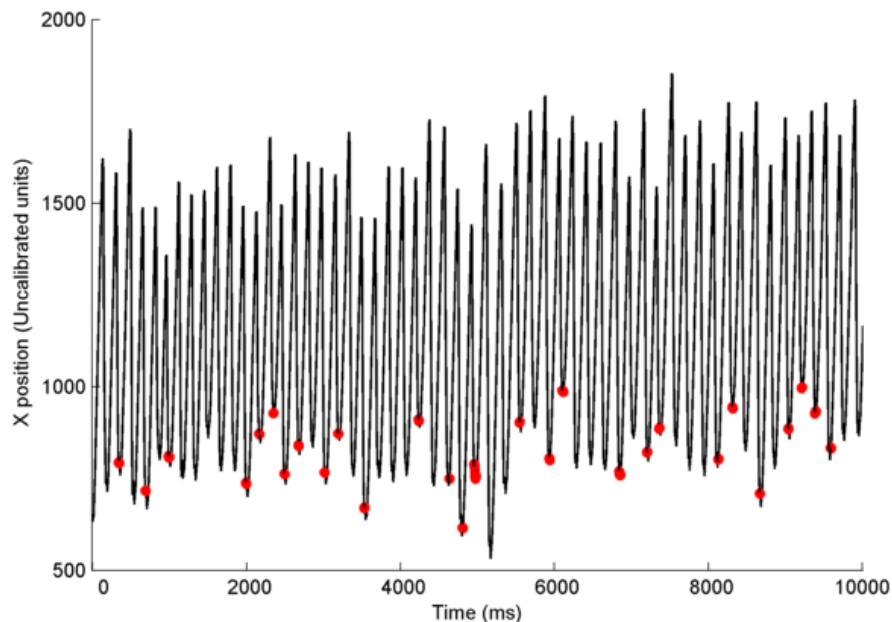


Figure 2.26: Example of foveations detected (red) using the new method of foveation detection, set to detect a foveation in 50% of nystagmus cycles (subject JS). Compare with Figure 2.1.

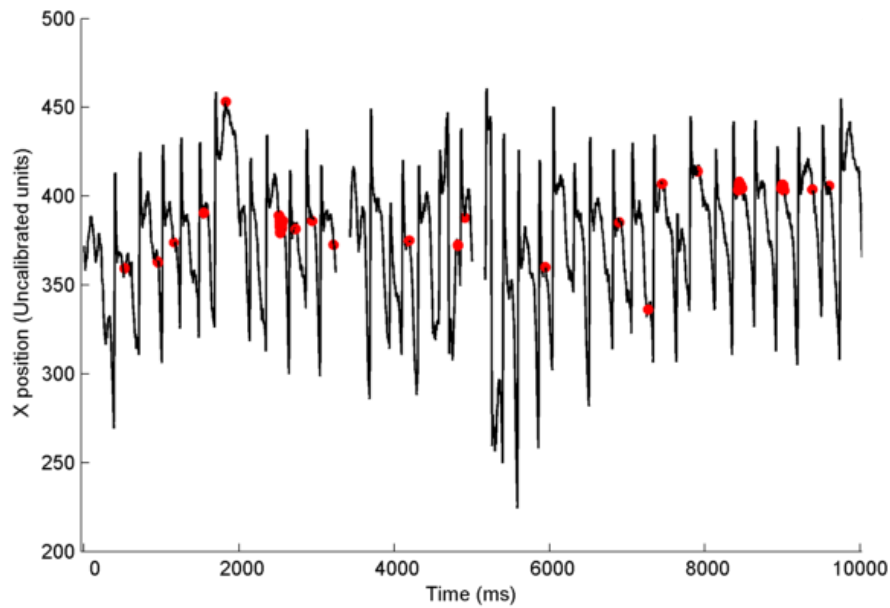


Figure 2.27: Example of foveations detected (red) using the new method of foveation detection, set to detect a foveation in 50% of nystagmus cycles (subject DB). Compare with Figure 2.2.

Notice that for each figure above, without specifying any absolute thresholds, a similar proportion of foveation data are detected for each subject using a single automated method. For subject JS above, *foveation velocity threshold* (as determined by the software following calibration) is $15^{\circ}/s$. For subject DB, this threshold is $3.1^{\circ}/s$. These figures provide a new way to define the best foveation parameters for each individual, and may provide a useful way of representing nystagmus severity in future studies. Nevertheless, the author recognises the potential usefulness of comparing foveation *duration* (for example, for intra-subject comparisons of foveation quality pre- and post-surgery), which require the use of the traditional *fixed threshold method*. For this reason, ‘traditional’ foveation detection is an optional feature, also included in the nystagmus analysis software described in this chapter. If using this feature, the user is prompted to specify velocity and position thresholds for foveation detection.

2.4.3 Saccade detection algorithm

The new saccade detection algorithm uses thresholds derived from the mean and standard deviation of the data in the EM trace. Using a relative threshold such as this (as opposed to pre-determined absolute thresholds) has the advantage of not requiring the input data to be calibrated. The improved performance of this algorithm (which uses information from the velocity channel) over that of Behrens, Mackeben and Schröder-Preikschat (which does not) is evident from comparison of Figures 2.8 and 2.15.

Nonetheless, the new method does have its limitations. Since it derives *saccadic velocity threshold* from a function of the *entire* EM trace, this method is best suited to EM traces in which jerk nystagmus is manifest for the majority of the recording, and is only useful in recordings of attempted ‘fixation’. Any voluntary saccades made during the recording would affect the standard deviation of velocity for the entire recording, thus changing the saccadic velocity threshold. Similarly, if nystagmus is pendular, the absence of any saccades in the EM trace could lead to an erroneous *saccadic velocity threshold*. However, all the subjects used in the studies throughout this thesis had jerk or jerk subtype waveforms.

2.4.4 Future work

2.4.4.1 Limitations in contaminated data

The main limitation of the proposed analysis algorithm is that it can only work in the presence of ‘clean’ EM data. Although it effectively filters out blinks/missing data and low-pass filters the data to remove some noise, it assumes the subject is attempting to fixate a target for the entirety of a recording. This is suitable for most adults, but in children and adults with a short attention span, non-nystagmoid EMs contaminating the data may hinder data analysis. One possible way to deal with contaminated data is to use a similar approach to that of Felius et. al (2011) in the calculation of NOFF (see Section 1.3.8.5), which uses a moving window to automatically detect the ‘cleanest’ segment of data, based on the velocity and positional variability of the data in the segment.

2.4.4.2 Time series analysis / template matching

Since the nystagmus waveform is split into cycles, it would be possible to perform a time series analysis to extract the average waveform shape from an EM trace. Using such a template matching technique, it might be possible to automatically diagnose the nystagmus waveform *type* (see Section 1.3.1). In addition, time series analysis could allow for the subtraction of the nystagmus oscillation from the EM trace, allowing for an in-depth assessment of fixation accuracy and identification of voluntary saccades.

2.4.4.3 Finding foveations in every cycle

An alternative method for foveation detection could be to determine a new foveation velocity threshold for *each* cycle. This would be done in a similar way to the protocol set out above, except that, after the waveform is split into cycles, foveations would be determined based on contiguous samples that have velocities below a threshold set by that cycle’s mean and standard deviation velocity. This would ensure that *every* cycle has a foveation detected, and also would not rely on sampling the *entire* recording to detect foveations, allowing waveforms

that change significantly over time (e.g. PAN). Of course, this method would rely heavily on accurate cycle detection.

2.4.4.4 Foveation weighting

Although the current foveation detection method adjusts iteratively to find the optimum foveation velocity threshold, when calculating the mean foveation position, equal weighting is given to all foveations regardless of their quality. A future development of the foveation detection algorithm could provide greater weighting to those foveations that are slower and/or longer. Furthermore, *within* a foveation, calibration could be weighted towards the slowest parts of the foveation. This recursive optimisation would inevitably lead to increased calibration accuracy.

2.4.4.5 Improved cycle detection

Notice that the waveform shown in Figure 2.13 contains some cycles that beat in different directions. At present, the cycle detection algorithm confuses the two cycles at the time of a direction change as a single cycle. Ultimately, it would be desirable to devise a solution that is able to overcome this problem when it arises.

2.4.4.6 Calibration of subjects with FMNS

FMNS waveforms do not exhibit foveation periods. Due to the presence of decelerating slow phases, calibration by the method described here would be likely to produce a constant error equal to the nystagmus amplitude (since ‘foveations’ would be detected just before the reorienting quick phases). This could be overcome by incorporating a software mode specifically for FMNS, which could use eye position *immediately following the quick phases* for calibration. As described earlier, there are some IN waveforms for which this approach would not work, but it should be well suited for subjects with FMNS.

2.4.4.7 Tests of fixation accuracy in IN

The software developed in this chapter produces large quantities of data without the need to manually mark foveations in EM traces. As such, it may prove useful as a tool to assess the accuracy of individual patients’ fixation. An example of the type of analysis possible is shown in Figure 2.28. Each colour on the plot represents a different participant – every foveation recorded over a 10 s period is plotted relative to the mean position of all foveations recorded in that period. This effectively demonstrates the variability in foveation position for each participant. Clearly, some individuals are more variable than others, and this will invariably have an impact on visual performance. As a research topic, foveation position variability has been investigated before (Bedell, White and Abplanalp 1989). However, in the

aforementioned study, all EM analysis had to be performed by hand. The new software performs this in just a few seconds, potentially making this accessible as a clinical tool.

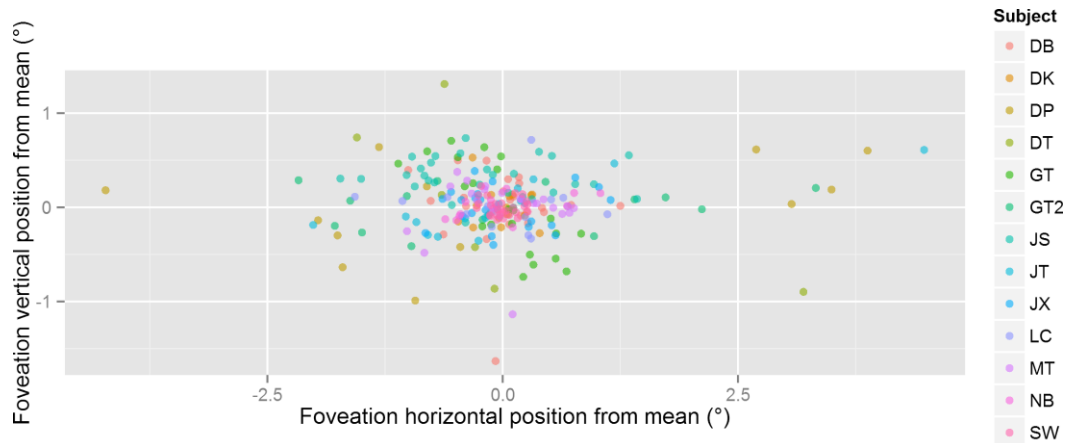


Figure 2.28: For subjects with IN, each foveation detected over a 10 s period, plotted relative to the mean position of all foveations during this period. This type of analysis may provide a useful method for assessing foveation accuracy of individuals with IN.

2.5 Summary

The software developed in this chapter provides a rapid method of calibrating and analysing nystagmus EM traces, as well as detecting saccades and parsing waveforms into their component parts. Not having to rely on laborious manual marking to analyse data makes large scale data analysis feasible, increasing statistical power. This software was originally developed to aid the experiment set out in the following chapter; however, due to a change in protocol (see Section 3.2.4.3), eye tracking was not used for the study. Chapters 4 and 5 make use of the saccade detection algorithm, and Chapter 6 includes a pilot study which sees the software used to its full potential.

Chapter 3 Visual acuity in the absence of image motion

The following chapter details a psychophysical study aiming to understand the limits of spatial vision in IN in the absence of image motion. The results have recently been published in *Investigative Ophthalmology and Visual Science* (Dunn et al. 2014) and can be found in Appendix VII.

3.1 Introduction

In optometric primary care, VA is estimated using optotypes on a static chart. Patients are encouraged to take as much time as they need to read the smallest optotypes possible, and quantification of central visual function is often based solely on this measurement.

VA is typically used as an outcome measure in the clinical vision sciences as it represents the finest level of detail that the visual system is able to resolve – a basic prerequisite for higher visual processing and function.

In normally sighted individuals, an increase in image velocity (above $2.5^\circ/\text{s}$) results in a concordant reduction in VA and perceived contrast intensity, regardless of the direction of movement (Ludvigh and Miller 1958; Miller 1958; Westheimer and McKee 1975). Figure 3.1 shows the relationship between VA and the velocity of an optotype moving vertically in a sinusoidal path in normally-sighted subjects. Note that up to $2^\circ/\text{s}$, VA is independent of retinal slip velocity (Demer and Amjadi 1993). Obviously, the average eye velocity in the presence of nystagmus exceeds this (see Section 1.3.1), so it has been assumed until now that motion blur is deleterious to vision in individuals with IN.

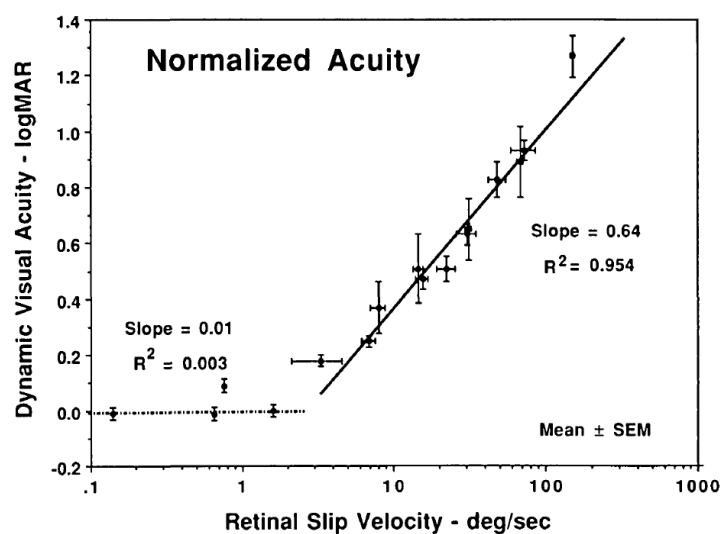


Figure 3.1: The relationship between retinal image velocity and VA with optotypes (Demer and Amjadi 1993)

Weiss, Kelly and Phillips (2011) used the above data to surmise that image degradation by retinal slip is not the limiting factor of VA in albinism-related IN. Instead, they concluded that in these patients, macular hypoplasia is the major limiting factor.

Between subjects, VA correlates with characteristics of the nystagmus waveform, such as foveation duration and accuracy (Sheth et al. 1995; Dell'Osso and Jacobs 2002; Abadi and Pascal 1991; Abadi and Worfolk 1989). In addition, experiments presenting normally-sighted subjects with image motion similar to that produced by nystagmus waveforms causes a worsening of VA as simulated foveation duration decreases (Chung and Bedell 1997; Currie, Bedell and Song 1993; Chung and Bedell 1995; Chung and Bedell 1996). This wealth of evidence has led to the assumption that modifying the nystagmus waveform through therapeutic intervention might lead to an improvement in VA.

In nystagmus with sufficient amplitude, at some point in each cycle of the waveform, the fovea will not be directed towards the object of regard. Therefore, as with all patients, giving nystagmats as long as they need to read a letter chart in practice is wise when trying to determine best possible VA. However, using charts in this way fails to address the underlying issue that when nystagmats view a chart, *the eyes are still moving*. In other words, an equivalent measure between nystagmats and controls cannot be made with a standard chart. VA is usually reduced in individuals with IN, even in the absence of comorbid ocular pathology (Abadi and Bjerre 2002). However, whether these individuals (idiopaths) would be capable of 'normal' VA if the eyes weren't moving is not known.

One way to 'level the playing field' might be to measure the contrast sensitivity function of normally-sighted individuals in response to visual targets that oscillate with similar characteristics to nystagmus waveforms. Whilst this has been done before (Chung, LaFrance and Bedell 2011; Dickinson and Abadi 1985), comparing the results of these studies (which find similar CSFs to subjects with IIN) to data from nystagmats fails to address the fact that people with IN *don't perceive an oscillating retinal image*. The solution to this problem might be to take the opposite approach: present a stable image to the nystagmat. This could be achieved by stabilising the image on the retina, through computerised gaze-contingent presentation. However, this presents yet another problem: a stabilised image in IN often causes perception of oscillopsia (Dell'Osso 2011). Perhaps a more appropriate solution is to measure VA using presentations sufficiently brief so as to minimise image motion.

Remarkably, the true impact of image motion on VA in IN has never been tested. Abadi and King-Smith (1979) measured the luminance required in order to detect the presence of a

horizontal or vertical line under continuous or tachistoscopic²⁰ (0.2 ms) presentation in four individuals with IN (diagnosis not specified) and three control subjects. By presenting visual stimuli to both groups with a brief flash of light, it was surmised that image motion would be eliminated, so that the impact of image motion on visual sensitivity could be estimated. They found that sensitivity to a line in the same axis as the nystagmus is higher than that in the orthogonal axis (this is attributed to meridional amblyopia), but the differences between the thresholds obtained by tachistoscopic and continuous presentation were not discussed, and quantifiable VAs were not reported. In the *presence* of retinal image motion (i.e. when measured under constant light), individuals with horizontal IN (both IIN and IN associated with albinism) have been shown to have significantly better VA for horizontally oriented gratings (Meiusi, Lavoie and Summers 1993; Abadi and Sandikcioglu 1975; Bedell and Loshin 1991; Loshin and Browning 1983; Jones 2011).

From its widespread use in photography, it is well known that flashes of light can be used to reduce motion blur in an imaging system. An experiment was devised in which VA could be measured under tachistoscopic and continuous illumination conditions, to determine the effect of retinal image motion on VA in IN. Any difference in VA obtained from subjects with IN as compared to controls under tachistoscopic and constant illumination conditions will inform the extent to which motion blur is detrimental to visual function in IN.

A thorough literature search was conducted to investigate whether any previous study has determined if there is an underlying VA deficit in IN in the absence of comorbid ocular pathology (i.e. in IIN). No experimental paradigm has thus far managed to determine VA in IN independent from the EMs.

3.1.1 Aims

In the present study, tachistoscopic presentations of visual stimuli were employed to ascertain the impact of image motion on VA in IN. By comparing VA under continuous presentation to a brief flash of light in both nystagmats and controls, it was possible to estimate the effect that image motion has on VA in IN. In addition, VA was measured for both horizontally and vertically oriented grating stimuli, in order to quantify meridional amblyopia and confirm (in a larger sample size) the results of a previous study (Abadi and King-Smith 1979).

²⁰ The word *tachistoscopic* refers to an image that is presented momentarily.

3.2 Materials and methods

3.2.1 Participants

Twenty-four subjects reporting to have IIN were recruited from the *Cardiff Research Unit for Nystagmus* cohort. Only subjects with *idiopathic* IN were sought since these individuals have no other known visual deficit. Nine normally-sighted control subjects with no history of ocular disease were also enrolled.

3.2.1.1 Inclusion / exclusion criteria

Subjects were questioned about their ocular history and previous diagnosis of IIN. EM recordings were made to ensure that participants had IN (as opposed to any other oculomotor instability). Accelerating slow phases were an essential criterion for diagnosis. Binocular indirect ophthalmoscopy, slit-lamp examination and optical coherence tomography were also performed. Subjects with any of the following were excluded:

- Signs or reports of comorbid congenital ocular pathology
- Active ocular pathology (other than strabismus and ametropia)
- A history of photosensitive epilepsy (due to the use of flashes of light in the experiment)

3.2.2 Apparatus

An instrument was designed and built with the purpose of measuring VA using brief flashes of light. VA was estimated by assessing subjects' ability to discriminate tilt of gratings; a technique previously employed by Jones (2011). Due to the nature of the experiment (using a flash to measure VA), stimuli could not be presented on a computer screen. The device comprised: an EyeLink 1000 eye tracker (see Section 1.4.3.3); a camera flash unit; a grating presentation and tilting mechanism; a series of printed gratings; and a MATLAB program which automated data collection, recorded EMs, and controlled flash delivery (see Appendix I – *flashtrack_test.m*).

3.2.2.1 Flash equipment

In order to present a flash with a specific duration, a Metz Mecablitz 76 MZ-5 Digital flash unit was used, which is capable of producing flashes of light with durations ranging from 0.05 to 6.67 ms (Metz 2009).

Spectral content

For safety reasons, heat resistant glass was placed over the flash unit to attenuate output. The combined spectral output of the flash unit and heat resistant glass is shown in Figure 3.2.

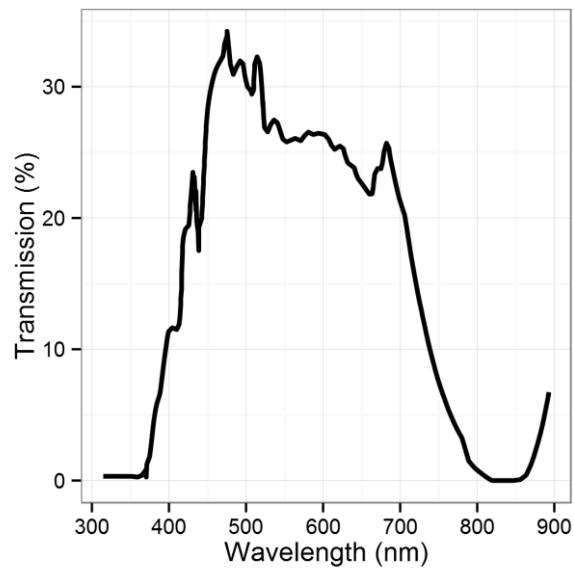


Figure 3.2: Combined spectral transmission of flash unit and heat resistant glass

Brightness

The flash unit can be operated over 30 different levels of brightness. Brighter flashes have a longer duration, deplete the battery more quickly, and require a longer ‘recycle’ time (recovery time before another flash can be initiated). The ideal flash would be bright, brief, and allow for fast recycle times. The flash brightness decided upon equated to $1/8^{2/3}$ of the maximum flash output level. See Section 3.2.2.3 for the reason this brightness level was chosen.

The brightness of the flash was measured using a ILT1700 Research Radiometer/Photometer; the output of 25 flashes was measured. The mean flash brightness (as reflected towards subject participants) was $4.64 \log \text{cd}\cdot\text{s}/\text{m}^2$.

Duration

A storage oscilloscope (Hewlett Packard, model 54603B) was used to measure the duration of ten flashes at $1/8^{2/3}$ output. Based on these measurements, the mean flash duration was 0.76 ms, with a standard deviation of 0.01 ms.

Computer control

The flash unit was connected to a computer-controlled relay switch (AR-2, by EECI) using a modified Metz standard sync cable (36-50), communicating with the computer over a RS-232

serial port via an extension cable (see Figure 3.3). An RS-232 connection was chosen instead of USB to reduce signal transmission latency (Ramadoss and Hung 2008).

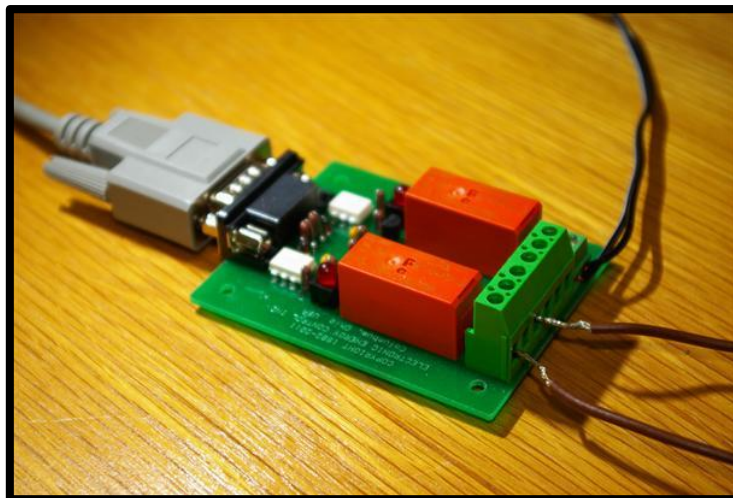


Figure 3.3: AR-2 relay device, connected to RS-232 cable. Brown wires lead to Metz standard sync cable; black wires lead to a 9V power supply.

To facilitate computer control of the flash, code was compiled in C++ capable of triggering the AR-2 relay on demand (see Appendix I – *flash.cpp*).

VA was measured using large gratings subtending a visual angle of 12° . Grating targets were chosen because they can be presented over a large area. The flash unit was triggered at random intervals so that for any given flash, the fovea could be at any position within the nystagmus waveform. A grating which covers a large part of the visual field should appear the same no matter which part is being viewed, whereas a Sloan letter at threshold is best viewed directly.

3.2.2.2 Test stimuli, housing and set-up

A frame was designed and constructed, which housed large (50 cm^2) gratings at a distance of 2 m from the subject. The frame contained a circular aperture with a 12° diameter. Four small bull's-eye targets were arranged around the aperture, each 2° from the edge of the aperture (see Figure 3.4). These provided a reference point, to aid in judgement of tilt under both lighting conditions. The bull's-eye targets were illuminated by spots of light from a projector, situated behind the subject's head. These were generated using a program written in Multimedia Fusion (an event-based programming language), run through a separate computer.

A series of 20 square wave gratings at equally-spaced logMAR steps were produced by a high-quality professional printer (Durst Epsilon photographic printer, RA-4 process) with

fundamental spatial frequencies ranging from -0.46 to 1.48 logMAR²¹ on heat-treated, non-glossy, strong photographic card large enough to fill the 12° aperture of the frame. The frame, with a grating mounted inside, is shown in Figure 3.4.

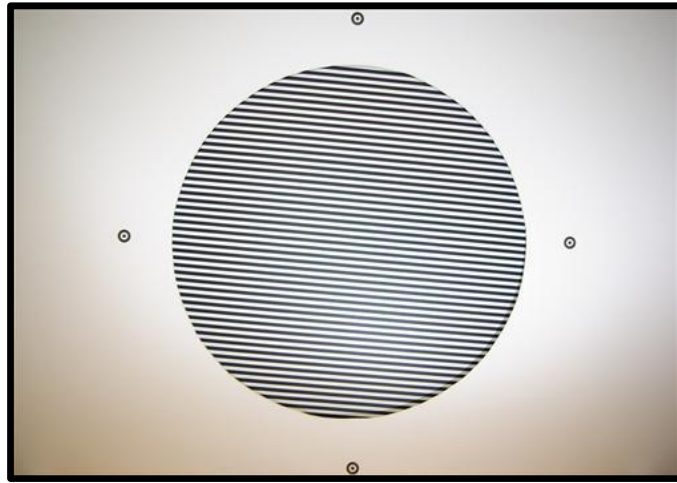


Figure 3.4: Photograph of the aperture frame illuminated by the flash unit, with a grating mounted inside (tilted 5° up to the left), as viewed by subjects. The bull's-eye targets serving as horizontal and vertical axis references can be seen around the grating edge.

In order to change the stimulus orientation, the targets needed to be physically tilted. An aluminium see-saw with a maximum tilt of 5° in each direction was constructed on which the gratings could be placed (see Figure 3.5). This mechanism was controlled by an eight-channel USB solenoid relay switch, driving a servo motor (see Figure 3.6). This allowed the up/down or left/right tilt of the gratings to be automated under computer control.



Figure 3.5: Servo-controlled aluminium see-saw and frame for grating mounting and tilting

²¹ The series of gratings was originally designed to run in 0.10 logMAR steps from -0.30 to 1.60 logMAR at a distance of 1.5 m, but the test distance was adjusted to 2 m due to high-performing control subjects in the early stages of the study.

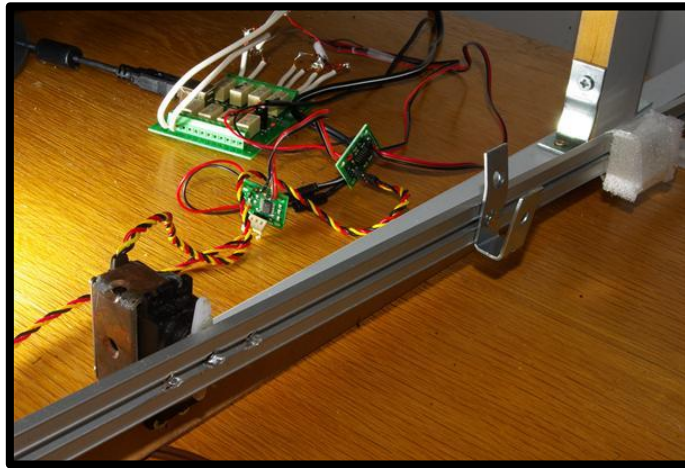


Figure 3.6: The tilt mechanism in detail, showing servo motor and eight channel USB solenoid relay switch

The rotating servo and tilting metal frame of the see-saw generated audible noise which subjects could potentially have used as a cue to the orientation in which the stimulus would next be presented. To circumvent this problem, auditory white noise was generated using Pure Data (an open source sound synthesis scripting language). This was played from a loudspeaker whenever a signal was sent to tilt the grating. Even if the grating's next orientation was due to be the *same* as its current orientation, the motor was programmed to jolt halfway in one direction, before returning to its original location. This ensured that the mechanism produced the same impact on the table at each presentation.

3.2.2.3 Stimulus illumination

The grating stimuli were illuminated in one of two ways: tachistoscopic presentation using a Metz Mecablitz 76 MZ-5 flash unit at $1/8^{2/3}$ power (with an output of $1.52 \log \text{ cd/m}^2$), or constant illumination by an angle-poise lamp, providing $4.64 \log \text{ cd}\cdot\text{s/m}^2$. Subjects were given as much time as desired to respond to each stimulus. The flash was strobed at a variable (random) frequency between 2-6 Hz in order to prevent flash timing prediction.

The decision to use a power level of $1/8^{2/3}$ was based on a short pilot experiment on a single subject, rendered emmetropic and with no known ocular pathology. The flash output was adjusted so that the VA under tachistoscopic presentation was close to the VA obtained with the constant illumination provided by the lamp. Since the outcome of the present study was determined by the *relative difference* in VA obtained under the different lighting conditions between subjects, the absolute parameters of each condition were of little importance, as long as they remained constant for all subjects and experimental paradigms.

3.2.2.4 Automated occluder

An automated occluder was constructed. This comprised an acrylic sheet attached to a servo motor. This was connected to two of the channels of the same USB relay switch used to control the tilt mechanism (see Figure 3.6). The occluder, mounted next to a chin/forehead rest, is shown in Figure 3.7.

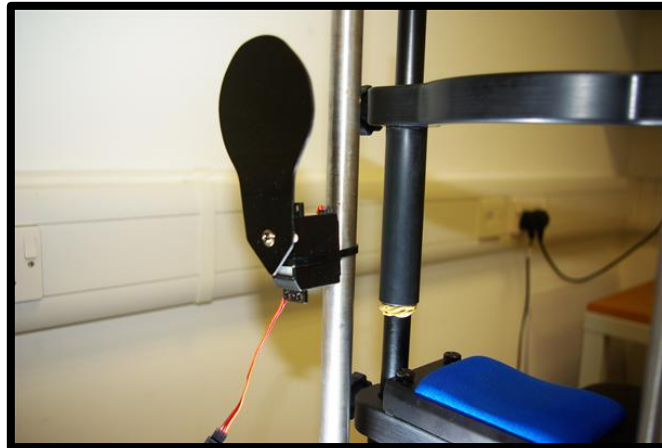


Figure 3.7: Automated occluder and chin/forehead rest

3.2.2.5 Response box

Subjects responded to visual stimuli using a Microsoft SideWinder game pad (see Figure 3.8). This device connects to a PC using a USB connection. Two buttons were used for subject responses: triggers located under the left and right index fingers.



Figure 3.8: Microsoft SideWinder game pad

3.2.2.6 Computer control

In order to synchronously control the eye tracker, flash unit, tilt mechanism and automated occluder, a program was written in the MATLAB programming language (The MathWorks, Natick MA) which activated the flash when the EyeLink 1000 was able to find the subject's eye. The flash therefore did not fire when the eye was closed (e.g. during a blink). This feature served to both preserve battery life in the flash, and provide an additional safety mechanism

in case of inducing an epileptic seizure. The source code can be found in Appendix I – *flashtrack_test.m*.

3.2.2.7 Laboratory setup

The frame was placed against a Sony GDM-F520 21" CRT monitor (used for calibration of the eye tracker; see Chapter 2), at a distance of 2 m directly in front of the chin/forehead rest and automated occluder. The flash unit (or angle poise lamp) was placed 55 cm in front of the aperture frame, with the illumination directed toward its centre. The eye tracker was placed 50-70 cm from the chin/forehead rest, in the optimum position prior to calibration in order to minimise glare from spectacle reflections (if worn).

Figure 3.9 shows the complete laboratory setup.



Figure 3.9: Laboratory setup for experiment

3.2.3 Procedures

Clinical VA for each eye was first measured using a self-illuminated logMAR chart, using distance spectacle correction at a distance of 3 m under clinical conditions. Subjects were encouraged to continue reading until at least four letters on a line were identified incorrectly. The eye with the best VA was tested. Subjects with equal VA had their dominant eye tested, as determined by investigation of suppression using a distance Mallett unit. In the case of equidominance, the right eye was tested by default. For the test eye, distance spectacle correction was provided if refractive error (which was determined for both eyes by the author, a qualified optometrist) exceeded ± 0.50 D (mean sphere) from their habitual correction (see Section 3.2.4.2).

Subjects were then seated in darkness with their head in the chin/forehead rest, 2 m from the grating. Subjects with an eccentric null zone were encouraged to turn their head into that

position. The non-test eye was patched to reduce the chance of an epileptic seizure being triggered by the flash (Anyanwu 1999).

EMs were recorded by an EyeLink 1000 (see Section 1.4.3.3). Subjects with IIN were calibrated using the method described in Chapter 2 to a screen subtending a visual angle of $11 \times 8.5^\circ$. Control subjects were calibrated on the same screen, using the standard EyeLink 1000 nine point calibration method (Stampe 1993).

The frame described in Section 3.2.2 was used to house gratings tilted either 5° left/right or up/down. Subjects were encouraged to view the centre of each grating, and report perceived tilt. Subjects were allowed as much time (or as many flashes) as they desired to give a response, which was given using one of two buttons on a Microsoft SideWinder game pad. No feedback was given for correct or incorrect responses. The finest grating available that provided a VA equivalent to or worse than the subject's clinical VA was used for the first presentation. The orientation of each subsequent presentation was determined by the use of Gellerman-Fellows sequences (see Section 3.2.3.1). VA was estimated using a two-alternative forced choice transformed up-down psychophysical staircase procedure of eight reversals with a three-up / one-down criterion; gratings were physically replaced with one of the 20 available sizes (see Section 3.2.2), and VA was estimated at a 79.4% chance of correctly identifying the stimulus, by averaging the last six reversals (Levitt 1971). The first two reversals were ignored to reduce bias inherent from the staircase starting position.

This procedure was undertaken under four different conditions:

1. Gratings oriented $\pm 5^\circ$ about the horizontal axis, under constant illumination
2. Gratings oriented $\pm 5^\circ$ about the horizontal axis, illuminated by flashes
3. Gratings oriented $\pm 5^\circ$ about the vertical axis, illuminated by flashes
4. Gratings oriented $\pm 5^\circ$ about the vertical axis, under constant illumination

Test presentation order was randomised. Statistical analysis of the resulting dataset was performed in the R Environment for Statistical Computing (R Core Team 2012).

3.2.3.1 Gellerman-Fellows sequences

The Gellerman-Fellows sequences are a series of 24 binary sequences (each with 12 elements) developed for use in psychophysical studies (Fellows 1967). A truly random binary sequence will often produce long runs of the same value. Gellerman (1933) argued that humans have a tendency to alternate their responses occasionally. The Gellerman-Fellows sequences do not contain any 'runs' of the same number longer than three; for example, one such sequences is

001011000111. The 24 sequences can be ‘joined together’ in such a way that this rule is still obeyed for a single looping sequence with 288 elements. By assigning each presentation of a 2AFC paradigm to this binary sequence, it is believed a more reliable result can be obtained (Fellows 1967). MATLAB code for running psychophysical studies with these ‘joined’ sequences is presented in Appendix I – *gellermanfellows.m*. Using this code, the sequence is started at a random location at the beginning of the experiment, in order to minimise the chance of memorising the sequence for subsequent experiments.

3.2.4 Paradigm development

This study went through several incarnations prior to the final experimental protocol outlined above. Automation of the stimulus, flash and response reporting was implemented to overcome extremely lengthy testing times (before automation, a single threshold could take in excess of 20 minutes to obtain).

3.2.4.1 Limited flashes

The decision to allow an unlimited number of flashes was made because a randomly timed flash can occur at any point during the nystagmus waveform and, whilst unproven, visual sensitivity *may* vary throughout the waveform of nystagmus. The investigation of this possible variation in sensitivity was another original investigative aim. If this variation truly exists, then providing a finite number of flashes would unfairly disadvantage nystagmats (as compared to control subjects). Since this hypothesis was left untested, it seemed prudent to control for the potential effect, whether or not it exists.

3.2.4.2 Habitual / full refractive correction

Initially, study participants were encouraged to wear their habitual refractive correction, whether or not it was close to their actual refractive error. This was done in order to prevent visual ‘stress’ associated with wearing an unfamiliar correction exacerbating the nystagmus. However, the decision was later made to limit residual refractive errors up to a maximum of ± 0.50 D (mean sphere). This constraint was imposed in order to reduce the effect of uncorrected astigmatism on the results. Since the flash was capable of isolating image motion, any changes in nystagmus intensity brought on by an increase in stress were deemed to be unlikely to affect the results. The analyses performed in Section 3.3 exclude those subjects that fall outside of this limit when investigating orientation-specific effects.

3.2.4.3 Abandoned paradigms

The following paradigms were dropped prior to the final experimental design:

Waveform-contingent flash triggering

Initially, one of the desired outcomes of the present study was to measure VA at different *times* throughout the nystagmus waveform. The intention was to trigger the flash unit at various waveform loci (see Figure 3.10), by parsing the nystagmus waveform in real time using the technology developed in Chapter 2. The results, it was hoped, would inform whether there is a graduated suppression of vision as the eyes reach full extension of the nystagmus waveform. Following a foveation period, the flash would be triggered at given deviations from the foveation location. However, due to constraints in computer processing power, the waveform analysis program was unable to report the position of the eyes in the nystagmus waveform sufficiently quickly, leading to a variable and unpredictable delay in flash triggering. Although it was possible to know the exact moment at which the flash had been triggered post-hoc, it was not feasible to perform a psychophysical staircase procedure to determine threshold at specific positions along the waveform. Furthermore, many participants exhibited multiple or variable waveforms which would have further complicated testing.

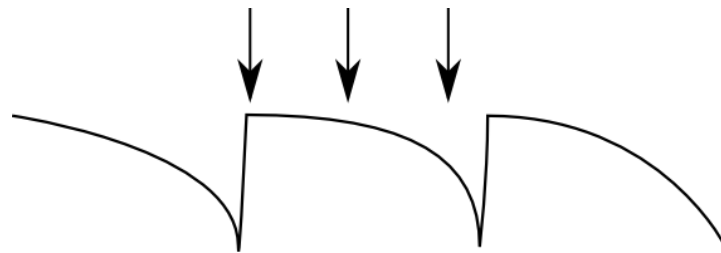


Figure 3.10: Schematic to explain the triggering of flash at different waveform loci. Although the absolute position of the waveform in the orbit varies from cycle to cycle, it might be possible to step through the waveform in real time and trigger a flash unit at (for example) the loci shown by the arrows.

Gaze-contingent flash triggering

A second, also unsuccessful, study outcome was to measure parafoveal VA by triggering the flash at various positions of gaze. For this part of the study, the 12° viewing window was reduced to 0.62° with the use of an additional baffle, to stimulate only specific parts of the visual field. The intention was to ascertain whether parafoveal VA is higher along the axis of nystagmus (for example, left and right of the fovea for an individual with horizontal nystagmus), due to increased exposure of these retinal loci to the point of regard during visual development. Software to perform this function was developed, and the functionality remains as an option in the code presented in Appendix I. The program allows the user to specify an angle of gaze and a ‘tolerance zone’ around that point at which the flash should trigger. The flash relay then resets when the eyes leave the zone. The tolerance zone was intended to be very small; it was specified to ensure that the relay still triggers if the eyes move past the exact

angle of gaze at such a velocity that they do not register at the exact desired co-ordinates during one of the samples taken at the 1000 Hz sampling rate of the EyeLink 1000.

Despite completion of this software, many of the finer details of the foveation detection algorithm were not implemented until the study was underway. At the time of data collection, calibrations were still poor (the software detailed in Chapter 2 was still in its infancy), and flash delivery proved to be sporadic in individuals with nystagmus, despite working well in control subjects. Data for this study were only collected from four participants with nystagmus, and are not included in the current report.

3.3 Results

3.3.1 Participants and exclusions

Twenty-four subjects with early-onset nystagmus were recruited from the *Cardiff Research Unit for Nystagmus* cohort. Of these, eight were excluded for having the following conditions:

- 3 FMNS (subjects KL, LL and MB)
- 1 Acquired downbeat nystagmus (resulting from hereditary motor and sensory neuropathy [type 2]) (subject IG)
- 1 Achromatopsia (subject DT)
- 1 Albinism (subject RC)
- 1 Nystagmus that was only present in right-gaze (subject JC)
- 1 Active pathology: bilateral Fuch's endothelial dystrophy, a mature cataract in the right eye and a distorted pupil in the left eye following previous surgery (subject RW)

A further four participants were excluded following a change of protocol²². The remaining 12 subjects, all with IIN, were included (3 female, 21-69 years [mean age 43]). Nine normally-sighted individuals with no history of ocular disease also took part (4 female, 21-48 years [mean age 28]). General information and biometrics for each subject can be found in Appendix II.

3.3.2 Threshold data

Tables 3.1 and 3.2 show the VAs obtained under each of the four conditions listed in Section 3.2.3. Note the final column in these tables; these indicate whether or not subjects' habitual correction was within 0.50 D (mean sphere) of their refractive error.

²² The flash unit was originally programmed to discharge only when the gaze fell within 1° of the centre of the grating. At the time of testing, the nystagmus calibration system (Chapter 2) was in its infancy. In practice, this led to the flash failing to fire at the 2-6 Hz rate specified in the protocol.

Table 3.1: VA (logMAR) obtained for subjects with IIN

Subject	Sex	Age	Clinical VA	Constant horizontal	Tachistoscopic horizontal	Tachistoscopic vertical	Constant vertical	Uncorrected ametropia > 0.50 D (mean sphere)
GT2	M	59	0.78	0.80	0.70	0.91	0.86	FALSE
DB	M	53	0.64	0.65	0.80	0.65	0.65	FALSE
JT	M	24	0.42	0.21	0.33	0.41	0.33	FALSE
SW	F	69	0.16	0.21	0.17	0.34	0.37	FALSE
JC2	F	54	0.54	0.42	0.34	0.54	0.53	FALSE
GS	M	28	0.54	0.39	0.28	0.42	0.51	FALSE
NB	M	44	0.26	-0.06	-0.11	0.33	0.31	FALSE
DP	M	38	0.60	0.16	-0.02	0.68	0.54	FALSE
LC	M	27	0.52	0.38	0.33	0.52	0.66	TRUE
DK	F	50	0.72	0.44	0.58	0.61	0.52	TRUE
JS	M	55	0.34	0.42	0.44			FALSE
VW	F	21	0.34	0.36	0.23	0.52	0.46	FALSE

Table 3.2: VA (logMAR) obtained for control subjects

Subject	Sex	Age	Clinical VA	Constant horizontal	Tachistoscopic horizontal	Tachistoscopic vertical	Constant vertical	Uncorrected ametropia > 0.50 D (mean sphere)
LP	F	23	0.10	0.03	0.17	0.08	0.01	FALSE
JS2	M	24	-0.16	-0.04	0.01	-0.07	-0.03	FALSE
FE	M	47	-0.08	-0.14	-0.08	-0.03	-0.11	FALSE
PG	M	20	-0.20	-0.11	-0.17	-0.08	-0.14	FALSE
TM	M	48	-0.22	-0.11	-0.11	-0.04	-0.03	FALSE
AS	F	23	-0.14	-0.03	-0.01	-0.10	-0.06	FALSE
MU	F	21	-0.08	0.03	-0.03	0.02	-0.07	FALSE
BF	F	26	-0.10	-0.08	0.02	0.07	0.01	FALSE
JT2	M	23	-0.14	-0.09	-0.20	0.00	-0.09	FALSE

The data from Tables 3.1 and 3.2 are summarised in Table 3.3 and expressed graphically in Figure 3.11. Subjects who took part with an uncorrected refractive error ≥ 0.50 D (mean sphere) are excluded from both Table 3.3 and Figure 3.11.

Table 3.3: Mean and standard errors of VAs (logMAR) shown in Tables 3.1 and 3.2 for all conditions and both groups. Subjects who took part with uncorrected refractive error ≥ 0.50 D (mean sphere) are excluded.

		IIN	Controls
Constant	Horizontal	0.35 ± 0.08	-0.06 ± 0.02
	Vertical	0.51 ± 0.06	-0.06 ± 0.01
Tachistoscopic	Horizontal	0.32 ± 0.09	-0.05 ± 0.04
	Vertical	0.50 ± 0.06	-0.02 ± 0.02

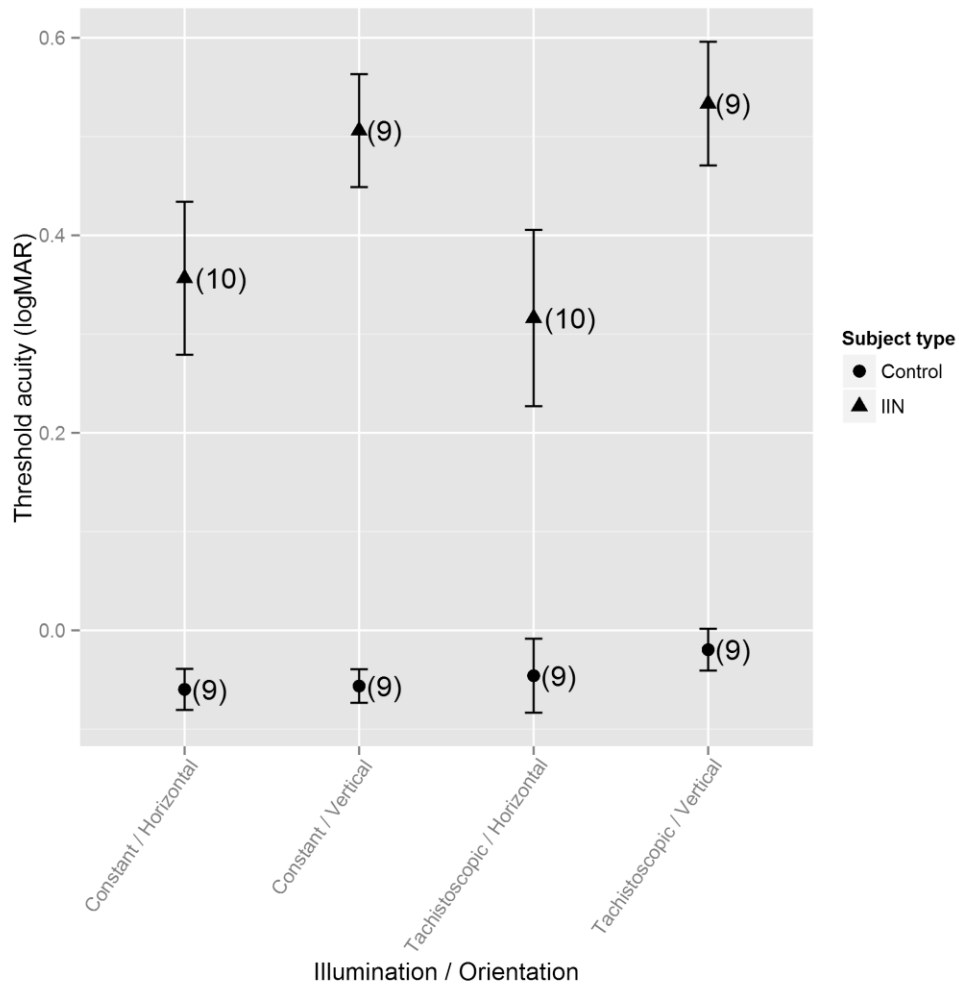


Figure 3.11: Graphical representation of the mean VA recorded for subjects with < 0.50 D (mean sphere) uncorrected refractive error. Error bars indicate standard error. The number of subjects for each datum is shown in parentheses.

3.3.3 Tachistoscopic vs constant illumination

The effect of tachistoscopic presentation on VA was analysed using paired samples t-tests. Since the two orientations were analysed separately, subjects whose habitual correction was ≥ 0.50 DS mean sphere from their true refractive error were included in the analysis.

Tachistoscopic presentation caused no significant difference to VA in controls for both horizontal ($p = 0.6224$) and vertical ($p = 0.0807$) gratings. Similarly, in nystagmats, there was no significant difference between lighting conditions for either orientation (horizontal: $p = 0.2545$; vertical: $p = 0.2431$).

3.3.4 Effect of orientation

The effect of horizontally vs vertically oriented gratings is shown in Table 3.4. For this table, subjects who participated with an uncorrected refractive error ≥ 0.50 D (mean sphere) are excluded. This table differs from Table 3.3 by just one subject (JS), who is not included as he did not complete the vertical/constant illumination condition due to time constraints on the day of testing.

Table 3.4: Mean and standard errors of VAs shown in Tables 3.1 and 3.2 for all conditions and both groups. Subjects who took part with uncorrected refractive error ≥ 0.50 D (mean sphere), and those who did not complete all conditions are excluded.

		IIN	Controls
Constant	Horizontal	0.35 \pm 0.09	-0.06 \pm 0.02
	Vertical	0.51 \pm 0.06	-0.06 \pm 0.01
Tachistoscopic	Horizontal	0.30 \pm 0.10	-0.05 \pm 0.04
	Vertical	0.53 \pm 0.06	-0.02 \pm 0.02

The data from Table 3.4 are shown in Figure 3.12, with error bars indicating standard error. Again, note that this figure only differs by one subject (JS) from Figure 3.11.

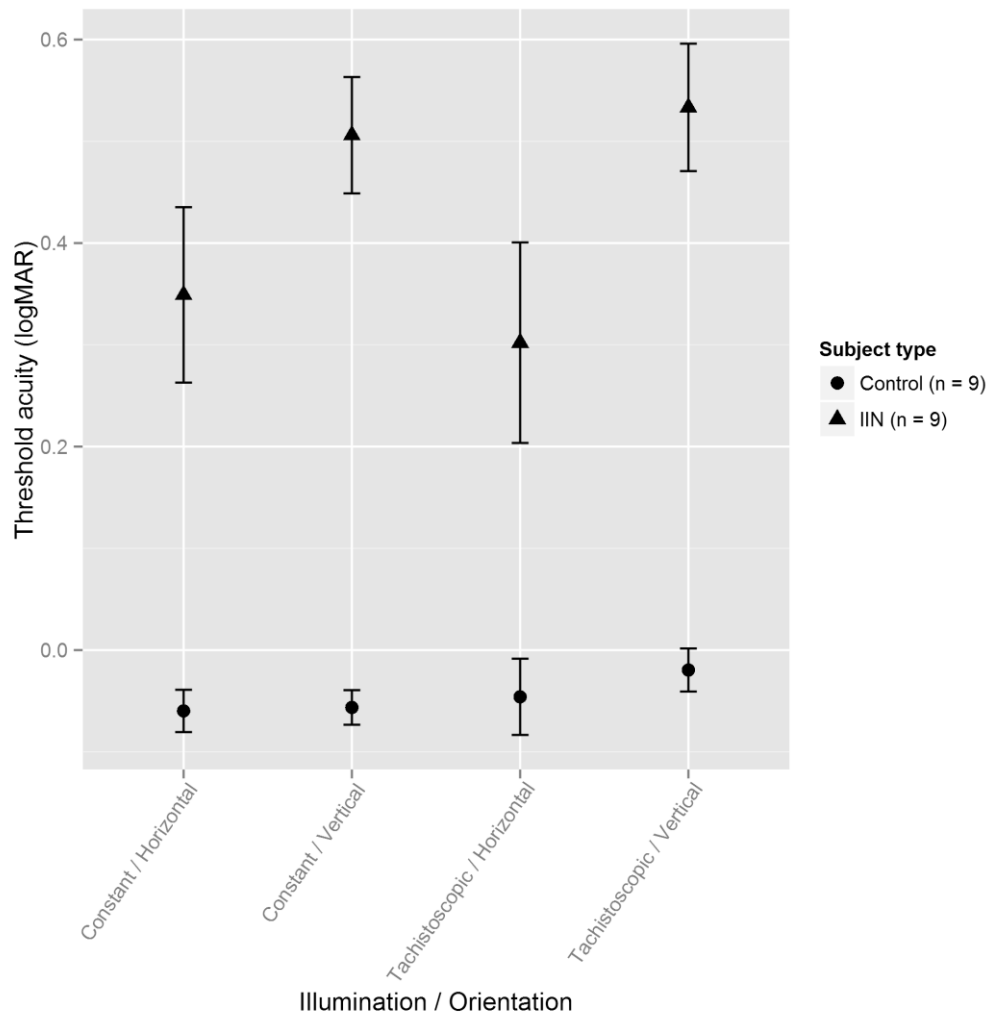


Figure 3.12: Data from Table 3.4 represented graphically. Error bars indicate standard error.

Paired samples t-tests indicate a significant effect of orientation in nystagmats under both constant ($p = 0.00755$) and tachistoscopic ($p = 0.01881$) conditions. However, this effect is not present in controls for either condition ($p = 0.8672$ for constant light and $p = 0.4426$ for tachistoscopic presentation).

3.3.5 Effect of age

Control subjects who participated in this study were from a lower age range than those with IIN. For this reason, an investigation into whether there was an effect of age on the difference in VA obtained under each illumination condition was undertaken. Figure 3.13 presents the distribution of the differences in VA observed with respect to the age of either control or nystagmus subjects. In the figure, a positive number indicates an improvement in VA under constant illumination as compared to tachistoscopic. Statistical analysis found no evidence for any correlation between difference in VA and age in either group (Pearson's product-moment correlation; controls: $p = 0.79$; nystagmats: $p = 0.84$). In other words, the slopes for both groups were not significantly different from zero, and thus, age matching was unnecessary for this study.

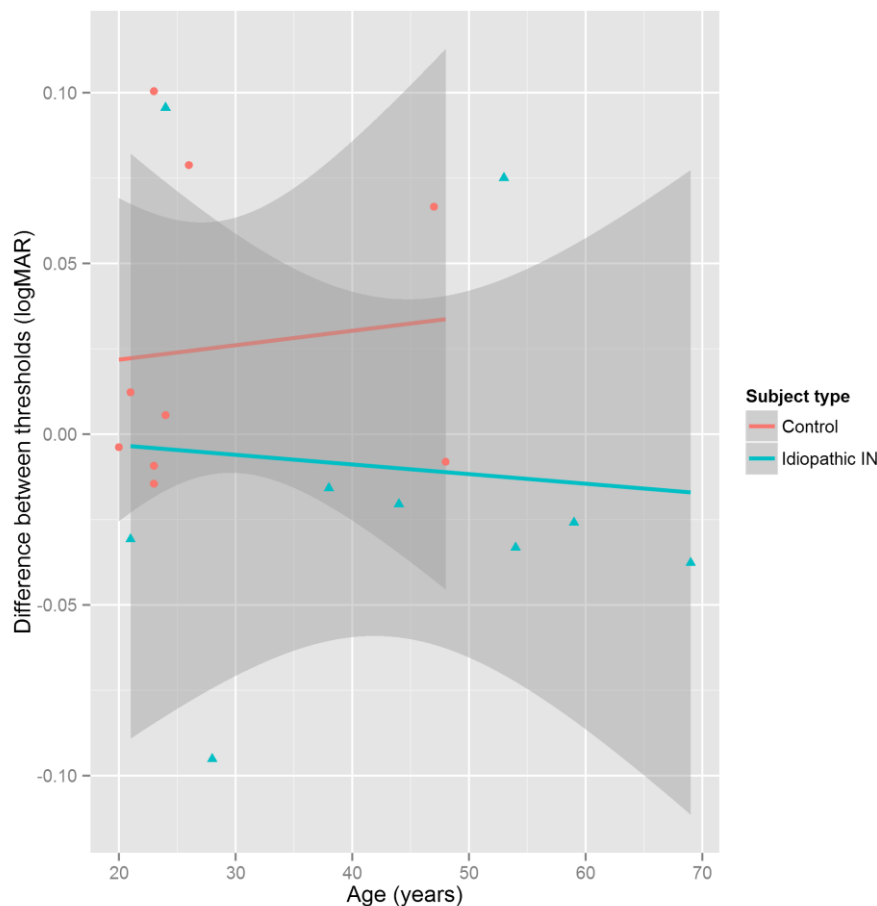


Figure 3.13: Graph showing the effect of age on the difference in mean thresholds obtained for constant and tachistoscopic stimulus presentation in both nystagmats and control subjects. A positive number indicates a worsening of VA with the flash. Linear regression and confidence intervals are shown.

3.4 Discussion

Under all lighting conditions and stimulus orientations, VA was worse for subjects with IIN than controls. Crucially, the fact that VA did not improve under tachistoscopic illumination suggests that *image motion is not the limiting factor to VA in IIN*. Moreover, under both lighting conditions, subjects with IIN had significantly poorer VA for vertical gratings as compared to horizontal, whereas controls showed no effect of orientation. This finding is strongly suggestive of meridional amblyopia in IN, and has previously been reported under constant illumination (Meiusi, Lavoie and Summers 1993). Abadi and King-Smith (1979) found a similar effect under tachistoscopic illumination although this is the first study to measure VA under tachistoscopic conditions.

In the presence of image motion, VA is known to be mediated (in normally sighted individuals) by larger spatial filters than when viewing a stable retinal image (Chung and Bedell 1998). Assuming that this is also the case in IN, it is possible that amblyopia development could be mediated by a relative under-use of smaller spatial filters (receptive fields) associated with high VA. Interestingly, Currie, Bedell and Song (1993) demonstrated that although nystagmoid retinal image motion causes a reduction in VA in normally-sighted individuals, this reduction is not large enough to reach the average VA of individuals with IN. This further suggests that nystagmats suffer from a sensory deficit beyond that which can be explained by image motion alone.

Previous studies have reported a correlation between foveation quality (duration, accuracy, etc.) and VA. Therefore, it has been concluded that EM characteristics can be used to predict VA (Sheth et al. 1995; Dell'Osso and Jacobs 2002; Currie, Bedell and Song 1993; Theodorou 2006). Whilst this has been shown with simulated waveforms in controls and *between* individuals with IN, the correlation does not appear to be evident in response to waveform changes *within* the same subject (Erichsen et al. 2013; Jones et al. 2013). The lack of an effect on VA in the present study strongly suggests that there is an upper limit on the VA possible in adults with IIN, and that stopping the eyes moving altogether would *not* result in 'normal' vision, indeed, halting nystagmus may not even produce a clinically significant change in VA. This has profound implications for current IN treatments, and suggests that future research efforts ought to focus on prophylaxis.

Despite the findings of this study (that VA is fundamentally limited in adults with IN), some therapeutic interventions that aim to improve visual function by reducing the EMs of nystagmus have resulted in (at least to a certain extent) a beneficial effect on VA (Kumar et al.

2011b; McLean et al. 2007; Helveston, Ellis and Plager 1991). These measurements were taken using standard clinical protocol, which allows patients as long as desired to respond. However, testing time is inevitably constrained by patient confidence and the need to ‘move on’ to the next test. It may be interesting to run a study in which subjects are given a fixed, lengthy period of time (e.g. five minutes), in which they are encouraged to scrutinise the chart in detail and are not permitted to respond until the end of the time. Perhaps, the improvements in VA shown in some studies could be the result of non-strict psychophysical methods. In any event, the use of a two-alternative forced choice paradigm in the present study removes any issues relating to confidence.

Some studies investigating therapies for IN have not shown a significant change in acuity, but *did* result in subjective reports of improved vision (Hertle et al. 2003). Therefore, it seems the VA benefit available from such treatments (if any) is small. In light of the present results, which indicate that reducing image motion does not significantly affect VA, additional outcome measures may be required, such as visual processing speed (e.g. time-restricted optotype recognition tasks [Yang et al. 2005], visual response speed measurements [Hertle et al. 2002] or target acquisition timing).

An alternative explanation for the small improvement in VA seen in some studies could be that abnormal conditions elicited changes in the waveform *in excess of* that normally experienced by the subject (and thus masked by amblyopia). If subjects are stressed by the prospect of undergoing treatment when their VA is first measured, the increase in nystagmus intensity brought on by this could potentially result in vision worse than their amblyopic VA limit. Naturally, subjects would be more relaxed following (or during) treatment, and this may bring VA back to their amblyopic limit. Of course, these are speculative hypotheses; further research is required to better understand the marginal improvements in VA that have been reported with some treatments.

3.4.1 Orientation

Orientation sensitivity has been previously investigated in IN (see Section 1.3.9.5). It is known that individuals with horizontal IN are typically less sensitive to gratings oriented in the vertical axis, even under tachistoscopic conditions (Abadi and Sandikcioglu 1975; Jones 2011; Loshin and Browning 1983; Bedell and Loshin 1991; Abadi and King-Smith 1979). The data presented here support these previous results.

The tasks performed in the present study involved discrimination of tilt $\pm 5^\circ$ about either the horizontal or vertical axes. Therefore, it is fair to say that the targets used in this study were

never *truly* horizontal or vertical. Nonetheless, there was a significant orientation effect for visual discrimination of gratings *about* the horizontal and vertical axes.

3.4.2 What does this mean for people with nystagmus?

The major conclusion of this study is that *image motion is not the limiting factor to VA in IN*. This means that although treatments and therapies that aim to improve visual function by reducing the EMs of nystagmus may have, to a certain extent, a beneficial effect on VA, the absolute benefit available from such treatments (to VA at least) appears to be fundamentally limited. Perhaps research efforts would be better spent identifying further ocular (or neurological) abnormalities in children at the time of presentation, rather than on therapies to reduce the nystagmus. However, other potential benefits from these therapies, such as the time taken to obtain visual information, should not be overlooked (see Chapter 4 for a study investigating this aspect of IN).

3.4.2.1 Extrapolation to infantile nystagmus

The conclusions of this study ought not only to apply to subjects with IIN, but to all forms of IN. Since IIN is usually considered to be an isolated form of IN, it is reasonable to believe that although additional pathophysiological mechanisms are in play in other forms of IN, the same reduction in VA is likely to be inherent from the EMs themselves. Participation in this study was limited to individuals with a diagnosis of IIN in order to test the hypothesis that VA might improve under tachistoscopic illumination, without the results being confounded by known visual deficits.

3.4.3 Implications for clinical practice

Given that no significant difference was found between the constant and tachistoscopic presentations in subjects with IIN, there appears to be no need to advise changes in optometric clinical practice. As long as patients with nystagmus are given plenty of time to read a letter chart, it seems that the actual motion of the eyes does not significantly impact on their ability to perform the task. However, what has not been tested is whether or not clinical VA provides a reliable approximation to the actual underlying VA when measured under strict psychophysical conditions. This would be a worthwhile future study which could further inform clinical practice.

In the past, clinical studies have relied heavily on VA as an outcome measure. Treatments such as biofeedback have been shown to cause increased foveation duration, but were abandoned due to the lack of a change in VA (Mezawa, Ishikawa and Ukai 1990; Ciuffreda, Goldrich and Neary 1982). In light of results indicating that VA cannot be *expected* to

improve, it may now be worth revisiting this and other therapies, as there may be tangible benefits to biofeedback that are not measurable using VA.

When first designing the present study, the possibility of developing the apparatus into a clinical instrument for predicting maximum VA was considered. The development of such an instrument would now appear to be unnecessary for use in IN. However, it might prove useful in clinical testing of individuals with *acquired* nystagmus since it should (in theory) remove oscillopsia. This is as yet untested.

3.4.4 Assumptions and potential improvements

3.4.4.1 Tilt discrimination and torsional nystagmus

IN waveforms frequently contain a significant torsional component. This component does not exhibit foveation periods, in the same way as the horizontal or vertical components. Torsional variability in IN is typically between $0.53 - 2^\circ$ ($0.35 - 1.14^\circ$ during foveations), as compared to 0.2° in controls (Ukwade, Bedell and White 2002). One might therefore expect that a task involving discrimination of tilt would be more difficult for nystagmats. On the contrary, Ukwade, Bedell, and White (2002) found that the torsional variability in eye position does not limit orientation thresholds *even in the absence of a reference stimulus*, presumably due to the influence of extra-retinal signals. This is convenient, as it allows us to use tilt discrimination as a means of obtaining VA through a two-alternative forced choice paradigm with a repeating stimulus that can be presented over a wide field of view (as used in the present study).

3.4.4.2 Diagnoses

Ophthalmoscopy was carried out on all subjects by a qualified optometrist in order to exclude those with obvious signs of undiagnosed pathology. However, a complete assessment to arrive at the diagnosis of IIN involves electrodiagnostic testing (such as electroretinography and visual evoked potentials), which was not available for the present study. It was assumed that subjects received the appropriate level of ophthalmic care in childhood to exclude other diagnoses, yet it remains possible (as always with IIN) that some subjects have an undiagnosed underlying pathology of the visual system.

3.4.4.3 Accommodative control

The visual stimuli used in this study were presented 2 m away from the subject. Since tachistoscopic presentations were made in a darkened room, it may have been preferable to

have provided each subject with a +0.50 DS over-correction (to focus the image at the retina without the need for accommodation). However, this was *not* done for two reasons:

1. Proximal accommodation may have been stimulated, causing unnecessary blur.
2. All paradigms were performed at the same distance for all subjects. Therefore, the results remain comparable without the additional complexity of adjusting refractive correction.

3.4.4.4 Use of a computer screen

This study could have been performed using a computer screen, by presenting gratings for the duration of a single frame. This approach was not taken due to hardware limitations. The following issues make commercially available monitors unsuitable:

- *Refresh rate*: the flash unit used provided a flash duration of approximately 0.76 ms (see Section 3.2.2). A monitor would require a refresh rate of 1316 Hz in order to achieve an equally brief presentation. Needless to say, such a monitor would be hard to find.
- *Resolution*: in order to reliably perform visual psychophysics using a monitor, either a very high resolution is required, or the study participant must sit sufficiently far away that the test target can be rendered in detail below their VA threshold.
- *Physical size*: for the present study, a large-field visual stimulus was used so that the same stimulus was presented to the fovea regardless of the part of the nystagmus waveform in which the presentation was made. Due to resolution limitations (and the confounding factor of possible convergence null in nystagmus), moving closer to the monitor to rectify the issue was not an option. Thus, any monitor used would have to be very large.

3.5 Summary

The results of the present study suggest that, in addition to meridional amblyopia, there remains an underlying pathology and/or motion-induced stimulus deprivation amblyopia in adults with IN as a result of reduced visual input during development. Motion blur presumably has the same deleterious effect on vision in nystagmats as it does in the rest of the population. The fact that removing this motion does not improve VA in adults suggests that the adverse impact of this motion may have occurred earlier in visual development. If this is true, then the parameters of the adult waveform (foveation duration, average eye velocity, etc.) may well be adapted to provide the maximum VA available. This would explain the strong correlation between, for example, foveation duration and VA between subjects (Abadi and Pascal 1991). In other words, poor quality nystagmus waveforms may not lead to poor VA; rather, IN waveforms in adults are perhaps adapted to the underlying VA. A recent study on the development of IN has proposed a similar idea (Felius and Muhanna 2013). For all these reasons, interventional studies predicated on reducing nystagmus intensity are likely to require better outcome measures than VA alone.

Having established that image motion is *not* the major limiting factor to VA in IIN (and by extrapolation, possibly in all forms of IN), an alternative test of visual function will now be investigated in Chapter 4: the time taken to see.

Chapter 4 Time to see

4.1 Introduction

There is a growing consensus within the nystagmus research community that visual *timing* and the *time taken to see* are important concepts in the visual experience of individuals with nystagmus (Yang et al. 2005; Hertle et al. 2002; Wang and Dell’Osso 2007). Regardless of the stable visual perceptual experience of adults with IN, vision simply cannot be optimal when the fovea is not directed at the locus of attention. It is hardly surprising therefore that VA, a static measure of visual function in which viewing time is unlimited, may not be able to adequately quantify the visual experience of IN (see Chapter 3). Quantitative measures of waveform characteristics (such as NOFF and NAFX) are currently predicated on the *inter*-subject relationship between VA and foveation characteristics (Felius et al. 2011; Dell’Osso and Jacobs 2002). Moreover, nystagmats have subjectively reported improvements to their vision following waveform-modifying treatment, even when VA is not significantly affected (Hertle et al. 2003). Therefore, additional assessments of visual performance need to be developed to adequately measure the efficacy of therapeutic intervention. Ideally, these measures would correlate with aspects of the waveform better than VA, especially *within* individual subjects.

With regards to *time* and vision, nystagmats are potentially faced with two distinct yet related problems:

1. It takes longer to move the eyes towards visual targets (Wang and Dell’Osso 2007).
2. Due to fixation instability, once a visual target has been acquired, additional time may be required to recognise it (this assumption has not yet been tested).

In addition to these time-related issues, individuals with IN typically have an underlying VA deficit (see Chapter 3). This complex situation means that adequate measures of visual function in IN must be multidimensional; taking into account both spatial and temporal aspects. Previous attempts to quantify temporal visual perception in IN have used time-restricted VA. In one such study, optotypes were presented at a fixed location for 550 ms, and VA was measured one letter at a time in sets of four letters. If at least three of four letters were correctly identified in a set, optotype size was decreased until a threshold was reached (Yang et al. 2005). Another study used *tumbling E* optotypes, presented for 0.1 s at a given spatial frequency (Sprunger, Fahad and Helveston 1997). If the orientation was not correctly identified, it was presented again, this time at 0.2 s. This was repeated, with the presentation duration increasing by 0.1 s each time, until the target was correctly identified. The whole

process was then repeated for different spatial frequencies. Whilst these solutions adequately measured VA whilst taking into account the time used to identify a visual target, targets were always presented in the primary position, and thus these methods do not fully address the problem of oculomotor target acquisition time (point 1 above). Another study looked at the time taken to acquire targets that were displaced peripherally (Wang and Dell'Osso 2007). This study only looked at oculomotor target acquisition time, and did not include a perceptual measure. As discussed in Section 1.3.11.2, Hertle et al. (2002) measured the time taken to identify static and moving (constant velocity) letter 'E' optotypes, and suggested that such a test might be useful clinically, since it takes into account not only the time taken to see, but also the ability of the subject to perform smooth pursuit.

Previous studies into visual reaction times in IN have used latency of fixation on peripherally presented targets as a measure of reaction time (Wang and Dell'Osso 2007; Wang and Dell'Osso 2009). Whilst these studies found that there is a greater latency if the new target is presented around the time of nystagmus quick phase, they did not distinguish whether the delay in target acquisition was due to the interplay of multiple saccades (causing an inherent increase in saccadic latency) or suppression of visual perception during those periods (causing a delay in the time taken to notice that the target had moved). A study tackling these particular issues is presented in Chapter 5. For the present study, a novel (combined) method of oculomotor and psychophysical assessment of IN was designed and implemented.

4.1.1 Aims

The present study aimed to determine the time taken by nystagmats (versus normally-sighted control subjects) to interpret visual information as opposed to the time required to fixate visual targets. This builds on the knowledge gained from Hertle et al. (2002)'s study, which examined the time taken to recognise an optotype moving at a constant velocity. In the present study, the oculomotor task was different: targets were displaced to fixed locations horizontally or vertically, so that participants had to perform a saccade to acquire the new target. Following target acquisition, the target remained in a fixed location until the subject gave a response. Unlike the dynamic task reported in Hertle et al.'s study, the two-step nature of the task in the present study (fixate, respond) allows 'time to fixation' to be differentiated from 'time to recognition'. It is hoped that the results of this study will inform understanding of the visual difficulties experienced by nystagmats; specifically to what extent the 'slow to see' phenomenon is due to the time taken to locate and fixate visual targets and to what extent it is due to the time taken to process visual information following fixation.

4.2 Materials and methods

4.2.1 Participants

Twenty-one subjects with IN were recruited from the *Cardiff Research Unit for Nystagmus* cohort. Eleven normally-sighted control subjects with no history of ocular disease were also enrolled.

4.2.1.1 Inclusion / exclusion criteria

EM recordings were made to ensure that participants had IN (as opposed to any other oculomotor instability). Accelerating slow phases were an essential criterion for diagnosis. Subjects with active non-congenital ocular pathology were excluded from the study.

4.2.2 Apparatus

Subjects were seated in a room lit at $\sim 1.78 \text{ log cd/m}^2$, 2 m from a Sony GDM-F520 21" CRT monitor (see Section 2.2.4). EMs were recorded with an EyeLink 1000 (see Section 1.4.3.3). The chin and head were supported by a rest (see Figure 3.7), and subjects were encouraged to adopt a comfortable position in order to view the screen. Habitual spectacle correction (if any) was worn, and viewing was binocular. A Microsoft SideWinder game pad was used to detect participant responses (see Section 3.2.2.5).

4.2.3 Procedures

Clinical binocular VA was first measured using a self-illuminated logMAR chart with distance spectacle correction at 3 m under clinical conditions. Subjects were encouraged to continue reading until at least four letters on a line were identified incorrectly.

4.2.3.1 Static task

On a mid-grey background, a simple black cross was displayed in the centre of the screen (see Figure 2.19). Subjects were instructed to view the cross, which was extinguished after a random delay of between 1-3 s. In its place was displayed a Gabor patch with a spatial frequency equivalent to the subject's clinical VA + 0.30 logMAR (i.e. sufficiently coarse that each subject ought to be able to identify the grating with the same level of difficulty). The Gabor patch was bounded by a Gaussian transparency envelope with a standard deviation of 0.25° . The grating was oriented either 45° to the left or right of vertical (see Figure 4.1) according to Gellerman-Fellows sequences (see Section 3.2.3.1). Subjects were instructed to use the response box to indicate the orientation of the grating as soon as possible. A switch behind the right index finger indicated the grating was tilted to the right, and vice versa. No feedback was given for correct or incorrect responses. Following the subject's response, the

grating was replaced with the fixation cross. Figure 4.2 illustrates the sequence of on-screen stimuli described above. This procedure was repeated 20 times. If subjects attempted to respond before the grating appeared, the 1-3 s delay was reset. EMs and subject response times were recorded throughout.

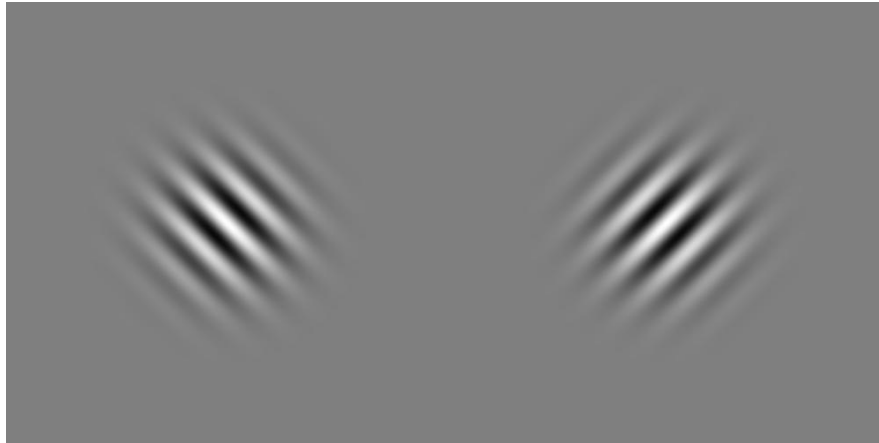


Figure 4.1: Examples of Gabor patches oriented 45° to the left and right

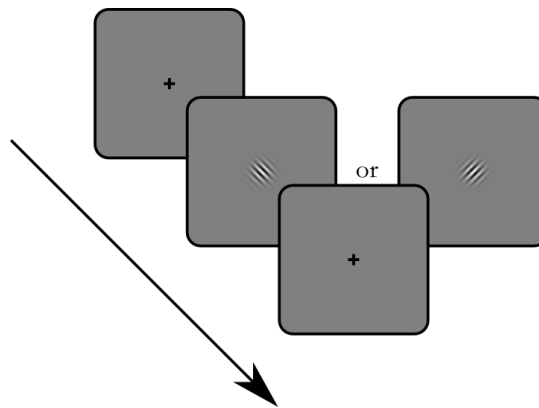


Figure 4.2: Schematic explanation of the sequence of stimuli presented on-screen for the static task

4.2.3.2 Saccadic task

Following completion of the first task, the procedure was repeated, but instead of appearing in the centre of the screen, Gabor patches were presented 3° away from fixation in any of four cardinal positions (above, below, left or right). The instruction for the subject was the same; however, the targets had to be fixated before a response could be made (since the spatial frequency of the targets were 0.30 logMAR coarser than the subjects' clinical VA, they ought not to be visible at 3° eccentricity [Randall, Brown and Sloan 1966]). Multiple Gellerman-Fellows sequences determined the on-screen position in which the Gabor patches appeared. One sequence determined whether the presentation location would be horizontal or vertical, whilst another determined in which of the two remaining possible locations (i.e.

left/right or up/down) the grating would be shown. The fixation cross returned to the screen centre between each presentation. Figure 4.3 illustrates this sequence of on-screen stimuli. The task was repeated until at least 10 presentations in each of the four locations had occurred.

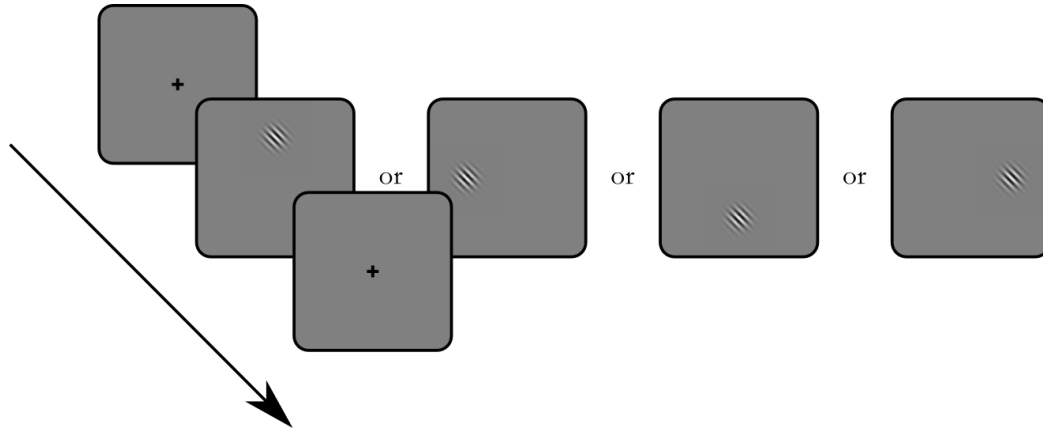


Figure 4.3: Schematic explanation of the sequence of stimuli presented on-screen for the saccadic task. Gabor patches were presented in either orientation; only one is shown here for illustrative purposes.

4.2.3.3 Repetition of the static task

In order to estimate the effect of task familiarity and exhaustion (i.e. the *learning* and *fatigue* effects) on response times, some control subjects repeated the static task after completing the saccadic task. This paradigm was added to the experimental protocol at a late stage; as a result, eight out of 11 control subjects and one subject with IN completed this section of the study.

4.2.4 Analysis

Data from the first five presentations were discarded to afford participants time to familiarise themselves with the task. In addition, any false positive responses (i.e. responses made before a stimulus appeared) were ignored.

For each presentation, up to three values were calculated:

- The time taken to respond (correctly) since the grating's appearance
- For peripherally presented gratings:
 - The time taken between target presentation and initiation of a targeting saccade
 - The time taken to respond (correctly) to the target, relative to completion of the targeting saccade

Note that for subjects with nystagmus, the last two parameters could only be determined unambiguously for *vertically* displaced grating presentations. An established saccade detection

algorithm was used to identify voluntary saccades (Behrens, Mackeben and Schröder-Preikschat 2010; see Section 2.1.5.1 for detail). All of the participants in the present study had primarily horizontal nystagmus, and the target displacements employed in the present study (3°) were too small to be able to reliably differentiate voluntary (target-acquiring) saccades from the involuntary (quick phase) saccades of nystagmus in the horizontal axis. Figure 4.4 illustrates this difficulty; saccades are readily identified in the vertical axis, but horizontal targeting saccades would be very difficult (if not impossible) to accurately parse from the EM trace.

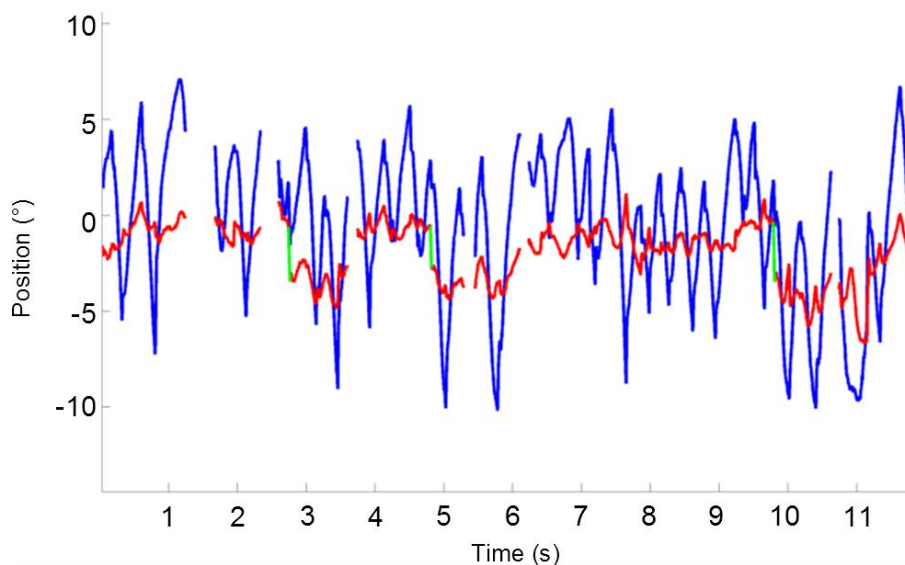


Figure 4.4: EM trace showing horizontal eye position (blue) and vertical eye position (red). Targeting saccades identified in the vertical axis are marked in green. The difficulty faced by automatic saccade detection in the horizontal axis is evident; it is not clear from the EM trace when these target-acquiring saccades took place.

Despite the fact that most IN waveforms exhibit oscillations with a greater magnitude in one axis than the other (typically horizontal), there is often residual motion in the orthogonal axis which potentially could be erroneously detected by the *Behrens, Mackeben and Schröder-Preikschat* saccadic filter. As a result, it was necessary to ensure that, for each target jump in the vertical axis, only the voluntary saccades were detected. Since the grating displacements of 3° were (usually) much larger than the comparatively minimal nystagmoid motion in the orthogonal axis, these were readily identified using an algorithm that finds the saccade with the largest amplitude in the correct direction for each target displacement. Detected saccades with a very short latency (< 100 ms) were rejected from the analysis, since these would be very unlikely to represent true voluntary saccades (Gilchrist 2011).

Three degree target jumps were used because the monitor had to be placed far enough away from participants to adequately display targets at a resolution 0.30 logMAR below each

participant's clinical VA. Due to limitations in the monitor's physical size, this compromise in the maximum target jump size had to be made. See Section 3.4.4.4 for a discussion of the limitations imposed by computer monitors in psychophysical studies.

Statistical analysis of the resulting dataset was performed in the R Environment for Statistical Computing (R Core Team 2012).

4.2.5 Paradigm development

4.2.5.1 Gaze-contingent stimulus triggering

In an early incarnation of the experiment, an additional feature was built into the stimulus presentation software to check whether the gaze was within 0.5° of the fixation cross before displaying the grating target. This feature was included to ensure that participants were always looking in the correct location at the time of stimulus onset, in an attempt to 'normalise' the starting position of the eyes in the subjects with nystagmus. However, during the early stages of data collection, some nystagmats did not have accurately calibrated eye position data (the software detailed in Chapter 2 was still being developed), which led to increased presentation delays (more than the expected 1-2 s) with some participants in some instances. Since these occasionally lengthy delays could have impacted on the response times of participants, the feature was dropped from the final study protocol, and all participants who undertook this paradigm (eight subjects with IN) were excluded from the analysis. Instead, the issue of stimulus onset timing and its relationship to saccade initiation timing was addressed in a separate study, which is described in detail in Chapter 5.

4.2.5.2 Effect of near damping

Some participants performed the experiment twice; at both 2 m and 80 cm, in order to quantify the effect of convergence on 'time to see'. It is known that in many individuals with IN, convergence causes a dampening of nystagmus intensity (see Section 1.3.8.2). However, the effect of this dampening on visual response speed has never been examined. In the study design, 80 cm was decided upon as the 'near' distance, in order to minimise the effects of presbyopia-related defocus on the task, since the study participants were drawn from a wide age range. However, during testing of presbyopic control subjects it soon became apparent that even at this distance, the difficulty of focusing on the targets impeded response times. It was considered that this extraneous factor might contaminate the results to such an extent as to render it impossible to draw conclusions. Therefore, this paradigm was dropped from the final protocol, and will not be discussed further in this chapter.

4.3 Results

4.3.1 Participants and exclusions

Twenty-one subjects from the *Cardiff Research Unit for Nystagmus* cohort with early-onset nystagmus took part in the present study. One subject (KL) was excluded for having FMNS. One (RW) was excluded for having active pathology: bilateral Fuch's endothelial dystrophy, a mature cataract in the right eye and a distorted pupil in the left eye following previous surgery. A further eight were excluded following a change in protocol (see Section 4.2.5.1). The remaining 11 subjects, all with IN, were included (ranging from 22-69 years of age, with a mean of 48 years). Sixteen normally-sighted individuals with no history of ocular disease also took part. Of these, five were excluded due to the change in protocol, leaving 11 controls ranging from 21-72 years of age, with a mean of 53 years. General information and biometrics for each subject can be found in Appendix II. Subjects with IN who participated were DB, DP, DT, GT2, JC2, JS, KL, LC, NB, RC and SW. Control subjects who participated were SS, NH2, FE, RE, TM, JG, JMW, ROD, JTE, SH2 and MD.

4.3.2 Central vs peripheral presentation

In order to produce normally distributed data (for parametric statistical analysis), response times were transformed logarithmically. Figure 4.5 displays the back-transformed mean response time data (from the time of stimulus onset) for both subject groups, separated into gratings that were presented centrally and peripherally.

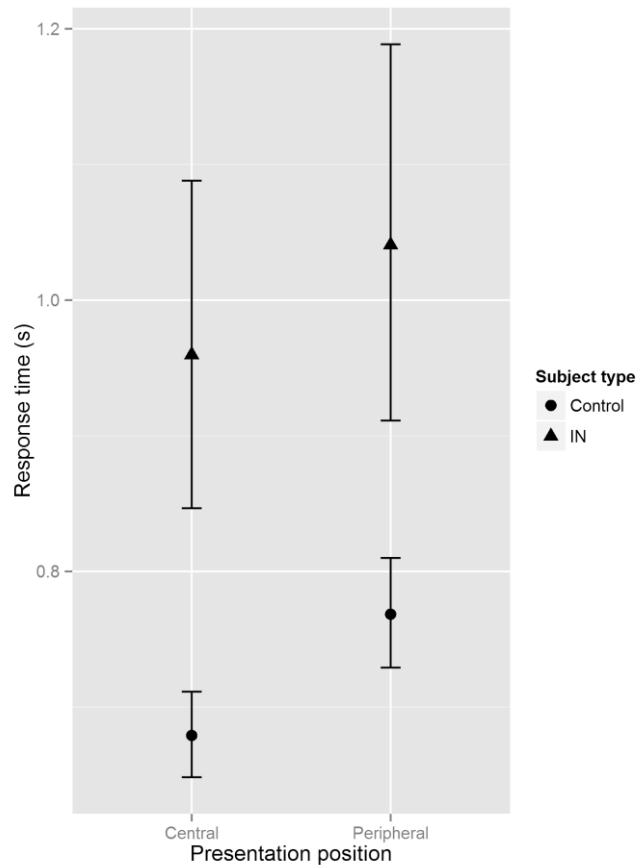


Figure 4.5: The effect of central or peripherally presented gratings on subject response time in subjects with and without IN. Error bars indicate standard error.

Welch two samples t-tests indicate that subjects with IN took significantly longer to respond than controls for centrally presented gratings (IN: 0.96 s [95% CI 0.75 – 1.23 s], controls: 0.68 s [95% CI 0.62 – 0.74 s], $p = 0.023$). For peripherally presented gratings, the difference between controls and nystagmats did not reach significance (IN: 1.04 s [95% CI 0.80 – 1.35 s], controls: 0.77 s [95% CI 0.69 – 0.85 s], $p = 0.054$).

Paired samples t-tests indicate that control subjects took significantly longer to respond to peripherally presented gratings than centrally presented gratings ($p = 0.00029$). However, whether gratings were presented centrally or peripherally made no significant difference to the speed of response in subjects with IN ($p = 0.30$). The lack of a significant effect in nystagmats may be due to the variability of response times in this group.

4.3.3 Horizontal vs vertical presentation

Figure 4.6 shows the median response times for horizontally vs vertically presented peripheral grating targets for subjects with and without IN.

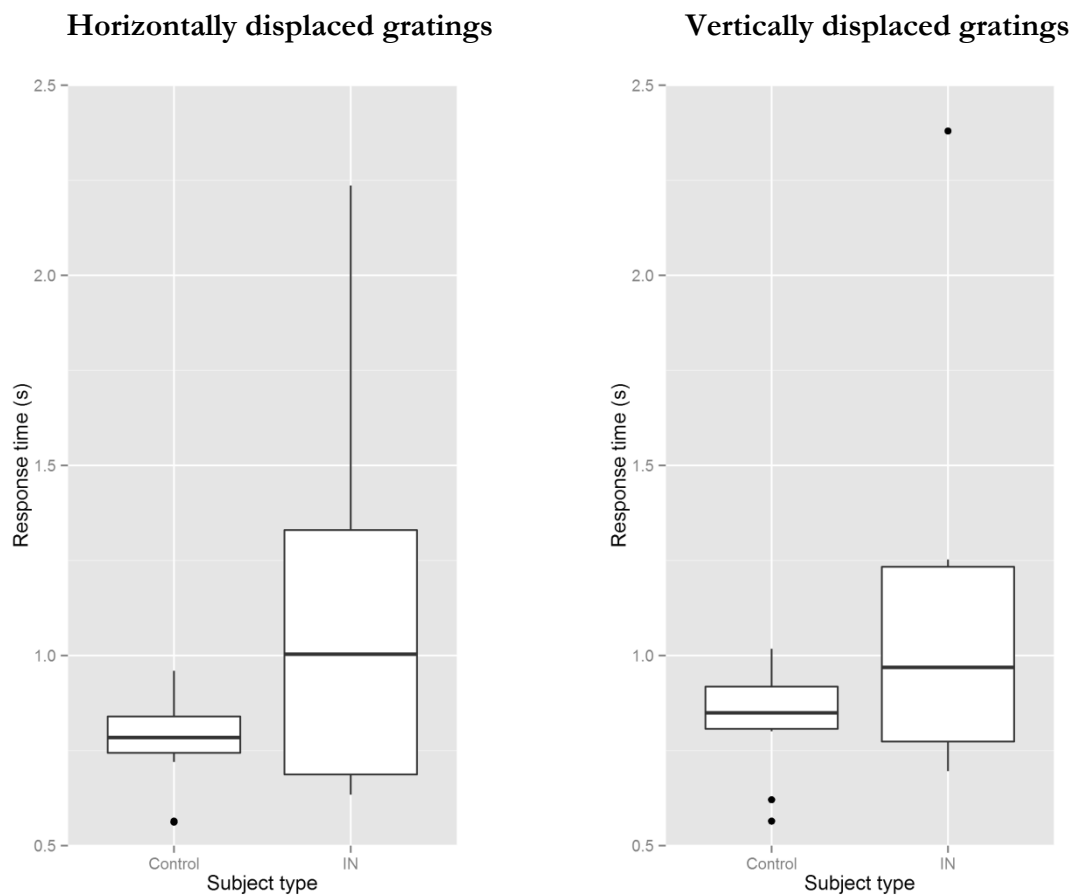


Figure 4.6: Box plots showing the effect of horizontally or vertically displaced gratings on subject response time in subjects with and without IN. Outliers are displayed as black dots.

Response time data for subjects with IN were not normally distributed (Shapiro-Wilk test $p < 0.05$), and could not be normalised through the use of a logarithmic transformation. Therefore, non-parametric statistical analyses were applied to the data.

Control subjects exhibited a median increase in response time of 34.7 ms for vertically displaced gratings as compared to horizontally displaced gratings, whilst nystagmats had the opposite effect, taking 65.0 ms longer for gratings displaced in the *horizontal* axis. Wilcoxon signed-rank tests indicate that both of these differences in response time are statistically significant (controls: $p = 0.0029$, IN: $p = 0.042$).

4.3.4 Time to fixate vs time to respond

For subjects with IN, a total of 241 vertically displaced grating presentations occurred with a correct response. Of these, 127 had target-acquiring saccades successfully identified using the automated algorithm (53%). For control subjects, this number was 232/257 (90%). Section 4.3.8 discusses the reasons for which automated saccade detection failed in some instances.

For these successfully identified vertical target acquiring saccades, Table 4.1 shows for each participant the mean time taken to execute the saccade and the mean time from the end of

the saccade until the response was made. Note that the mean values presented in Table 4.1 are derived from differing numbers of observations, as shown in the table.

Table 4.1: From response data for which saccade detection was possible, the mean time until execution of the vertical target acquiring saccade and the mean time from saccade termination until subject response. The number of recorded observations for each participant are shown.

Control subjects				Subjects with IN			
Subject initials	Mean time to saccade start (s)	Mean time from saccade end to response (s)	Number of observations analysed	Subject initials	Mean time to saccade start (s)	Mean time from saccade end to response (s)	Number of observations analysed
FE	0.1835	0.6315	30	DB	0.3706	0.5315	8
JG	0.1769	0.8112	20	DP	0.2471	0.4367	20
JMW	0.2464	0.6036	19	DT	-	-	0
JTE	0.1873	0.6009	26	GT2	0.5716	0.6436	22
MD	0.1389	0.3969	18	JC2	-	-	0
NH2	0.1874	0.6424	22	JS	0.4573	2.3707	18
RE	0.3132	0.6749	19	LC	0.2409	0.4997	19
ROD	0.2341	0.6261	15	NB	0.2018	0.9861	18
SH2	0.1870	0.6635	20	RC	0.2118	0.4211	6
SS	0.1908	0.4107	21	RD	-	-	0
TM	0.1921	0.5831	22	SW	0.2472	0.7949	16

The *time to saccade start time* data do not exhibit similar variance between subject groups (F test $p < 0.05$). Logarithmic transformation of these data corrected for this. However, the *time from saccade end to response* data were not normally distributed (Shapiro-Wilk test $p < 0.05$), and could not be normalised through the use of logarithmic or reciprocal transformations. Therefore, parametric statistical analyses were applied to the *time to saccade start time* data, whilst non-parametric analyses were used when interpreting *time from saccade end to response*. Figures 4.7 and 4.8 show the data from Table 4.1 graphically. Note that Figure 4.7 displays back-transformed means, as used for statistical analysis.

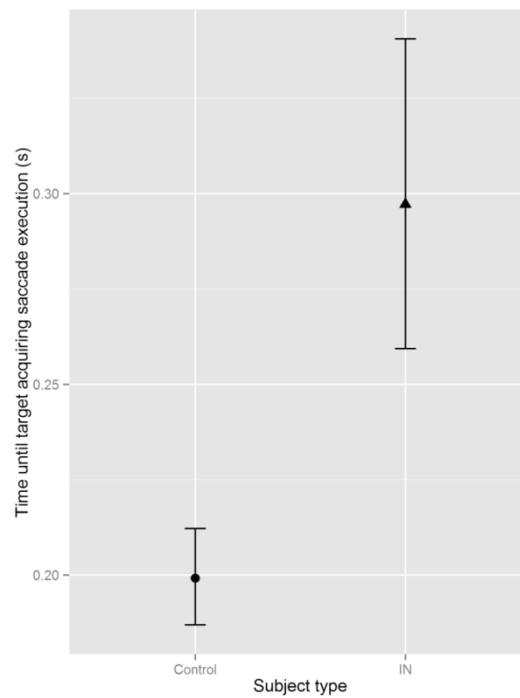


Figure 4.7: For vertically displaced grating targets, the average time taken for a target-acquiring saccade to be executed. Note that not all target displacements were associated with a detected saccade.

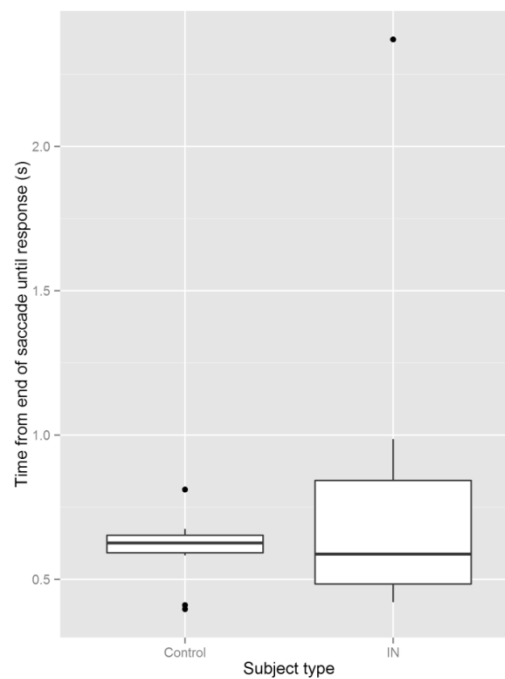


Figure 4.8: For vertically displaced grating targets, the time taken from completion of the target-acquiring saccade until the response was made by the subject. Note that not all target displacements were associated with a detected saccade. Outliers are displayed as black dots.

Welch two samples t-tests indicate that subjects with IN took significantly longer than controls to execute saccades towards vertically displaced gratings (IN: 0.30 s [95% CI 0.23 - 0.39 s], controls: 0.20 s [95% CI 0.18 – 0.23 s], $p = 0.024$). However, a Mann-Whitney U test shows no significant difference between the groups in the median time taken to respond *after* moving the eyes towards the gratings (IN: 0.59 s, controls: 0.63 s, $p = 0.78$). An F test indicates that there was significantly more variance in the response times following the saccadic EM in nystagmats ($p = 1.02 \times 10^{-5}$).

4.3.4.1 Left vs right; above vs below

Paired samples t-tests indicate that there was *no* significant difference in the time taken to execute saccades to targets located to the left vs right of the fixation point in controls, and no significant difference in the time taken to execute saccades to targets above vs below fixation in both controls and nystagmats (all $p > 0.05$). Similarly, there was no significant effect for the response times following target acquisition in any of these groups (all $p > 0.05$). Left/right comparisons were not made for nystagmats due to the inability to distinguish the time of the acquiring saccade (see Section 4.2.4). Using larger target jumps, Wang and Dell'Osso (2007) have previously noted that *horizontal* position (left vs right) made no difference to saccadic acquisition time in nystagmats.

4.3.5 Horizontal vs vertical fixation and response times in controls

Whilst it was not possible to detect saccades to horizontally displaced targets for nystagmats (see Section 4.2.4), no such difficulties were faced for the data collected from controls. In the interests of completeness (and to further investigate the finding that controls took longer to respond to vertical displacements than horizontal), the saccadic initiation latency and response times for these instances were also analysed. Out of a total of 253 horizontally displaced grating presentations with a correct response, 223 (88%) had their targeting saccade identified by the automated algorithm. Figures 4.9 and 4.1 show the relative differences in the time taken to initiate a target acquiring saccade and to make a response (after saccade termination) for control subjects for both horizontally and vertically displaced gratings.

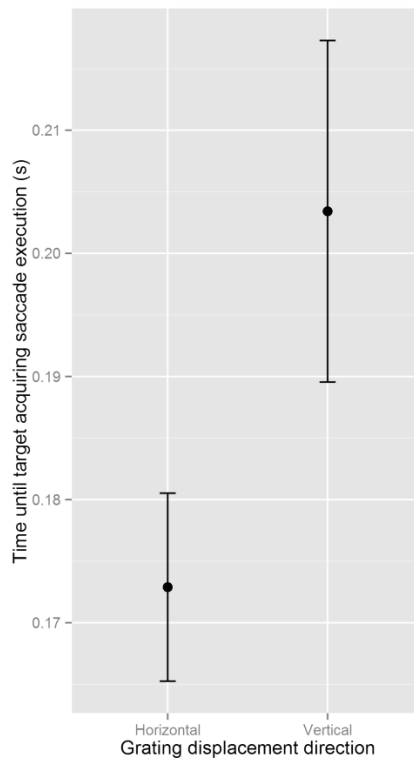


Figure 4.9: For control subjects, the time taken for a target-acquiring saccade to be executed towards horizontally or vertically displaced gratings. Note that not all target displacements were associated with a detected saccade. Outliers are displayed as black dots.

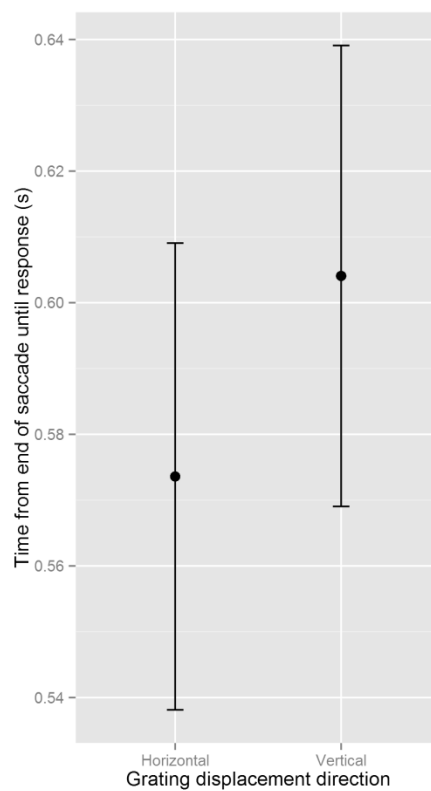


Figure 4.10: For control subjects, the time taken from completion of the target-acquiring saccade until the response was made by the subject for horizontally or vertically displaced gratings. Note that not all target displacements were associated with a detected saccade. Error bars indicate standard error.

Paired samples t-tests indicate that control subjects took significantly longer to initiate saccades towards vertically displaced gratings than horizontally displaced gratings (horizontal: 0.17 ± 0.03 s, vertical: 0.20 ± 0.05 s, $p = 0.0014$), as well as taking longer to respond to these targets once the saccade has terminated (horizontal: 0.57 ± 0.12 s, vertical: 0.60 ± 0.12 s, $p = 0.026$).

4.3.6 Effect of age

The effect of participant age on the response times obtained for all stimuli by *all* participants are shown in Figure 4.11.

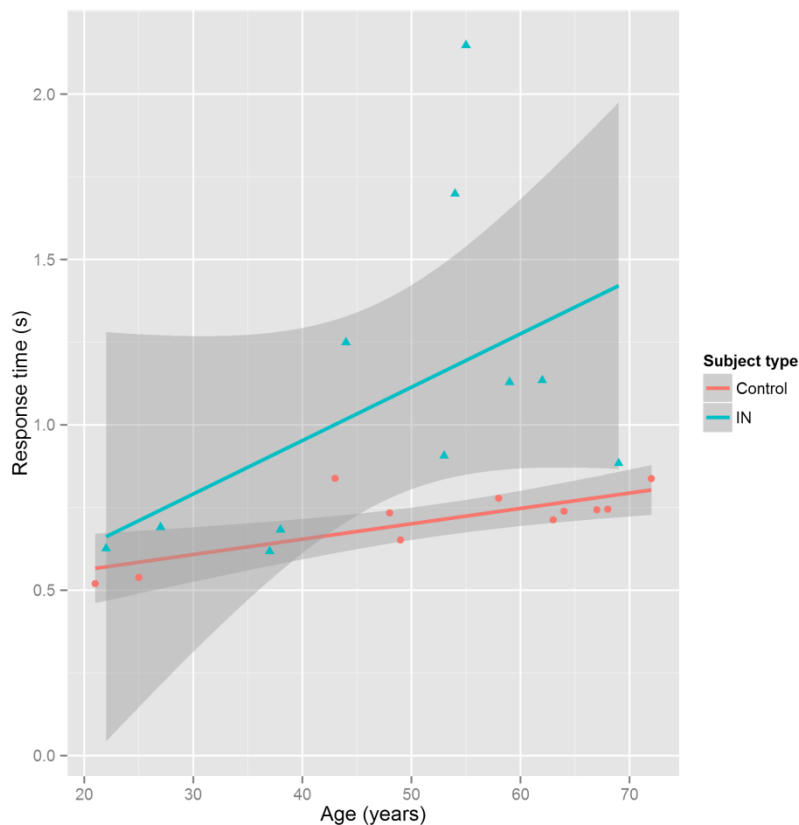


Figure 4.11: Scatter plot showing the effect of age on response times to all stimuli in nystagmats and control subjects. Regression lines and 95% confidence intervals (shaded areas) are shown.

Linear regression models indicate that age did *not* significantly affect response time in nystagmats ($p = 0.12$), whereas it *did* significantly affect the response times of control subjects ($p = 0.0061$). Presumably, the increased variance of the IN data (F test $p < 0.05$) accounts for the lack of a detectable age effect in these subjects.

4.3.7 Effect of learning/fatigue

Eight control subjects and one subject with IN underwent the third part of the experiment (see Section 4.2.3.3), which essentially repeated the protocol of the first part in order to determine whether a learning/fatigue effect is likely to have influenced the study results. Paired samples t-tests comparing the response times obtained for these subjects in the first and third parts of the experiment indicate that there was no significant learning/fatigue effect during the course of the experiment ($p = 0.61$). It is assumed that this effect ought to be similar for subjects with IN as in control subjects.

4.3.8 Instances in which automated analysis failed

The relatively small target jump size (3°) occasionally made saccade detection difficult. In nystagmats with a large orthogonal component to their waveform, the target-acquiring saccade was sometimes undetected, since the *Behrens, Mackeben and Schröder-Preikschat* saccade detection algorithm seeks fluctuations in eye position which can be masked by regular nystagmoid oscillations. A similar problem was encountered in the analysis of Chapter 5; see Section 5.3.7.2 for more detail.

Some saccades were also missed simply due to dropped data or blinks occurring around the time of the saccade; this accounts for the missed saccades in control subjects.

4.4 Discussion

Wang and Dell'Osso (2007) demonstrated that the presence of IN increases the time taken to direct gaze towards objects of interest. The results of the present study confirm this finding, but also indicate that IN does *not* affect the time taken to process visual information following target acquisition. In other words, any visual 'timing' delays arise solely as a result of an increased saccadic latency, rather than impaired visual processing *per se*.

This finding sheds new light on the perceptual experience of IN. The presence of a gaze targeting difficulty, rather than slowed visual processing, suggests that the ideal outcome of therapeutic intervention ought to be an improvement in oculomotor targeting speed. The work presented in Chapter 3 indicates that spatial vision (i.e. VA) is unlikely to improve with intervention, possibly due to bilateral amblyopia. The subjective improvements to visual function that some patients report following surgical intervention (Hertle et al. 2003) might therefore be explained by a decrease in gaze acquisition time.

In control subjects, age exerted a significant influence on response times. In order to control for this effect, normally-sighted subjects deliberately came from a similar age range as the

nystagmats (controls ranged from 21-72 years with a mean age of 53; nystagmats ranged from 22-69 years with a mean age of 48). Comparison of the response times of eight control subjects between the first and third parts of the experiment indicated that the study was unlikely to have been affected by a learning/fatigue effect.

The finding that controls took significantly longer to make targeting saccades towards vertically displaced targets than horizontally displaced targets was not unexpected, since saccadic latency is known to be longer for elevation and depression than for adduction and abduction (Thomas 1969). Figures 4.9 and 4.10 indicate that the increased delay for responses to vertically presented targets (as compared with horizontally presented targets) is due to a combination of an increased saccadic latency *and* an increased recognition time once the target had been acquired. It is not clear why response times following saccadic acquisition were significantly longer for targets displaced in the vertical axis. This finding has no counterpart in the literature and thus may require further work to fully understand. It is also interesting to note that nystagmats took longer (overall) to respond to horizontally displaced targets than to those that were displaced vertically. Understanding the reason(s) for this (and why this relationship is the exact opposite to that seen in controls) will require an analysis of horizontal saccade initiation time, which is not possible for the small target jump sizes used in this experiment. It would be therefore be wise to repeat the study with larger target jumps, and a greater number of participants in order to increase statistical power.

In both subject groups, centrally presented gratings were recognised more quickly than those that were presented peripherally. This too was not unexpected. However, the fact that nystagmats were shown to take *no longer than controls* to recognise vertically displaced visual targets once they had been 'acquired', yet took significantly longer (0.28 s longer) than controls to respond to *centrally* presented targets would suggest that the centrally presented targets were not foveated immediately. Rather, it seems likely that a latency between the grating appearance and the next foveation period could have introduced this discrepancy in the response times of the two groups. This is significant, as it demonstrates a mechanism by which nystagmats could be 'slow to see', even when viewing static scenes.

Since the results of this study indicate that there is no delay in visual processing in IN, it seems reasonable to suggest that an appropriate test of visual function would *not* need to include a perceptual measure of timing; rather, a measure of saccadic acquisition latency ought to be sufficient to capture all the relevant information related to the visual timing deficit.

4.4.1 Limitations

4.4.1.1 Simon effect

The nature of the task (judging tilt and responding with the left or right hand) may have occasionally been confusing. Where targets were displaced to the left or right, subjects may have accidentally responded to the *position* of the gratings rather than the *orientation*. In order to circumvent this potential problem, subjects were given clear instruction prior to beginning this part of the study, and in fact, no subjects reported this being a source of confusion. Nonetheless, it is known that response times for tasks involving spatially displaced stimuli may be increased if the required response does not correlate with the spatial location of the stimulus, even when stimulus position is irrelevant to the task. This is known as the ‘Simon effect’ and is potentially applicable to the results of the present study (Simon and Wolf 1963; Simon and Rudell 1967). However, since confusion may only have arisen from the left/right tilt decision, there is no reason to suspect that the Simon effect would have had an effect on the response speeds for grating displacements in the vertical axis.

4.4.1.2 Variable spatial frequency

The spatial frequency of the sine wave gratings was adjusted to the subject’s binocular VA + 0.30 logMAR, in order to make the task equally difficult for all participants. However, this may still have had an influence on the results of the study. It is worth noting that saccadic latency towards a Gabor patch is known to be influenced by the spatial frequency of the patch, with higher spatial frequencies eliciting slower targeting saccades (Ludwig, Gilchrist and McSorley 2004). Thus, it is possible that the saccadic latencies of control subjects were increased by the generally higher spatial frequencies of the gratings used in these subjects. Nonetheless, control subjects still exhibited significantly faster target acquiring saccades than those with IN.

In addition, the Gabor patches used were bounded by a Gaussian transparency envelope with a standard deviation of 0.25° for *all* participants. This was kept constant in order to demand the same amplitude of targeting saccades from all participants. However, since the spatial frequency of Gabor patches varied, a different number of grating cycles would have been visible depending on the VA of the participant. The participant in this study with the poorest VA (subject DT; 0.92 logMAR) viewed grating stimuli with an angular subtense of 1.81 cycles/ $^\circ$. It is impossible to say exactly how many cycles were visible for this subject due to the Gaussian envelope of the Gabor patch; however, it is quite possible that this subject

may have had greater difficulty in performing the task due to less visible cycles within the patch.

4.4.1.3 USB buffer latency

The Microsoft SideWinder game pad response device uses a USB connection which, due to the use of a buffer, introduces a variable signal transmission latency of up to 1 ms. In reaction time experiments, variable latency inevitably leads to an increase in response time variability, potentially reducing the likelihood of detecting real timing effects statistically. However, previous work has demonstrated that the quantisation effect of clocks with resolution as poor as 30 ms is negligible in human reaction time experiments, because the variability of human response times far exceeds this (Ulrich and Giray 1989).

4.4.1.4 Subject numbers

Human response time experiments yield inherently variable results. The fact that subjects with IN exhibited significantly more variance in their response times than controls indicates the value of large sample sizes for performing statistical analyses. Statistical power would have been improved by increasing the sample sizes. For example, as explained in Section 4.3.2, independent samples t-tests indicated no significant difference between the response times of controls and nystagmats for peripherally presented targets ($p = 0.054$). The lack of an effect at the 5% significance level is difficult to explain, but the near-significance suggests that a larger sample size would be useful to determine whether or not this is a real effect.

4.4.2 Future work

4.4.2.1 Effect of near damping

As mentioned in Section 4.2.5.2, some participants performed the study at two distances: 80 cm and 2 m. The aim of this paradigm was to investigate the effects of the ‘convergence null’ exhibited by some subjects with IN (see Section 1.3.8.2). However, the effects of presbyopia increased response times, even in control subjects. Nonetheless, it may be possible to repeat this paradigm, simply omitting subjects with amplitudes of accommodation less than 2.50 D (a stimulus at 80 cm demands 1.25 D of accommodation, and an amplitude of accommodative reserve greater than or equal to double the accommodative demand is typically considered sufficient for comfortable viewing [Elliot 2003]). Alternatively, since accommodative convergence is not believed to be a factor in the convergence nulls of nystagmats (Dickinson 1986), it may be possible to justify the use of reading additions for near viewing in presbyopic subjects.

4.4.2.1 Number of nystagmus cycles before response

Notice that the average increase in response latency for nystagmats for centrally presented gratings (0.28 s; as compared to controls) could reasonably be explained as the duration of a single nystagmus cycle (at 3.6 Hz). For peripherally presented gratings, it should be possible to investigate the number of nystagmus cycles that occur after target acquisition, but before a response is made. This would require custom software which could be based on the functions developed for Chapter 2, and might uncover the number of ‘snapshots’ that individuals with IN require before being confident in their visual responses.

4.4.2.2 Larger grating displacements

Figure 4.4 illustrates the problem faced in attempting to detect target-acquiring saccades in the horizontal axis for small target displacements. For this reason, horizontal saccades were not analysed for subjects with nystagmus in the present study. However, for some subjects with low amplitude nystagmus, this may still have been possible. Figure 4.12 shows an example of one subject (KL) for whom this may be an option. Nonetheless, the inability to apply this analysis to all subjects is somewhat limiting. A simpler solution may simply be to repeat the experiment with larger grating displacements.

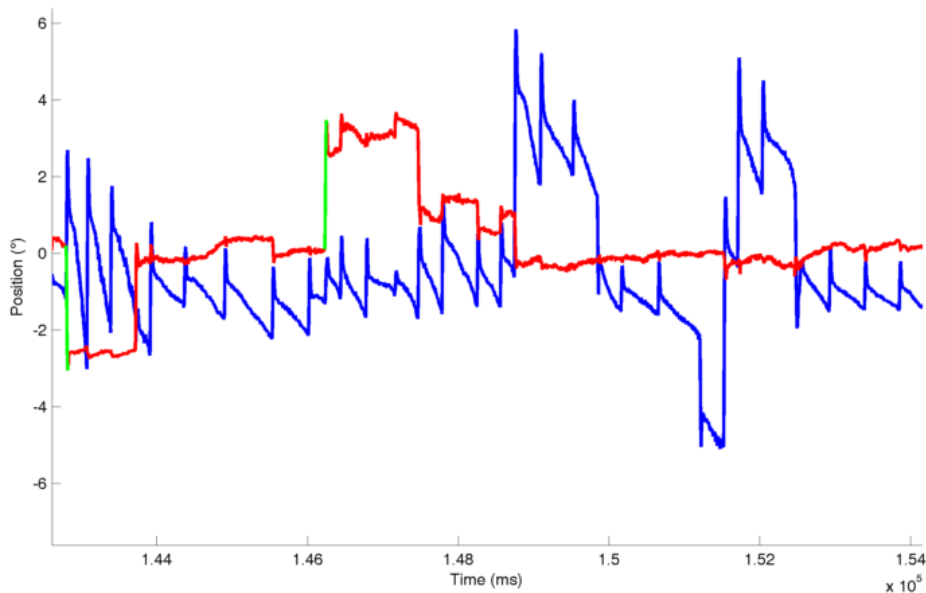


Figure 4.12: EM trace showing horizontal eye position (blue) and vertical eye position (red). Targeting saccades identified in the vertical axis are marked in green. Unlike Figure 4.4, this subject has low enough nystagmus amplitude that automated saccade detection may be feasible in the horizontal axis.

4.5 Summary

The work presented in Chapter 3 strongly suggests that therapies aimed at reducing the EMs of IN are unlikely to elicit significant improvements in VA. The results of the present chapter show that nystagmats take considerably longer than control subjects to execute saccades towards objects of interest; a finding that has been demonstrated previously in four individuals (Wang and Dell’Osso 2007). In addition, the present chapter provides new evidence that *visual processing in IN is not slow*. Taken together, it is possible to posit that the visual impairment experienced by individuals with IN stems from a combination of poor underlying VA and difficulty in redirecting the gaze towards objects of regard in a timely manner. Based on this evidence, it is gradually becoming clearer why situations such as “finding a person in a crowd” (Jones 2011) are so troublesome for the patient affected by IN.

During the analysis of EM traces obtained for this study, an unexpected and interesting observation was made. Almost every voluntary vertical saccade elicited by individuals with IN appeared to be accompanied by a simultaneous horizontal nystagmus quick phase. The chapter that follows details further investigation into this incidental finding that may shed light on the extent to which the involuntary EMs of IN can be subconsciously controlled.

Chapter 5 Interaction and timing of voluntary and involuntary saccades

5.1 Introduction

Although IN causes involuntary oscillations of the eyes, affected individuals are generally unaware of the EMs occurring on a moment-by-moment basis (Cham, Anderson and Abel 2008a). Therefore, both the slow and quick phases are usually considered to be involuntary. However, since quick phases usually realign the fovea with the object of regard, they can be considered as a corrective EM. Two previous studies have looked at the temporal relationship between voluntary saccades and the ‘involuntary’ quick phases of nystagmus (Wang and Dell’Osso 2007; Worfolk and Abadi 1991). Another established that individuals with jerk nystagmus sometimes extend their slow phases to acquire targets rather than making saccades (Bedell, Abplanalp and McGuire 1987). Each of these studies only looked at EMs in the horizontal plane. Since all their participants had horizontal nystagmus, the voluntary and involuntary saccades analysed in these studies occurred in the same axis, and hence, the opportunity to compare voluntary and involuntary saccades in relative isolation was missed. Are quick phases combined with voluntary saccades, do they occur separately, or is one substituted for the other? It seems feasible that there might be no distinction between the two at all. Understanding this will undoubtedly inform our understanding of the oculomotor pathology that underlies IN.

Inspiration for the present study came during the analysis of the data in Chapter 4. Whilst examining the saccadic target acquisition timings in the vertical meridian, it was noted that vertical saccades often occurred in synchrony with a horizontal nystagmus quick phase. This prompted a thorough investigation into the temporal relationship between the horizontal and vertical aspects of these saccades.

This finding has not previously been reported in the literature. One possible reason for this relates to the type of equipment typically employed for EM studies. Although eye trackers that record both horizontal and vertical EMs have been available for some time, much of the nystagmus literature either reports findings obtained using uniaxial eye trackers (such as the Skalar IRIS system [Section 1.4.3.1]) or data that were only *analysed* in the primary axis of nystagmus.

Since a thorough review of the literature revealed no existing report of this phenomenon, the following chapter is, to the author's knowledge, the first time this interaction has been investigated.

5.1.1 Aims

The primary aim of the present study was to determine how often voluntary vertical saccades are combined with horizontal quick phases in individuals with early-onset nystagmus. A secondary aim was to identify the 'driving force' behind this coordination; i.e. to understand whether the timing of the voluntary saccade is modified to 'ride' the nystagmus, or the nystagmus waveform is modified to ensure that a quick phase occurs at the time of the saccade. To this end, parameters of the nystagmus waveform (amplitude and cycle length) *at* the time of target-acquiring saccades were compared to waveform parameters *prior to* target acquisition.

5.2 Materials and methods

5.2.1 Participants

Seventeen subjects with early-onset nystagmus were recruited for the study from the Cardiff *Research Unit for Nystagmus* cohort.

5.2.2 Procedures

Subjects were seated in a room lit at $\sim 1.78 \log \text{ cd/m}^2$, 2 m from a Sony GDM-F520 21" CRT monitor (see Section 2.2.4). The chin and head were supported by a rest (see Figure 3.7), and subjects were encouraged to adopt a comfortable position in order to view the screen. Subjects wore their habitual refractive correction (if any), and viewed the monitor binocularly. Binocular EMs were recorded by an EyeLink 1000 (see Section 1.4.3.3). On a mid-grey background, a simple black cross was displayed in the centre of the screen (see Figure 2.19 for details). Subjects were instructed to view the cross, which stepped after a random delay of between 1-2 s to either 3 or 5° from the screen centre in one of four directions (up, down, left or right). After another random delay of 1-2 s, the target stepped back to the centre. Figure 5.1 illustrates the sequence of on-screen stimuli shown during the experiment. This process was repeated until all eight of the peripheral target positions had been presented at least 10 times. Peripheral target presentation order was randomised, with the target returning to centre between each peripheral location. Target jump times were recorded in the EM trace.

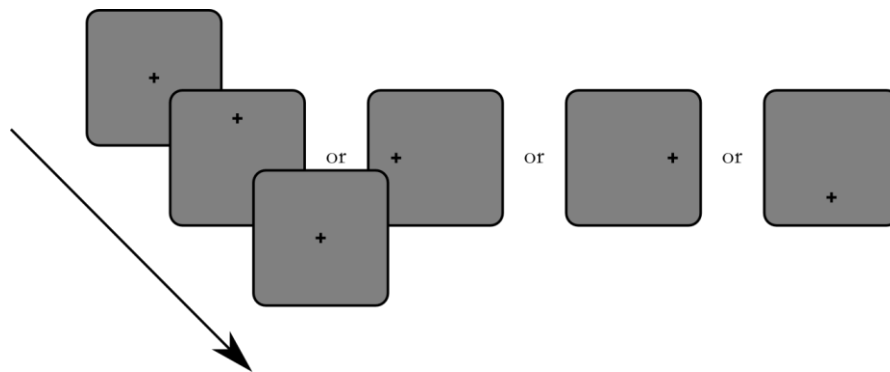


Figure 5.1: Schematic explanation of the sequence of stimuli presented on-screen. Note that two magnitudes of target displacement were used; only one is shown here for illustrative purposes.

5.2.3 Analysis

Data were analysed using custom-made software written in MATLAB (The MathWorks, Natick MA); the code is presented in Appendix I – *saccadetiming_analyse.m*. This software utilises many of the algorithms described in Chapter 2. Data from the subject’s dominant eye (as determined by a distance Mallett unit test) were used for analysis, or the right eye was used by default in the case of equidominance.

No attempts to calibrate the data were made since analysis only involved calculation of the timing of *changes* in eye position, rather than the use of absolute values.

5.2.3.1 Saccade detection

Since the primary aim of the present study was to determine the relationship between the timing of voluntary and involuntary saccades in nystagmus, only target jumps in the vertical axis were used for data analysis (despite the fact that the test stimulus moved in four directions²³). Given that most IN is primarily uniaxial (horizontal), this meant that vertical (voluntary) saccades were readily identified in the eye position trace. Saccadic detection was performed *separately* in each axis of the EM trace, so that the timing of each component could be determined independently and then compared.

²³ Horizontal target jumps were included in the study paradigm for three reasons:

1. To maximise data capture for potential future analyses
2. To reduce prediction of the upcoming target location
3. In case any study participants had primarily vertical nystagmus (in fact, none did)

In addition, participants completed a paradigm consisting of oblique target jumps. Data from this paradigm are not reported here.

Saccades in the axis orthogonal to nystagmus

Saccades in the vertical axis were identified using the same, established saccadic detection algorithm as used in the analysis of Chapter 4 (Behrens, Mackeben and Schröder-Preikschat 2010); see Section 2.1.5.1 for detail.

Saccades in the axis of nystagmus

Saccades in the axis of nystagmus (i.e. horizontal quick phases) were detected using the algorithm developed for Chapter 2. As described in Section 2.2.2.7, for this filter to work correctly, the EM trace data must solely contain attempted ‘fixation’ (albeit in the presence of nystagmus); if the data are contaminated by other (voluntary) EMs, the *saccadic velocity threshold* becomes erroneously high. For the current study however, the vertical and horizontal aspects of the EM trace were analysed separately. As a result, the saccadic filter could be applied, so long as non-nystagmoid horizontal EMs were removed from the data. To achieve this, all data collected during times at which the fixation cross was displaced in the *same axis as nystagmus* were removed. An extra 500 ms of data following each of the fixation cross’ returns to centre were also removed to allow time for subjects to reacquire the target. Figure 5.2 shows an example of the data regions removed in this way.

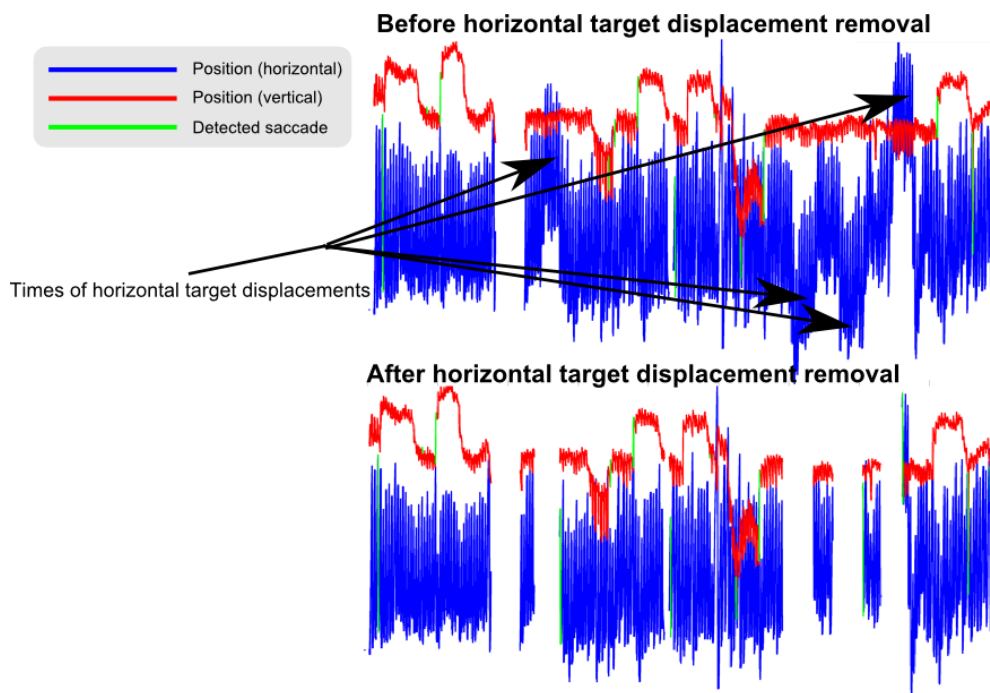


Figure 5.2: Diagram to illustrate regions of data removed in order to analyse target displacements solely in the vertical axis

The resulting EM traces contained target displacements solely in the vertical axis. In the horizontal axis, the only EMs present were assumed to represent pure nystagmus. Saccades in the horizontal axis (i.e. nystagmus quick phases) were then detected in the manner described

in Section 2.2.2.7. However, for the present study, only the major *quick phases* of nystagmus were sought (i.e. in waveforms with multiple saccades per cycle, only the saccade with the highest *peak velocity* in any given cycle was considered to be the ‘quick phase’). Figure 5.3 gives an example of a waveform for which this distinction had to be made. Of course, in order to determine this, a further stage of signal pre-processing was required: nystagmus *cycles* were isolated using the method described in Section 2.2.2.6.

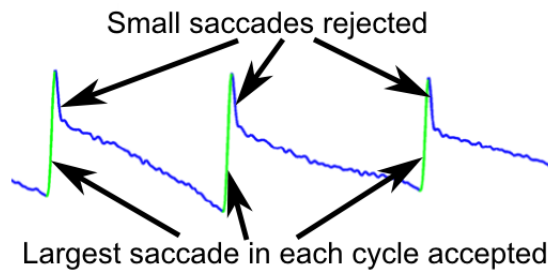


Figure 5.3: Illustration of a waveform containing multiple saccades in each cycle. Only the saccade with the highest peak velocity in each cycle is chosen to represent the 'quick phase'.

5.2.3.2 Saccade overlap detection

Having determined the times of horizontal and vertical saccades, the following metrics were determined for each vertical target displacement:

- Whether or not the vertical saccadic movement overlapped with a horizontal quick phase
- The latency of the voluntary saccade from the time of target displacement²⁴
- The time within the nystagmus cycle at which the target was displaced, measured from the end of the last quick phase²⁵
- For each voluntary saccade, saccade amplitude
- For each horizontal quick phase that coincided with a vertical target-acquiring saccade:
 - The amplitude of the quick phase
 - The amplitude of the last quick phase preceding the target jump²⁶
 - The latency of the quick phase (i.e. the inverse of instantaneous nystagmus frequency; measured from the end of the previous quick phase)
 - The latency of the last quick phase preceding the target jump from the one prior to that²⁶

²⁴ This metric is equivalent to **Lt** in Wang and Dell'Osso (2007)

²⁵ This metric is equivalent to **Tc** in Wang and Dell'Osso (2007)

²⁶ This metric was calculated to represent the nystagmus waveform *prior to* target acquisition.

Figure 5.4 illustrates the times from which some of the above metrics were calculated. Note that data shown in the figures are not calibrated, since the analyses only rely on *relative* changes in eye position.

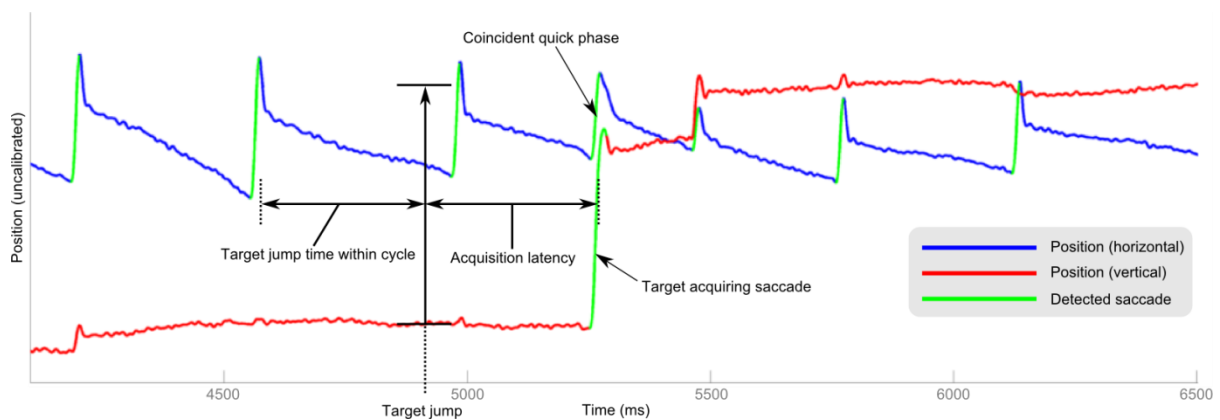


Figure 5.4: Example EM trace illustrating how some of the analysis metrics were determined

5.2.3.3 Missing data

For each target displacement, if any data were dropped (e.g. due to a blink) at any time between the *previous* target displacement and the *next* target displacement, no metrics were calculated for that target jump. This conservative method of data rejection ensured that only clean EM data were analysed.

The first three vertical target displacements were removed from the analysis of each participant. This provided a brief period in which subjects could familiarise themselves with the task. In addition, instances in which a target jump occurred during a nystagmus quick phase were removed from the analysis; this was done to simplify calculation of the time during the slow phase at which each target jump occurred.

5.2.3.4 Manual inspection

To confirm that saccade detection had been successful, the EM trace was manually inspected around the time of every target jump. If any saccades appeared to have been erroneously detected (either false positives or negatives), data from these target jumps were excluded from the final analysis. Examples of instances in which this was necessary are given in Section 5.3.2.

Statistical analysis of the resulting dataset was performed in the R Environment for Statistical Computing (R Core Team 2012).

5.3 Results

5.3.1 Participants and exclusions

Thirteen of the 17 individuals with early-onset nystagmus produced data suitable for analysis. The remaining participants had too much data dropped by the EyeLink 1000 during acquisition and/or the saccade detector failed to accurately detect saccades. Table 5.1 shows all of the participants who took part, along with their data capture rate. Additional biometrics are available in Appendix II. Subject JC only exhibited nystagmus in right-gaze, so was asked to orient the head turned to the left (in order to ensure nystagmus was present throughout the recording). Note that data capture rate doesn't necessarily correlate with the number of analysable target jumps, since analysis depends on the presence of *contiguous* data from the eye tracker. In some instances (e.g. subject JC2), some satisfactory periods of contiguous data were obtained, despite a low overall data capture rate. The last column indicates the number of target jumps that were used in the final data analysis; these are the trials for which the automatically-detected saccades were *not* manually rejected. Section 5.3.2 details why the saccade detection algorithm did not work in every instance.

Table 5.1: List of subjects who participated in the present study, along with the data capture rate, number of analysable target jumps (based on the presence of contiguous data), and number of target jumps that were used in the final analysis

Subject	Data capture rate (%)	Number of target jumps with contiguous data	Number of target jumps included in analysis
DB	69.5	0	0
DK	97.6	21	17
DP	97.1	32	16
DT	92.3	4	0
GS	98.6	31	15
GT2	97.3	43	31
GT	99.4	39	18
JC2	57.1	5	4
JC	99.5	51	46
JS	95.6	19	8
JT	93.9	19	8
KL	99.8	47	41
LC	99.7	48	19
NB	97.4	19	9
RC	81.0	0	0
RW	91.2	1	0
SW	100	20	6

5.3.2 Saccadic overlap

Having excluded each of the target jumps for which automatic saccade detection failed (see Section 5.3.7), the remainder of the target-acquiring saccades (for all subjects combined) had a coincident nystagmus quick phase on **80%** of occasions. Giving equal weighting to each participant, the average percentage of target jumps with a coincident nystagmus quick phase was 76%. In other words, **the majority of voluntary vertical saccades were combined with nystagmus quick phases** into a single oblique EM. Figure 5.4 above shows an example of this typical behaviour.

For those instances in which saccadic overlap was *not* detected, the waveforms often showed an extension of the slow phase and a small disturbance at the time of the vertical saccade. Figure 5.5 (subject DK) gives two examples in which such a disturbance is visible in the waveform, whilst the accelerating portion of the slow phase appears to have been suppressed. It is impossible to say whether this represents a failure of the saccade detection algorithm, whether the quick phases are present but dampened, or if there is no quick phase at all. Interestingly, in the lower of these two figures, the cycle detection algorithm (see Section 2.2.2.6) *did* identify a cycle boundary at the time of the disturbance.

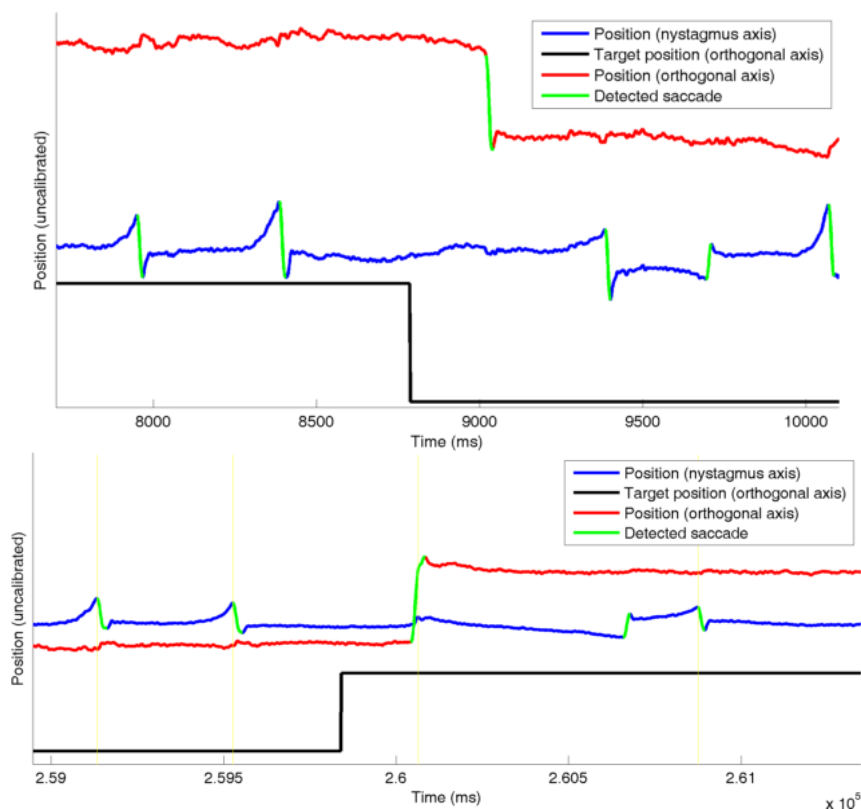


Figure 5.5: Examples of instances in which nystagmus quick phases were *not* detected as coinciding with vertical saccades, although visible inspection reveals small disturbances around the time that the quick phase would have been expected, as well as a lack of slow phase acceleration and an approximate doubling of slow phase length. The lower figure also shows an apparent change in nystagmus beat direction.

For one subject (LC), vertical target acquisition was occasionally performed by a fast drift, rather than a typical saccade (see Figure 5.7). This occurred in the case of *five* target displacements throughout the trial, and *only* in this subject. On these occasions, the horizontal eye trace did not exhibit a quick phase. Rather, the waveform changed to an *asymmetric pendular* type (see Figure 5.6), and target acquisition occurred during the faster portion of the waveform.



Figure 5.6: Schematic of an asymmetric pendular waveform (Dell'Osso and Daroff 1975).

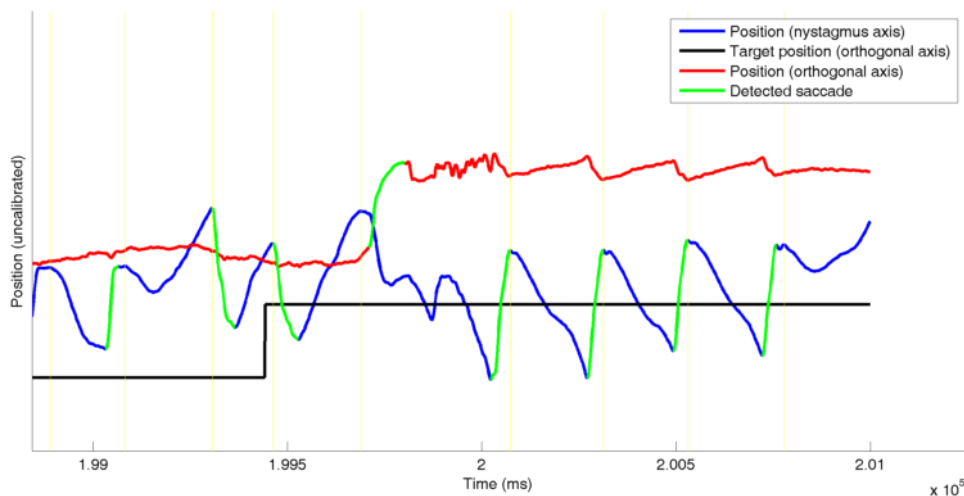


Figure 5.7: An example of target acquisition occurring with a fast drift (marked in green on the red eye trace) and modification of the waveform to asymmetric pendular type.

As explained above, most subjects made target acquiring saccades in conjunction with nystagmus quick phases (or displayed a dampened quick phase at the expected time of the quick phase as shown in Figure 5.5). However, in three subjects (DP, NB and SW), on very rare occasions a vertical saccade was made in the midst of a slow phase, after which the nystagmus cycle completed relatively unperturbed. Figure 5.8 shows examples of this behaviour. These saccades occurred *three* times in subject DP, *once* in subject NB, and *once* in subject SW. Note that both subjects NB and DP exhibit the waveform type *pseudo pendular with foveating saccades*, whereas SW has a typical *jerk with extended foveation* waveform. Note that for *every* other subject (with the exception of the fast drifts seen in subject LC discussed above), *every* instance in which quick phases and vertical saccades were not coincident exhibited small disturbances in the waveform and extended slow phases.

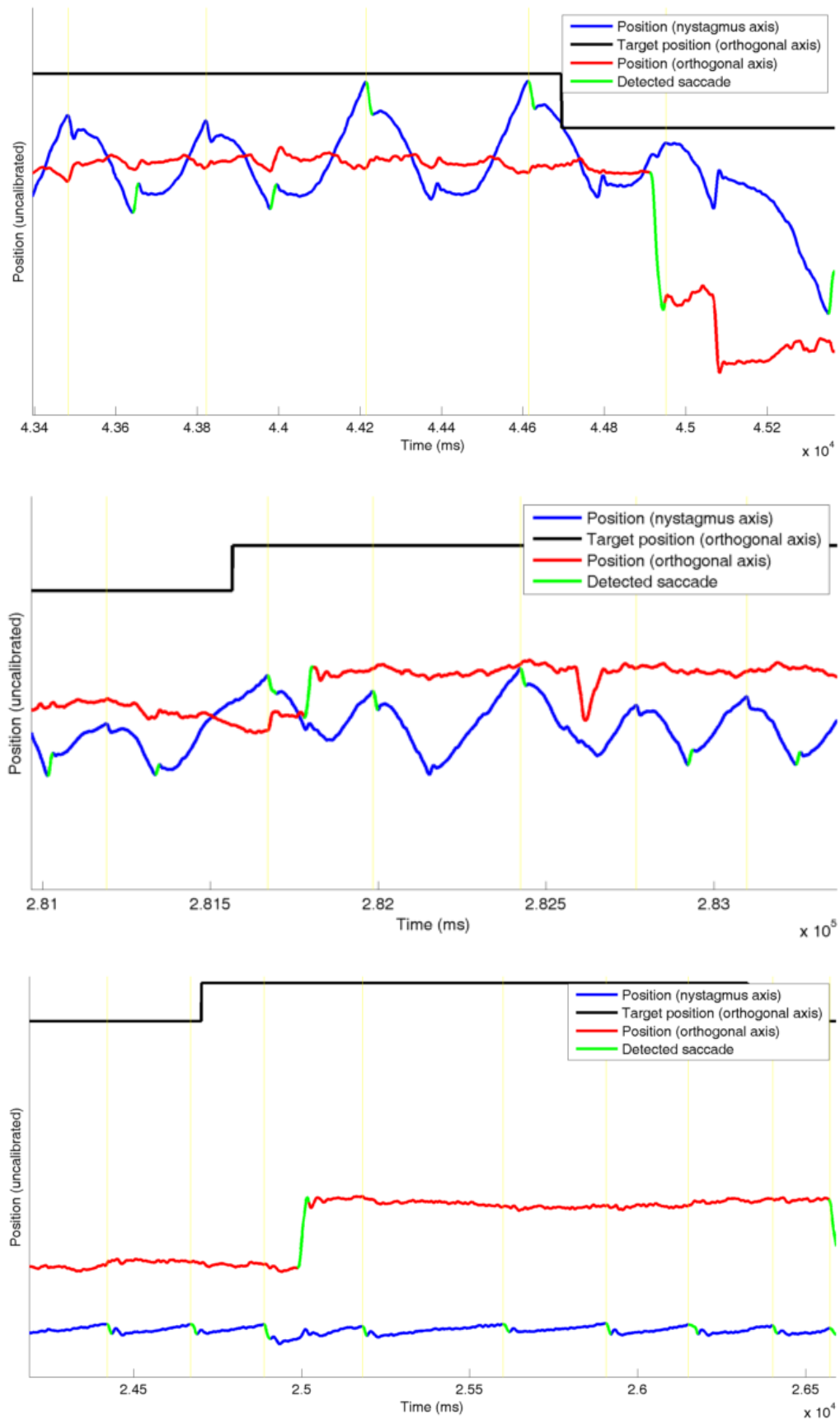


Figure 5.8: Examples of vertical target acquiring saccades occurring mid-slow phase. These occurred only rarely (top, subject NB; middle, subject DP; bottom, subject SW).

5.3.3 Changes to waveform metrics

Table 5.2 reports several quantitative properties of the nystagmus waveform both prior to the target jump and at the time of the target-acquiring saccade.

Table 5.2: Subject-specific saccadic metrics. Quick phase metrics are not shown for subjects DP and NB, as explained in Section 5.3.7.1.

Subject	Diagnosis	Number of target jumps included in analysis		Percentage of acquiring saccades that coincide with nystagmus quick phase	Acquiring saccade latency from target jump (ms)	Corresponding nystagmus quick phase amplitude (°)	Quick phase amplitude prior to target jump (°)	Corresponding nystagmus quick phase latency from previous quick phase (ms)	Inter-quick phase interval prior to target jump (ms)
DK	IIN	17	29	202	1.16	2.14	490	453	
DP	IIN	16	50	226	-	-	-	-	
GS	IIN	15	73	191	7.93	6.51	194	194	
GT	IIN	31	77	289	3.22	3.43	317	295	
GT2	IIN	18	100	1014	10.14	8.54	486	390	
JC	Unknown	46	98	225	5.09	4.96	349	314	
JC2	IIN	4	75	322	3.44	3.14	366	396	
JS	IIN	8	88	388	11.23	10.66	336	243	
JT	IIN	8	75	248	14.87	15.56	260	328	
KL	FMNS	41	98	249	1.36	1.44	462	469	
LC	IIN	19	58	287	8.12	6.72	315	258	
NB	Macular defect?	9	89	203	-	-	-	-	
SW	IIN	6	83	233	0.92	0.96	303	303	

5.3.3.1 Effect of voluntary saccades on quick phase amplitude

As described in Section 5.3.7.3, nystagmus amplitude appeared to occasionally be modified by the onset of a target jump. Figure 5.9 shows, for each target-acquiring saccade that had a coincident nystagmus quick phase, the relationship between the quick phase's amplitude and the amplitude of the last quick phase immediately preceding the target jump. This attempts to investigate the extent to which the saccadic task modified quick phase amplitude.

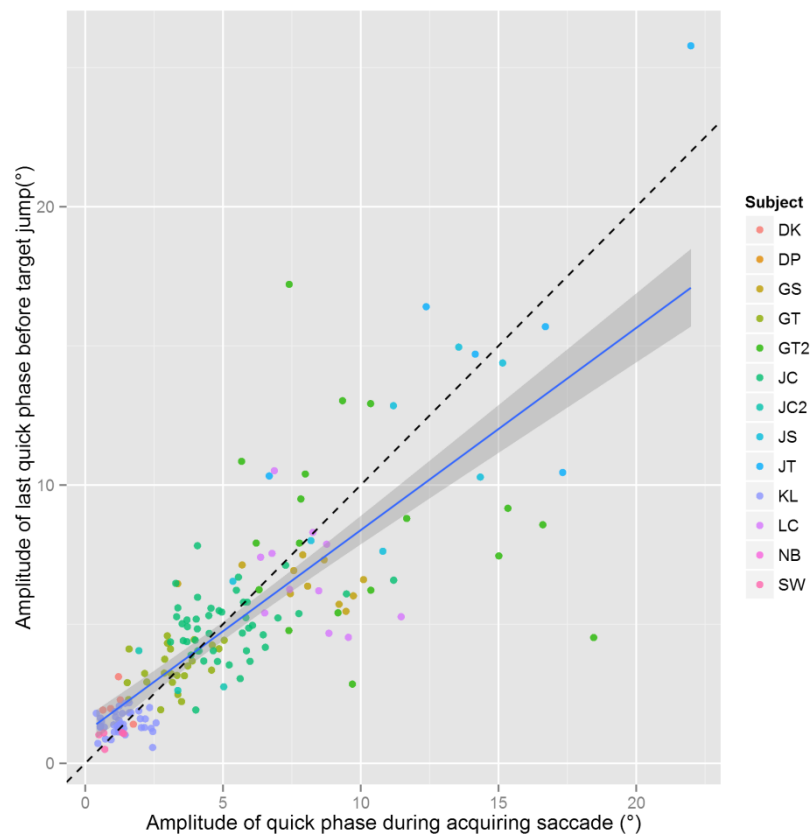


Figure 5.9: For coincident targeting saccades and quick phases, the relationship between the amplitude of the quick phase and the last quick phase to occur prior to the target jump. Regression line is shown (solid line); the shaded region indicates standard error. The dashed line represents the expected (1:1) relationship if there were no effect.

The slope of the regression line shown in Figure 5.9 is 0.89 (95% CI 0.79 – 0.99), indicating that nystagmus **quick phase amplitude is significantly reduced when occurring in conjunction with a voluntary vertical saccade** as compared to quick phase amplitude prior to a target jump.

5.3.3.1 Effect of voluntary saccades on nystagmus cycle length

Figure 5.10, like Figure 5.9, compares the quick phase at the time of the coincident targeting saccade with the last quick phase before the target jump. This time, the comparison is of nystagmus *cycle length*.

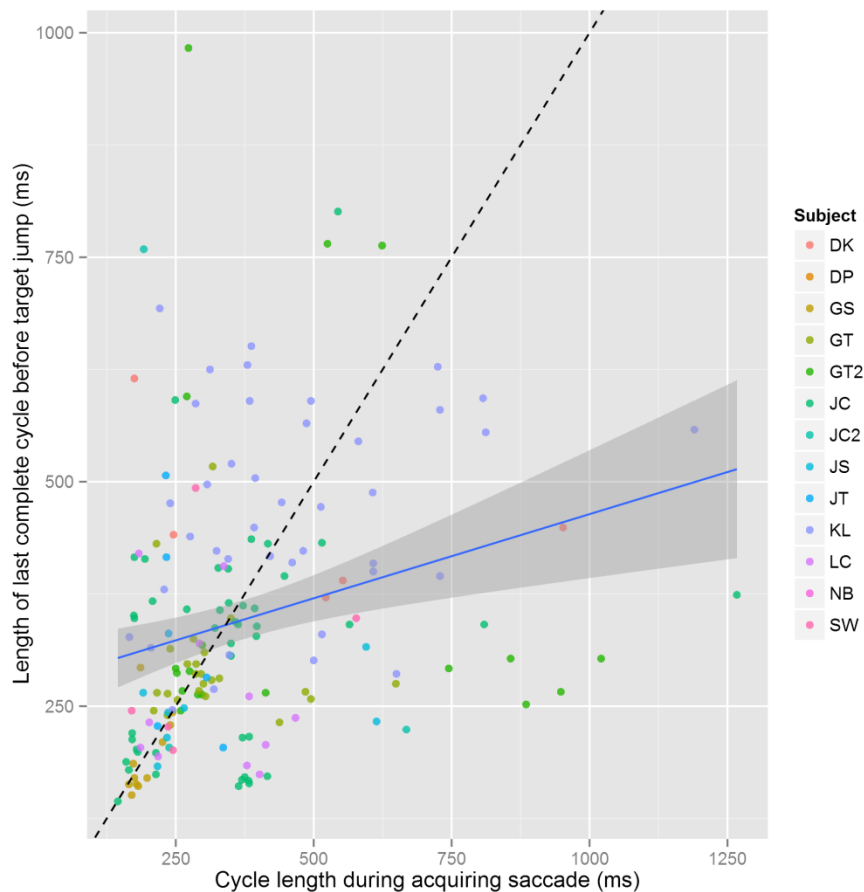


Figure 5.10: For coincident targeting saccades and quick phases, the relationship between the nystagmus cycle length at the time of target acquisition and the length of the last cycle to occur prior to the target jump. Regression line is shown (solid line); the shaded region indicates standard error. The dashed line represents the expected (1:1) relationship if there were no effect.

The data in Figure 5.10 have a regression slope of 0.34 (95% CI 0.14 – 0.53). This indicates that **nystagmus cycles containing a voluntary saccade were significantly longer** than those occurring immediately before the target jump.

5.3.4 Waveform modification prior to target acquisition

One subject in particular (GT2) repeatedly showed a marked change in nystagmus amplitude and waveform prior to target acquisition. Of all the participants in the experiment, this individual consistently took the greatest time to acquire the target (mean acquisition initiation time of 1014 ms, as opposed to 255 ms for the rest of the participants). Figure 5.11 shows an example of a target-acquiring saccade, made more than 1.5 s after the target jump. Notice that the waveform appears to change to a pendular type (i.e. it lacks a quick phase) for two cycles before the target-acquiring saccade is executed.

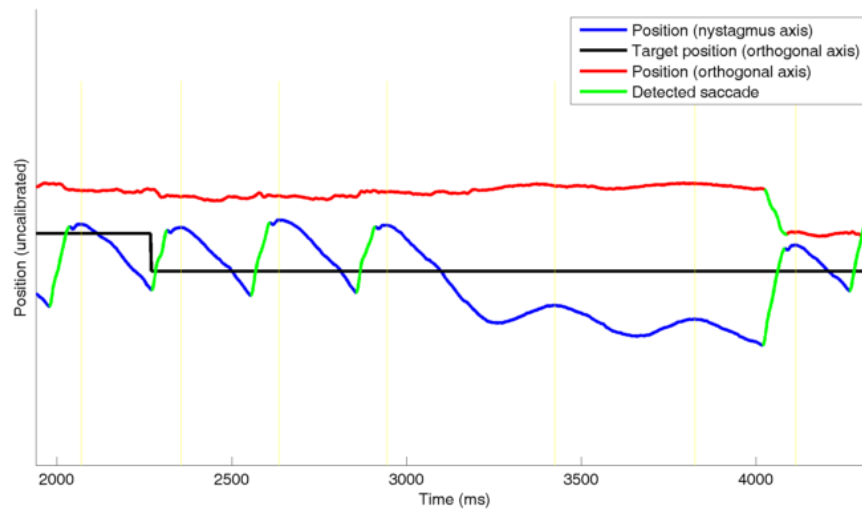


Figure 5.11: Results from subject GT2 show an obvious modification of the waveform prior to target acquisition. This feature was a common finding in this subject.

5.3.5 Waveform modification prior to target jumps

During analysis it was noted that one subject (JC)'s waveform occasionally changed to a pendular type in anticipation of upcoming target jumps. Presumably, this was done as an adaptation to the visual demand of the task, similar to that reported in Wiggins et al. (2007). Since target jumps occurred randomly with delays between 1 and 2 s, it seems feasible that some target jump anticipation could have occurred, especially as the delay approached 2 s. Figure 5.12 shows an example of this incidental finding. Note that JC was unique in this study as the only participant with no nystagmus in any position except right-gaze.

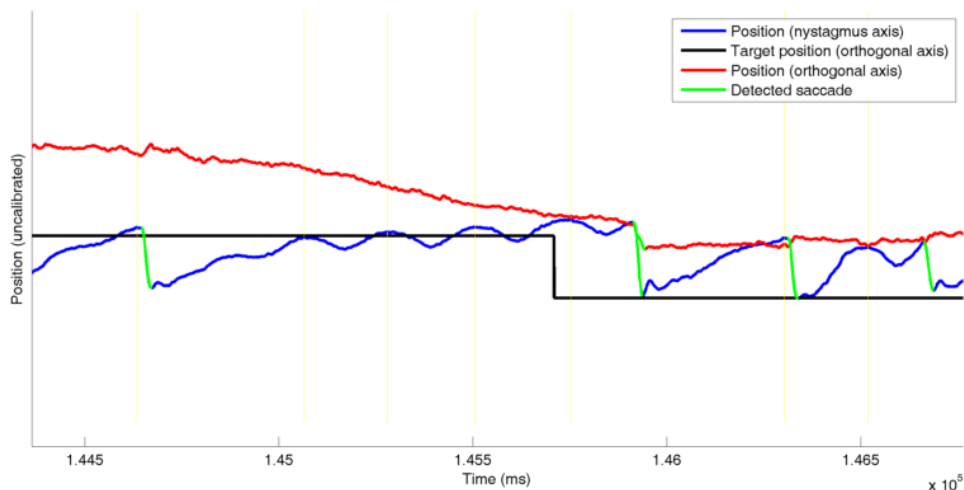


Figure 5.12: Subject JC exhibits a change to a pendular waveform *prior to* the target jump, possibly as an adaptation to improve visual function in anticipation of the jump.

5.3.6 Effect of target jump timing on targeting saccade latency

Figure 5.13 shows, for each subject, the effect of target jump timing (as a function of time since the last nystagmus quick phase) on the latency of the (vertical) target acquiring saccade.

Data plotted here are only from subjects with IN; subjects KL (FMNS) and JC (no nystagmus in primary position) are excluded in order to relate the results to the perceptual experience of IN, which is hypothesised to be continuous (rather than intermittent; see Section 1.3.9.1).

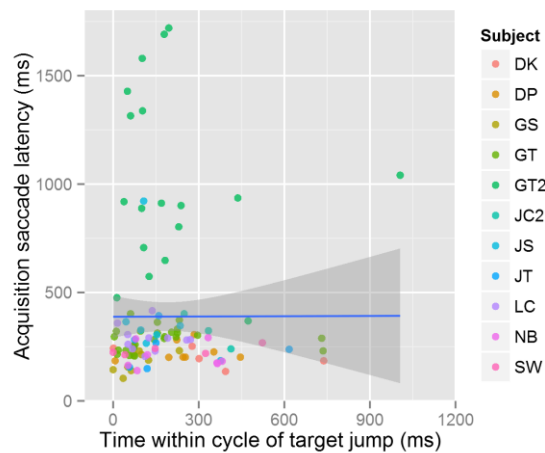


Figure 5.13: The effect of the timing of target jumps (with respect to the last nystagmus quick phase) on vertical saccade latency for subjects with IN. Regression line is shown; the shaded region indicates standard error.

The slope of the linear regression model for the data in Figure 5.13 has a p value of 0.98, indicating that the slope is not significantly different from zero. This suggests that the time during the nystagmus cycle at which the target jump occurred had no effect on the latency of target acquiring (vertical) saccades. However, these data are from multiple participants with varying nystagmus frequencies. In an attempt to normalise across subjects, Figure 5.14 shows the same data, with the abscissa expressed as a fraction: how far through the nystagmus cycle the target jump occurred, as a percentage of the total cycle length (measured to the first quick phase occurring after the target jump). The concept of ‘normalising’ cycle durations in this way was previously employed by Wang and Dell’Osso (2007).

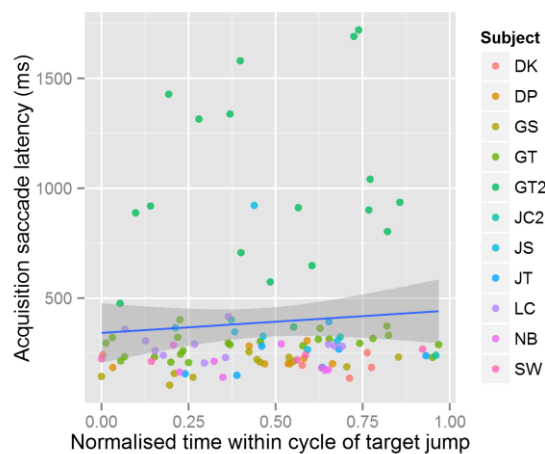


Figure 5.14: The effect of target jump timing during the nystagmus cycle (as a fraction of the total cycle length) on vertical saccade latency for subjects with IN. Regression line is shown; the shaded region indicates standard error.

The p value of the slope of the regression line in Figure 5.14 is 0.43, indicating (as above) that the time within the cycle that the target jump occurred did *not* have an effect on voluntary (vertical) saccadic latency. However, this still shows data for all the subjects plotted together. In order to investigate whether there are any *individual* effects, Figure 5.15 shows the same data with each subject presented separately.

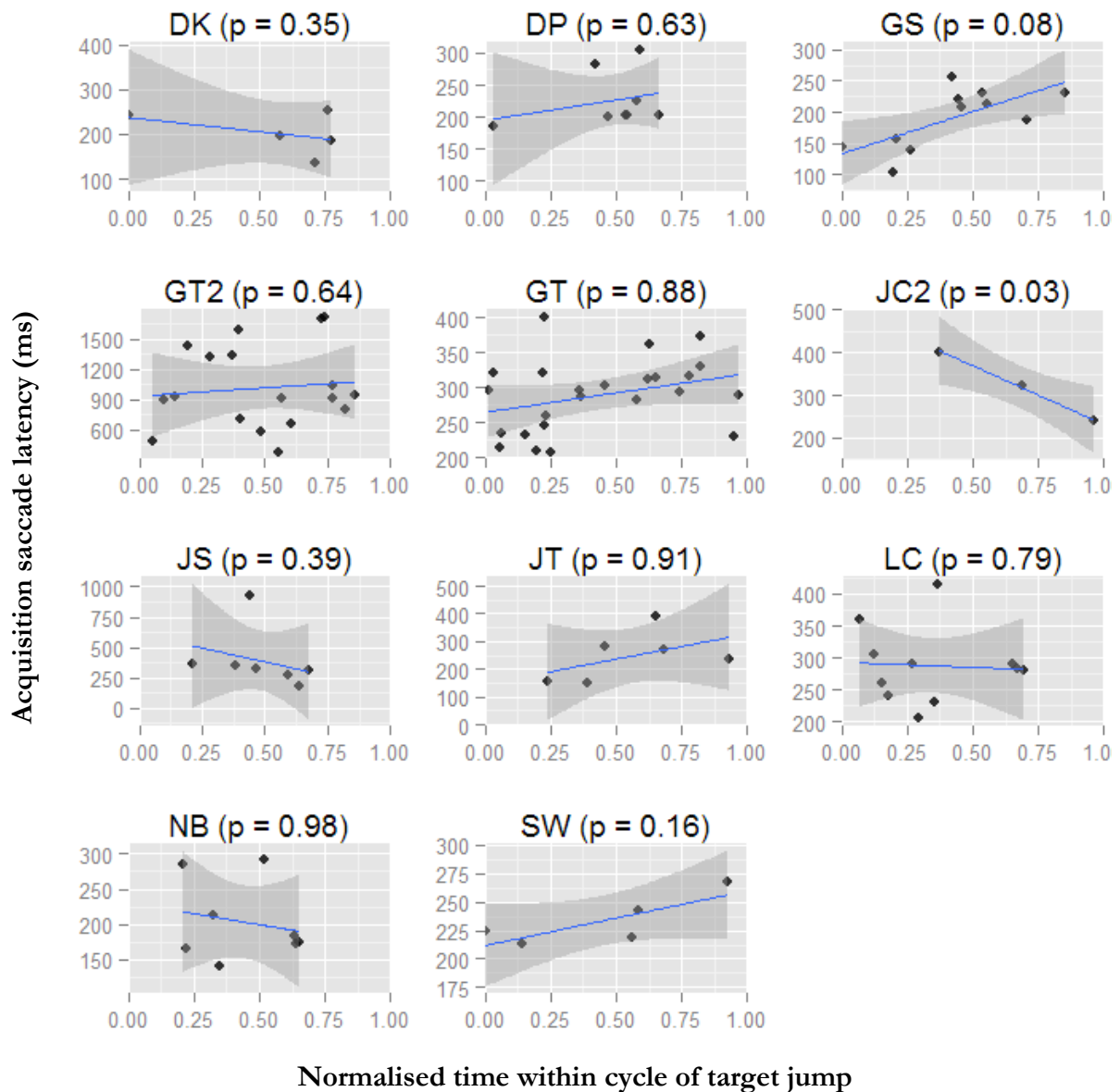


Figure 5.15: For each subject with IN, the relationship between the time during the nystagmus cycle at which the target jump occurred (since the last quick phase) and the latency of the targeting saccade. For each participant, linear regression lines are shown with standard error (shaded region). p values indicate the probability that each regression slope is equal to zero.

Figure 5.15 shows that, with the exception of subject JC2, the time during nystagmus cycles at which the target jump occurred had no significant effect on voluntary vertical saccade timing. In other words, **voluntary (vertical) saccade latency was unaffected by the time during**

the cycle at which the stimulus was presented (using a linear model to test the hypothesis). Note that subject JC2 only had three target jumps included in the analysis; the other participants had an average of 10.3. The lack of data for this participant may explain why statistical testing reached a different conclusion in this instance.

In the interests of completeness, similar data from subjects KL and JC are shown in Figure 5.16.

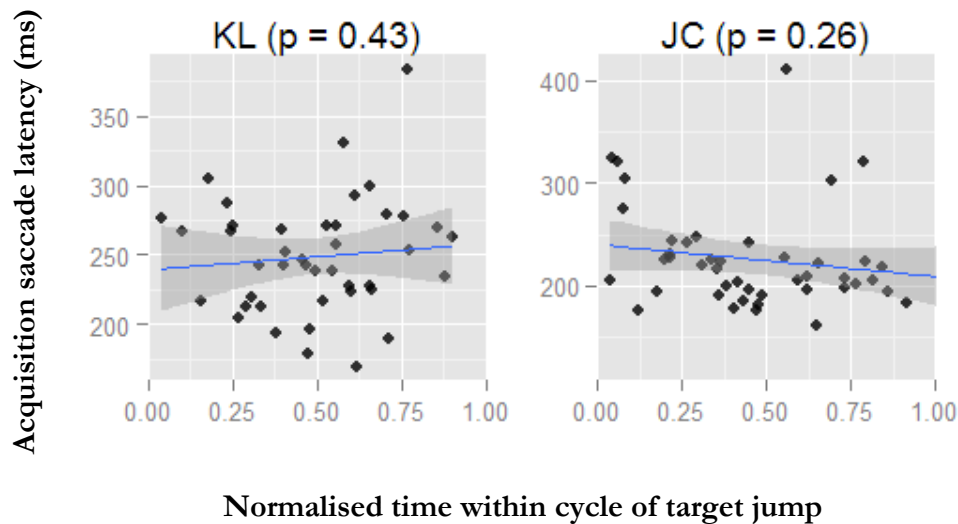


Figure 5.16: For subjects KL (FMNS) and JC (no nystagmus in primary position), the effect of target jump timing on voluntary saccade latency. Format is identical to Figure 5.15.

As seen in the subjects with IN, target jump timing appears to have no effect on saccadic latency in these two subjects.

Note that the assertion made above is based on the assumption that a linear regression model ought to be applied to interpret the data; see Section 5.4.3.1 for a discussion on the appropriateness of this model.

It must also be pointed out that the normalisation of cycle lengths as presented above are based on the assumption that the nystagmus cycle length is unperturbed by the target jump. As has been demonstrated in this study, nystagmus cycle length *is* affected by the saccadic task (see Section 5.3.3.1), so the ‘normalised time within cycle’ metric may produce distorted results. In order to test this hypothesis, the data from Figure 5.15 were replotted, but with the ‘normalised time within cycle’ derived from a *prediction* of cycle length, based on the length of the last complete cycle to occur before the target jump. Figure 5.17 shows these data.

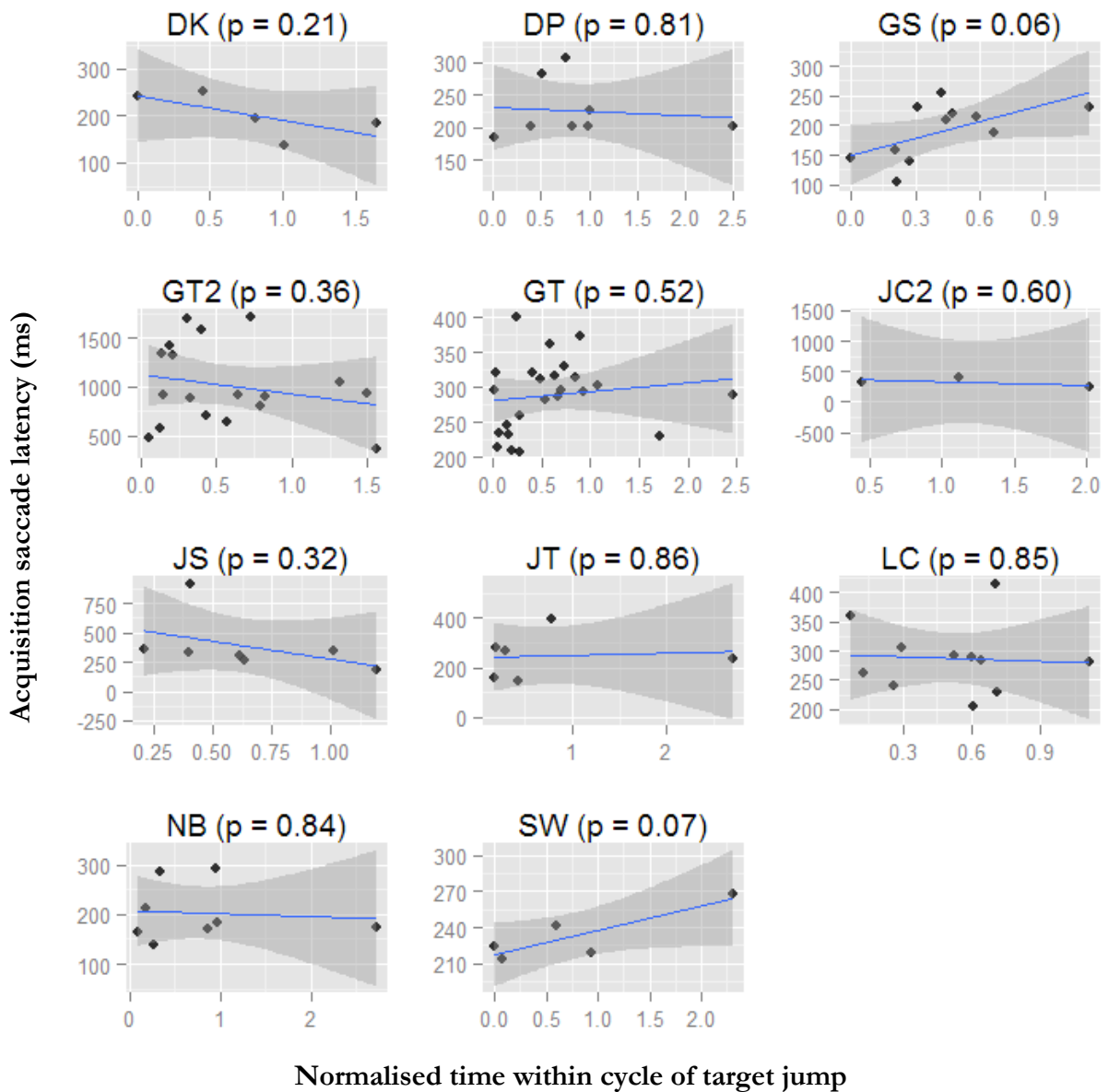


Figure 5.17: The same data as shown in Figure 5.17, but with the ordinate based on a *prediction* of nystagmus cycle length, based on the length of the last complete cycle preceding the target jump

Note that in Figure 5.17, some of the normalised cycle lengths are greater than 1. This is due to the variability of nystagmus cycle length between beats, and indicates that the last cycle prior to the target jump was shorter than the one that included the target jump. Nonetheless, the same result is reached (using linear regression modelling): there is no significant effect of target jump timing on the latency of the vertical saccade.

As with Figure 5.16, in the interests of completeness, similar data using *predictive* normalised cycle lengths are shown from subjects KL and JC in Figure 5.18.

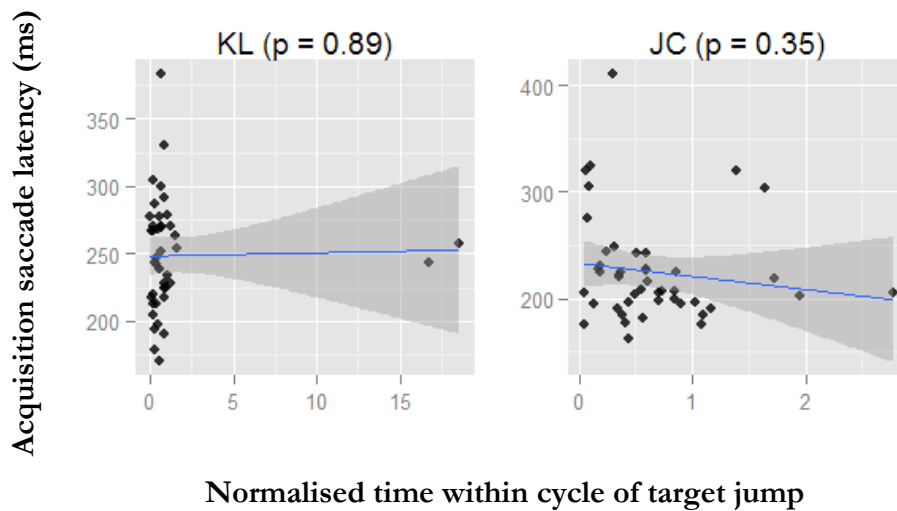


Figure 5.18: For subjects KL (FMNS) and JC (no nystagmus in primary position), the effect of target jump timing on voluntary saccade latency, where ‘normalised’ cycle length is a prediction based on the length of the last complete cycle to occur prior to the target jump. Format is identical to Figure 5.17.

As before, Figure 5.18 shows no significant effect of target jump timing on voluntary saccade latency in these two subjects. Notice that subject KL exhibits two instances in which the cycle length prior to the target jump was more than 15 times shorter than the cycle in which the target jump occurred. Removing these two points from the analysis still produces a regression line with an insignificant slope ($p = 0.53$).

5.3.7 Instances in which automated analysis failed

Visual inspection of each target jump confirmed that automated saccade detection worked for 59.6% of target jumps. The remainder of the automatically detected saccades were rejected from the analysis. Examples and explanations for these situations are given below.

5.3.7.1 Waveforms with multiple quick phases

Subjects DP and NB both have *pseudo pendular* waveforms, which contain two quick phases in each cycle. Since the algorithm was designed to choose only one quick phase per cycle, it was not possible to determine quick phase latency for these subjects (illustrated by Figure 5.19). For this reason, although the final analysis includes these subjects for *whether or not saccades were coincident*, metrics relating to the nystagmus quick phase (such as *time within cycle of target jump*, *previous quick phase latency*, etc.) are not included.

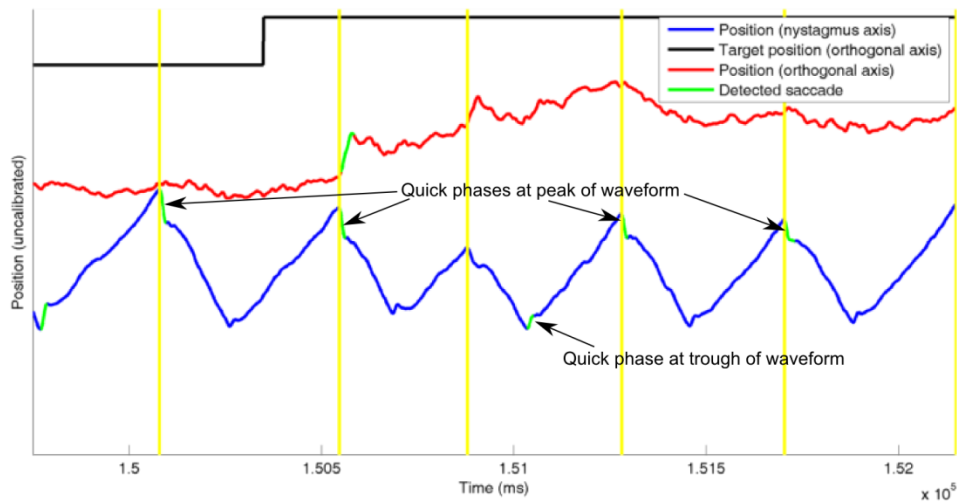


Figure 5.19: Data from subject DP showing cycle boundaries (vertical yellow lines), leading to variable 'quick phase' selection for each cycle

5.3.7.2 Ambiguous acquisition saccades

Wrong saccade detected

Since the algorithm was programmed to identify the saccade with the largest amplitude in the direction of each target jump, there was potential for non-target-acquiring saccades to be incorrectly identified as the 'acquiring' saccade. One such example is given in Figure 5.20, in which there is a non-saccadic drift towards the target (similar to that reported by Worfolk and Abadi [1991], which typically occurred in response to target jumps in the opposite direction of the nystagmus quick phase). In the case of the example in the figure, the algorithm incorrectly identifies what appears to be a saccadic intrusion as the target-acquiring saccade. Instances such as these were rejected from the analysis.

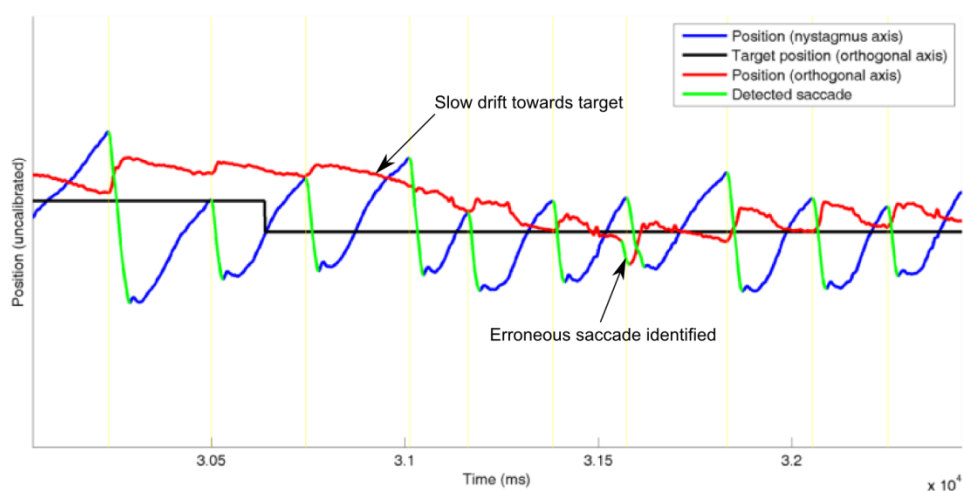


Figure 5.20: Example of a target jump with a non-saccadic target acquisition. The algorithm has instead detected a later erroneous saccade.

Two-dimensional waveforms and small target jumps

The relatively small target jump sizes (3 and 5°) occasionally made saccade detection difficult. In subjects whose axis of nystagmus was significantly oblique (i.e. not horizontal), the target-acquiring saccade was sometimes ambiguous (see Figure 5.21)²⁷. These instances were rejected from the analysis.

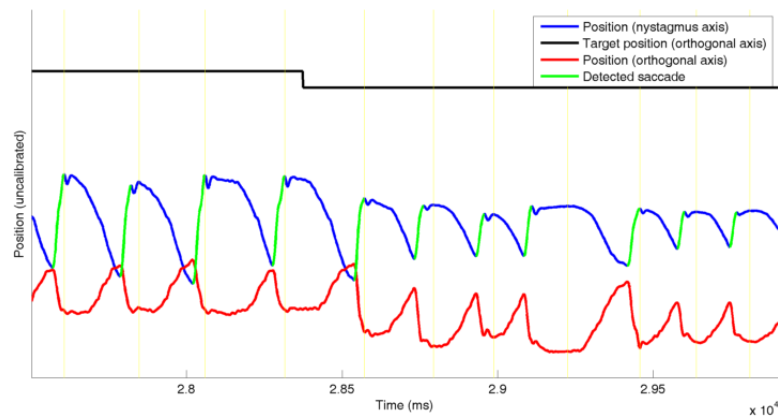


Figure 5.21: A subject with an oblique nystagmus axis (JT) exhibits significant vertical and horizontal components. For small target jumps, this makes detection of the target-acquiring saccade difficult.

5.3.7.3 Dampened nystagmus causing incorrect cycle detection

In some instances, the nystagmus amplitude appeared to be dampened for the few cycles between the stimulus jump and execution of the target-acquiring saccade. This caused the cycle detection algorithm to miss cycles, which in turn meant that some of the true quick phases were not identified (since the program only detects one quick phase per cycle; see Figure 5.22). Events in which cycles were incorrectly identified were rejected from the analysis.

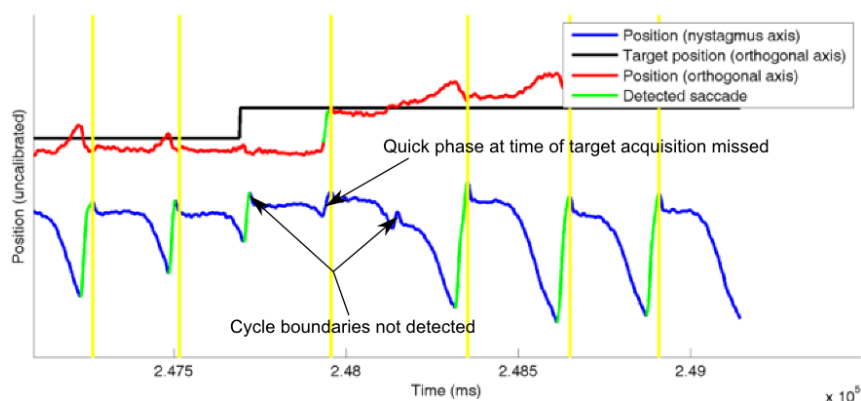


Figure 5.22: Dampened nystagmus amplitude around the time of the target-acquiring saccade causes incorrect cycle detection, which leads to a quick phase not being identified. Vertical yellow lines indicate cycle boundaries as detected by the algorithm.

²⁷ This is of course the same reason that the *Behrens, Mackeben and Schröder-Preikschat* saccade detector was *not* used to detect nystagmus quick phases in the horizontal axis; see Sections 5.2.3.1 and 2.1.5.1 for detail.

5.3.7.4 Dysmetric saccades

In a few cases, vertical target-acquiring saccades were dysmetric, and corrective saccades were made to account for this. Due to the small target step size, these were rare. However, since the saccade detection algorithm was programmed to identify only a single saccade for each target jump, when they *did* occur, they caused the saccade detection algorithm to fail. Figure 5.23 shows an example of this. These cases were rejected from the analysis.

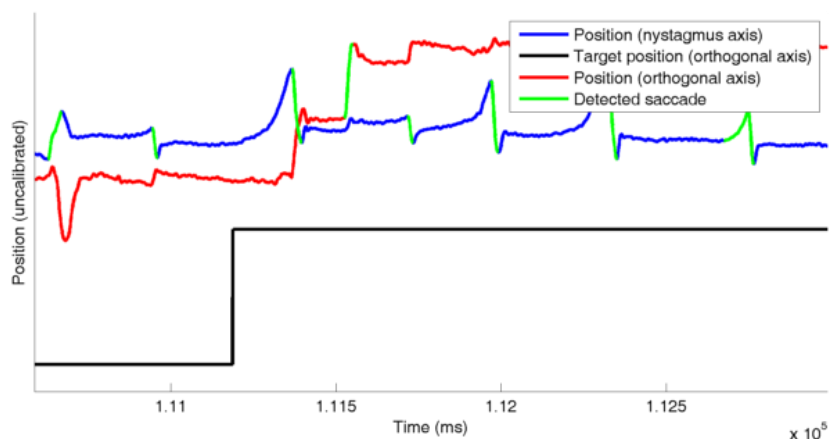


Figure 5.23: An initial hypometric vertical saccade causes the algorithm to fail to detect overlap with a nystagmus quick phase.

5.4 Discussion

5.4.1 Coincidence of quick phases and targeting saccades

The results indicate an extremely strong relationship between the timing of voluntary and involuntary saccades in 11 subjects with IN, one with FMNS and one with IN which was not present in the primary position of gaze. This modification of the waveform at the time of target acquisition provides further evidence that nystagmus is under adaptive control. Previous studies have shown that nystagmus can be modified by alertness, stress and ‘effort to see’ (Abadi and Dickinson 1986; Wiggins et al. 2007; Tkalcevic and Abel 2005; Jones et al. 2013). The present study constitutes compelling evidence that nystagmus quick phase programming works with the voluntary saccadic system (or indeed that both represent the same system). This finding is supported by the work of Worfolk and Abadi (1991), who found that the latency of the first quick phase following a target jump is directly related to the latency of the quick phase that follows. However, their finding was only exhibited in 2/19 subjects, both of whom had IIN. By isolating the horizontal and vertical axes in the present study, coincident voluntary saccades and nystagmus quick phases were easier to determine and clearly appear to be present in all individuals for whom sufficient data were available (13 participants). Although only 80% of the voluntary vertical saccades analysed had a coincident nystagmus quick phase identified algorithmically, visual inspection confirmed the presence of

dampened quick phases in almost every instance (with the exception of the *five* instances out of 280 mentioned in Section 5.3.2 and the peculiar behaviour of subject LC, who occasionally used fast drifts to acquire the target). Previous studies have shown that, when presented at closely spaced intervals, saccadic EMs are often combined into a single movement (Hou and Fender 1979). The phenomenon described in this chapter may represent a similar mechanism.

5.4.2 Changes in nystagmus waveform prior to target acquisition

One subject in particular (GT2) demonstrated a remarkable change in nystagmus waveform prior to executing target-acquiring saccades (see Figure 5.11). More generally, subjects exhibited a decrease in nystagmus frequency (increase in slow phase duration) prior to executing voluntary saccades, as well as a dampening of quick phase amplitude. These changes further indicate active modification of the nystagmus waveform during saccadic programming. In a similar manner, Van Beuzek and Van Gisbergen (2002) have shown that generation of voluntary prosaccades and antisaccades can cause suppression and modification of VOR nystagmus quick phases during yaw rotation. The results of the present study suggest that the quick phases of IN are under a similar degree of conscious control.

5.4.3 Lack of an effect of stimulus onset on saccade timing

The fact that there was no significant effect of the timing of the target jumps (within the nystagmus cycle) on the latency of target acquisition suggests that saccadic programming is independent of phenomena such as foveation periods. The lack of an effect provides further weight to the argument that visual perception is continuous throughout the entire nystagmus slow phase; i.e. that visual processing (for the purposes of saccadic programming) may be unimpaired by the image falling off the fovea at the time of the target jump (see Section 1.3.9.1 for a summary of other evidence supporting this theory).

Taking together the fact that nystagmus quick phases tended to occur at the same time as voluntary saccades *and* that there was no significant correlation between the *time within the nystagmus cycle at which the target jump occurred* and the *voluntary saccade latency* suggests that **the nystagmus waveform is modified to fit in with the time course of voluntary saccades**. In other words, it appears as though the timing of the nystagmus quick phase is modified to ‘ride’ the voluntary saccade, rather than the other way around. This is relevant, as it suggests that nystagmus can be directly modified by the voluntary saccadic system, and that voluntary saccades take priority over nystagmus quick phases.

5.4.3.1 Comparison to Wang and Dell'Osso (2007)

Previous work has examined the relationship between target jump timing and target acquisition latency for voluntary *horizontal* saccades in IN (Wang and Dell'Osso 2007). Figure 5.24 shows these data. Note that these data were collected for *large* target jumps ranging from 15 - 60°. The same study also presented data derived from a computerised model of nystagmus, which produced simulated results similar to those that were collected from the real participants (shown in Figure 5.24). However, the present author argues that there are not enough data in either their study, nor the present one to justify the use of polynomial regression curve fitting. The data in the present study appear to show similar features to the data collected by Wang and Dell'Osso. For example, in Figure 5.15, subject GT (with a pseudo cycloid waveform) appears to show a similar pattern to the bottom-left panel (marked 'PC') in Figure 5.24. However, the scarcity of the data make it difficult to justify the use of polynomial regression modelling. Therefore, it is difficult to conclude anything other than the *lack* of a relationship between saccade timing and target acquisition time. Clearly, future work ought to be undertaken, specifically to collect much larger quantities of data to test the predictions made by Wang and Dell'Osso's model.

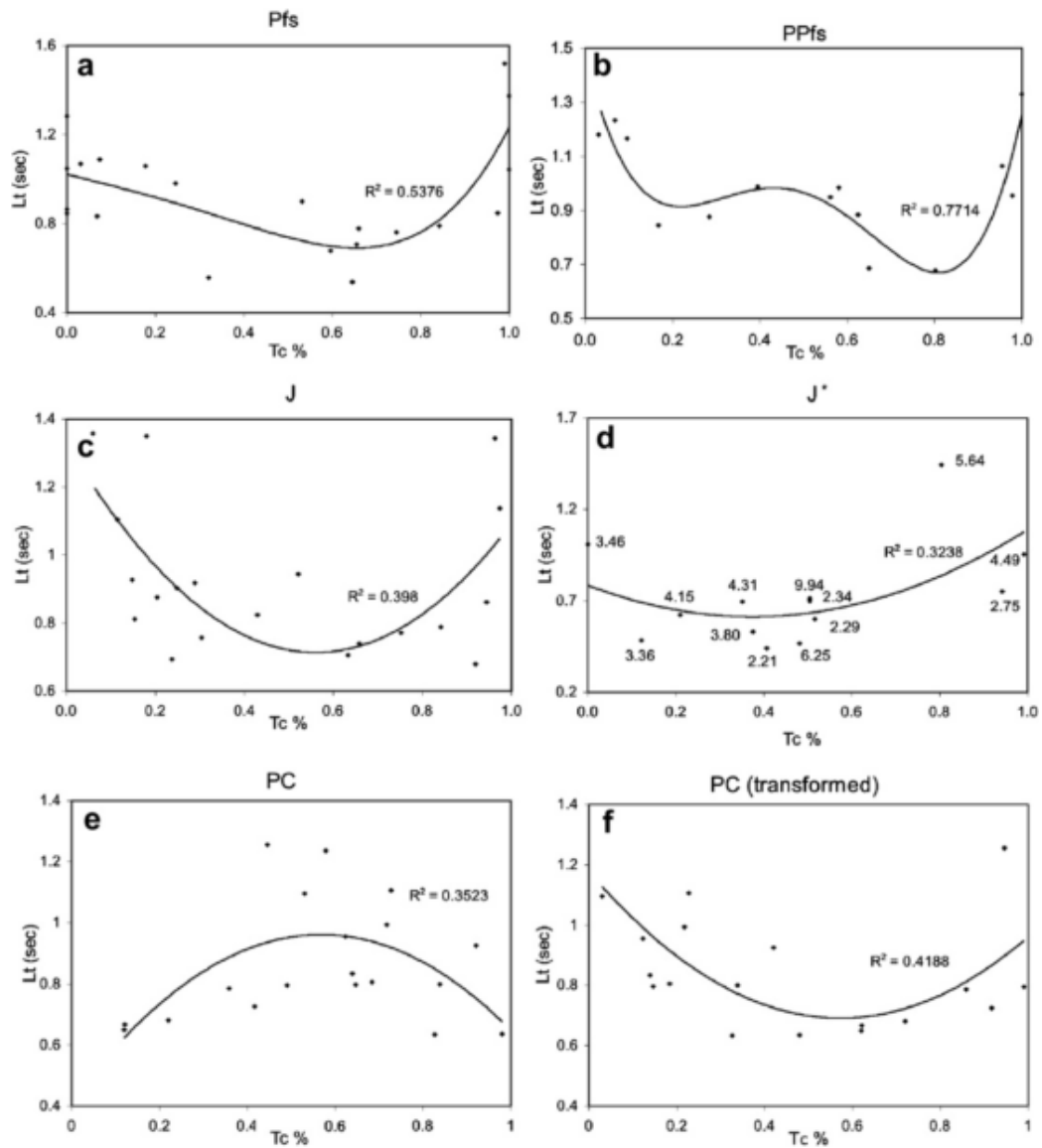


Figure 5.24: Data from Wang and Dell'Osso (2007), showing horizontal target acquisition time (L_t) against the normalised time within the nystagmus cycle of the target jump (T_c %) for different waveform types. Polynomial regression curves are shown.

In addition to the ambiguity introduced by polynomial regression modelling, Wang and Dell'Osso calculated the 'normalised time within cycle' metric under the assumption that cycle length is unperturbed by the presence of the target jump. This is the reason that the concept of *predicted* normalised cycle lengths was introduced in the present study. Nonetheless, regardless of how 'normalised' cycles were calculated, the same conclusion was reached: there was *no* linear relationship between voluntary vertical saccade latency and the time during the nystagmus cycle at which the target jump occurred.

5.4.4 Implications

The fact that nystagmus quick phases are both modified by, and coincident with, voluntary saccades implies a certain amount of voluntary control over the nystagmus waveform, albeit

subconscious. This suggests that nystagmats economise their quick phases, perhaps to reduce saccadic suppression time. As discussed in Section 5.4.3.1, whether or not voluntary saccade programming can be initiated at any time during a slow phase is still unclear. More data are required to confirm this conclusion. However, if so, this would suggest that visual perception (at least, for the purposes of saccadic programming) is present during the *entire* nystagmus slow phase. Note that any target jumps that occurred *during* a nystagmus quick phase were excluded from the study, as one would expect saccadic suppression to be active during nystagmus quick phases, just as they are during normal saccades.

5.4.5 Limitations

5.4.5.1 Algorithm limitations

The automated data analysis algorithms allow for quick processing of hundreds of saccades with a minimum of effort. Whilst this method has its advantages, as can be seen in Section 5.3.2, there are many instances in which the algorithm fails. This is testament to the challenge presented by the extreme variability and complexity of nystagmus waveforms.

For the present study, a total of 1352 target jumps were performed, with up to 15 metrics being calculated for each. If these data were to be analysed manually, the only feasible approach would be to sample a subset of the data. It is assumed that the shortcomings of the algorithmic approach are counteracted by the statistical power of attempting to analyse *every* target jump. Visual confirmation/rejection of the results was required to ensure that erroneous ‘saccades’ were excluded from the analysis.

5.4.5.2 Noisy data

As can be seen from Table 5.1, a large proportion of eye tracker data were dropped at the time of capture. Five subjects had data dropout for more than 5% of the total recording time, and two subjects had such infrequent data capture that no target jumps qualified for attempted analysis at all (the criterion was for clean data between the previous and next target jump). This raises questions about the suitability of the EyeLink 1000 as a device for EM analysis in the presence of nystagmus.

5.4.5.3 Target jump size

In Wang and Dell’Osso’s (2007) study of the timing of saccades in IN (in the horizontal plane only), their results were split into two sections. ‘*Small target jumps*’ investigated target jumps of 5°, whereas ‘*large target jumps*’ looked at target jump sizes from 15 – 60°. Essentially, the present study has only investigated one half of the 2007 study. This was primarily due to

limitations in laboratory equipment; a much larger screen would be required to expand the study. As discussed in Section 5.3.7.2, the small target jumps hindered automated analysis. Aside from the greater yield of analysable data that larger target jumps would surely provide, it would be interesting to see whether the relationship between voluntary saccades and nystagmus quick phases remains when target jump size is increased.

5.4.5.4 Jump time prediction

As shown in Section 5.3.5, one subject (JC) appears to have occasionally anticipated the onset of the following target jump, and modified the nystagmus amplitude accordingly. Although this fascinating phenomenon certainly warrants further investigation, it is possible that these instances may have hindered the automated analysis of data from this participant. Despite the fact that no other participants appear to exhibit this effect, it is worth remembering when designing experimental paradigms that psychological effects such as this can have a measurable effect on the nystagmus waveform.

5.5 Summary

The findings presented in this chapter provide the first evidence that, in nystagmats, small voluntary vertical saccades almost always coincide with quick phases. In addition, the timing of quick phases appears to be modified to accommodate the voluntary saccade. Taking together the evidence for direct modification of nystagmus frequency/waveform from this study and the work of Worfolk and Abadi (1991), we now have a compelling argument that nystagmus is directly modified by the saccadic system. This further suggests that voluntary saccades and nystagmus quick phases are under the control of a common system, and that nystagmus quick phases are a non-pathological mechanism employed to strategically control the pathological drift of nystagmus slow phases.

Further work must now be done to confirm that the effects shown here are consistent for larger target jump sizes, and to use larger numbers of subjects in order to enhance the statistical power of the analyses.

Chapter 6 Preliminary work and future investigations

During the course of the work presented in this thesis, a number of other studies were designed to measure aspects of visual perception and oculomotor characteristics in subjects with IN. The following chapter details these experiment designs. For one (section 6.1 below), preliminary data are presented. In this study, waveform characteristics were analysed over long periods of inattention. This exploratory study aimed to uncover the waveform in its ‘natural’ state; unperturbed by the need to fixate anything in particular. The remaining studies, which were designed but not undertaken for this thesis, aim to better understand aspects of spatial and temporal visual perception experienced by individuals with IN.

Preliminary work

6.1 Waveform characteristics during visual inattention

6.1.1 Introduction

Waveform parameters of IN are known to be affected by psychological factors such as stress, consciousness, visual task demand and ‘effort to see’ (Abadi and Dickinson 1986; Wiggins et al. 2007; Tkalcevic and Abel 2005; Cham, Anderson and Abel 2008b; Jones et al. 2013). As discussed in Chapter 5, nystagmus quick phases appear to serve the function of realigning the fovea with the object of interest. Therefore, it follows that in the absence of a specific visual target to fixate, nystagmus waveforms might be expected to change, with less quick phases being observed.

The pilot study detailed here was a simple paradigm investigating the parameters of IN in the absence of any specific visual stimulus or mental activity. As described above, many studies have looked at the effects of stress in nystagmus. Yet, there are few formal reports of IN motor characteristics during times of ‘non-activity’; this study aimed to fill this gap in the literature. As noted in Section 1.3.10, many of the treatments that have been shown to reduce nystagmus intensity (except for those that aim to move the null zone) may be considered as sedative in their effect. Since increased ‘effort to see’ causes a concurrent reduction in nystagmus intensity (Wiggins et al. 2007), one might expect intensity to increase in the absence of any specific visual task. Or, perhaps, nystagmus intensity will *decrease* due to inattention and relaxation.

One previous report has documented the effect of visual inattention on the nystagmus waveform (Reinecke 1997). Figure 6.1 shows the effect of an individual with jerk nystagmus

switching from visual attention to performing mental arithmetic (i.e. no visual attention required). Note the extension of the slow phases and the absence of quick phases (i.e. change to a pendular waveform) in the shaded region C_1 . The lack of quick phases during these periods (in which fixation is functionally less important) lends further evidence supporting the theory that the quick phases of IN are non-pathological, and exist solely to redeploy gaze.

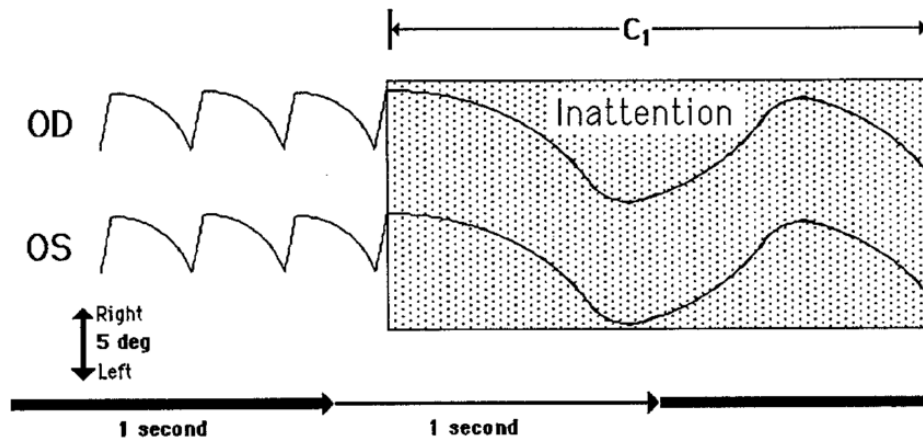


Figure 6.1: The effect of inattention on a jerk nystagmus waveform (Reinecke 1997)

6.1.1.1 Aims

The present study was of an exploratory nature, aiming to observe changes in nystagmus parameters occurring over five minutes of inattention. Subjects were instructed to simply gaze ‘more or less’ straight ahead whilst sitting in silence. It also served as a functional verification of the software developed in Chapter 2, since the experiment produced a large quantity of data for the software to analyse. It was hoped that the results of this, and the large quantity of data generated, might inform future work. As explained above, inattention has previously been shown to cause extension of slow phases and an absence of quick phases. By recording lengthy periods of inattention, it may be possible to unmask an underlying pendular waveform and observe changes in intensity over time.

6.1.2 Materials and methods

6.1.2.1 Participants

Eleven subjects with IN were recruited for the study from the Cardiff *Research Unit for Nystagmus* cohort. Subjects wore their habitual refractive correction.

Inclusion / exclusion criteria

EM recordings were made to ensure that participants had IN (as opposed to any other oculomotor instability). Accelerating slow phases were an essential criterion for diagnosis. In

addition, any subjects whose data quality was not sufficient for analysis (due to dropped samples) were excluded post-hoc.

6.1.2.2 Procedures

Subjects were seated in a room lit at $\sim 1.78 \log \text{ cd/m}^2$, facing a monitor, which was turned off. The chin and head were supported by a rest (see Figure 3.7), and subjects were encouraged to adopt a comfortable position (adopting a habitual head posture if desired). Calibration was performed using the software developed in Chapter 2. Subjects wore their habitual refractive correction (if any), and were instructed *not* to fixate anything in particular; the only constraint was that they should “more or less” keep their eyes looking ahead so that an eye tracker could monitor them. Binocular EMs were recorded by an EyeLink 1000 (see Section 1.4.3.3). Subjects were informed that the room would be silent for five minutes, and they would go home after this time. No further instruction was given.

6.1.2.3 Data analysis

EM traces were analysed using the software written for Chapter 2. Foveations were defined as periods of data exceeding 7 ms with velocities $< 6^\circ/\text{s}$. Foveations separated by less than 35 ms were combined into single foveations (these parameters are identical to those used by Felius et al. [2011]). The software detected saccades, cycles, slow phases and foveations throughout the recordings and created reports containing each of the metrics listed in Section 2.1.3. For the purposes of this report, changes in nystagmus intensity over time were analysed. In order to minimise the effect that voluntary changes in gaze angle might have had on the results, quadratic regression models were generated for each participant, comparing gaze angle with nystagmus intensity over the entire recording session. These models were then used to decorrelate gaze angle effects (i.e. the null zone) from the recordings in order to reveal changes in intensity over time that were *not* due to the effects of the null zone. Statistical analysis was performed in the R Environment for Statistical Computing (R Core Team 2012).

6.1.3 Results

6.1.3.1 Participants and exclusions

Eleven subjects with IN took part in the study. Subjects who took part also contributed to other studies during the same day. General information and biometrics for each subject can be found in Appendix II. The subjects who took part in this study were:

- DB, DK, DP, DT, GT, GT2, JS, JX, LC, MT and NB

Data from subject LC were not analysed due to a corrupt (unreadable) data file. The 10 remaining participants were included in the analysis.

6.1.3.2 Nystagmus intensity

For each cycle detected by the nystagmus analysis software, Figure 6.2 shows how nystagmus intensity changed with time for each participant. Only those cycles containing no dropped data are included.

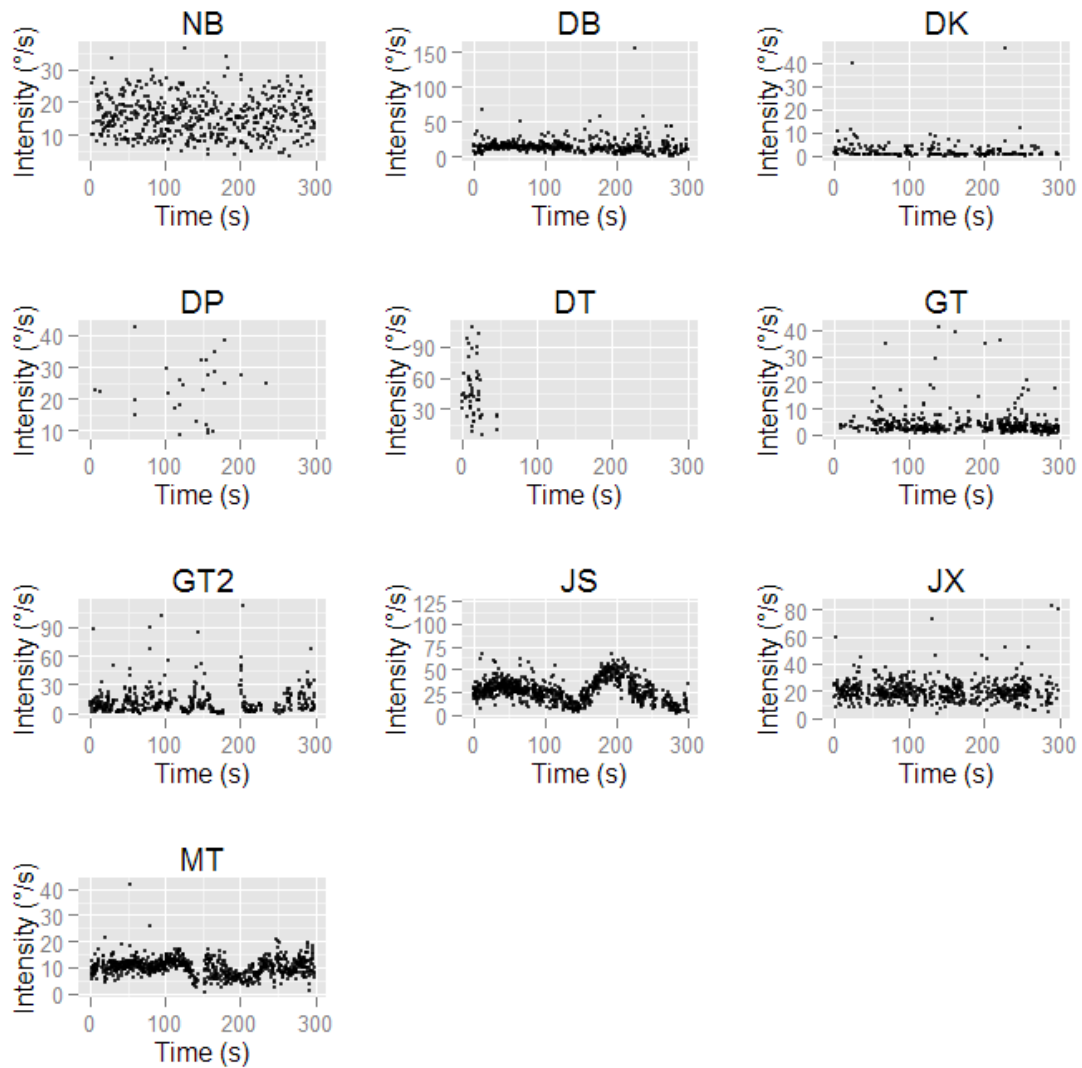


Figure 6.2: Nystagmus intensity plotted against time since the start of the recording for each participant. Only 'clean' cycles (i.e. those containing no dropped data) are shown.

Since subjects were free to look wherever they wished during the experiment, it was necessary to control for the effect of gaze angle (null zone) when interpreting the data. Quadratic

regression models²⁸ were constructed for each participant in order to model horizontal gaze angle against nystagmus intensity from the dataset available in the recordings. The resulting models are shown in Figure 6.3.

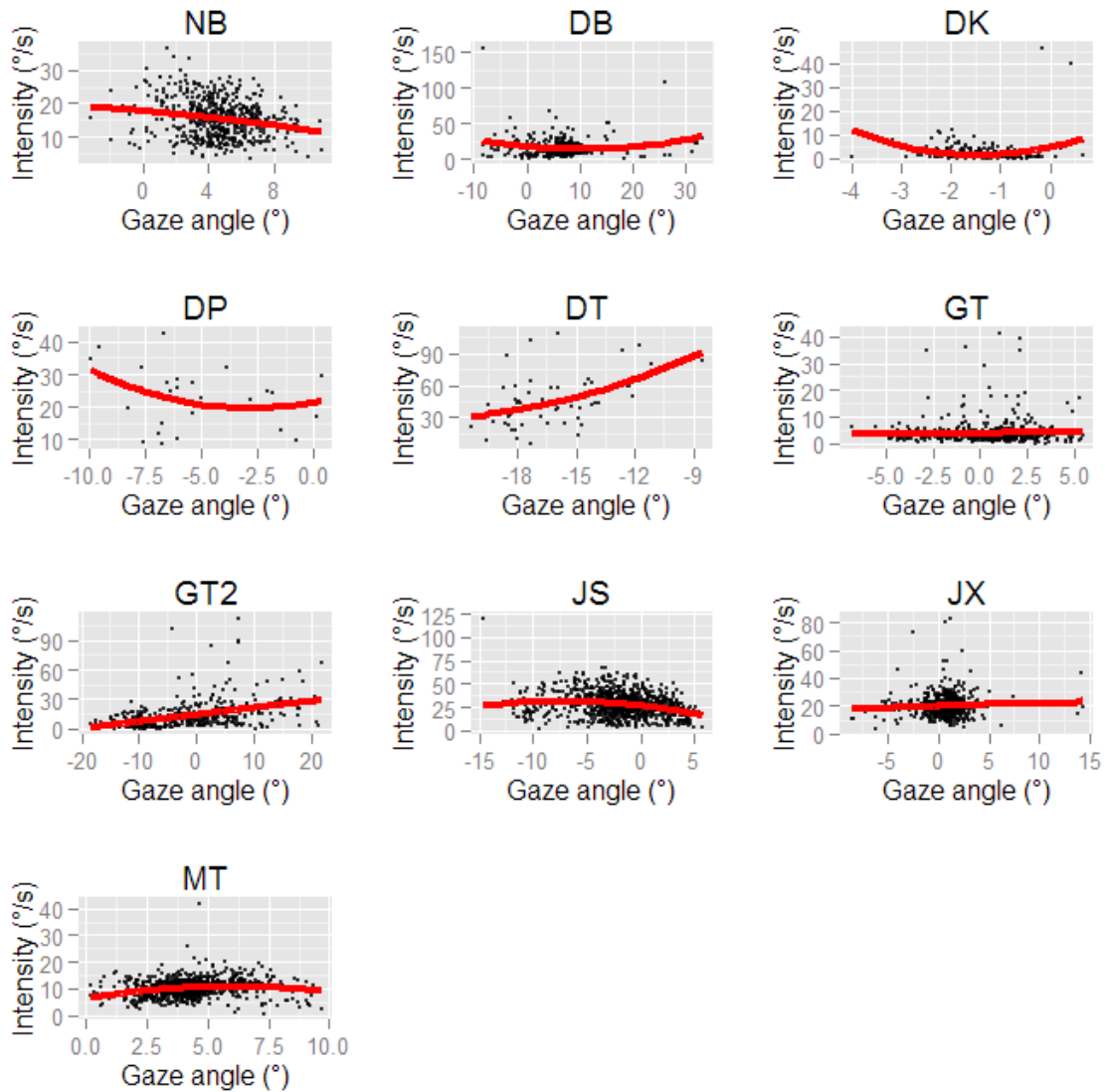


Figure 6.3: Quadratic regression models for the null zones of each participant, based on data available from the range of viewing angles recorded during the experiment

Figure 6.4 shows locally weighted polynomial regression models (fitted using weighted least squares; span = 0.75), plotting nystagmus intensity against time for each participant, with the effects of gaze angle controlled for (using the quadratic regression models above). In this figure, the ordinate shows *change in intensity*; i.e. the variation in nystagmus intensity over time

²⁸ The use of *quadratic* regression to model the null zone is based on the assumption that individuals with IN have a single null zone. This notion has not been formally tested, although work currently being conducted at Cardiff University aims to address the issue.

that is not accounted for by changes in gaze angle as predicted by the regression models above.

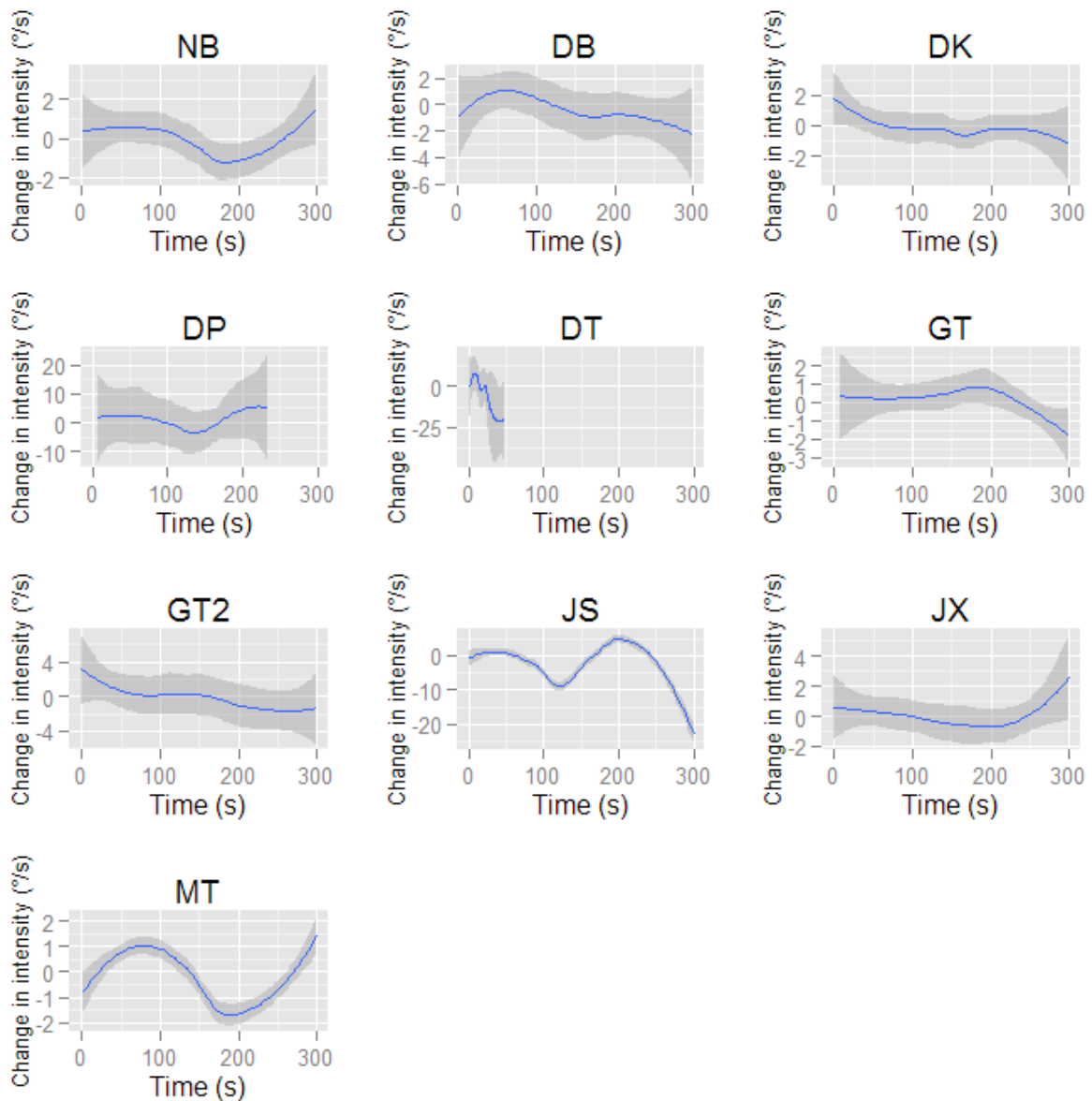


Figure 6.4: Locally weighted polynomial regression models showing change in nystagmus intensity plotted against time for each participant. Changes in intensity due to variation in horizontal gaze angle are controlled for (using the quadratic regression models shown in Figure 6.3). Hence, the ordinate shows the *change* in nystagmus intensity relative to values predicted by the quadratic regression model at each moment in time.

6.1.4 Discussion

The results presented here provide a glimpse into the large scale analyses that could be performed using the nystagmus analysis software. Figure 6.4 demonstrates how variable different participants' waveforms were during long periods of visual inattention. There are a number of possible psychological factors that might have been in play during the course of the experiments, so it is not possible to derive any specific conclusions from these data alone;

however, it may be interesting to perform similar experiments in conjunction with physiological measures, such as heart rate, galvanic skin response and/or electroencephalography²⁹. Since the work of Reinecke (1997) demonstrated an absence of nystagmus quick phases during inattention, it would also be interesting to identify such periods of data from the recordings in this study, and look specifically at changes in waveform *amplitude* over time. These periods of time might represent an ‘unmasking’ of the nystagmus waveform in its pure form (undisturbed by quick phases), and may therefore be a very useful topic of study.

The visual environment used in the present study was probably not optimal for ‘unmasking’ an underlying pendular oscillation. Since the quick phases of IN are likely to represent attempts of the oculomotor system to realign the fovea with the intended visual target (see Chapter 5), whether or not subjects intended to fixate, it is likely that retinal slip (of the laboratory environment) acted as visual feedback, causing reorienting quick phases to occur. If this experiment were to be repeated, it would be useful to do so in the presence of a homogenous visual field, such as viewing a Ganzfeld bowl, or in the dark.

The quadratic regression models that were used to control for the effects of gaze angle on nystagmus intensity (see Figure 6.3) were likely over-simplified. Firstly, quadratic models may not be complex enough to explain individual nuances of the null zone. In addition, only horizontal gaze angle was used in the construction of each model. Ideally, the null zone would be modelled in two dimensions prior to each experiment, and over a wider oculomotor range than that likely to be used during the experiment. Nonetheless, these data provide a good starting point for the design of future studies.

Future investigations

The following sections detail a range of potential psychophysical techniques that it might be possible to use in the future to further investigate aspects of visual perception in IN. Some of these are additional paradigms for exploring spatial vision using the flash equipment developed for Chapter 3, whilst the others are novel methods for investigating functional aspects of the *slow to see* phenomenon seen in IN.

²⁹ A pilot study attempting to measure EMs in conjunction with electroencephalographic recordings was in fact carried out with a single subject. Unfortunately, it was not possible to decorrelate the EMs from brain activity, so no conclusions could be drawn from the results. This study is not detailed in this thesis. Alternative brain imaging techniques such as magnetoencephalography may yield greater success, since keeping the eyes still is not a prerequisite for obtaining good data.

6.2 Determination of the complete contrast sensitivity function

VA is a measure of only one part of the contrast sensitivity function – the point at maximum contrast. It may be informative to measure visual function of individuals with IIN using low contrast stimuli – again using the flash paradigm (from Chapter 3) to eliminate image motion. Given our poor understanding of the reduced visual function in IIN (which is often reported as being worse through visual function questionnaires than would be predicted from clinical measures [Hertle et al. 2003]), it is essential that all aspects of visual function be measured. Since we now know that there is likely to be an underlying pathology or amblyopia in IIN (see Chapter 3), understanding the perceptual difficulties may provide clues to uncover the nature of the defect. If IN is indeed a developmental adaptation serving to enhance contrast of low spatial frequencies (as predicted by Harris and Berry's [2006] model of IN development), then there may well be nuances of the contrast sensitivity function that have been missed by the paradigm presented in Chapter 3 due to only measuring VA (i.e. at maximum contrast) in the absence of image motion (Dunn et al. 2014).

6.3 Measurement of parafoveal acuity

As described in Section 3.2.4.3, the flash unit can be made to trigger based on eye position (instead of strobing at a random frequency). Programming for this function has been completed, and calibration using the method detailed in Chapter 2 would allow accurate flash delivery timing, which in turn would allow peripheral VA to be measured for individuals with nystagmus. Specifically, *parafoveal* VA in IIN could be compared to normative data (Mandelbaum and Sloan 1947). Since it is likely that conscious visual input in IN is constant throughout the slow phase (see Section 1.3.9.1), it seems feasible that nystagmats could have a 'spread' of their functional foveae. This might develop as a result of greater use of the retinal loci associated with the waveform during the plastic period than normally-sighted individuals, leading to increased representation in the visual cortex. For example, horizontal nystagmus might lead to a wider region of high acuity about the horizontal meridian, but this might not be the case vertically. This theory could be tested using the flash delivery equipment built for Chapter 3 (with small gratings to stimulate specific parts of the visual field), and may help to understand the developmental adaptations inherent to early-onset nystagmus that do not manifest in acquired nystagmus. This paradigm was not pursued during the course of the experiments presented in this thesis due to the calibration algorithm being in its infancy at the time. However, with the improved programmatic efficiency of the current algorithm, it may now be possible to deliver gaze-contingent flashes of light.

6.4 Partitioning the waveform: assessing temporal effects of nystagmus

It ought to be possible to assess whether there is a time-dependent suppression throughout the nystagmus waveform (i.e. a moment-to-moment variation in visual sensitivity, perhaps higher during foveations and lower with increased eccentricity from the point of regard) by having subjects undergo repeated measures of VA at various spatial frequencies. Using the flash delivery equipment, subjects could be presented with a *single* flash illuminating a large tilted grating (i.e. exactly as in Chapter 3, except with only one flash). The time of the flash would be marked on an EM trace. Subjects would then report the perceived tilt of the grating – this would be repeated several times. Using the same large gratings as in Chapter 3, it would be possible to ensure that the fovea is always directed towards the grating, regardless of the time during the waveform at which the flash was delivered.

The technique above would result in an EM trace with flashes marked. The waveform could then be separated into histogram ‘bins’; for example, from the time since the last foveation or quick phase. For each bin, the frequency of correct responses given to a flash at each spatial frequency would be recorded. This might demonstrate variability in the frequency of correct responses when the eyes are in different positions along the waveform, despite the gratings *always* being imaged on the fovea. Note that this would not be possible using the data already collected for Chapter 3, since multiple flashes were used for each response; hence it would not be possible to attribute a specific waveform location to each response.

6.5 Further measures of the ‘slow to see’ phenomenon

Chapter 4 investigated the time taken to locate and recognise the orientation of a grating target presented in different retinal locations. Alternative paradigms were also designed to measure different functional aspects of visual ‘timing’. These included the time taken to notice a change in a visual scene, a visual search paradigm, and a measure of the time taken to recognise a change in motion. Although these were not run as experiments for this report, programming was completed for each, and they could be used in the future in order to gain a greater understanding of the functional difficulties experienced by nystagmats. Each paradigm is briefly explained in the sections that follow.

6.5.1 Visual change recognition time

Although it is generally accepted that there is no suppression of vision during non-foveating periods of the waveform (see Section 1.3.9.1), it could be argued that a salient event, such as a light turning on, might break through suppression if it were present. For example, Jin,

Goldstein and Reinecke (1989) demonstrated constant conscious visual input in IN by showing that subjects were equally likely to perceive a 0.8° or 10° flash of light during all phases of their nystagmus. This is one of the major pieces of evidence upon which the ‘visual remapping’ theory (that states that vision is not suppressed during non-foveating periods of the waveform) is based. However, it seems feasible that if suppression *were* present, complex features such as a flash of light might be capable of breaking through that suppression. A potentially more appropriate way to test ‘time to see’ that would avoid this potential pitfall would be to have participants detect a visual change that is minimally salient, i.e. not likely to break through visual suppression. For this purpose, a program was written which displays a simple 2×2 checkerboard against a mid-grey background (see Figure 6.5). After a random delay of 1-3 s, the checkerboard pattern reverses. Subjects are instructed to indicate their perception of the change using a response box. Concurrent EM recordings would make it possible to know exactly where the eyes were when the reversal occurred, and the average time until a response could be investigated at various periods throughout the waveform.

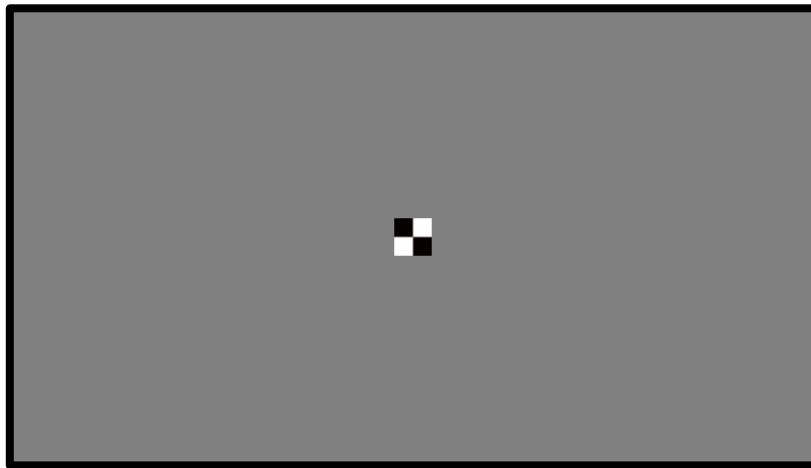


Figure 6.5: Program for testing visual reaction speed

6.5.2 Visual search

In a recent questionnaire study, one of the most stressful situations for individuals with IN was identified as being “finding a person in a crowd” (Jones 2011). This situation is analogous to a visual search task in which many of the search targets are moving. A simple visual search paradigm was created to simulate this. Subjects have to find a single reversed *Landolt C* character amongst a group of normal ‘C’ characters (see Figure 6.6). The task can be performed either with static targets, or with the targets slowly drifting around the search field. Based on the evidence presented in Chapter 4 (that nystagmats have significant difficulties in deploying gaze appropriately), this may provide a more sensitive clinical measure of visual function in IN than static, time-unlimited tests. Analysis of the scanpaths employed may also

reveal interesting differences to those used by normally-sighted individuals, owing to the typically horizontal oscillatory waveforms seen in subjects with IN.

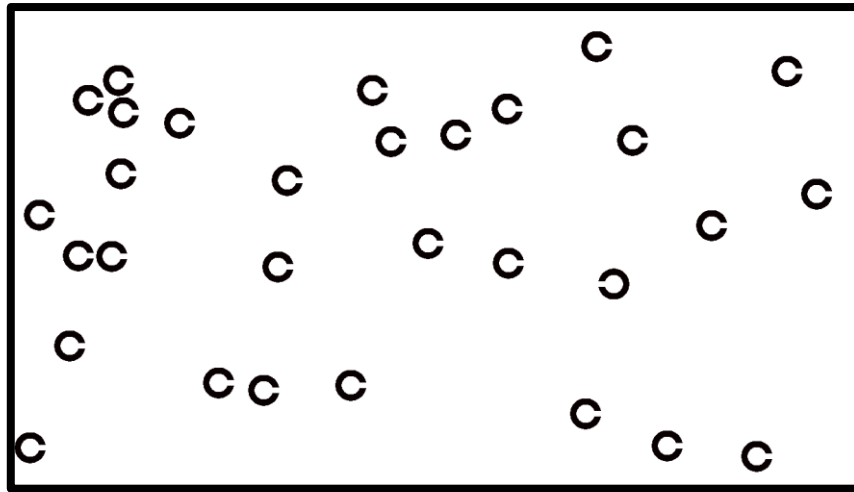


Figure 6.6: Screenshot from visual search paradigm

6.5.3 Motion change detection

The same questionnaire study mentioned above (Jones 2011) also identified “crossing the road in heavy traffic” as a particularly stressful task for people with IN. In response to this, another paradigm was created. In this, subjects view a target that drifts laterally across the screen (see Figure 6.7). After a random delay, the target reverses direction. This is designed to measure the time taken to notice changes in direction of motion, and can be performed at a range of stimulus velocities. As above, this might provide a more sensitive measure of visual function than standard clinical tests. This test (and the others presented here) could be performed under varying levels of nystagmus intensity, elicited through modifications in viewing angle (i.e. viewing in and out of the null zone).

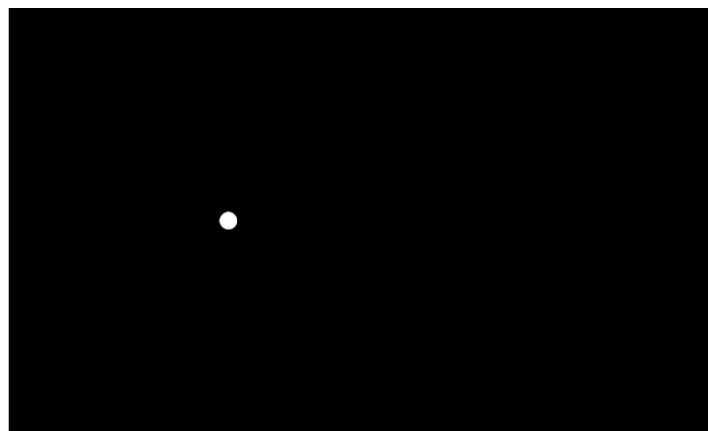


Figure 6.7: Motion change detection paradigm. The white circle is moving to the right, and will change direction at a random time

The paradigm above is likely to suffer from prediction bias; the further the target travels towards the screen edge, the more likely it is to reverse direction, since it will always reverse before reaching the screen edge. In order to circumvent this potential problem, the paradigm could be adapted. An alternative would be to use a full screen of drifting dots; the direction would change at a random time, but there would be less prediction bias inherent in the task, since the individual dots would be permitted to drift beyond the screen edge.

6.6 Summary

The additional studies presented in the chapter above may yield valuable insights into various aspects of visual perception and oculomotor control in IN. The work presented in Section 6.1 shows some interesting variability in nystagmus waveforms over long periods of inattention, but must now be repeated under visually homogenous conditions, in order to ‘unmask’ underlying pendular oscillations. Since the completion of the software presented in Chapter 2, it is now feasible to perform gaze contingent flash delivery, thus enabling the paradigms outlined in Sections 6.3 and 6.4 to be performed reliably. Finally, having established in Chapters 4 and 5 that the ‘slow to see’ phenomenon observed in individuals with IN is the result of difficulty reorienting the gaze, the additional studies described in Section 6.5 may be useful to quantify *functional* deficits in visual processing.

Chapter 7 Discussion

The overarching aim of the work presented in this thesis was to better understand the visual experience of people with IN. For a lay summary of the findings to emerge from the work presented in this thesis, please see Appendix IV. This letter was sent to all subjects, thanking them for their participation in the studies. The following chapter summarises the work in more detail.

Chapter 1 reviewed the literature concerning the characteristics and therapeutic intervention of IN. Although currently available treatments can produce significant changes in waveform parameters, little, if any, improvement in VA is found. Despite this, subjective reports following treatment tend to be positive, with some patients reporting ‘improved vision’. There was a need to address this important discrepancy in order to develop more appropriate visual outcome measures.

In Chapter 2, a method to objectively quantify IN waveforms was designed and tested. This method allows for rapid calibration of eye trackers in the presence of nystagmus, and serves as the basis for the experimental chapters that follow.

Chapter 3 detailed a study designed to determine the maximum VA available to individuals with IN in the absence of image motion. The aim of many IN therapies is to slow nystagmoid EMs, since it is assumed that motion blur (resulting from ocular oscillations) is detrimental to VA. The results of this chapter indicate that VA is fundamentally limited in adults with IN and that even if nystagmus was halted altogether, VA would *not* improve (if measured under strict psychophysical conditions). So, what hope exists for the nystagmat undergoing treatment? Clearly, subjective reports following treatment indicate that visual function can be improved *somehow*.

In Chapter 4, the concept of visual *timing* was explored. It has been reported that IN causes an increase in the time taken to recognise visual stimuli (Hertle et al. 2002), yet the cause of this timing deficit had not, until now, been explicitly defined. Using a task involving both oculomotor and perceptual components, it was revealed that the deficit is *not* due to visual processing time, but the time taken to accurately direct the gaze towards the object of regard.

Chapter 5 further investigated this oculomotor targeting deficit, by examining *when* in the nystagmus waveform subjects were able to elicit voluntary saccades towards displaced targets. One possibility was that the quick phases might produce a delay in the voluntary saccade, or alternatively, any suppression of vision during the non-foveating periods of the slow phases

might delay detection of the stimulus. In fact, the overwhelming majority of voluntary saccades were shown to coincide with nystagmus quick phases, which were often delayed in order to accommodate timing of the voluntary saccade. This suggests that the quick phases of nystagmus are non-pathological, and serve simply to reorient the gaze when the (pathological) slow phases have moved the eye too far from the object of regard.

The major findings of the studies are discussed in more detail below, separated into those findings that solely implicate visual perception, and those that relate to oculomotor control (which, of course, have consequences for visual perception).

7.1 Perception

The study presented in Chapter 3 concluded that VA is fundamentally limited in adults with IN, and that therapeutic interventions to slow the EMs are unlikely to yield demonstrable effects if VA is used as the primary outcome measure. The importance of this finding is that it implies that stopping nystagmus altogether would be unlikely to yield significant improvements in VA when measured under controlled psychophysical conditions. This may explain the lack of consistent VA improvements following therapies, despite reductions in nystagmus intensity and reported improvements in subjective visual function. The idea that VA may be a poor indicator of visual function in IN has been suspected for some time, which is why metrics to quantify the EMs themselves have come to be relied on as an outcome measure (see Section 1.3.8.5). Nevertheless, the applicability of measures such as NAFX are currently predicated on the relationship between NAFX and VA when plotted *between* subjects (Dell’Osso and Jacobs 2002). This relationship was assumed to hold true *within* subjects (due, in part, to results demonstrating that the vision of normally-sighted individuals can be similarly degraded by simulated nystagmoid image motion [Chung, LaFrance and Bedell 2011; Currie, Bedell and Song 1993; Chung and Bedell 1996]). Owing to this evidence, NAFX was believed to be useful as a *predictor* of VA. Recent work has refuted this, instead showing that waveform changes elicited by variations in gaze angle and stress have mixed effects on VA. Although a few individuals demonstrate some improvement in VA in the null zone, many get worse and others show no significant effect at all (Erichsen et al. 2013; Wiggins 2008; Jones et al. 2013).

The evidence in this report demonstrates that VA (when measured using a strict psychophysical protocol) cannot be *expected* to significantly improve with treatments that aim to reduce nystagmus intensity. This not only indicates that NAFX is unlikely to be an accurate predictor of VA following treatment, but also suggests that VA is itself an inappropriate

outcome measure for these treatments, as it is not significantly impacted by nystagmoid EMs in adulthood. This opens up the possibility of revisiting many nystagmus therapies that have been refuted in the past on the basis that they did not improve VA. Examples of these treatments include auditory biofeedback and intermittent photic stimulation (see Sections 1.3.10.4 and 1.3.10.7).

So, the question remains: Are NAFX, NOFF, NAEF and ANAF of any use at all? Certainly these metrics provide convenient ways of quantifying motor characteristics, and NAFX appears to correlate with *subjective* accounts of visual function following surgical intervention (Hertle et al. 2003). It is intuitive to assume that increasing the amount of time that the photoreceptor-rich fovea spends directed towards objects of interest ought to improve the visual experience in some way. Therefore, it is likely that improved NAFX would be a desirable outcome of any nystagmus therapy. The challenge now will be to identify exactly which aspects of visual perception NAFX might be associated with. Without a *perceptual* measure that correlates with NAFX, it is hard to justify its use as a therapeutic outcome measure. The work set out in Chapter 4 may provide clues as to how to resolve this.

Difficulties in visual ‘timing’ have long been suspected in IN, and in Chapter 4, this phenomenon was investigated in detail. The fact that individuals with IN take longer than controls to execute saccades towards peripherally presented targets (Wang and Dell’Osso 2007) was corroborated by the results of this study. In addition, the time taken to *recognise* visual targets was measured. The results showed that visual response time was not significantly different between subjects with and without IN, once the targeting saccade had completed. This suggests that visual processing in IN is *not* slow, and that the ‘slow to see’ phenomenon may be attributable *solely* to an increase in gaze targeting time.

Taken together, the results of Chapters 3 and 4 indicate that visual impairment in adults with IN is due to a combination of poor underlying VA and a difficulty in redirecting gaze towards objects of interest in a timely manner. Since VA appears to be limited in adults with IN, the most likely candidate for a perceptual correlate with waveform metrics such as NAFX appears to be target acquisition time; i.e. the time taken to foveate a peripherally presented target. An important next step is to identify whether target acquisition time is affected by factors known to affect waveform parameters, such as gaze angle or therapeutic intervention. Target acquiring saccade latency may provide a good objective measure of visual function in IN. Higher level visual function tests (such as those outlined in Chapter 6) may also prove to be useful prototypes for clinical measures, and might help to explain some of the functional difficulties faced by individuals with the condition.

7.2 Oculomotor characteristics

In addition to psychophysical measures of visual function, another outcome of the studies in this thesis was the development of a rapid method of quantifying the motor characteristics of IN waveforms. Chapter 2 described the development of a software package designed to calibrate and analyse large quantities of EM data. A saccade detection algorithm specialised for use in IN was also devised. This algorithm proved useful in analysing the data from Chapters 4 and 5. The ability to rapidly calibrate an eye tracking system in the presence of nystagmus makes future work using gaze-contingent stimuli more feasible, since calibration can now realistically be performed *before* beginning experiments. In addition, we are now witnessing the advent of gaze-interactive technology on mobile devices and computers. The algorithms presented in Chapter 2 may provide a means for nystagmats to interact with these devices.

An incidental finding during the analysis of Chapter 4 led to the work presented in Chapter 5. It was discovered that subjects with IN typically combine voluntary saccades and nystagmus quick phases into unified saccadic EMs. Furthermore, these combined saccades cause instantaneous modification of waveform dynamics (frequency and amplitude). This is significant, as it provides new evidence that the oculomotor system has control over the quick phases of nystagmus, reinforcing the theory that the *slow phases* of nystagmus are pathological, whereas quick phases represent normal (albeit unconscious) saccades.

It is still unclear whether or not individuals with IN are able to initiate saccadic programming at any point during the slow phase. Although the results of Chapter 5 show no evidence of a *linear* relationship between the timing of presentation of a stimulus for saccades and the actual saccadic latency, previous work (Wang and Dell’Osso 2007) has suggested the presence of curvilinear relationships that cannot be accurately tested with the quantities of data obtained in this study (or, this author would argue, their own data). Nonetheless, whether or not the ability to program saccades varies with the time course of nystagmus slow phases, it is clear from the results of Chapter 4 that saccadic programming is, on the whole, slower in IN than it is in normally-sighted individuals.

7.3 ‘Chicken and egg’

The results of Chapter 3 bring us no closer to answering the question “*Does nystagmus cause poor vision, or does poor vision cause nystagmus?*” Clearly, because eliminating image motion in adults does not improve VA, one might assume that, in each individual, nystagmus intensity is sufficiently low as to not cause a *worsening* of vision below the VA available. However, it is

possible that either amblyopia exists as a result of motion blur during the critical period of visual development or that poor VA may have pre-existed and contributed towards the development of IN. It is unlikely that this ‘chicken and egg’ conundrum will be untangled by experiments involving adult participants. Future work and treatment efforts should involve participants whose visual system is still developing, as stimulus deprivation amblyopia or hard-wired oculomotor oscillations are unlikely to resolve following the critical periods of visual and oculomotor development.

7.4 Final remarks

Nystagmus is an incredibly complex and variable condition, which is still very poorly understood. Although the work in this thesis provides a glimpse into the spatial and temporal limits of visual perception, the question “how does someone with nystagmus see the world?” is yet to be answered in full. Perceptual stability is assumed to be achieved by efference copy, but this hypothesis relies on experiments purported to refute suppression, in which observers detected salient stimuli during non-foveating periods of the waveform. In order to be certain of the absence of visual suppression during the slow phases of nystagmus, testing must be done with less salient visual stimuli (see Section 6.5.1).

It is unlikely that a cure or prevention for nystagmus will be discovered without first discovering the cause(s). Recent genetic work is making tremendous advances in this area (see Section 1.3.7). However, genetics cannot currently explain all forms of IN, and there is great variability in presentation of the condition, even within the idiopathic subcategory. Improved diagnostic techniques such as optical coherence tomography are identifying more and more ocular abnormalities related to IN (Thomas and Gottlob 2012; Thomas et al. 2014). The discipline of psychophysics is only one avenue through which advances may be made. By better understanding how perception with IN differs from that of normally-sighted individuals, it may be possible to identify new areas on which to focus future research.

It is hoped that the nystagmus calibration and analysis software developed here will prove useful clinically. Perhaps reducing the workload required to perform EM analyses will allow for greater acceptance of eye trackers within the clinic. A greater clinical awareness of nystagmus will surely improve patient care and inspire others to conduct further research into this fascinating, little understood condition.

References

- Abadi R V and Bjerre A (2002) Motor and sensory characteristics of infantile nystagmus. *Br J Ophthalmol* **86**: 1152–1160.
- Abadi R V, Carden D and Simpson J (1980) A new treatment for congenital nystagmus. *Br J Ophthalmol* **64**: 2–6.
- Abadi R V and Dickinson CM (1986) Waveform characteristics in congenital nystagmus. *Doc Ophthalmol* **64**: 153–167.
- Abadi R V and King-Smith PE (1979) Congenital nystagmus modifies orientational detection. *Vision Res* **19**: 1409–1411.
- Abadi R V and Pascal E (1991) Visual resolution limits in human albinism. *Vision Res* **31**: 1445–1447.
- Abadi R V and Sandikcioglu M (1975) Visual resolution in congenital pendular nystagmus. *Am J Optom Physiol Opt* **52**: 573–581.
- Abadi R V and Scallan CJ (2001) Ocular oscillations on eccentric gaze. *Vision Res* **41**: 2895–2907.
- Abadi R V and Whittle J (1991) The nature of head postures in congenital nystagmus. *Arch Ophthalmol* **109**: 216–220.
- Abadi R V and Worfolk R (1989) Retinal slip velocities in congenital nystagmus. *Vision Res* **29**: 195–205.
- Abel LA (2006) Infantile nystagmus: current concepts in diagnosis and management. *Clin Exp Optom* **89**: 57–65.
- Abel LA, Dell’Osso LF and Daroff RB (1978) Analog model for gaze-evoked nystagmus. *IEEE Trans Biomed Eng* **25**: 71–75.
- Alió JL, Chipont E, Mulet E and De La Hoz F (2003) Visual performance after congenital nystagmus surgery using extended hang back recession of the four horizontal rectus muscles. *Eur J Ophthalmol* **13**: 415–423.
- Allen ED and Davies PD (1983) Role of contact lenses in the management of congenital nystagmus. *Br J Ophthalmol* **67**: 834–836.
- Anyanwu E (1999) Evaluation of the laboratory and environmental factors that induce seizures in photosensitive epilepsy. *Acta Neurol Belg* **99**: 126–132.
- Arkin AM, Lutzky H and Toth MF (1972) Congenital nystagmus and sleep: a replication. *Psychophysiology* **9**: 210–217.
- Arkin AM, Weitzman ED and Hasteley JM (1966) An observational note on eye movement patterns during REM and non-REM sleep in subjects with congenital nystagmus. *Psychophysiology* **3**: 69–72.

- Atila H, Erkam N and Işıkçelik Y (1999) Surgical treatment in nystagmus. *Eye (Lond)* **13**: 11–15.
- Avallone JM, Bedell HE, Birch EE, Cotter S, Dell’Osso LF, Demer JL, Good W V, Granet DB, Hertle RW, Leigh RJ, Madigan Jr. WP, Maybodi M, McKee SP, Oberdorfer MD, Optican LM, Parks MM, Reinecke RD, Repka MX, Scheiman M, Schor CM, Scott WE and Tychsen L (2001) *A Classification of Eye Movement Abnormalities and Strabismus* [Online]. Available at: <http://www.nei.nih.gov/news/statements/cemas.pdf>.
- Bahill AT, Adler D and Stark L (1975) Most naturally occurring human saccades have magnitudes of 15 degrees or less. *Invest Ophthalmol* **14**: 468–469.
- Bahill AT, Clark MR and Stark L (1975) The main sequence, a tool for studying human eye movements. *Math Biosci* **24**: 191–204.
- Bahill AT, Kallman JS and Lieberman JE (1982) Frequency limitations of the two-point central difference differentiation algorithm. *Biol Cybern* **45**: 1–4.
- Baloh RW, Honrubia V and Konrad HR (1976) Periodic alternating nystagmus. *Brain* **99**: 11–26.
- Banks AZ and Wall C (1989) An improved clinical nystagmus algorithm. In: *Images of the Twenty-First Century. Proceedings of the Annual International Engineering in Medicine and Biology Society*. IEEE, pp. 648–649.
- Barker RA and Barasi S (1999) *Neuroscience at a Glance*. 1st ed. Cambridge: Blackwell Publishing Ltd.
- Barlow HB (1952) Eye movements during fixation. *J Physiol* **116**: 290–306.
- Barnes GR, Schmid AM and Jarrett CB (2002) The role of expectancy and volition in smooth pursuit eye movements. *Prog Brain Res* **140**: 239–254.
- Barnes GR and Smith R (1981) The effects of visual discrimination of image movement across the stationary retina. *Aviat Space Environ Med* **52**: 466–472.
- Becker W and Fuchs AF (1969) Further properties of the human saccadic system: eye movements and correction saccades with and without visual fixation points. *Vision Res* **9**: 1247–1258.
- Becker W and Klein HM (1973) Accuracy of saccadic eye movements and maintenance of eccentric eye positions in the dark. *Vision Res* **13**: 1021–1034.
- Bedell HE (2000) Perception of a clear and stable visual world with congenital nystagmus. *Optom Vis Sci* **77**: 573–581.
- Bedell HE (2006) Visual and perceptual consequences of congenital nystagmus. *Semin Ophthalmol* **21**: 91–95.
- Bedell HE, Abplanalp PL and McGuire CA (1987) Oculomotor responses to target displacements by patients with congenital idiopathic nystagmus and nystagmus associated with albinism. *Clin Vision Sci* **2**: 21–31.

- Bedell HE and Bollenbacher MA (1996) Perception of motion smear in normal observers and in persons with congenital nystagmus. *Invest Ophthalmol Vis Sci* **37**: 188–195.
- Bedell HE and Currie DC (1993) Extraretinal signals for congenital nystagmus. *Invest Ophthalmol Vis Sci* **34**: 2325–2332.
- Bedell HE and Loshin DS (1991) Interrelations between measures of visual acuity and parameters of eye movement in congenital nystagmus. *Invest Ophthalmol Vis Sci* **32**: 416–421.
- Bedell HE and Tong JL (2009) Asymmetrical perception of motion smear in infantile nystagmus. *Vision Res* **49**: 262–267.
- Bedell HE, White JM and Abplanalp PL (1989) Variability of foveations in congenital nystagmus. *Clin Vision Sci* **4**: 247–252.
- Behrens F, Mackeben M and Schröder-Preikschat W (2010) An improved algorithm for automatic detection of saccades in eye movement data and for calculating saccade parameters. *Behav Res Meth* **42**: 701–708.
- Berg P and Scherg M (1991) Dipole models of eye movements and blinks. *Electroen Clin Neurophysiol* **79**: 36–44.
- Van Beuzekom AD and Van Gisbergen JAM (2002) Interaction between visual and vestibular signals for the control of rapid eye movements. *J Neurophysiol* **88**: 306–322.
- Bifulco P, Cesarelli M, Loffredo L, Sansone M and Bracale M (2003) Eye movement baseline oscillation and variability of eye position during foveation in congenital nystagmus. *Doc Ophthalmol* **107**: 131–136.
- Billauer E (2012) *peakdet: Peak detection using MATLAB* [Online]. Available at: <http://www.billauer.co.il/peakdet.html> [Accessed: 22 January 2013].
- Biousse V, Tusa RJ, Russell B, Azran MS, Das V, Schubert MS, Ward M and Newman NJ (2004) The use of contact lenses to treat visually symptomatic congenital nystagmus. *J Neurol Neurosurg Psychiatry* **75**: 314–316.
- Birch EE, Subramanian V and Weakley DR (2013) Fixation instability in anisometric children with reduced stereopsis. *J AAPOS* **17**: 287–290.
- Bishop JE (2011) A novel new [yet again] procedure for correction of compensatory head posture in infantile nystagmus; augmented Anderson plus Dell'osso-Hertle. *Binocul Vis Strabolog Q Simms Romano* **26**: 37–42.
- Blekher T, Yamada T, Yee RD and Abel LA (1998) Effects of acupuncture on foveation characteristics in congenital nystagmus. *Br J Ophthalmol* **82**: 115–120.
- Boghen D, Troost BT, Daroff RB, Dell'Osso LF and Birkett JE (1974) Velocity characteristics of normal human saccades. *Invest Ophthalmol* **13**: 619–623.
- Bojanic S, Simpson T and Bolger C (2001) Ocular microtremor: a tool for measuring depth of anaesthesia? *Br J Anaesth* **86**: 519–522.

- Bolger C, Bojanic S, Sheahan NF, Coakley D and Malone JF (2001) Effect of age on ocular microtremor activity. *J Gerontol A Biol Sci Med Sci* **56**: 386–390.
- Bollen E, Bax J, van Dijk JG, Koning M, Bos JE, Kramer CG and van der Velde EA (1993) Variability of the main sequence. *Invest Ophthalmol Vis Sci* **34**: 3700–3704.
- Boyle NJ, Dawson ELM and Lee JP (2006) Benefits of retroequatorial four horizontal muscle recession surgery in congenital idiopathic nystagmus in adults. *J AAPOS* **10**: 404–408.
- Braddick O, Atkinson J and Wattam-Bell J (2003) Normal and anomalous development of visual motion processing: motion coherence and “dorsal-stream vulnerability”. *Neuropsychologia* **41**: 1769–1784.
- Brickner RM (1936) Oscillopsia - A new symptom commonly occurring in multiple sclerosis. *Arch Neurol Psych* **36**: 586–589.
- Brodsky MC and Dell’Osso LF (2014) A unifying neurologic mechanism for infantile nystagmus. *JAMA Ophthalmology*
- Broomhead DS, Clement RA, Muldoon MR, Whittle JP, Scallan C and Abadi R V (2000) Modelling of congenital nystagmus waveforms produced by saccadic system abnormalities. *Biol Cybern* **82**: 391–399.
- Burr DC, Morrone MC and Ross J (1994) Selective suppression of the magnocellular visual pathway during saccadic eye movements. *Nature* **371**: 511–513.
- Butterworth S (1930) On the theory of filter amplifiers. *Wireless Engineer* **7**: 536–541.
- Buttner-Ennever JA, Cohen B, Pause M and Fries W (1988) Raphe nucleus of the pons containing omnipause neurons of the oculomotor system in the monkey, and its homologue in man. *J Comp Neurol* **267**: 307–321.
- Cambridge Research Systems (2007) *Skalar IRIS Eyetracker* [Online]. Available at: www.crs Ltd.com/catalog/skalar.
- Cannon SC and Robinson DA (1987) Loss of the neural integrator of the oculomotor system from brain stem lesions in monkey. *J Neurophysiol* **57**: 1383–1409.
- Carl JR, Optican LM, Chu FC and Zee DS (1985) Head shaking and vestibulo-ocular reflex in congenital nystagmus. *Invest Ophthalmol Vis Sci* **26**: 1043–1050.
- Carruthers J (1995) The treatment of congenital nystagmus with Botox. *J Pediatr Ophthalmol Strabismus* **32**: 306–308.
- Casteels I, Harris CM, Shawkat F and Taylor D (1992) Nystagmus in infancy. *Br J Ophthalmol* **76**: 434–437.
- Cavegn D, Rensbergen J and d’Ydewalle G (1993) An artificial eye for evaluating videobased eye recording systems. *Behav Res Meth Ins C* **25**: 472–476.

- Cesarelli M, Bifulco P, Loffredo L and Bracale M (2000) Relationship between visual acuity and eye position variability during foveations in congenital nystagmus. *Doc Ophthalmol* **101**: 59–72.
- Cham KM, Anderson AJ and Abel LA (2008a) Factors influencing the experience of oscillopsia in infantile nystagmus syndrome. *Invest Ophthalmol Vis Sci* **49**: 3424–3431.
- Cham KM, Anderson AJ and Abel LA (2008b) Task-induced stress and motivation decrease foveation-period durations in infantile nystagmus syndrome. *Invest Ophthalmol Vis Sci* **49**: 2977–2984.
- Chen C-C, Bockisch CJ, Olasagasti I, Weber KP, Straumann D and Huang MY-Y (2014) Positive or negative feedback of optokinetic signals: degree of the misrouted optic flow determines system dynamics of human ocular motor behavior. *Invest Ophthalmol Vis Sci* **55**: 2297–2306.
- Choudhuri I, Sarvananthan N and Gottlob I (2007) Survey of management of acquired nystagmus in the United Kingdom. *Eye (Lond)* **21**: 1194–1197.
- Chung ST (2012) Vision in the presence of infantile nystagmus. In: Harris CM, Gottlob I, and Sanders J eds. *The Challenge of Nystagmus*. 1st ed. Cardiff: Nystagmus Network, pp. 261–271.
- Chung ST and Bedell HE (1998) Vernier and letter acuities for low-pass filtered moving stimuli. *Vision Res* **38**: 1967–1982.
- Chung ST, LaFrance MW and Bedell HE (2011) Influence of motion smear on visual acuity in simulated infantile nystagmus. *Optom Vis Sci* **88**: 200–207.
- Chung STL and Bedell HE (1997) Congenital nystagmus image motion: influence on visual acuity at different luminances. *Optom Vis Sci* **74**: 266–272.
- Chung STL and Bedell HE (1995) Effect of retinal image motion on visual-acuity and contour interaction in congenital nystagmus. *Vision Res* **35**: 3071–3082.
- Chung STL and Bedell HE (1996) Velocity criteria for “foveation periods” determined from image motions simulating congenital nystagmus. *Optom Vis Sci* **73**: 92–103.
- Ciuffreda KJ, Goldrich SG and Neary C (1982) Use of eye movement auditory biofeedback in the control of nystagmus. *Am J Optom Physiol Opt* **59**: 396–409.
- Coakley D and Thomas JG (1977) The ocular microtremor record and the prognosis of the unconscious patient. *Lancet* **1**: 512–515.
- Collewijn H (1999) Eye movement recording. In: Carpenter RHS and Robson JG eds. *Vision Research: a Practical Guide to Laboratory Methods*. Oxford: Oxford University Press, pp. 245–285.
- Comer RM, Dawson EL and Lee JP (2006) Baclofen for patients with congenital periodic alternating nystagmus. *Strabismus* **14**: 205–209.
- Cornsweet TN (1956) Determination of the stimuli for involuntary drifts and saccadic eye movements. *J Opt Soc Am* **46**: 987–993.

- Crawford JD, Cadera W and Vilis T (1991) Generation of torsional and vertical eye position signals by the interstitial nucleus of Cajal. *Science* **252**: 1551–1553.
- Cronin TH, Hertle RW, Ishikawa H and Schuman JS (2009) Spectral domain optical coherence tomography for detection of foveal morphology in patients with nystagmus. *J AAPOS* **13**: 563–566.
- Currie DC, Bedell HE and Song S (1993) Visual-acuity for optotypes with image motions simulating congenital nystagmus. *Clin Vision Sci* **8**: 73–84.
- Dell’Osso LF (2002) Development of new treatments for congenital nystagmus. *Ann N Y Acad Sci* **956**: 361–379.
- Dell’Osso LF (1998) Extraocular muscle tenotomy, dissection, and suture: a hypothetical therapy for congenital nystagmus. *J Pediatr Ophthalmol Strabismus* **35**: 232–233.
- Dell’Osso LF (1989) Nystagmus, saccadic intrusions/oscillations, and oscillopsia. In: Lessell S and van Dalen JTW eds. *Current Neuro-Ophthalmology*. Chicago: Year Book Medical Publishers, Inc., pp. 147–182.
- Dell’Osso LF (2011) The mechanism of oscillopsia and its suppression. *Ann N Y Acad Sci* **1233**: 298–306.
- Dell’Osso LF and Daroff RB (1975) Congenital nystagmus waveforms and foveation strategy. *Doc Ophthalmol* **39**: 155–182.
- Dell’Osso LF, Daroff RB and Tomsak RL (2001) Migraine aura and diplopia phenomenology associated with congenital nystagmus. *Neuro-Ophthalmology* **26**: 79–83.
- Dell’Osso LF, Hertle RW, Leigh RJ, Jacobs JB, King S and Yaniglos S (2011) Effects of topical brinzolamide on infantile nystagmus syndrome waveforms: eyedrops for nystagmus. *J Neuroophthalmol* **31**: 228–233.
- Dell’Osso LF, Hertle RW, Williams RW and Jacobs JB (1999) A new surgery for congenital nystagmus: effects of tenotomy on an achiasmatic canine and the role of extraocular proprioception. *J AAPOS* **3**: 166–182.
- Dell’Osso LF and Jacobs JB (2002) An expanded nystagmus acuity function: intra- and intersubject prediction of best-corrected visual acuity. *Doc Ophthalmol* **104**: 249–276.
- Dell’Osso LF, Leigh RJ and Daroff RB (1991) Suppression of congenital nystagmus by cutaneous stimulation. *Neuro-Ophthalmology* **11**: 173–175.
- Dell’Osso LF, van der Steen J, Steinman RM and Collewijn H (1992a) Foveation dynamics in congenital nystagmus. I: Fixation. *Doc Ophthalmol* **79**: 1–23.
- Dell’Osso LF, van der Steen J, Steinman RM and Collewijn H (1992b) Foveation dynamics in congenital nystagmus. II: Smooth pursuit. *Doc Ophthalmol* **79**: 25–49.
- Dell’Osso LF, van der Steen J, Steinman RM and Collewijn H (1992c) Foveation dynamics in congenital nystagmus. III: Vestibulo-ocular reflex. *Doc Ophthalmol* **79**: 51–70.

- Dell'Osso LF, Traccis S, Abel LA and Erzurum SI (1988) Contact lenses and congenital nystagmus. *Clin Vision Sci* **3**: 229–232.
- Demer JL and Amjadi F (1993) Dynamic visual acuity of normal subjects during vertical optotype and head motion. *Invest Ophthalmol Vis Sci* **34**: 1894–1906.
- Dickinson CM (1986) The elucidation and use of the effect of near fixation in congenital nystagmus. *Ophthalmic Physiol Opt* **6**: 303–311.
- Dickinson CM and Abadi R V (1984) Corneal topography of humans with congenital nystagmus. *Ophthalmic Physiol Opt* **4**: 3–13.
- Dickinson CM and Abadi R V (1985) The influence of nystagmoid oscillation on contrast sensitivity in normal observers. *Vision Res* **25**: 1089–1096.
- Duchowski AT (2007) *Eye Tracking Methodology*. 2nd ed. London: Springer.
- Dunn MJ, Margrain TH, Woodhouse JM, Ennis F, Harris CM and Erichsen JT (2014) Grating visual acuity in infantile nystagmus in the absence of image motion. *Invest Ophthalmol Vis Sci* **55**: 2682–2686.
- Easter SS and Schmidt JT (1977) Reversed visuomotor behavior mediated by induced ipsilateral retinal projections in goldfish. *J Neurophysiol* **40**: 1245–1254.
- Eggert T (2007) Eye movement recordings: methods. *Dev Ophthalmol* **40**: 15–34.
- Eggert T, Straube A and Schroeder K (1997) Visually induced motion perception and visual control of postural sway in congenital nystagmus. *Behav Brain Res* **88**: 161–168.
- ElKamshoushy A, Shawky D, Elmassry A, Elbaha S, Abdel Wahab MM and Sprunger D (2012) Improved visual acuity and recognition time in nystagmus patients following four-muscle recession or Kestenbaum-Anderson procedures. *J AAPOS* **16**: 36–40.
- Elliot DB (2003) *Clinical Procedures in Primary Eye Care*. 2nd ed. Edinburgh: Butterworth-Heinemann.
- Engelken EJ and Stevens KW (1990) A new approach to the analysis of nystagmus: an application for order-statistic filters. *Aviat Space Environ Med* **61**: 859–864.
- Erichsen JT, Wiggins D, Woodhouse JM, Margrain TH and Harris CM (2013) Effect of eye orientation on visual acuity in infantile nystagmus (INS). In: *17th European Conference on Eye Movements*. Lund, p. 514.
- Evans BJW V, Jordahl-Moroz J and Nabee M (1998) Randomised double-masked placebo-controlled trial of a treatment for congenital nystagmus. *Vision Res* **38**: 2193–2202.
- Evinger C, Kaneko CR and Fuchs AF (1982) Activity of omnipause neurons in alert cats during saccadic eye movements and visual stimuli. *J Neurophysiol* **47**: 827–844.
- Felius J, Fu VL, Birch EE, Hertle RW, Jost RM and Subramanian V (2011) Quantifying nystagmus in infants and young children: relation between foveation and visual acuity deficit. *Invest Ophthalmol Vis Sci* **52**: 8724–8731.

- Felius J and Muhanna ZA (2013) Visual deprivation and foveation characteristics both underlie visual acuity deficits in idiopathic infantile nystagmus. *Invest Ophthalmol Vis Sci* **54**: 3520–3525.
- Fellows BJ (1967) Chance stimulus sequences for discrimination tasks. *Psychol Bull* **67**: 87–92.
- Fishman RS (2006) Dark as a dungeon: the rise and fall of coal miners' nystagmus. *Arch Ophthalmol* **124**: 1637–1644.
- Fresina M, Benedetti C, Marinelli F, Versura P and Campos EC (2013) Astigmatism in patients with idiopathic congenital nystagmus. *Graefes Arch Clin Exp Ophthalmol* **251**: 1635–1639.
- Fu VL, Bilonick RA, Felius J, Hertle RW and Birch EE (2011) Visual acuity development of children with infantile nystagmus syndrome. *Invest Ophthalmol Vis Sci* **52**: 1404–1411.
- Garbutt S, Harwood MR and Harris CM (2001) Comparison of the main sequence of reflexive saccades and the quick phases of optokinetic nystagmus. *Br J Ophthalmol* **85**: 1477–1483.
- Garbutt S, Harwood MR and Harris CM (2006) Infant saccades are not slow. *Dev Med Child Neurol* **48**: 662–667.
- Van der Geest JN and Frens MA (2002) Recording eye movements with video-oculography and scleral search coils: a direct comparison of two methods. *J Neurosci Methods* **114**: 185–195.
- Gellerman (1933) Chance orders of alternating stimuli in visual discrimination experiments. *J Gen Psychol* **42**: 29–50.
- Gilchrist ID (2011) Saccades. In: *The Oxford Handbook of Eye Movements*. First. Oxford: Oxford Library of Psychology, pp. 85–94.
- Goldstein HP, Gottlob I and Fendick MG (1992) Visual remapping in infantile nystagmus. *Vision Res* **32**: 1115–1124.
- Good GW and Augsburger AR (1986) Use of horizontal gaze nystagmus as a part of roadside sobriety testing. *Am J Optom Physiol Opt* **63**: 467–471.
- Good W V, Hou C and Carden SM (2003) Transient, idiopathic nystagmus in infants. *Dev Med Child Neurol* **45**: 304–307.
- Gottlob I (1997) Infantile nystagmus. Development documented by eye movement recordings. *Invest Ophthalmol Vis Sci* **38**: 767–773.
- Gottlob I (2000) Nystagmus. *Curr Opin Ophthalmol* **11**: 330–335.
- Gottlob I and Proudlock FA (2014) Aetiology of infantile nystagmus. *Curr Opin Neurol* **27**: 83–91.
- Gottlob I, Wizov SS and Reinecke RD (1995) Spasmus nutans. A long-term follow-up. *Invest Ophthalmol Vis Sci* **36**: 2768–2771.

Gottlob I, Zubcov A, Catalano RA, Reinecke RD, Koller HP, Calhoun JH and Manley DR (1990) Signs distinguishing spasmus nutans (with and without central nervous system lesions) from infantile nystagmus. *Ophthalmology* **97**: 1166–1175.

Gradstein L, Goldstein HP, Wizov SS, Hayashi T and Reinecke RD (1998) Relationships among visual acuity demands, convergence, and nystagmus in patients with manifest/latent nystagmus. *J AAPOS* **2**: 218–229.

Gradstein L, Reinecke RD, Wizov SS and Goldstein HP (1997) Congenital periodic alternating nystagmus. Diagnosis and management. *Ophthalmology* **104**: 928–929.

Gresty MA, Bronstein AM, Page NG and Rudge P (1991) Congenital-type nystagmus emerging in later life. *Neurology* **41**: 653–656.

Gupta M, Mulvihill AO, Lascaratos G, Fleck BW and George NDLD (2009) Nystagmus and reduced visual acuity secondary to drug exposure in utero: long-term follow-up. *J AAPOS* **13**: e17.

Hanson KS, Bedell HE, White JM and Ukwade MT (2006) Distance and near visual acuity in infantile nystagmus. *Optom Vis Sci* **83**: 823–829.

Harris CM and Berry D (2006) A developmental model of infantile nystagmus. *Semin Ophthalmol* **21**: 63–69.

Harvey EM (2009) Development and treatment of astigmatism-related amblyopia. *Optom Vis Sci* **86**: 634–639.

Helveston EM, Ellis FD and Plager DA (1991) Large recession of the horizontal recti for treatment of nystagmus. *Ophthalmology* **98**: 1302–1305.

Helveston EM and Pogrebniak AE (1988) Treatment of acquired nystagmus with botulinum A toxin. *Am J Ophthalmol* **106**: 584–586.

Hernández-García E and Gómez-De-Liaño-Sánchez R (2012) Use of botulinum toxin in a patient with pendular congenital nystagmus. *Arch Soc Esp Oftalmol* **87**: 330–332.

Hertle RW and Dell'Osso LF (2007) Benefits of retroequatorial four horizontal muscle recession surgery in congenital idiopathic nystagmus in adults. *J AAPOS* **11**: 313.

Hertle RW, Dell'Osso LF, FitzGibbon EJ, Thompson D, Yang D and Mellow SD (2003) Horizontal rectus tenotomy in patients with congenital nystagmus: results in 10 adults. *Ophthalmology* **110**: 2097–2105.

Hertle RW, Maybodi M, Bauer RM and Walker K (2001) Clinical and oculographic response to Dexedrine in a patient with rod-cone dystrophy, exotropia, and congenital aperiodic alternating nystagmus. *Binocul Vis Strabismus Q* **16**: 259–264.

Hertle RW, Maybodi M, Reed GF, Guerami AH, Yang D and Fitzgibbon EJ (2002) Latency of dynamic and gaze-dependent optotype recognition in patients with infantile nystagmus syndrome versus control subjects. *Ann N Y Acad Sci* **956**: 601–603.

- Hertle RW, Reznick L and Yang DS (2009) Infantile aperiodic alternating nystagmus. *J Pediatr Ophthalmol Strabismus* **46**: 93–103.
- Hertle RW, Yang D, Jeng J, Carey K and Mitchell E (2012) A systematic approach to eye muscle surgery for infantile nystagmus syndrome: general results in 100 patients. In: Harris CM, Gottlob I, and Sanders J eds. *The Challenge of Nystagmus*. 1st ed. Cardiff, pp. 339–366.
- Hittinger M and Horn AKE (2012) The anatomical identification of saccadic omnipause neurons in the rat brainstem. *Neuroscience* **210**: 191–199.
- Holmström G, Bondeson M-L, Eriksson U, Akerblom H and Larsson E (2013) “Congenital” nystagmus may hide various ophthalmic diagnoses. *Acta Ophthalmologica*
- Hou RL and Fender DH (1979) Processing of direction and magnitude by the saccadic eye-movement system. *Vision Res* **19**: 1421–1426.
- Huang MY-Y, Chen C-C, Huber-Reggi SP, Neuhauss SCF and Straumann D (2011) Comparison of infantile nystagmus syndrome in achiasmatic zebrafish and humans. *Ann N Y Acad Sci* **1233**: 285–291.
- Huang Y-Y, Rinner O, Hedinger P, Liu S-C and Neuhauss SCF (2006) Oculomotor instabilities in zebrafish mutant belladonna: a behavioral model for congenital nystagmus caused by axonal misrouting. *J Neurosci* **26**: 9873–9880.
- Huber-Reggi SP, Chen C-C, Grimm L, Straumann D, Neuhauss SCF and Huang MY-Y (2012) Severity of infantile nystagmus syndrome-like ocular motor phenotype is linked to the extent of the underlying optic nerve projection defect in zebrafish belladonna mutant. *J Neurosci* **32**: 18079–18086.
- Huurneman B and Boonstra FN (2013) Monocular and binocular development in children with albinism, infantile nystagmus syndrome, and normal vision. *Strabismus* **21**: 216–224.
- Irving EL, Zacher JE, Allison RS and Callender MG (2003) Effects of scleral search coil wear on visual function. *Invest Ophthalmol Vis Sci* **44**: 1933–1938.
- Ishikawa S, Ozawa H and Fujiyama Y (1987) Treatment of nystagmus by acupuncture. In: Boyd BF ed. *Highlights in neuro-ophthalmology. Proceedings of the sixth meeting of the International Neuro-Ophthalmology Society (INOS)*. Amsterdam: Aeolus Press, pp. 227–232.
- Jacobs JB and Dell’Osso LF (2004) Congenital nystagmus: hypotheses for its genesis and complex waveforms within a behavioral ocular motor system model. *J Vis* **4**: 604–625.
- Jacobs JB and Dell’Osso LF (2009) Extending the eXpanded Nystagmus Acuity Function for vertical and multiplanar data. *Vision Res* **50**: 271–278.
- Janczewski G, Zajac J, Pierchala K, Dawidowicz J, Kowalski W and Kochanek K (1996) [Computer analysis of nystagmus]. *Otolaryngologia polska* **50**: 428–434.
- Jin YH, Goldstein HP and Reinecke RD (1989) Absence of visual sampling in infantile nystagmus. *Korean J Ophthalmol* **3**: 28–32.

- Jones DH (2001) Bell's phenomenon should not be regarded as pathognomonic sign. *Br Med J* **323**: 935.
- Jones PH (2011) The impact of stress on visual function in nystagmus. Cardiff University.
- Jones PH, Harris CM, Woodhouse JM, Margrain TH, Ennis F and Erichsen JT (2013) Stress and visual function in infantile nystagmus syndrome. *Invest Ophthalmol Vis Sci* **54**: 7943–7951.
- Jones PH, Woodhouse JM, Margrain TH and Erichsen JT (2008) Perception of the world through wobbly eyes - it's stressing me out! In: *ARVO*.
- Juhola M (1988) Detection of nystagmus eye movements using a recursive digital filter. *IEEE Trans Biomed Eng* **35**: 389–395.
- Keller EL (1974) Participation of medial pontine reticular formation in eye movement generation in monkey. *J Neurophysiol* **37**: 316–332.
- Keller EL, McPeck RM and Salz T (2000) Evidence against direct connections to PPRF EBNs from SC in the monkey. *J Neurophysiol* **84**: 1303–1313.
- Khanna S and Dell'Osso LF (2006) The diagnosis and treatment of infantile nystagmus syndrome (INS). *ScientificWorldJournal* **6**: 1385–1397.
- Kumar A, Gottlob I, McLean RJ, Thomas S, Thomas MG and Proudlock FA (2011a) Clinical and oculomotor characteristics of albinism compared to FRMD7 associated infantile nystagmus. *Invest Ophthalmol Vis Sci* **52**: 2306–2313.
- Kumar A, Shetty S, Vijayalakshmi P and Hertle RW (2011b) Improvement in visual acuity following surgery for correction of head posture in infantile nystagmus syndrome. *J Pediatr Ophthalmol Strabismus* **48**: 341–346.
- Kurzan R and Buttner U (1989) Smooth pursuit mechanisms in congenital nystagmus. *Neuro-Ophthalmology* **9**: 313–325.
- Lappin JS, Tadin D, Nyquist JB and Corn AL (2009) Spatial and temporal limits of motion perception across variations in speed, eccentricity, and low vision. *J Vis* **9**: 1–14.
- Lee AG and Brazis PW (2006) Localizing forms of nystagmus: symptoms, diagnosis, and treatment. *Curr Neurol Neurosci Rep* **6**: 414–420.
- Lee J (2002) Surgical management of nystagmus. *J R Soc Med* **95**: 238–241.
- Leigh RJ, Dell'Osso LF, Yaniglos SS and Thurston SE (1988) Oscillopsia, retinal image stabilization and congenital nystagmus. *Invest Ophthalmol Vis Sci* **29**: 279–282.
- Leigh RJ and Kennard C (2004) Using saccades as a research tool in the clinical neurosciences. *Brain* **127**: 460–477.
- Leigh RJ and Zee DS (2006) *The Neurology of Eye Movements*. Fourth. Oxford: Oxford University Press.

- Levitt H (1971) Transformed up-down methods in psychoacoustics. *J Acoust Soc Am* **49**: 467–477.
- Li L, Xiao X, Yi C, Jiao X, Guo X, Hejtmancik JF and Zhang Q (2012) Confirmation and refinement of an autosomal dominant congenital motor nystagmus locus in chromosome 1q31.3-q32.1. *J Hum Genet* **57**: 756–759.
- Liu Z, Mao S, Pu J, Ding Y, Zhang B and Ding M (2013) A novel missense mutation in the FERM domain containing 7 (FRMD7) gene causing X-linked idiopathic congenital nystagmus in a Chinese family. *Mol Vis* **19**: 1834–1840.
- Lorenz B and Gampe E (2001) Analysis of 180 patients with sensory defect nystagmus (SDN) and congenital idiopathic nystagmus (CIN). *Klin Monbl Augenheilkd* **218**: 3–12.
- Loshin DS and Browning RA (1983) Contrast sensitivity in albinotic patients. *Am J Optom Physiol Opt* **60**: 158–166.
- Ludvigh E and Miller JW (1958) Study of visual acuity during the ocular pursuit of moving test objects. I. Introduction. *J Opt Soc Am* **48**: 799–802.
- Ludwig CJH, Gilchrist ID and McSorley E (2004) The influence of spatial frequency and contrast on saccade latencies. *Vision Res* **44**: 2597–2604.
- Mallett RFJ (1983) The treatment of congenital idiopathic nystagmus by intermittent photic-stimulation. *Ophthalmic Physiol Opt* **3**: 341–356.
- Mandelbaum J and Sloan LL (1947) Peripheral visual acuity with special reference to scotopic illumination. *Am J Ophthalmol* **30**: 581–588.
- Manni R (2005) Rapid eye movement sleep, non-rapid eye movement sleep, dreams, and hallucinations. *Curr Psychiatry Rep* **7**: 196–200.
- Martinez-Conde S, Macknik SL and Hubel DH (2004) The role of fixational eye movements in visual perception. *Nat Rev Neurosci* **5**: 229–240.
- Martinez-Conde S, Macknik SL, Troncoso XG and Hubel DH (2009) Microsaccades: a neurophysiological analysis. *Trends Neurosci* **32**: 463–475.
- May PJ and Corbett JJ (1997) Visual Motor Systems. In: Haines D ed. *Fundamental Neuroscience*. First. Philadelphia: Churchill Livingstone, pp. 399–416.
- McGlone L, Hamilton R, McCulloch DL, Mackinnon JR, Bradnam M and Mactier H (2013) Visual outcome in infants born to drug-misusing mothers prescribed methadone in pregnancy. *Br J Ophthalmol* **98**: 238–245.
- McLean RJ and Gottlob I (2009) The pharmacological treatment of nystagmus: a review. *Expert Opin Pharmacother* **10**: 1805–1816.
- McLean RJ, Proudlock F, Thomas S, Degg C and Gottlob I (2007) Congenital nystagmus: randomized, controlled, double-masked trial of memantine/gabapentin. *Ann Neurol* **61**: 130–138.

- Meiusi RS, Lavoie JD and Summers CG (1993) The effect of grating orientation on resolution acuity in patients with nystagmus. *J Pediatr Ophthalmol Strabismus* **30**: 259–261.
- Metz (2009) *Mecablitz* [Online]. Available at: <http://www.metz.de/en/photo-electronics/instruction-manuals/mecablitz.html>.
- Mezawa M, Ishikawa S and Ukai K (1990) Changes in wave-form of congenital nystagmus associated with biofeedback treatment. *Br J Ophthalmol* **74**: 472–476.
- Miller JW (1958) Study of visual acuity during the ocular pursuit of moving test objects. II. Effects of direction of movement, relative movement, and illumination. *J Opt Soc Am* **48**: 803–808.
- Millodot M (2004) *Dictionary of Optometry and Visual Science*. 6th ed. Edinburgh: Butterworth-Heinemann.
- Mitchell DE, Freeman RD, Millodot M and Haegerstrom G (1973) Meridional amblyopia: evidence for modification of the human visual system by early visual experience. *Vision Res* **13**: 535–558.
- Møller F, Laursen ML and Sjølie AK (2006) The contribution of microsaccades and drifts in the maintenance of binocular steady fixation. *Graefes Arch Clin Exp Ophthalmol* **244**: 465–471.
- Mulvihill AO, Cackett PD, George ND and Fleck BW (2007) Nystagmus secondary to drug exposure in utero. *Br J Ophthalmol* **91**: 613–615.
- Murphy PJ, Duncan AL, Glennie AJ and Knox PC (2001) The effect of scleral search coil lens wear on the eye. *Br J Ophthalmol* **85**: 332–335.
- National Information Display Laboratory (2001) Evaluation of the Sony GDM-F520 21-inch diagonal color CRT monitor for monoscopic and stereoscopic imagery Alliance NT ed.
- Optican LM and Zee DS (1984) A hypothetical explanation of congenital nystagmus. *Biol Cybern* **50**: 119–134.
- Oyster CW (1999) *The Human Eye: Structure and Function*. Sunderland: Sinauer.
- Pander T, Czabanski R, Przybyla T, Jezewski J, Pojda-Wilczek D, Wrobel J, Horoba K and Bernys M (2012) A new method of saccadic eye movement detection for optokinetic nystagmus analysis. In: *Annual International Conference of the IEEE Engineering in Medicine and Biology Society*. pp. 3464–3467.
- Pasquariello G, Cesarelli M, Bifulco P, Fratini A, La Gatta A and Romano M (2009) Characterisation of baseline oscillation in congenital nystagmus eye movement recordings. *Biomed Signal Proces* **4**: 102–107.
- Pasquariello G, Cesarelli M, Romano M, La Gatta A, Bifulco P and Fratini A (2010) Waveform type evaluation in congenital nystagmus. *Comput Meth Prog Bio* **100**: 49–58.
- Pel J, Does L V, Boot F, Faber TD, Steen-Kant S V, Willemsen S and Steen H V (2011) Effects of visual processing and congenital nystagmus on visually guided ocular motor behaviour. *Dev Med Child Neurol* **53**: 344–349.

- Pel JJM, Kooiker MJG, Does JME van der, Boot FH, Faber JT de, Steen-Kant SP van der and Steen J van der (2013) Orienting responses to various visual stimuli in children with visual processing impairments or infantile nystagmus syndrome. *J Child Neurol*
- Pradeep A, Thomas S, Roberts EO, Proudlock FA and Gottlob I (2008) Reduction of congenital nystagmus in a patient after smoking cannabis. *Strabismus* **16**: 29–32.
- Pritchard RM (1961) Stabilized images on the retina. *Sci Am* **204**: 72–78.
- Proudlock F and Gottlob I (2011) Foveal development and nystagmus. *Ann N Y Acad Sci* **1233**: 292–297.
- Pu J, Li Y, Liu Z, Yan Y, Tian J, Chen S and Zhang B (2011) Expression and localization of FRMD7 in human fetal brain, and a role for F-actin. *Mol Vis* **17**: 591–597.
- R Core Team (2012) R: a language and environment for statistical computing.
- Radhakrishna U, Ratnamala U, Deutsch S, Bartoloni L, Kuracha MR, Singh R, Banwait J, Bastola DK, Johar K, Nath SK and Antonarakis SE (2012) Novel homozygous, heterozygous and hemizygous FRMD7 gene mutations segregated in the same consanguineous family with congenital X-linked nystagmus. *Eur J Hum Genet* **20**: 1032–1036.
- Radinsky I and Galiana HL (2004) Improved algorithm for classification of ocular nystagmus. In: *Annual International Conference of the IEEE Engineering in Medicine and Biology Society*. pp. 534–537.
- Ramadoss L and Hung JY (2008) A study on universal serial bus latency in a real-time control system. In: *2008 34th Annual Conference of IEEE Industrial Electronics*. IEEE, pp. 67–72.
- Ramat S, Leigh RJ, Zee DS and Optican LM (2005) Ocular oscillations generated by coupling of brainstem excitatory and inhibitory saccadic burst neurons. *Exp Brain Res* **160**: 89–106.
- Randall HG, Brown DJ and Sloan LL (1966) Peripheral visual acuity. *Arch Ophthalmol* **75**: 500–504.
- Reinecke RD (1997) Idiopathic infantile nystagmus: diagnosis and treatment. *J AAPOS* **1**: 67–82.
- Reinecke RD, Guo S and Goldstein HP (1988) Waveform evolution in infantile nystagmus: An electro-oculo-graphic study of 35 cases. *Binocular Vision* **3**: 191–202.
- Reinecke RD, Hertle RW, FitzGibbon EJ, Avallone JM, Cheeseman E and Tsilou EK (2001) Onset of oscillopsia after visual maturation in patients with congenital nystagmus. *Ophthalmology* **108**: 2301–2307.
- Remington LA (1998) *Clinical Anatomy of the Visual System*. Newton: Butterworth-Heinemann.
- Repka MX, Friedman DS, Katz J, Ibrionke J, Giordano L and Tielsch JM (2012) The prevalence of ocular structural disorders and nystagmus among preschool-aged children. *J AAPOS* **16**: 182–184.

- Reulen JPH, Marcus JT, Vangilst MJ, Koops D, Bos JE, Tiesinga G, Devries FR, Boshuizen K and de Vries FR (1988) Precise recording of eye movement: the IRIS technique. Part 1. *Med Biol Eng Comput* **26**: 20–26.
- Robinson DA (1963) A method of measuring eye movement using a scleral search coil in a magnetic field. *IEEE Trans Biomed Eng* **10**: 137–145.
- Robinson DA, Gordon JL and Gordon SE (1986) A model of the smooth pursuit eye movement system. *Biol Cybern* **55**: 43–57.
- Ron S, Robinson DA and Skavenski AA (1972) Saccades and the quick phase of nystagmus. *Vision Res* **12**: 2015–2022.
- Ross J, Burr D and Morrone C (1996) Suppression of the magnocellular pathway during saccades. *Behav Brain Res* **80**: 1–8.
- Rowe FJ (1997) *Clinical Orthoptics*. Oxford: Blackwell Science.
- Sampath V and Bedell HE (2002) Distribution of refractive errors in albinos and persons with idiopathic congenital nystagmus. *Optom Vis Sci* **79**: 292–299.
- Sanders J (2006) The UK Nystagmus Network (NN). *Semin Ophthalmol* **21**: 61.
- Sarvananthan N, Proudlock FA, Choudhuri I, Dua H and Gottlob I (2006) Pharmacologic treatment of congenital nystagmus. *Arch Ophthalmol* **124**: 916–918.
- Sarvananthan N, Surendran M, Roberts EO, Jain S, Thomas S, Shah N, Proudlock FA, Thompson JR, McLean RJ, Degg C, Woodruff G and Gottlob I (2009) The prevalence of nystagmus: the Leicestershire nystagmus survey. *Invest Ophthalmol Vis Sci* **50**: 5201–5206.
- Schütz AC, Braun DI, Kerzel D and Gegenfurtner KR (2008) Improved visual sensitivity during smooth pursuit eye movements. *Nat Neurosci* **11**: 1211–1216.
- Schütz AC and Morrone MC (2010) Compression of time during smooth pursuit eye movements. *Vision Res* **50**: 2702–13.
- Self J and Lotery A (2007) A review of the molecular genetics of Congenital Idiopathic Nystagmus (CIN). *Ophthalmic Genet* **28**: 187–191.
- Shadlen MN and Newsome WT (2001) Neural basis of a perceptual decision in the parietal cortex (area LIP) of the rhesus monkey. *J Neurophysiol* **86**: 1916–1936.
- Shaikh AG, Ramat S, Optican LM, Miura K, Leigh RJ and Zee DS (2008) Saccadic burst cell membrane dysfunction is responsible for saccadic oscillations. *J Neuroophthalmol* **28**: 329–336.
- Shaikh AG, Wong AL, Optican LM, Miura K, Solomon D and Zee DS (2010) Sustained eye closure slows saccades. *Vision Res* **50**: 1665–1675.
- Shallo-Hoffmann JA, Faldon M and Tusa RJ (1999) The incidence and waveform characteristics of periodic alternating nystagmus in congenital nystagmus. *Invest Ophthalmol Vis Sci* **40**: 2546–2553.

- Shallo-Hoffmann JA, Wolsley CJ, Acheson JF and Bronstein AM (1998) Reduced duration of a visual motion aftereffect in congenital nystagmus. *Doc Ophthalmol* **95**: 301–314.
- Sharma P, Tandon R, Kumar S and Anand S (2000) Reduction of congenital nystagmus amplitude with auditory biofeedback. *J AAPOS* **4**: 287–290.
- Shawkat FS, Harris CM and Taylor DS (2001) Spontaneous reversal of nystagmus in the dark. *Br J Ophthalmol* **85**: 428–431.
- Shery T, Proudlock FA, Sarvananthan N, McLean RJ and Gottlob I (2006) The effects of gabapentin and memantine in acquired and congenital nystagmus: a retrospective study. *Br J Ophthalmol* **90**: 839–843.
- Sheth N V, Dell’Osso LF, Leigh RJ, Vandoren CL, Peckham HP and Van Doren CL (1995) The effects of afferent stimulation on congenital nystagmus foveation periods. *Vision Res* **35**: 2371–2382.
- Siderov J and Tiu AL (1999) Variability of measurements of visual acuity in a large eye clinic. *Acta Ophthalmol Scand* **77**: 673–676.
- Simon JR and Rudell AP (1967) Auditory S-R compatibility: the effect of an irrelevant cue on information processing. *J Appl Psychol* **51**: 300–304.
- Simon JR and Wolf JD (1963) Choice reaction time as a function of angular stimulus-response correspondence and age. *Ergonomics* **6**: 99–105.
- Sjödell L, Sjöström A and Abrahamsson M (1996) Transillumination of iris and subnormal visual acuity - ocular albinism? *Br J Ophthalmol* **80**: 617–623.
- Solomon D, Shepard N and Mishra A (2002) Congenital periodic alternating nystagmus: response to baclofen. *Ann N Y Acad Sci* **956**: 611–615.
- Sparks DL (2002) The brainstem control of saccadic eye movements. *Nat Rev Neurosci* **3**: 952–964.
- Spauschus A, Marsden J, Halliday DM, Rosenberg JR and Brown P (1999) The origin of ocular microtremor in man. *Exp Brain Res* **126**: 556–562.
- Sprunger DT, Fahad B and Helveston EM (1997) Recognition time after four muscle recession for nystagmus. *Am Orthopt J* **47**: 122–125.
- SR Research (2010) *EyeLink 1000* [Online]. Available at: http://www.sr-research.com/EL_1000.html [Accessed: 3 February 2013].
- St Cyr GJ and Fender DH (1969) The interplay of drifts and flicks in binocular fixation. *Vision Res* **9**: 245–265.
- Stahl JS, Plant GT and Leigh RJ (2002) Medical treatment of nystagmus and its visual consequences. *J R Soc Med* **95**: 235–237.
- Stampe DM (1993) Heuristic filtering and reliable calibration methods for video-based pupil-tracking systems. *Behav Res Meth Ins C* **25**: 137–142.

- Stern RM, Ray WJ and Quigley KS (2001) *Psychophysiological Recording*. 2nd ed. Oxford: Oxford University Press US.
- Strupp M, Thurtell MJ, Shaikh AG, Brandt T, Zee DS and Leigh RJ (2011) Pharmacotherapy of vestibular and ocular motor disorders, including nystagmus. *J Neurol* **258**: 1207–1222.
- Tai Z, Hertle RW, Bilonick RA and Yang D (2011) A new algorithm for automated nystagmus acuity function analysis. *Br J Ophthalmol* **95**: 832–836.
- Taki M, Hasegawa T, Adachi N, Fujita T, Sakaguchi H and Hisa Y (2014) Periodic alternating nystagmus during caloric stimulation. *Auris, Nasus, Larynx* **41**: 211–214.
- Tarpey P, Thomas S, Sarvananthan N, Mallya U, Lisgo S, Talbot CJ, Roberts EO, Awan M, Surendran M, McLean RJ, Reinecke RD, Langmann A, Lindner S, Koch M, Jain S, Woodruff G, Gale RP, Degg C, Droutsas K, Asproudis I, Zubcov AA, Pieh C, Veal CD, Machado RD, Backhouse OC, Baumber L, Constantinescu CS, Brodsky MC, Hunter DG, Hertle RW, Read RJ, Edkins S, O'Meara S, Parker A, Stevens C, Teague J, Wooster R, Futreal PA, Trembath RC, Stratton MR, Raymond FL and Gottlob I (2006) Mutations in FRMD7, a newly identified member of the FERM family, cause X-linked idiopathic congenital nystagmus. *Nat Genet* **38**: 1242–1244.
- Theodorou M (2006) Predicting visual acuity in early onset nystagmus. *Semin Ophthalmol* **21**: 97–101.
- Thomas JG (1969) The dynamics of small saccadic eye movements. *J Physiol* **200**: 109–127.
- Thomas MG, Crosier M, Lindsay S, Kumar A, Araki M, Leroy BP, McLean RJ, Sheth V, Maconachie G, Thomas S, Moore AT and Gottlob I (2014) Abnormal retinal development associated with FRMD7 mutations. *Hum Mol Genet*
- Thomas MG and Gottlob I (2012) Optical coherence tomography studies provides new insights into diagnosis and prognosis of infantile nystagmus: a review. *Strabismus* **20**: 175–180.
- Thomas S, Proudlock FA, Sarvananthan N, Roberts EO, Awan M, McLean R, Surendran M, Kumar AS, Farooq SJ, Degg C, Gale RP, Reinecke RD, Woodruff G, Langmann A, Lindner S, Jain S, Tarpey P, Raymond FL and Gottlob I (2008) Phenotypical characteristics of idiopathic infantile nystagmus with and without mutations in FRMD7. *Brain* **131**: 1259–1267.
- Thomas S, Thomas MG, Andrews C, Chan W-M, Proudlock FA, McLean RJ, Pradeep A, Engle EC and Gottlob I (2013) Autosomal-dominant nystagmus, foveal hypoplasia and presenile cataract associated with a novel PAX6 mutation. *Eur J Hum Genet* **22**: 344–349.
- Tinelli F, Gamucci A, Battini R and Cioni G (2013) Congenital nystagmus in two infants born from mothers exposed to methadone during pregnancy. *Italian Journal of Pediatrics* **39**: 40.
- Tkalcevic L and Abel LA (2005) The effects of increased visual task demand on foveation in congenital nystagmus. *Vision Res* **43**: 1139–1146.
- Tobii Technology (2011) *Tobii X300 Eye Tracker* [Online]. Available at: <http://www.tobii.com/eye-tracking-integration/global/products-services/hardware/tobii-tx300-eye-tracker/>.

- Tong J, Patel SS and Bedell HE (2006) The attenuation of perceived motion smear during combined eye and head movements. *Vision Res* **46**: 4387–4397.
- Tovée MJ (1996) *An Introduction to the Visual System*. Cambridge: Cambridge University Press.
- Tusa RJ, Mustari MJ, Das VE and Boothe RG (2002) Animal models for visual deprivation-induced strabismus and nystagmus. *Ann N Y Acad Sci* **956**: 346–360.
- Ukwade MT and Bedell HE (1992) Variation of congenital nystagmus with viewing distance. *Optom Vis Sci* **69**: 976–985.
- Ukwade MT, Bedell HE and White JM (2002) Orientation discrimination and variability of torsional eye position in congenital nystagmus. *Invest Ophthalmol Vis Sci* **34**: 1125.
- Ulrich R and Giray M (1989) Time resolution of clocks: effects on reaction time measurement—good news for bad clocks. *Brit J Math Stat Psy* **42**: 1–12.
- Wang ZI and Dell’Osso LF (2007) Being “slow to see” is a dynamic visual function consequence of infantile nystagmus syndrome: model predictions and patient data identify stimulus timing as its cause. *Vision Res* **47**: 1550–1560.
- Wang ZI and Dell’Osso LF (2009) Eye-movement-based assessment of visual function in patients with infantile nystagmus syndrome. *Optom Vis Sci* **86**: 988–995.
- Wang ZI, Dell’osso LF, Prakash S and Chen X (2012) Smooth-pursuit changes after the tenotomy and reattachment procedure for infantile nystagmus syndrome: model predictions and patient data. *J Pediatr Ophthalmol Strabismus* **49**: 295–302.
- Warren S, Yeziarski RP and Capra NF (1997) The Somatosensory System I: Discriminative Touch and Position Sense. In: Haines DE ed. *Fundamental Neuroscience*. First. Philadelphia: Churchill Livingstone, pp. 219–235.
- Waugh SJ and Bedell HE (1992) Sensitivity to temporal luminance modulation in congenital nystagmus. *Invest Ophthalmol Vis Sci* **33**: 2316–2324.
- Weiss AH and Kelly JP (2007) Acuity development in infantile nystagmus. *Invest Ophthalmol Vis Sci* **48**: 4093–4099.
- Weiss AH, Kelly JP and Phillips JO (2011) Relationship of slow-phase velocity to visual acuity in infantile nystagmus associated with albinism. *J AAPOS* **15**: 33–39.
- Wertheim (1938) *Textbook of Ophthalmology*. First. Duke-Elder WS ed. St. Louis: C. V. Mosby Co.
- Westheimer G and McKee SP (1975) Visual acuity in the presence of retinal-image motion. *J Opt Soc Am* **65**: 847–850.
- Wiggins D (2008) Stress and nystagmus. *Focus: Newsletter of the Nystagmus Network*, pp. 6–7.
- Wiggins D (2007) The impact of orbital eye position, visual demand and stress on infantile nystagmus syndrome. Cardiff University.

- Wiggins D, Woodhouse JM, Margrain TH, Harris CM and Erichsen JT (2007) Infantile nystagmus adapts to visual demand. *Invest Ophthalmol Vis Sci* **48**: 2089–2094.
- Williams RW, Garraghty PE and Goldowitz D (1991) A new visual system mutation: achiasmatic dogs with congenital nystagmus. In: *Society for Neuroscience Abstracts*. p. 187.
- Winterson BJ and Collewijn H (1976) Microsaccades during finely guided visuomotor tasks. *Vision Res* **16**: 1387–1390.
- Woo S and Bedell HE (2006) Beating the beat: reading can be faster than the frequency of eye movements in persons with congenital nystagmus. *Optom Vis Sci* **83**: 559–571.
- Worfolk R and Abadi R V (1991) Quick phase programming and saccadic re-orientation in congenital nystagmus. *Vision Res* **31**: 1819–1830.
- World Medical Association (2008) *WMA Declaration of Helsinki - Ethical Principles for Medical Research Involving Human Subjects*.
- Wyatt HJ (1998) Detecting saccades with jerk. *Vision Res* **38**: 2147–2153.
- Xiao X, Li S, Guo X and Zhang Q (2012) A novel locus for autosomal dominant congenital motor nystagmus mapped to 1q31-q32.2 between D1S2816 and D1S2692. *Hum Genet* **131**: 697–702.
- Yang DS, Hertle RW, Hill VM and Stevens DJ (2005) Gaze-dependent and time-restricted visual acuity measures in patients with Infantile Nystagmus Syndrome (INS). *Am J Ophthalmol* **139**: 716–718.
- Yao J-P, Tai Z and Yin Z-Q (2014) A new measure of nystagmus acuity. *Int J Ophthalmol* **7**: 95–99.
- Yee RD, Baloh RW and Honrubia V (1980) Study of congenital nystagmus: optokinetic nystagmus. *Br J Ophthalmol* **64**: 926–932.
- Yee RD, Baloh RW, Honrubia V and Kim YS (1981) A study of congenital nystagmus: vestibular nystagmus. *J Otolaryngol* **10**: 89–98.
- Young M, Heidary G and VanderVeen DK (2011) Course of nystagmus in patients with bilateral infantile cataracts. *J AAPOS* **15**: 554–557.
- Young MP, Heidary G and Vanderveen DK (2012) Relationship between the timing of cataract surgery and development of nystagmus in patients with bilateral infantile cataracts. *J AAPOS* **16**: 554–557.
- Zubcov AA, Stark N, Weber A, Wizov SS and Reinecke RD (1993) Improvement of visual acuity after surgery for nystagmus. *Ophthalmology* **100**: 1488–1497.
- Zuber BL and Stark L (1965) Microsaccades and the velocity-amplitude relationship for saccadic eye movements. *Science* **150**: 1459–1460.

Appendix I Source code for experimental programs

flash.cpp

```
#include <windows.h>

int WINAPI WinMain (HINSTANCE hThisInstance,
                   HINSTANCE hPrevInstance,
                   LPSTR lpszArgument,
                   int nFunsterStil)
{
//Define the serial port procedure
HANDLE hSerial;

//Open the serial port
hSerial = CreateFile("COM1", GENERIC_WRITE, 0, 0, OPEN_EXISTING,
FILE_ATTRIBUTE_NORMAL, 0);
//Close the serial port
CloseHandle(hSerial);

return 0;
}
```

flashtrack_test.m

```
function flashtrack_test
% Eye tracker / flash co-ordinator for nystagmus research
% Version 2.1 - 2012 by Matt J Dunn

addpath(genpath('resources')); % must have the 'resources' subfolder
present

%
% *****
%
% *                               Subject parameters
% * %
%
% *****
%

subjectInitials = input('Please enter subject initials > ','s');
subjectVA = input('What is the subject's VA? > ');
controlExperiment = input('Is this a control experiment? (1 = yes, 0 =
no) > ');
if controlExperiment
    nystagmusAxis = 0;
else
    nystagmusAxis = input('What is the axis of nystagmus? (1 =
horizontal, 2 = vertical, 0 = don't know) > ');
    % The above parameter is overridden by the axis detected by the
calibration procedure, so
    % this only applies if we are bypassing calibration and the subject
has nystagmus
end

%
% *****
%
```

```

% *
% * %
%
% *****
%

experimentReferenceNumber = input('Which experiment would you like to
run? (1-8) > ','s');
% ...Or '0' to specify custom parameters (see below)

% If experimentReferenceNumber is set to zero, the following parameters
take effect:
flash = true; % set to false if using photopic conditions
horizontalGrating = true; % are we using horizontal or vertical
gratings?
largeAperture = true; % are we using the large or small aperture?
eyeTrackerIsWorking = true; % set to false if the tracker is broken for
some reason

%
% *****
%
% *
% * %
%
% *****
%

numberOfReversalsRequired = 8; % the number of reversals used to
determine threshold
numberOfReversalsToDiscard = 2; % number of initial reversals that we
ignore in threshold calculation
ScreenInfo.horizontalSize = 388; % the horizontal size of the visible
screen in millimetres
ScreenInfo.distance = 2000; % subject to grating distance (in mm)
toleranceDegrees = 1; % tolerance (in degrees) of flash detection zone
flashOutputPower = '1/(8 2/3)'; % this is the output level set on the
flash unit. This does not affect the program in any way, but is printed
in the output
flashComPort = 'COM1'; % the port that the flash unit is connected to
tiltComPort = 'COM3'; % the port that the grating mechanism and occluder
are connected to
% The widths of the bars on the grating cards in mm, from card #1 to 20:
gratingBarWidthValues = [0.2 0.3 0.4 0.5 0.6 0.7 0.9 1.1 1.4 1.7 2.2 2.8
3.5 4.4 5.5 6.9 8.7 11.0 13.8 17.4];
flashLimiter = false; % set to 'true' to limit number of flashes per
presentation
flashLimit = 5; % if the flashLimiter is 'true', set the maximum number
of flashes per presentation here
horizontalGazeOffsetDegrees = 0; % horizontal offset for the flash to be
triggered at. Positive values are to the right
verticalGazeOffsetDegrees = 0; % ... and vertical. Positive values are
up
triggerBasedSolelyOnAxisOfNystagmus = false; % if true, we ignore the
vertical axis in horizontal nystagmus for flash trigger and vice versa
useNystagmusCalibration = true; % set to 'false' to ignore nystagmus
calibration file and leave position scale transform at zero
minStrobeRate = 2; % only applies if the eye tracker is not working and
we need to strobe
maxStrobeRate = 6; % as above
peripheralTargetExpectedThresholdDifference = 0.30; % how far below
clinical foveal VA should we start for the peripheral targets

```

```

%
*****
%
% *
% * %
% *
%
*****
%

switch experimentReferenceNumber
  case '1' % large aperture, horizontal, steady illumination
    flash = false;
    horizontalGrating = true;
    largeAperture = true;
    peripheralTarget = false;
  case '2' % large aperture, horizontal, flash
    flash = true;
    horizontalGrating = true;
    largeAperture = true;
    peripheralTarget = false;
  case '3' % large aperture, vertical, flash
    flash = true;
    horizontalGrating = false;
    largeAperture = true;
    peripheralTarget = false;
  case '4' % large aperture, vertical, steady illumination
    flash = false;
    horizontalGrating = false;
    largeAperture = true;
    peripheralTarget = false;
  case '5' % small aperture, horizontal, flash, central fixation
    flash = true;
    horizontalGrating = true;
    largeAperture = false;
    peripheralTarget = false;
  case {'6', '7'} % small aperture, horizontal, flash, peripheral
    fixation (horizontally/vertically displaced)
    flash = true;
    horizontalGrating = true;
    largeAperture = false;
    peripheralTarget = true;
  case '8' % large aperture, horizontal, flash (attenuated output)
    flash = true;
    horizontalGrating = true;
    largeAperture = true;
    peripheralTarget = false;
    flashOutputPower = strcat(flashOutputPower, ' (attenuated)');
end

if largeAperture
  triggerBasedOnEyePosition = false;
else
  triggerBasedOnEyePosition = true;
end

driftCorrectionNumber = 0; % this keeps track of how many drift
corrections have taken place.
% It also numbers our EDF files since we need to split between drift
corrections

```

```

% Stop MATLAB from using default system colours
com.mathworks.services.Prefs.setBooleanPref('ColorsUseSystem',0);

% Change MATLAB colours
com.mathworks.services.Prefs.setColorPref('ColorsBackground',java.awt.Color.black);
com.mathworks.services.Prefs.setColorPref('ColorsText',java.awt.Color.red);
com.mathworks.services.ColorPrefs.notifyColorListeners('ColorsBackground');
com.mathworks.services.ColorPrefs.notifyColorListeners('ColorsText');

set(0,'DefaultFigureWindowStyle','docked') % ensure that the grating
number display is docked

ListenChar(2); % disable key output to MATLAB window

KbName('UnifyKeyNames'); % use named keys
escapeKey = KbName('ESCAPE'); % define the escape key so we can use it
to quit
leftKey = KbName('leftArrow'); % ... and left, so we can use it to
accept a response
rightKey = KbName('rightArrow'); % ... and right
pKey = KbName('p'); % ... and 'p', which will allow the experimenter to
call a new orientation
dKey = KbName('d'); % ... and 'd', which will allow the experimenter to
invoke a drift correction

verticalGazeOffsetDegrees = -verticalGazeOffsetDegrees; % invert the
sign of this value since computers work upside-down in the Y-axis
logMARValues =
log10((atan(gratingBarWidthValues/(ScreenInfo.distance))*60)*180/pi); %
convert the bar widths to logMAR values

if peripheralTarget % if we're testing peripherally, we must allow for
this in the starting VA
    startingVA = subjectVA +
peripheralTargetExpectedThresholdDifference;
else
    startingVA = subjectVA;
end

% The block below finds which grating we should be starting with. This
is
% the grating with a logMAR value just above the subject's VA
gratingNumber = 1;
while startingVA > logMARValues(gratingNumber)
    gratingNumber = gratingNumber + 1;
end

whichScreen = max(Screen('Screens')); % set to the primary monitor
ScreenInfoTEMP = ScreenInfo; % make a backup of ScreenInfo as it's about
to be overwritten
% Retrieve info about the screen:
ScreenInfo = Screen('resolution', whichScreen);
% Write the other variables back into the struct (TODO: make this more
efficient)
ScreenInfo.distance = ScreenInfoTEMP.distance;
ScreenInfo.horizontalSize = ScreenInfoTEMP.horizontalSize;

flashRelay = initialiseflashrelay(flashComPort);

```

```

tiltRelay = initialisetiltrelay(tiltComPort);

% Convert tolerance from degrees to px;
tolerance = oculomotorsuite_degrees2px(toleranceDegrees,
ScreenInfo.horizontalSize, ScreenInfo.width, ScreenInfo.distance);
% Convert gaze offset from degrees to px
horizontalGazeOffset =
oculomotorsuite_degrees2px(horizontalGazeOffsetDegrees,
ScreenInfo.horizontalSize, ScreenInfo.width, ScreenInfo.distance);
verticalGazeOffset =
oculomotorsuite_degrees2px(verticalGazeOffsetDegrees,
ScreenInfo.horizontalSize, ScreenInfo.width, ScreenInfo.distance);

try % this just means attempt to do the following, but if fails, go to
'catch'. Useful in debugging.
    window = Screen('OpenWindow', whichScreen); % 'window' will appear
on screen

    % ** EL1000 setup ** %
    dummymode=0; % set to 1 to run the EL1000 in dummy mode
    el=EyelinkInitDefaults(window); % initialise EL1000

    % Open EL1000 connection:
    if ~EyelinkInit(dummymode, 1)
        fprintf('Eyelink Init aborted.\n');
        shutdown(flashRelay, tiltRelay); % run cleanup function
        return;
    end

    EyelinkDoTrackerSetup(el); % begin camera setup program for any last
minute adjustments

    orientation = 0; % initialise the orientation. This means that
before each experiment, grating must be tilted left!
    GFIndex = 0; % initialise the Gellerman-Fellows index
    firstPresentation = true; % for the first presentation, GFIndex is
made random
    x = 0; % initialise these variables
    y = 0;
    numberOfFlashesArray = []; % initialise
    numberOfFlashesArrayCorrect = []; % initialise
    timeToRespondArray = []; % initialise
    timeToRespondArrayCorrect = []; % initialise

    diary(strcat(subjectInitials, '_', experimentReferenceNumber,
'_flashData.txt')); % record all MATLAB output to file
    currentTime = clock;
    fprintf('Time at start of session is %i:%02i\n', currentTime(4),
currentTime(5)); % print the time

    if ~controlExperiment && useNystagmusCalibration &&
triggerBasedOnEyePosition
        run calibrationFile;
        Eyelink('Message', 'New calibration parameters: slopeX = %s,
interceptX = %s, slopeY = %s, interceptY = %s'...
, num2str(slopeX), num2str(interceptX), num2str(slopeY),
num2str(interceptY)); % send a message to the EL1000
    else % if we aren't calibrating, we use unmodified calibration
        slopeX = 1
        interceptX = 0
        slopeY = 1

```

```

    interceptY = 0
    EYELINK('Message', 'New calibration parameters: slopeX = %s,
interceptX = %s, slopeY = %s, interceptY = %s'...
        , num2str(slopeX), num2str(interceptX), num2str(slopeY),
num2str(interceptY)); % send a message to the EL1000
    end
    %Screen('close', window); % shut the open window since there is no
need for it during the experiment

    % Drift correction:
    if triggerBasedOnEyePosition
        if ~controlExperiment % there are two types of drift correction
procedures; one for nystagmats and one for controls
            [interceptX, interceptY, driftCorrectionNumber,
nystagmusAxis] = nystagmus_driftcorrection(ScreenInfo, el, x, y, slopeX,
interceptX, slopeY, interceptY, subjectInitials,
experimentReferenceNumber, nystagmusAxis, driftCorrectionNumber); %
perform a drift-correction
        else
            fprintf('Performing drift correction...\n')
            EYELINKDoDriftCorrection(el);
        end
    end

    % ** Begin recording ** %
    edfFile = strcat(experimentReferenceNumber, 'flDat',
num2str(driftCorrectionNumber), '.edf'); % define the name of our EDF
file (must be 8 characters or less)
    eye_used = oculomotorsuite_beginrecording(edfFile);

    numberCorrect = 0; % initialise a variable to store number of
consecutive correct responses
    numberOfReversals = 0; % this will count our number of reversals
    reversalData = []; % this stores the value of each reversal
    lastFlashTime = 0; % initialise
    direction = 2; % direction begins at a nonsense value. 0 means
descending staircase, 1 means ascending.
    targetX = ScreenInfo.width / 2 + horizontalGazeOffset; % set the
location for the trigger
    targetY = ScreenInfo.height / 2 + verticalGazeOffset;

    orientation = awaitgrating(gratingNumber, direction); % request that
the first grating be put into place

    EYELINK('Message', 'Beginning experiment with subject %s (clinical
VA = %s logMAR)', subjectInitials, num2str(subjectVA));
    WaitSecs(0.01); % wait so the EL1000 messages don't collide
    EYELINK('Message', 'Trigger zone is (%s, %s) degrees from the
centre, with a tolerance zone of %s degrees',
num2str(horizontalGazeOffsetDegrees),
num2str(verticalGazeOffsetDegrees), num2str(toleranceDegrees));
    WaitSecs(0.01); % wait so the EL1000 messages don't collide
    EYELINK('Message', 'Subject is sat %s metres from stimuli. We will
obtain threshold using %s reversals and discarding the first %s',
num2str(ScreenInfo.distance/1000), num2str(numberOfReversalsRequired),
num2str(numberOfReversalsToDiscard));
    WaitSecs(0.01); % wait so the EL1000 messages don't collide
    fprintf('Beginning experiment with subject %s (clinical VA = %.2f
logMAR).\nTrigger zone is (%.2f, %.2f) degrees from the centre.\nSubject
is sat %.2f metres from stimuli. We will obtain threshold using %i
reversals and discarding the first %i.\n'...

```

```

        , subjectInitials, subjectVA, horizontalGazeOffsetDegrees,
verticalGazeOffsetDegrees, ScreenInfo.distance/1000,
numberOfReversalsRequired, numberOfReversalsToDiscard)
    if horizontalGrating
        Eyelink('Message', 'We are using horizontal gratings');
        fprintf('We are using horizontal gratings.\n')
    else
        Eyelink('Message', 'We are using vertical gratings');
        fprintf('We are using vertical gratings.\n')
    end
    WaitSecs(0.01); % wait so the EL1000 messages don't collide
    if controlExperiment
        Eyelink('Message', 'This is a control experiment');
        fprintf('This is a control experiment.\n')
    else
        Eyelink('Message', 'Our subject has nystagmus');
        fprintf('Our subject has nystagmus.\n')
    end
    WaitSecs(0.01); % wait so the EL1000 messages don't collide
    if largeAperture
        Eyelink('Message', 'We are using the large aperture stimulus');
        fprintf('We are using the large aperture stimulus.\n')
    else
        Eyelink('Message', 'We are using the small aperture stimulus');
        fprintf('We are using the small aperture stimulus.\n')
    end
    WaitSecs(0.01); % wait so the EL1000 messages don't collide
    if flash
        if flashLimiter
            Eyelink('Message', 'Each presentation will be illuminated by
up to %s flashes at %s power', num2str(flashLimit), flashOutputPower);
            fprintf('Each presentation will be illuminated by up to %i
flashes at %s power.\n', flashLimit, flashOutputPower)
        else
            Eyelink('Message', 'Each presentation will be illuminated by
an infinite number of flashes at %s power', flashOutputPower);
            fprintf('Each presentation will be illuminated by an
infinite number of flashes at %s power.\n', flashOutputPower)
        end
        WaitSecs(0.01); % wait so the EL1000 messages don't collide
        if triggerBasedOnEyePosition
            if triggerBasedSolelyOnAxisOfNystagmus
                Eyelink('Message', 'The trigger zone is determined
solely by the primary axis of nystagmus with a tolerance of %s degrees',
num2str(toleranceDegrees));
                fprintf('The trigger zone is determined solely by the
primary axis of nystagmus with a tolerance of %.1f degrees.\n',
toleranceDegrees)
            else
                Eyelink('Message', 'The trigger zone is a circle with a
tolerance zone of %s degrees', num2str(toleranceDegrees));
                fprintf('The trigger zone is a circle with a tolerance
zone of %.1f degrees.\n', toleranceDegrees)
            end
        else
            Eyelink('Message', 'There is no specific trigger zone');
            fprintf('There is no specific trigger zone.\n')
        end
    else
        Eyelink('Message', 'Presentations are made under constant
illumination');
        fprintf('Presentations are made under constant illumination.\n')
    end
end

```

```

end
% ** This is our experiment loop! ** %
while numberOfReversals < numberOfReversalsRequired
    [orientation, GFIndex, firstPresentation, numberOfFlashes,
timeAtStartOfPresentation] = orientgrating (orientation, tiltRelay,
GFIndex, firstPresentation); % orient the grating randomly
    responseGiven = false;

    % This loop runs and causes flashes until the subject responds
    while ~responseGiven
        % This block is picking up a new sample from the EL1000
        if Eyelink('NewFloatSampleAvailable') > 0 % checks the
buffer for a new sample
            % get the sample in the form of an event structure
            evt = Eyelink('NewestFloatSample');
            if eye_used ~= -1 % do we know which eye to use yet? If
we do, get current gaze position from sample
                % Scale and intercept from the custom calibration
program are applied here
                x = slopeX * evt.gx(eye_used+1) + interceptX; % +1
as we're accessing MATLAB array.
                y = slopeY * evt.gy(eye_used+1) + interceptY;
            else % if we don't, first find eye that's being tracked
                eye_used = Eyelink('EyeAvailable'); % get eye that's
tracked
            if eye_used == el.BINOCULAR; % if both eyes are
tracked
                eye_used = el.LEFT_EYE; % use left eye
            end
        end
        end
        if flash && (evt.gx(eye_used+1) ~= -32768 ||
~eyeTrackerIsWorking) % if the eye is found (-32768 indicates eye not
found)
            % Find the difference between the detected position and
the centre of the flash gaze position target
            differenceInPosition = [x y] - [targetX targetY];
            if triggerBasedSolelyOnAxisOfNystagmus % in case we
override the trigger setting to just base on a single axis
                totalDifferenceInPosition =
abs(differenceInPosition(nystagmusAxis));
            else
                % Find the Euclidian norm
                totalDifferenceInPosition =
norm(differenceInPosition);
            end

            if (numberOfFlashes < flashLimit || ~flashLimiter)... %
if we are using the flashLimiter, ensure we still have flashes left...
                & (totalDifferenceInPosition <= tolerance ||
~triggerBasedOnEyePosition)... % if eyes are within tolerance zone or we
are overriding to strobe mode
                & evt.time - lastFlashTime >= 1000/maxStrobeRate
% ensure that we've had enough time pass to provide another flash.
                % n.b. never allow the flash to fire more often than
the max strobe rate; this could destroy the bulb
                % Compare the Euclidian norm to that detected in the
previous sample. We check this since there is no sense in
                % discharging the flash when the eyes are at the
edge of the tolerance zone if they are still moving towards the
                % centre of the zone. We wait until they just start
to move away from the middle (or as close as they're going to

```

```

        % get), and then flash.
        if ~triggerBasedOnEyePosition ||
totalDifferenceInPosition > previousTotalDifferenceInPosition
            % If this happens, then the eyes have started
moving away from the target
            % In this case, we want to discharge the flash
immediately
            Eyelink('Message', 'FLASH'); % send a message to
the EL1000 to say a flash occurred
            flashstrobe(flashRelay, minStrobeRate,
maxStrobeRate);
            numberOfFlashes = numberOfFlashes + 1;
            lastFlashTime = evt.time;
        end
    end
    previousTotalDifferenceInPosition =
totalDifferenceInPosition; % record the last Euclidian norm
end

[ keyIsDown, seconds, keyCode ] = KbCheck;

    if numberOfFlashes > 0 || ~flash % only allow a response
after at least one flash if it's a flash paradigm
        if keyCode(leftKey) % if user presses left arrow
            Eyelink('Message', 'User response: left'); % send a
message to the EL1000
            keyPress = 0; % 0 = leftKey
            responseGiven = true; % leave the loop as the user
has responded
        elseif keyCode(rightKey) % if user presses right arrow
            Eyelink('Message', 'User response: right'); % send a
message to the EL1000
            keyPress = 1; % 1 = rightKey
            responseGiven = true; % leave the loop as the user
has responded
        end
    end

    if keyCode(escapeKey) % if user presses escape
        shutdown(flashRelay, tiltRelay); % exit the program
        return;
    elseif keyCode(pKey) % if experimenter wants to re-orient
the grating
        Eyelink('Message', 'Experimenter requested grating re-
orientation'); % send a message to the EL1000
        fprintf('Experimenter requested grating re-
orientation\n')
        [orientation, GFIndex, firstPresentation,
numberOfFlashes, timeAtStartOfPresentation] = orientgrating
(orientation, tiltRelay, GFIndex, firstPresentation); % orient the
grating randomly
    elseif keyCode(dKey) % if experimenter wants to perform a
drift-correction
        if ~controlExperiment
            oculomotorsuite_receivedatafile; % save the old data
file
            [interceptX, interceptY, driftCorrectionNumber,
nystagmusAxis] = nystagmus_driftcorrection(ScreenInfo, el, x, y, slopeX,
interceptX, slopeY, interceptY, subjectInitials,
experimentReferenceNumber, nystagmusAxis, driftCorrectionNumber); %
perform a drift-correction

```

```

        edfFile = strcat(experimentReferenceNumber, 'flDat',
num2str(driftCorrectionNumber), '.edf'); % define the name of our EDF
file (must be 8 characters or less)
        eye_used = oculomotorsuite_beginrecording(edfFile);
    else
        fprintf('Performing drift correction...\n')
        EYELINK('StopRecording');
        EYELINKDO('DriftCorrection', el);
        EYELINK('StartRecording');
    end

    % After drift correction we should re-orient the grating
    [orientation, GFIndex, firstPresentation,
numberOfFlashes, timeAtStartOfPresentation] = orientgrating
(orientation, tiltRelay, GFIndex, firstPresentation); % orient the
grating randomly
    end
end
timeToRespond = GetSecs - timeAtStartOfPresentation; % record
the time taken to respond
numberOfFlashesArray(end+1) = numberOfFlashes; % at the end we
calculate average number of flashes
timeToRespondArray(end+1) = timeToRespond;

% Orientation 0 is to the left.
% This 'if' block deals with whether the correct response was
given or not.
if orientation == 0
    if keyPress == 0
        response = 1;
    else
        response = 0;
    end
elseif orientation == 1 % orientation 1 is to the right.
    if keyPress == 1
        response = 1;
    else
        response = 0;
    end
end

% We tend to ascribe direction to tilt based on the highest
point of the object;
% therefore, if we're using horizontal gratings, we must reverse
the direction
if horizontalGrating
    response = ~response; % invert the value
end

if response == 0
    EYELINK('Message', 'Bad response', numberOfFlashes);
    WaitSecs(0.01); % wait so the EL1000 messages don't collide
    fprintf('Bad response after ')
    if flash
        fprintf('%u flashes and ', numberOfFlashes)
    end
    fprintf('%.2f seconds\n', timeToRespond)
    numberCorrect = 0;
    if direction == 1 % check whether we were ascending prior to
this
        numberOfReversals = numberOfReversals + 1; % if so, this
is a reversal
    end
end

```

```

        Eyelink('Message', 'Reversal %s of %s',
num2str(numberOfReversals), num2str(numberOfReversalsRequired));
        fprintf('Reversal %u of %u\n', numberOfReversals,
numberOfReversalsRequired)
        logMARValueOfThisReversal = logMARValues(gratingNumber);
% search the list of grating values for the corresponding card
        reversalData = [reversalData logMARValueOfThisReversal];
% append the reversal to the other stored reversals
        end
        gratingNumber = gratingNumber + 1;
        direction = 0; % we are now descending
        if numberOfReversals < numberOfReversalsRequired
            orientation = awaitgrating(gratingNumber, direction);
        end
    elseif response == 1
        Eyelink('Message', 'Good response', numberOfFlashes);
        WaitSecs(0.01); % wait so the EL1000 messages don't collide
        fprintf('Good response after ')
        if flash
            fprintf('%u flashes and ', numberOfFlashes)
        end
        fprintf('%.2f seconds\n', timeToRespond)
        numberCorrect = numberCorrect + 1;
        numberOfFlashesArrayCorrect(end+1) = numberOfFlashes;
        timeToRespondArrayCorrect(end+1) = timeToRespond;
    else % This should never happen:
        fprintf('ERROR: Neither good nor bad response detected.
Something is wrong.\n')
        shutdown(flashRelay, tiltRelay);
        return;
    end
    % If we have had three correct responses in a row, we should
reduce
    % the spatial frequency
    if numberCorrect == 3
        numberCorrect = 0; % reset the number of cumulative correct
responses counter
        if direction == 0 % check whether we were descending prior
to this
            numberOfReversals = numberOfReversals + 1; % if so, this
is a reversal
            Eyelink('Message', 'Reversal %s of %s',
num2str(numberOfReversals), num2str(numberOfReversalsRequired));
            fprintf('Reversal %u of %u\n', numberOfReversals,
numberOfReversalsRequired)
            logMARValueOfThisReversal = logMARValues(gratingNumber);
% search the list of grating values for the corresponding card
            reversalData = [reversalData logMARValueOfThisReversal];
% append the reversal to the other stored reversals
            end
            gratingNumber = gratingNumber - 1;
            direction = 1; % we are now ascending
            if numberOfReversals < numberOfReversalsRequired
                orientation = awaitgrating(gratingNumber, direction);
            end
        end
    end
    reversalData(1:numberOfReversalsToDiscard) = []; % remove the first
(usually two) reversals from the threshold calculation
    thresholdVA = mean(reversalData); % calculate the threshold VA
    WaitSecs(0.01); % wait so the EL1000 messages don't collide
    Eyelink('Message', 'Threshold is %s', num2str(thresholdVA));

```

```

fprintf('Threshold is %f\n', thresholdVA)
fprintf('Average number of flashes is %.2f, average number for a
correct response is %.2f\n', mean(numberOfFlashesArray),
mean(numberOfFlashesArrayCorrect));
fprintf('Average time to respond is %.2f secs, average time for a
correct response is %.2f secs\n', mean(timeToRespondArray),
mean(timeToRespondArrayCorrect));
player = playtone(2,1760); % make a noise for 2 seconds to indicate
we have finished

% ** Experiment ended: tidy up ** %
shutdown(flashRelay, tiltRelay); % run cleanup function
return;

catch
% ** Error handling block - any errors end up here ** %
shutdown( flashRelay, tiltRelay); % run cleanup function
psychrethrow(psychlasterror); % send error description to MATLAB
output
return;
end

function tiltRelay = initialisetiltrelay (tiltComPort);
% Initialises the USB RLY08 to control the grating orientation
% Commands such as 'RELAY1_ON' are sent by fprintf

warning off MATLAB:sprintf:InputForPercentSIsNotOfClassChar % prevent
receiving warning messages because we send numbers, not char strings

tiltRelay = serial(tiltComPort, 'BaudRate', 19200);
fopen(tiltRelay); % open the serial port
fprintf(tiltRelay, 110); % turn off all relays

% n.b. command codes for the RLY08 device can be found on the table at
% http://www.robot-electronics.co.uk/htm/usb\_rly08tech.htm

function flashRelay = initialiseflashrelay (flashComPort);
% Initialises the RS-232 relay switch for instantaneous flash control
% RTS controls relay #1; DTR controls relay #2

flashRelay = serial(flashComPort);
fopen(flashRelay);
flashRelay.RequestToSend = 'off';
flashRelay.DataTerminalReady = 'off';

function orientation = awaitgrating (gratingNumber, direction)
% Requests user to place a new grating in the frame

if direction == 0 % if we are descending in VA
directionSymbol = '- ';
elseif direction == 1 % if we are ascending in VA
directionSymbol = '+ ';
else % this will only be the case for the first grating

```

```

        directionSymbol = '';
    end

    orientation = 0; % always reset the orientation to left when manually
    replacing the grating

    uicontrol('Style', 'text', 'String', strcat(directionSymbol,
    num2str(gratingNumber)), 'FontSize', 120, 'ForegroundColor', 'red', ...
    'BackgroundColor', 'black', 'Units', 'normalized', 'Position', [0 0 1
    1]);
    drawnow; % force the window to update now; otherwise the system will
    wait until later
    player = playtone(2,880); % make a noise for 2 seconds
    % pop up number so it can be seen from the other side of the lab
    fprintf('Please insert grating number %u, then press SPACE\n',
    gratingNumber)
    WaitSecs(0.01); % wait so the EL1000 messages don't collide
    Eyelink('Message', 'We are now changing to grating number %s',
    num2str(gratingNumber));
    awaitspacepress;

function keyCode = flashstrobe (flashRelay, minStrobeRate,
maxStrobeRate)
% Generate strobe for control experiments

thisDelay = 1 / (minStrobeRate + rand * (maxStrobeRate -
minStrobeRate)); % the delay is randomly generated between the two
limits.
% this delay is then spread evenly between the 'on' and 'off'
% states, so that the relay has time to fire
flashRelay.DataTerminalReady = 'on'; % send command to activate flash
relay
keyCode = skippabledelay(thisDelay / 2); % pause (but allow the system
to cancel if a button is pressed)
flashRelay.DataTerminalReady = 'off'; % send command to deactivate flash
relay
keyCode = skippabledelay(thisDelay / 2);

function [orientation, GFIndex, firstPresentation, numberOfFlashes,
timeAtStartOfPresentation] = orientgrating (orientation, tiltRelay,
GFIndex, firstPresentation);
% selects orientation of grating randomly and controls the tilt
mechanism

previousOrientation = orientation;
[orientation, GFIndex, firstPresentation] = gellermanfellows(GFIndex,
firstPresentation);

% White noise mask the noise of the table banging:
waveFile = 'whiteNoise.wav';
[y, Fs, nbits, readinfo] = wavread(waveFile);
sound(y, Fs);

if orientation == 0
    Eyelink('Message', 'Tilting grating left'); % send a message to the
    EL1000
end

```

```

fprintf('Tilting grating left\n')
if previousOrientation == 0 % left from left
    fprintf(tiltRelay, 110); % turn off all relays
    fprintf(tiltRelay, 105); % turn on relay 5
    pause(1);
    fprintf(tiltRelay, 115); % turn off relay 5
    fprintf(tiltRelay, 101); % turn on relay 1
    pause(0.15);
    fprintf(tiltRelay, 111); % turn off relay 1
    fprintf(tiltRelay, 102); % turn on relay 2
    pause(0.85);
    fprintf(tiltRelay, 112); % turn off relay 2
    fprintf(tiltRelay, 104); % turn on relay 4
    pause(1);
    fprintf(tiltRelay, 114); % turn off relay 4
elseif previousOrientation == 1 % left from right
    fprintf(tiltRelay, 110); % turn off all relays
    fprintf(tiltRelay, 105); % turn on relay 5
    pause(1);
    fprintf(tiltRelay, 115); % turn off relay 5
    fprintf(tiltRelay, 102); % turn on relay 2
    pause(1);
    fprintf(tiltRelay, 112); % turn off relay 2
    fprintf(tiltRelay, 104); % turn on relay 4
    pause(1);
    fprintf(tiltRelay, 114); % turn off relay 4
end
elseif orientation == 1
    Eyelink('Message', 'Tilting grating right'); % send a message to the
EL1000
    fprintf('Tilting grating right\n')
    if previousOrientation == 1 % right from right
        fprintf(tiltRelay, 110); % turn off all relays
        fprintf(tiltRelay, 105); % turn on relay 5
        pause(1);
        fprintf(tiltRelay, 115); % turn off relay 5
        fprintf(tiltRelay, 102); % turn on relay 2
        pause(0.15);
        fprintf(tiltRelay, 112); % turn off relay 2
        fprintf(tiltRelay, 101); % turn on relay 1
        pause(0.85);
        fprintf(tiltRelay, 111); % turn off relay 1
        fprintf(tiltRelay, 104); % turn on relay 4
        pause(1);
        fprintf(tiltRelay, 114); % turn off relay 4
    elseif previousOrientation == 0 % right from left
        fprintf(tiltRelay, 110); % turn off all relays
        fprintf(tiltRelay, 105); % turn on relay 5
        pause(1);
        fprintf(tiltRelay, 115); % turn off relay 5
        fprintf(tiltRelay, 101); % turn on relay 1
        pause(1);
        fprintf(tiltRelay, 111); % turn off relay 1
        fprintf(tiltRelay, 104); % turn on relay 4
        pause(1);
        fprintf(tiltRelay, 114); % turn off relay 4
    end
end
end
numberOfFlashes = 0; % after orienting grating, we will always want the
% number of flashes to be reset
timeAtStartOfPresentation = GetSecs; % set the presentation start time
Eyelink('Message', 'Tilting complete'); % send a message to the EL1000

```



```

if firstPresentation % on first presentation, we jump to a random part
of the sequence
    GFIndex = round(rand * length(gellermanfellowsSequences));
    firstPresentation = false;
end

GFOutput = gellermanfellowsSequences(GFIndex); % output the part of the
sequence relating to the index number

if GFIndex >= length(gellermanfellowsSequences)
    GFIndex = 1; % if we reach the end of the sequence, loop back to the
beginning
end

GFIndex = GFIndex + 1; % advance the sequence

```

handmarkfoveationperiods.m

```

% Script to allow for hand marking of foveation periods in an eye trace.
% Analyse results by comparing the output of this to the automated
method.

```

```

addpath(genpath('resources')); % must have the 'resources' subfolder
present

debug.timeToUse = 9000; % how many samples to use in debug mode
debug.timeToStart = 1000; % sample number to start from in debug mode

eyeTrackerSamplingRate = 1000;
averagingWindow = 7;

%% File input
inputFile = uigetfile({'*.edf;*.csv', 'EDF or CSV files'}, 'Select data
file');
if inputFile == 0 % if no selection is made
    return; % exit
end
[unusedVariable inputFileNames, fileExtension] = fileparts(inputFile); %
separate the filename and extension

fprintf('\nConverting EDF file to ASCII...')
if exist(strcat(inputFileNames, '.asc'), 'file') % if the function was
terminated halfway through previously, we need to remove the temp file
before continuing
    delete(strcat(inputFileNames, '.asc'));
end
[unusedVariable unusedVariable] = system(['EDF2ASC -s -miss NaN ',
inputFileNames, '.edf']); % convert EDF file to ASCII using SR Research's
EDF2ASC tool
% If the above line fails, then either EDF2ASC is not installed, or you
need to check your environment variables
fprintf('\nImporting data to MATLAB...')
fid = fopen(strcat(inputFileNames, '.asc'));
inputData = textscan(fid, '%d %f %f %f %s'); % read the ASCII file in.
The file has the format [timestamp, X, Y, pupilSize, {...}]
inputData = [inputData{2:3}]; % we're only interested in the X and Y
columns
fclose(fid);
delete(strcat(inputFileNames, '.asc')); % clear up the new file

```

```

%% Array structuring
inputData(:,3) = 1:(size(inputData,1)); % generate timestamp column,
starting at one. n.b. this is in samples; not ms

% Remove all but the data to be hand marked
fprintf('\nSamples %i - %i are being analysed\n', debug.timeToStart,
debug.timeToStart + debug.timeToUse)
inputData(1:debug.timeToStart,:) = [];
inputData(debug.timeToUse+1:end,:) = [];

fprintf('\nCalculating velocity profile...')
inputData(:,4) = oculomotorsuite_datadifferentiator(inputData(:,1),
averagingWindow)*10; % take the differential of the position data and
apply it to column 4

%% Plotting
set(0, 'DefaultFigureWindowStyle', 'docked'); % dock figure window by
default
figure;
hold on; % we are about to plot graphs: prepare for multiple datasets
set(gcf, 'Renderer', 'OpenGL'); % set rendering mode to OpenGL to allow
hardware acceleration to visualisation
xlabel('Time (s)')
whitebg('black')
set(gcf, 'name', strcat(inputFile, ' eye movement plot'), 'numbertitle',
'off');
plot(inputData(:,3), inputData(:,4)-1000, 'cyan'); % plot the velocity
transform
plot3(inputData(:,3), inputData(:,1), inputData(:,2)); % plot position
data

set(gca, 'ytick', [], 'ztick', [])

%% Data selection
dataCursor = datacursormode(gcf);
set(dataCursor, 'DisplayStyle', 'datatip', 'SnapToDataVertex', 'off', 'Enable
', 'on'); % change to 'data cursor mode'

finished = false;
foveationTimeStamps = [];
foveationPeriodNumber = 0;
while ~finished
    foveationPeriodNumber = foveationPeriodNumber + 1;
    fprintf('Foveation period number %i\n', foveationPeriodNumber)
    input('Select foveation start point, then press enter');
    candidateFoveation.start = getCursorInfo(dataCursor); % grab info
from the cursor position
    input('Select foveation end point, then press enter');
    candidateFoveation.end = getCursorInfo(dataCursor); % grab info from
the cursor position
    startTime = round(candidateFoveation.start.Position(1)) -
debug.timeToStart;
    endTime = round(candidateFoveation.end.Position(1)) -
debug.timeToStart;
    plot3(inputData(startTime:endTime,3),
inputData(startTime:endTime,1), inputData(startTime:endTime,2), 'r')
    foveationTimeStamps = [foveationTimeStamps; startTime, endTime];
    done = input('Type 'y' if finished (hit enter if not) > ', 's');
    if strcmp(done, 'y')
        finished = true;

```

```

    end
end

```

```

csvwrite(strcat(inputFileName, '_hand_marked_foveation_times.csv'),
foveationTimeStamps);
fprintf('\nProgram terminated normally');

```

nystagmus_analyser.m

```

function [nystagmusAxis, Foveations, Saccades, SlowPhases, Cycles,
positionPeaks, positionTroughs, inputData] =
nystagmus_analyser(inputFile, eyeTrackerSamplingRate, nystagmusAxis,
Prefs)
% Analyse an eye position trace to detect nystagmus parameters
% Version 1.0 created by Matt J Dunn December 2011 - November 2013

% Input can be an EDF file, a two-column CSV file with the format
% [X, Y], a one-column CSV file containing uniaxial data, or a MATLAB
array
% of the same format

% Note that in the absence of a calibration file (calibrationfile.m),
all
% data are in arbitrary units. Once a calibration has been run and the
% file generated, subsequent runs will allow output of more detailed
% metrics relating to the waveform.

addpath(genpath('resources')); % must have the 'resources' subfolder
present

ExperimentalPrefs.deleteSaccades = false; % turn on to produce plots
without saccades

%% Set program defaults
if ~exist('eyeTrackerSamplingRate','var')
    eyeTrackerSamplingRate = 1000; % the temporal resolution of the eye
tracker (Hz)
end
if ~exist('nystagmusAxis', 'var')
    nystagmusAxis = nystagmus_setanalysisdefaults;
end

if ~exist('Prefs','var')
    [unusedVariable, Prefs.Plot, Prefs.FoveationDefinition,
Prefs.CycleDefinition, Prefs.SaccadeDefinition, Prefs.BlinkDefinition,
Prefs.General, Prefs.FilterDefinition, Prefs.Report] =
nystagmus_setanalysisdefaults;
end

% Program defaults (too technical to bother including in the GUI, but
you may want to adjust them here)
Prefs.FoveationDefinition.iterativeVelocityIncrementPercentage = 10; %
when iteratively adjusting foveation velocity thresholds, by what
percentage it should be adjusted each time
Prefs.FoveationDefinition.maxAttemptsAtFindingAVelocity = 100; % the
maximum attempts that the program should try to iteratively adjust the
foveation velocity window before giving up
Prefs.FoveationDefinition.maxVelocityStandardDeviations = -1; % how many
standard deviations above the mean slow phase velocity should be the
first value used to attempt to find foveations? (this should be a
negative number)

```

```

Prefs.Plot.useHardwareAcceleration = true; % render the plots using
OpenGL - disable if using a system that doesn't support hardware
acceleration

%% Read data file
if exist('inputFile', 'var')
    [inputData, inputFileNames] =
    oculomotorsuite_readeyetrace(inputFile);
else
    [inputData, inputFileNames] = oculomotorsuite_readeyetrace;
end

% TODO: Consider using structs for organising eye data instead of arrays

%% Remove unwanted data from trace
Prefs.General.timeToAnalyse.start =
round(Prefs.General.timeToAnalyse.start / 1000 *
eyeTrackerSamplingRate); % convert from ms to samples
Prefs.General.timeToAnalyse.end = round(Prefs.General.timeToAnalyse.end
/ 1000 * eyeTrackerSamplingRate); % convert from ms to samples
if Prefs.General.timeToAnalyse.constrainEnd
    if size(inputData,1) > Prefs.General.timeToAnalyse.end % if we
actually have enough data
        fprintf('\nRemoving all samples after %i from
analysis...', Prefs.General.timeToAnalyse.end)
        inputData(Prefs.General.timeToAnalyse.end:end,:) = []; % throw
away the end of the dataset
    else
        error('notEnoughData:notEnoughDataToRemoveEnd', 'Not enough data
recorded')
    end
end
if Prefs.General.timeToAnalyse.constrainStart
    if size(inputData,1) > Prefs.General.timeToAnalyse.start % if we
actually have enough data
        fprintf('\nRemoving the first %i samples from
analysis...', Prefs.General.timeToAnalyse.start)
        inputData(1:Prefs.General.timeToAnalyse.start,:) = []; % throw
away the start of the dataset
    else
        error('notEnoughData:notEnoughDataToRemoveStart', 'Not enough
data recorded')
    end
end

%% Filter position data
if Prefs.FilterDefinition.filterData
    fprintf('\nFiltering position data with a %ith order %iHz low pass
filter...', Prefs.FilterDefinition.order, Prefs.FilterDefinition.cutoff)
    inputData(:,1) = oculomotorsuite_lowpassfilter(inputData(:,1),
Prefs.FilterDefinition.order, Prefs.FilterDefinition.cutoff,
eyeTrackerSamplingRate); % filter X position data
    inputData(:,2) = oculomotorsuite_lowpassfilter(inputData(:,2),
Prefs.FilterDefinition.order, Prefs.FilterDefinition.cutoff,
eyeTrackerSamplingRate); % filter Y position data
end

%% Calibrate position data
if ~isfield(Prefs.General, 'calibrationFile') ||
isempty(Prefs.General.calibrationFile)
    Prefs.General.calibrationFile = [];
end

```

```

end

if ~Prefs.General.dataAreCalibrated
    [inputData, Prefs.General.dataAreCalibrated] =
nystagmus_applycalibration(inputData, Prefs.General.calibrationFile); %
calibrate position trace
end

%% Calculate axis of nystagmus
if nystagmusAxis == 0 % if nystagmus axis is unknown
    nystagmusAxis = findnystagmusaxis(inputData);
end

%% Generate timestamp, velocity and acceleration channels
inputData =
oculomotorsuite_generatecompleteeyetracearray(inputData, Prefs.General.av
eragingWindow, eyeTrackerSamplingRate, Prefs.General.constrainVelocityAnal
ysisToAxisOfNystagmus, nystagmusAxis); % generate timestamp, velocity and
acceleration channels

%% Remove blinks
if Prefs.BlinkDefinition.removeBlinksFromDataSet
    fprintf('\nRemoving blinks...')
    ColumnNumbers.xPosition = 1;
    ColumnNumbers.yPosition = 2;
    ColumnNumbers.velocity = 4;
    ColumnNumbers.acceleration = 5;
    [inputData nBlinks] = oculomotorsuite_removeblinks(inputData,
ColumnNumbers, Prefs.BlinkDefinition.considerLargeMovementsBlinks,
Prefs.BlinkDefinition.numberofStandardDeviationsAboveMedianForBlinkRemov
al); % remove blinks from data
    if nBlinks == 0
        fprintf('\nNo blinks were detected...')
    elseif nBlinks == 1
        fprintf('\nOne blink was detected and removed...')
    else
        fprintf('\n%i blinks were detected and removed...', nBlinks)
    end
end

percentageDataDropped = 100 / size(inputData,1) *
length(find(isnan(inputData(:,1)))));
fprintf('\n%.2f%% of the data were dropped', percentageDataDropped)

%% Detect cycles
fprintf('\nDetecting cycles...')
if strcmp(Prefs.CycleDefinition.method, 'juhola')
    [positionPeaks, positionTroughs, nCycles] =
nystagmus_cycledetection_juhola(inputData, nystagmusAxis,
Prefs.CycleDefinition.juhola.slopeAnalysisLength,
Prefs.CycleDefinition.juhola.smoothingFilterCutOff,
eyeTrackerSamplingRate);
elseif strcmp(Prefs.CycleDefinition.method, 'sd')
    [positionPeaks, positionTroughs, nCycles] =
nystagmus_cycledetection_sd(inputData, nystagmusAxis,
Prefs.CycleDefinition.sd.standardDeviationsPositionDifference);
end

%% Get cycle metrics
Cycles =
struct('startTime', [], 'endTime', [], 'amplitude', [], 'frequency', [], 'intens

```

```

ity', [], 'min_x', [], 'max_x', [], 'mean_x', [], 'min_y', [], 'max_y', [], 'mean_y'
, []); % initialise struct
for i = 1 : nCycles
    Cycles.startTime(i) = positionPeaks(i,3);
    Cycles.endTime(i) = positionPeaks(i+1,3);
    Cycles.frequency(i) = 1000 / (Cycles.endTime(i) -
Cycles.startTime(i));
    Cycles.amplitude(i) = abs(positionPeaks(i,nystagmusAxis) -
positionTroughs(i,nystagmusAxis));
    Cycles.intensity(i) = Cycles.frequency(i) * Cycles.amplitude(i);
    Cycles.min_x(i) =
nanmin(inputData(Cycles.startTime(i):Cycles.endTime(i),1));
    Cycles.max_x(i) =
nanmax(inputData(Cycles.startTime(i):Cycles.endTime(i),1));
    Cycles.mean_x(i) =
nanmean(inputData(Cycles.startTime(i):Cycles.endTime(i),1));
    Cycles.min_y(i) =
nanmin(inputData(Cycles.startTime(i):Cycles.endTime(i),2));
    Cycles.max_y(i) =
nanmax(inputData(Cycles.startTime(i):Cycles.endTime(i),2));
    Cycles.mean_y(i) =
nanmean(inputData(Cycles.startTime(i):Cycles.endTime(i),2));
    % Note: since we made sure that troughs always come *after* their
    % corresponding peak, there is no need to ensure that the peak and
    % trough occur in the same cycle
    if all(~isnan(inputData(Cycles.startTime(i) : Cycles.endTime(i),
1))) % mark clean cycles as we will only calculate amplitude and
frequency from these
        Cycles.isClean(i) = true;
    else
        Cycles.isClean(i) = false;
    end
end
if isfield(Cycles, 'isClean')
    nCleanCycles = sum(Cycles.isClean); % number of cycles without
dropped data
else
    nCleanCycles = 0;
    warning('cycles:notEnoughCleanCycles', 'Not enough clean nystagmus
cycles detected')
end

%% Detect foveations
if Prefs.FoveationDefinition.findFoveations
    fprintf('\nDetecting foveations...')
    Prefs.FoveationDefinition.minDuration =
Prefs.FoveationDefinition.minDuration / 1000 * eyeTrackerSamplingRate; %
convert from ms to samples
    if Prefs.FoveationDefinition.iterativelyAdjustFoveationWindow
        Prefs.FoveationDefinition.maxDriftAbsolute =
norm(nanstd(inputData(:,1:2))) *
Prefs.FoveationDefinition.maxDriftStandardDeviations; % set the max
drift in a foveation to a percentage of the SD of the drift present in
the whole dataset
        Prefs.FoveationDefinition.maxVelocityAbsolute =
abs(nanmean(abs(inputData(:,4))) +
Prefs.FoveationDefinition.maxVelocityStandardDeviations *
nanstd(inputData(:,4))); % threshold velocity for foveation (°/s).
        % TODO: The value above has to be positive, hence the abs().
Although it doesn't make a difference to the result, there may be a more
efficient way of doing this

```

```

    [foveationData, Prefs, errorCode] =
foveationwindowadjustment(positionPeaks, nCycles, Prefs, inputData); %
find the optimum foveation window size
    if errorCode
        fprintf('\nError: unable to find a foveation velocity
threshold within %i attempts...',
Prefs.FoveationDefinition.maxAttemptsAtFindingAVelocity)
    end
    else
        foveationData = identifyfoveations(Prefs, inputData);
    end

    % At this point, we have detected *at least* one 'foveation' for
however many cycles are required by
Prefs.FoveationDefinition.percentageOfCyclesThatMustHaveFoveationsFound

    if Prefs.FoveationDefinition.bridgeAdjacentFoveations
        foveationData = bridgefoveations(foveationData, inputData,
Prefs);
    end

    if Prefs.FoveationDefinition.onlyAllowOneFoveationPerCycle
        foveationData = optimisefoveations(Prefs, positionPeaks,
foveationData, nCycles); % eliminate all but one foveation for each
cycle
    end

    %% Get foveation metrics
    % Initialise struct:
    Foveations = struct('duration',NaN,'position',[NaN
NaN],'velocity',NaN,'startTime',NaN,'endTime',NaN);
    if ~isempty(foveationData) % if we have detected any foveation data
at all
        % Find contiguous elements (i.e. each foveation period)
        x = rot90(diff(foveationData(:,3)) ~=1); % mark the borders
between non-contiguous elements
        y = [1, cumsum(x) + 1]; % assign each contiguous group's
elements a reference number
        for i = 1 : max(y)
            Foveations.startTime(i) = foveationData(find(y == i, 1),3);
            Foveations.endTime(i) = foveationData(find(y == i, 1,
'last'),3);
            Foveations.duration(i) = sum(y == i);
            Foveations.position(i,:) = nanmean(foveationData(y == i,
1:2));
            Foveations.velocity(i) = nanmean(abs(foveationData(y == i,
4)));
        end
    end

    if ~isnan(Foveations.startTime)
        nFoveationsDetected = length(Foveations.startTime);
    else
        nFoveationsDetected = 0;
    end

    %% Calculate NAFX and NOFF
    if nFoveationsDetected > 0
        if Prefs.General.dataAreCalibrated
            % To calculate NAFX we need to first supply position data
zero'ed about the mean foveation position

```

```

        positionZeroedForNafx = inputData(:,nystagmusAxis) -
mean(Foveations.position(:,nystagmusAxis));

        % Set Prefs.FoveationDefinition.maxPositionAbsoluteForNafx
and Prefs.FoveationDefinition.maxVelocityAbsoluteForNafx each to one of
the values allowed by the Tau surface
        nafxPositionLimitPossibleValues = [0.5, 0.75, 1, 1.25, 1.5,
2, 2.5, 3, 3.5, 4, 5, 6]; % the list of values allowed by the NAFX tau
surface
        rangeOfFoveationPositionsInData =
max(Foveations.position(:,nystagmusAxis)) -
min(Foveations.position(:,nystagmusAxis)); % positional range of
foveations present in dataset
        if rangeOfFoveationPositionsInData/2 >
max(nafxPositionLimitPossibleValues)
            warning('nafx:positionLimitTooLow', 'Position limit used
for NAFX calculation may be too low to encompass all foveations')

Prefs.FoveationDefinition.maxPositionVariationAbsoluteForNafx =
max(nafxPositionLimitPossibleValues);
        else

Prefs.FoveationDefinition.maxPositionVariationAbsoluteForNafx =
nafxPositionLimitPossibleValues(find(rangeOfFoveationPositionsInData/2 -
nafxPositionLimitPossibleValues < 0, 1));
        end

        nafxVelocityLimitPossibleValues = [4, 5, 6, 7, 8, 9, 10]; %
the list of values allowed by the NAFX tau surface
        if Prefs.FoveationDefinition.maxVelocityAbsolute >
max(nafxVelocityLimitPossibleValues) % base the NAFX velocity limit on
the limit found by the Dunn algorithm
            warning('nafx:velocityLimitInappropriate', 'Velocity
limit used for NAFX calculation may not detect any foveations')
            Prefs.FoveationDefinition.maxVelocityAbsoluteForNafx =
max(nafxVelocityLimitPossibleValues);
        else
            Prefs.FoveationDefinition.maxVelocityAbsoluteForNafx =
nafxVelocityLimitPossibleValues(find(Prefs.FoveationDefinition.maxVeloci
tyAbsolute - nafxVelocityLimitPossibleValues < 1, 1));
        end

        [Nafx.value, Nafx.tau] =
nystagmus_calc_nafx(positionZeroedForNafx,inputData(:,4),eyeTrackerSampl
ingRate,nCycles,Prefs.FoveationDefinition.maxPositionVariationAbsoluteFo
rNafx,Prefs.FoveationDefinition.maxVelocityAbsoluteForNafx, Foveations,
inputData(:,3));
        Foveations.nafx = Nafx.value;
        [Noff.value, Noff.bestFoveation] =
nystagmus_calc_noff(inputData(:,nystagmusAxis), inputData(:,4),
eyeTrackerSamplingRate,
Prefs.FoveationDefinition.useManualOffsetForNoff,
Prefs.FoveationDefinition.maxPositionVariationAbsoluteForNoff,
Prefs.FoveationDefinition.maxVelocityAbsoluteForNoff,
Prefs.FoveationDefinition.minDuration,
Prefs.FoveationDefinition.maxGapToBridge);
        Foveations.noff = Noff.value;
    end
else
    warning('foveations:noFoveationsDetected', 'No foveations
detected')
    Nafx.value = NaN;

```

```

        Noff.value = NaN;
    end
else
    Foveations = [];
end

%% Detect saccades
fprintf('\nDetecting saccades...')

if strcmp(Prefs.SaccadeDefinition.detectorType, 'behrens') % Behrens'
detection is preferred for pendular nystagmus
    % Find all saccades and output their metrics:
    Saccades =
oculomotorsuite_findsaccades_behrens(inputData(:,nystagmusAxis),
inputData(:,4), inputData(:,5), eyeTrackerSamplingRate,
Prefs.SaccadeDefinition.Behrens.standardDeviationsForAccelerationThresho
ld);
elseif strcmp(Prefs.SaccadeDefinition.detectorType, 'dunn') % Dunn's
detection is preferred for jerk nystagmus
    [Saccades, saccadeVelocityThreshold] =
oculomotorsuite_findsaccades_dunn(inputData(:,nystagmusAxis),
inputData(:,4), inputData(:,5),
Prefs.SaccadeDefinition.Dunn.standardDeviationsForVelocityThreshold);
end

if isempty(Saccades.startTime)
    warning('saccades:noSaccadesFound', 'No saccades were detected. Try
changing saccade velocity threshold or disabling absolute thresholds')
end

%% Detect slow phases and back-to-back saccades
fprintf('\nDetecting slow phases...')
[SlowPhases, backToBackSaccadeTimes] = identifyslowphases(Saccades,
inputData); % find all slow phases (and back-to-back saccades)
if isempty(SlowPhases.startTime)
    warning('slowPhases:noSlowPhasesFound', 'No slow phases were
detected. This is probably due to a lack of detected saccades')
else
    for i = 1:length(SlowPhases.startTime)
        % To determine if slow phase is accelerating or decelerating,
        % compare velocity for first half of slow phase with velocity in
        % second half. Taking an average of instantaneous acceleration
        isn't
        % very informative due to local fluctuations.

        % TODO: This doesn't work well yet; acceleration detection could
        probably be improved
        if
nanmean(abs(inputData(SlowPhases.startTime(i):SlowPhases.startTime(i)+ro
und((SlowPhases.endTime(i)-SlowPhases.startTime(i))/2),4))) <
nanmean(abs(inputData(SlowPhases.startTime(i)+round((SlowPhases.endTime(
i)-SlowPhases.startTime(i))/2):SlowPhases.endTime(i),4)))
            SlowPhases.isAccelerating(i) = true;
        else
            SlowPhases.isAccelerating(i) = false;
        end
    end
end

%% Console output
meanAmplitude = nanmean(Cycles.amplitude);

```

```

stdAmplitude = nanstd(Cycles.amplitude);

meanFrequency = nanmean(Cycles.frequency);
stdFrequency = nanstd(Cycles.frequency);

meanIntensity = nanmean(Cycles.intensity);
stdIntensity = nanstd(Cycles.intensity);

if Prefs.FoveationDefinition.findFoveations && nFoveationsDetected > 1
    meanFoveationDuration = mean(Foveations.duration) * 1000 /
eyeTrackerSamplingRate; % convert to ms
    stdFoveationDuration = std(Foveations.duration) * 1000 /
eyeTrackerSamplingRate; % convert to ms
    meanFoveationPosition = mean(Foveations.position(:,1:2));
    rangeFoveationPosition = max(Foveations.position(:,1:2)) -
min(Foveations.position(:,1:2));
    stdFoveationPosition = std(Foveations.position(:,1:2));
    meanFoveationVelocity = mean(Foveations.velocity);
    stdFoveationVelocity = std(Foveations.velocity);
end
meanSaccadeMeanVelocity = mean(Saccades.meanVelocity); % TODO: Should
this really be mean? Why not median? Same applies for the other metrics
output here
stdSaccadeMeanVelocity = std(Saccades.meanVelocity);
meanSaccadePeakVelocity = mean(Saccades.peakVelocity);
stdSaccadePeakVelocity = std(Saccades.peakVelocity);
meanSaccadeAmplitude = mean(Saccades.amplitude);
stdSaccadeAmplitude = std(Saccades.amplitude);
meanSaccadeDuration = mean(Saccades.duration) * 1000 /
eyeTrackerSamplingRate; % convert to ms
stdSaccadeDuration = std(Saccades.duration) * 1000 /
eyeTrackerSamplingRate; % convert to ms
nSaccadesDetected = length(Saccades.duration);
meanSlowPhaseMeanVelocity = mean(SlowPhases.meanVelocity);
stdSlowPhaseMeanVelocity = std(SlowPhases.meanVelocity);
meanSlowPhasePeakVelocity = mean(SlowPhases.peakVelocity);
stdSlowPhasePeakVelocity = std(SlowPhases.peakVelocity);
nBackToBackSaccadesDetected = length(backToBackSaccadeTimes);

fprintf('\n\n*** WAVEFORM ANALYSIS ***\n%i cycles were detected (%i of
these were free from blinks)\nFrequency = %.1fHz (SD = %.1fHz)',
nCycles, nCleanCycles, meanFrequency, stdFrequency)
if Prefs.General.dataAreCalibrated
    fprintf('\nAmplitude = %.1f° (SD = %.1f°)\nIntensity = %.1f (SD =
%.1f)', meanAmplitude, stdAmplitude, meanIntensity, stdIntensity)
end

if Prefs.FoveationDefinition.findFoveations && nFoveationsDetected > 1
    fprintf('\n\n*** FOVEATION ANALYSIS ***\n%i foveations were
detected\nFoveation duration = %.1fms (SD = %.1fms)',
nFoveationsDetected, meanFoveationDuration, stdFoveationDuration)
    if Prefs.General.dataAreCalibrated
        if Prefs.FoveationDefinition.iterativelyAdjustFoveationWindow
            extraText = strcat('to detect a foveation on >=',
num2str(Prefs.FoveationDefinition.percentageOfCyclesThatMustHaveFoveatio
nsFound), '% of cycles');
        else
            extraText = 'fixed';
        end
        fprintf('\nFoveation velocity threshold (%s) is %.1f°/s',
extraText, Prefs.FoveationDefinition.maxVelocityAbsolute)
    end
end

```

```

    if Prefs.FoveationDefinition.limitDrift
        fprintf('\nIntra-foveation drift limit is %.1f°',
Prefs.FoveationDefinition.maxDriftAbsolute)
    end
    fprintf('\nFoveation position = (%.1f°, %.1f°) ± (%.1f°, %.1f°)
(SD = [%.1f°, %.1f°])\nFoveation velocity = %.1f°/s (SD = %.1f°/s)',
meanFoveationPosition(1), meanFoveationPosition(2),
rangeFoveationPosition(1)/2, rangeFoveationPosition(2)/2,
stdFoveationPosition(1), stdFoveationPosition(2), meanFoveationVelocity,
stdFoveationVelocity)
    fprintf('\nNAFX = %.2f, using a velocity limit of %.1f°/s,
position limit of %.1f° and tau value of %.2fms', Nafx.value,
Prefs.FoveationDefinition.maxVelocityAbsoluteForNafx,
Prefs.FoveationDefinition.maxPositionVariationAbsoluteForNafx, Nafx.tau)
    fprintf('\nNOFF = %.2f, using a velocity limit of %.1f°/s and
position limit of %.1f°', Noff.value,
Prefs.FoveationDefinition.maxVelocityAbsoluteForNoff,
Prefs.FoveationDefinition.maxPositionVariationAbsoluteForNoff)
    end
end

fprintf('\n\n*** SACCADIC ANALYSIS ***\n%i saccades were
detected\nSaccade duration = %.1fms (SD = %.1fms)\n%i saccades had no
intersaccadic interval', nSaccadesDetected, meanSaccadeDuration,
stdSaccadeDuration, nBackToBackSaccadesDetected)
if Prefs.General.dataAreCalibrated
    if strcmp(Prefs.SaccadeDefinition.detectorType, 'dunn')
        fprintf('\nSaccade velocity threshold is %.2f°/s',
saccadeVelocityThreshold)
    elseif strcmp(Prefs.SaccadeDefinition.detectorType, 'behrens')
        fprintf('\nSaccade acceleration threshold is %i SDs from the
previous 200 ms',
Prefs.SaccadeDefinition.Behrens.standardDeviationsForAccelerationThresho
ld)
    end
end

% Calculate which is the dominant saccade direction by adding up the
% total amplitudes of all saccades in each direction and comparing:
totalRightOrUpSaccadeSize = 0;
totalLeftOrDownSaccadeSize = 0;
for i = 1 : size(Saccades.amplitude)
    if Saccades.direction(i) == 1 % up or right saccade
        totalRightOrUpSaccadeSize = totalRightOrUpSaccadeSize +
Saccades.amplitude(i);
    else
        totalLeftOrDownSaccadeSize = totalLeftOrDownSaccadeSize +
Saccades.amplitude(i);
    end
end

if nystagmusAxis == 1 % horizontal
    if totalRightOrUpSaccadeSize > totalLeftOrDownSaccadeSize
        dominantSaccadeDirection = 'right';
    elseif totalLeftOrDownSaccadeSize > totalRightOrUpSaccadeSize
        dominantSaccadeDirection = 'left';
    else
        dominantSaccadeDirection = 'unknown';
    end
elseif nystagmusAxis == 2 % vertical
    if totalRightOrUpSaccadeSize > totalLeftOrDownSaccadeSize
        dominantSaccadeDirection = 'up';
    end
end

```

```

elseif totalLeftOrDownSaccadeSize > totalRightOrUpSaccadeSize
    dominantSaccadeDirection = 'down';
else
    dominantSaccadeDirection = 'unknown';
end
end

fprintf('\nDominant saccade direction is %s: ',
dominantSaccadeDirection)

nUpOrRightSaccades = sum(Saccades.direction == +1);
nDownOrLeftSaccades = sum(Saccades.direction == -1);

if nystagmusAxis == 1 % horizontal
    fprintf('%i right saccades and %i left saccades were detected',
nUpOrRightSaccades, nDownOrLeftSaccades)
elseif nystagmusAxis == 2 % vertical
    fprintf('%i up saccades and %i down saccades were detected',
nUpOrRightSaccades, nDownOrLeftSaccades)
end

if Prefs.General.dataAreCalibrated
    fprintf('\nSaccade peak velocity = %.1f°/s (SD = %.1f°)\nSaccade
mean velocity = %.1f°/s (SD = %.1f°)\nSaccade amplitude = %.1f° (SD =
%.1f°)', meanSaccadePeakVelocity, stdSaccadePeakVelocity,
meanSaccadeMeanVelocity, stdSaccadeMeanVelocity, meanSaccadeAmplitude,
stdSaccadeAmplitude)
end

fprintf('\n\n*** SLOW PHASE ANALYSIS ***')
if isfield(SlowPhases, 'isAccelerating') &&
sum(SlowPhases.isAccelerating) > length(SlowPhases.isAccelerating)/2 %
if more than half of slow phases are accelerating
    fprintf('\nSlow phases appear to be accelerating')
else
    fprintf('\nSlow phases do not appear to be accelerating')
end

if Prefs.General.dataAreCalibrated
    fprintf('\nSlow phase peak velocity = %.1f°/s (SD = %.1f°)\nSlow
phase mean velocity = %.1f°/s (SD = %.1f°)', meanSlowPhasePeakVelocity,
stdSlowPhasePeakVelocity, meanSlowPhaseMeanVelocity,
stdSlowPhaseMeanVelocity)
end

fprintf('\n')

%% Figure output
if Prefs.Plot.displayFigure
    figure;
    if Prefs.Plot.mainSequence
        subplot('position', [0.1 0.35 0.8 0.6]);
    end

    hold on;
    if Prefs.Plot.useWhiteBackground
        whitebg('white'); % set figure background to white
    else
        whitebg('black'); % set figure background to black
    end
end

```

```

    if ExperimentalPrefs.deleteSaccades % to visualise nystagmus without
the resets
        for i = 1 : length(Saccades.startTime) % for each detected
saccade
            warning('experimentalPrefs:deleteSaccades','Deleting all
saccades from eye trace')
            inputData(Saccades.startTime(i):Saccades.endTime(i),:) =
NaN; % delete the data
            end
        end

    if Prefs.Plot.useHardwareAcceleration
        set(gcf,'Renderer','OpenGL'); % set rendering mode to OpenGL to
allow hardware acceleration to visualisation
        end
        yAxisLabel = 'X Position (°)'; % This is a variable and will be
modified if there are more things to show
        set(0,'Units','pixels'); % prepare to use pixel units to find the
screen size
        screenSize = get(0,'ScreenSize'); % find the screen size
        set(gcf,'name',strcat(inputFileName,' analysis'), 'numbertitle',
'off', 'position', [screenSize(3)*0.1 screenSize(4)*0.1
screenSize(3)*0.8 screenSize(4)*0.8]); % position the figure window
relative to screen size
        plot3(inputData(:,3), inputData(:,1), inputData(:,2),
'b','LineWidth',Prefs.Plot.lineWidth); % plot the position data

        if nystagmusAxis == 2 % if we're looking at vertical nystagmus data
            view(0,180); % rotate the plot so we're looking from the
appropriate angle
        end % we don't need to do anything for horizontal nystagmus, since
the default view is (0,90)

    if Prefs.Plot.saccades
        for i = 1 : length(Saccades.startTime) % for each detected
saccade

plot3(inputData(Saccades.startTime(i):Saccades.endTime(i),3),
inputData(Saccades.startTime(i):Saccades.endTime(i),1),
inputData(Saccades.startTime(i):Saccades.endTime(i),2),
'green','LineWidth',Prefs.Plot.lineWidth); % plot saccades in green
            end
        end

    if Prefs.Plot.lockAspect
        tmpAspect=daspect(); % get the aspect ratio of the axes scales
        daspect(tmpAspect([1 2 2])); % make the Y and Z axes equal in
scale (to better visualise the data)
        pbaspect([2 1 0.4]); % set the plot box size to maximise on-
screen data
        end

    if Prefs.Plot.velocityTransform
        plot(inputData(:,3), inputData(:,4)/100,
'cyan','LineWidth',Prefs.Plot.lineWidth); % plot the velocity/100
transform
        yAxisLabel = strcat(yAxisLabel, ' | Velocity/100 (°/s)');
        end

    if Prefs.Plot.accelerationTransform

```

```

        plot(inputData(:,3), inputData(:,5)/1000,
'magenta','LineWidth',Prefs.Plot.lineWidth); % plot the
acceleration/1000 transform
        yAxisLabel = strcat(yAxisLabel, ' | Acceleration/1000 (°/s²)');
    end

    if Prefs.Plot.backToBackSaccades && ~isempty(backToBackSaccadeTimes)
        if Prefs.Plot.useWhiteBackground
            plot(backToBackSaccadeTimes([1 1],:) ,
ylim,'black','LineWidth',Prefs.Plot.lineWidth); % plot vertical dotted
lines showing back-to-back saccade locations
        else
            plot(backToBackSaccadeTimes([1 1],:) ,
ylim,'white','LineWidth',Prefs.Plot.lineWidth); % plot vertical dotted
lines showing back-to-back saccade locations
        end
    end

    if Prefs.Plot.velocityThresholds
        plot(xlim, saccadeVelocityThreshold(:, [1
1])/100,'red','LineWidth',Prefs.Plot.lineWidth); % plot the saccadic
velocity threshold
        plot(xlim, -saccadeVelocityThreshold(:, [1
1])/100,'red','LineWidth',Prefs.Plot.lineWidth); % plot the saccadic
velocity threshold (negative)
        plot(xlim, Prefs.FoveationDefinition.maxVelocityAbsolute(:, [1
1])/100,'red--','LineWidth',Prefs.Plot.lineWidth); % plot the foveation
velocity threshold
        plot(xlim, -Prefs.FoveationDefinition.maxVelocityAbsolute(:, [1
1])/100,'red--','LineWidth',Prefs.Plot.lineWidth); % plot the foveation
velocity threshold (negative)
    end

    if Prefs.Plot.waveformBounds && nCycles >= 1 % if we have at least
one cycle to plot
        if Prefs.Plot.useWhiteBackground
            % Generate a plot with our maxima and minima envelope on to
visually confirm the amplitude
            plot3(positionTroughs(:,3), positionTroughs(:,1),
positionTroughs(:,2), 'black','LineWidth',Prefs.Plot.lineWidth);
            plot3(positionPeaks(:,3), positionPeaks(:,1),
positionPeaks(:,2), 'black','LineWidth',Prefs.Plot.lineWidth);
        else
            % Generate a plot with our maxima and minima envelope on to
visually confirm the amplitude
            plot3(positionTroughs(:,3), positionTroughs(:,1),
positionTroughs(:,2), 'white','LineWidth',Prefs.Plot.lineWidth);
            plot3(positionPeaks(:,3), positionPeaks(:,1),
positionPeaks(:,2), 'white','LineWidth',Prefs.Plot.lineWidth);
        end
    end

    if Prefs.Plot.cycleBoundaries && nCycles >= 1 % if we have at least
one cycle to plot
        if Prefs.Plot.useWhiteBackground
            plot(positionPeaks(:, [3 3]), ylim,
'black','LineWidth',Prefs.Plot.lineWidth);
        else
            plot(positionPeaks(:, [3 3]), ylim,
'white','LineWidth',Prefs.Plot.lineWidth);
        end
    end
end

```

```

if Prefs.General.dataAreCalibrated
    ylabel(yAxisLabel); % Put the relevant Y axis label on the plot
    xlabel('Y Position (°)');
else
    ylabel('X position (Uncalibrated units)');
    xlabel('Y position (Uncalibrated units)');
end

if Prefs.FoveationDefinition.findFoveations
    if nFoveationsDetected > 0 && Prefs.Plot.foveations % if we have
        collected some foveation data
            for i = 1 : nFoveationsDetected % for each foveation

plot3(inputData(Foveations.startTime(i):Foveations.endTime(i),3),
inputData(Foveations.startTime(i):Foveations.endTime(i),1),
inputData(Foveations.startTime(i):Foveations.endTime(i),2),
'red','LineWidth', Prefs.Plot.lineWidth); % plot foveation position data
with red lines

plot3(inputData(Foveations.startTime(i):Foveations.endTime(i),3),
inputData(Foveations.startTime(i):Foveations.endTime(i),1),
inputData(Foveations.startTime(i):Foveations.endTime(i),2),
'red.','MarkerSize', Prefs.Plot.markerSize); % overlay foveation data
points with red dots (to increase visibility)
                end
            end

                if Prefs.Plot.noffFoveations && ~isnan(Noff.value)
                    plot3(inputData(Noff.bestFoveation,3),
inputData(Noff.bestFoveation,1), inputData(Noff.bestFoveation,2),
'white.','MarkerSize', Prefs.Plot.markerSize); % plot NOFF data points
with white dots
                    end
                end

if Prefs.Plot.mainSequence
    if ~Prefs.General.dataAreCalibrated
        warning('uncalibrated:dataNotCalibrated', '\nData are not
calibrated. Main sequence of saccades are therefore inaccurate')
    end
    plotmainsequence(Saccades); % plot main sequence of saccades
end

hold off; % we have finished plotting; turn off hold

% Convert X axis from timestamp to ms
xTicks = get(gca, 'XTick');
xLabels = get(gca, 'XTickLabel');
set(gca, 'XTick', xTicks, 'XTickLabel', num2str(str2num(xLabels) *
1000 / eyeTrackerSamplingRate));
xlabel('Time (ms)');
end

%% Generate CSV reports
if Prefs.Report.generateReports
    if Prefs.Report.cycles
        cyclesReport(:,1) = Cycles.startTime;
        cyclesReport(:,2) = Cycles.endTime;
        cyclesReport(:,3) = Cycles.amplitude;
        cyclesReport(:,4) = Cycles.frequency;
    end
end

```

```

cyclesReport(:,5) = Cycles.intensity;
cyclesReport(:,6) = Cycles.min_x;
cyclesReport(:,7) = Cycles.max_x;
cyclesReport(:,8) = Cycles.mean_x;
cyclesReport(:,9) = Cycles.min_y;
cyclesReport(:,10) = Cycles.max_y;
cyclesReport(:,11) = Cycles.mean_y;
cyclesReport(:,12) = Cycles.isClean;
fileName = strcat(inputFileName, '_cycles.csv');
header =
'start_time,end_time,amplitude,frequency,intensity,min_x,max_x,mean_x,mi
n_y,max_y,mean_y,is_clean';
    generatecsv(cyclesReport,fileName,header);
end

if Prefs.Report.foveations
    foveationsReport(:,1) = Foveations.startTime;
    foveationsReport(:,2) = Foveations.endTime;
    foveationsReport(:,3) = Foveations.position(:,1);
    foveationsReport(:,4) = Foveations.position(:,2);
    foveationsReport(:,5) = Foveations.velocity;
    foveationsReport(:,6) = Foveations.duration;
    fileName = strcat(inputFileName, '_foveations.csv');
    header =
'start_time,end_time,position_x,position_y,velocity,duration';
    generatecsv(foveationsReport,fileName,header);
end

if Prefs.Report.slowPhases
    slowPhasesReport(:,1) = SlowPhases.startTime;
    slowPhasesReport(:,2) = SlowPhases.endTime;
    slowPhasesReport(:,3) = SlowPhases.meanVelocity;
    slowPhasesReport(:,4) = SlowPhases.peakVelocity;
    fileName = strcat(inputFileName, '_slowphases.csv');
    header = 'start_time,end_time,mean_velocity,peak_velocity';
    generatecsv(slowPhasesReport,fileName,header);
end

if Prefs.Report.saccades
    saccadesReport(:,1) = Saccades.startTime;
    saccadesReport(:,2) = Saccades.endTime;
    saccadesReport(:,3) = Saccades.duration;
    saccadesReport(:,4) = Saccades.meanVelocity;
    saccadesReport(:,5) = Saccades.peakVelocity;
    saccadesReport(:,6) = Saccades.amplitude;
    saccadesReport(:,7) = Saccades.direction;
    fileName = strcat(inputFileName, '_saccades.csv');
    header =
'start_time,end_time,duration,mean_velocity,peak_velocity,amplitude,dire
ction';
    generatecsv(saccadesReport,fileName,header);
end

end

function generatecsv(report,fileName,header)
outid = fopen(fileName, 'w+');
fprintf(outid, '%s', header);
fclose(outid);
dlmwrite(fileName,report,'roffset',1,'-append', 'precision', 8); %
increased precision to allow all digits to be saved

```

```

disp(strcat('Generated report ', fileName, ''))

function nystagmusAxis = findnystagmusaxis(inputData)
% Look at the standard deviations of the oscillations in both the
horizontal and vertical axes to determine if nystagmus is
% horizontal or vertical
inputDataStandardDeviation = nanstd(inputData);

% The following block determines if the nystagmus is primarily
horizontal or vertical, and applies the amplitude analysis on the
% appropriate axis:
if inputDataStandardDeviation(1) > inputDataStandardDeviation(2)
    fprintf('\nSubject has horizontal nystagmus')
    nystagmusAxis = 1; % Type 1 indicates horizontal
elseif inputDataStandardDeviation(2) > inputDataStandardDeviation(1)
    fprintf('\nSubject has vertical nystagmus')
    nystagmusAxis = 2; % Type 2 indicates vertical
else % this will only happen if our standard deviations are equal
    dialogResponse = questdlg('What is nystagmus axis?', 'Unable to
determine nystagmus axis', 'Horizontal', 'Vertical', 'Horizontal');
    switch dialogResponse
        case 'Horizontal'
            nystagmusAxis = 1;
        case 'Vertical'
            nystagmusAxis = 2;
        otherwise
            error('unknownNystagmusAxis:userExitedDialog', 'Unable to
determine nystagmus axis')
    end
end

function [SlowPhases, backToBackSaccadeTimes] =
identifyslowphases(Saccades, inputData)
% Finds slow phases. In addition, identifies any back-to-back saccades
% present in the data.

SlowPhases =
struct('startTime', [], 'endTime', [], 'meanVelocity', [], 'peakVelocity', []);
% initialise struct

% Find the slow phases by finding times not in Saccades
SlowPhases.startTime = Saccades.endTime(1:end - 1) + 1; % slow phase
starts after saccade. Don't use last saccade
SlowPhases.endTime = Saccades.startTime(2:end) - 1; % slow phase
finishes just before saccade. Don't use first saccade

% It is possible that if a back-to-back saccade occurs without an
% intersaccadic interval, we will have erroneous data in the
% slowPhaseTimesArray matrix. So, the block below removes these
instances:
backToBackSaccades = []; % initialise a vector which will contain the row
number (within slowPhaseTimesArray) of any back-to-back saccades that
are detected
for i = 1 : length(SlowPhases.startTime)
    if SlowPhases.endTime(i) - SlowPhases.startTime(i) < 1 % if slow
phase lasts less than a single sample in length
        backToBackSaccades = [backToBackSaccades, i];
    end
end

```

```

end
backToBackSaccadeTimes = SlowPhases.startTime(backToBackSaccades)-1; %
keep a record of the times of the back-to-back saccade junction
SlowPhases.startTime(backToBackSaccades) = []; % remove back-to-back
saccades identified from the slowPhaseTimesArray matrix
SlowPhases.endTime(backToBackSaccades) = []; % remove back-to-back
saccades identified from the slowPhaseTimesArray matrix

% Having weeded out all back-to-back saccades, we now have a matrix
containing slow phase start and end times only
for i = 1 : length(SlowPhases.startTime) % for each slow phase...
    SlowPhases.meanVelocity(i) =
nanmean(abs(inputData(SlowPhases.startTime(i):SlowPhases.endTime(i),4)))
; % find mean velocity
    SlowPhases.peakVelocity(i) =
max(abs(inputData(SlowPhases.startTime(i):SlowPhases.endTime(i),4))); %
find peak velocity
end

```

```

function foveationData = identifyfoveations(Prefs, inputData)
% Actually identify foveations based on
Prefs.FoveationDefinition.maxVelocityAbsolute and
Prefs.FoveationDefinition.minDuration

foveationData = inputData(abs(inputData(:,4)) <=
Prefs.FoveationDefinition.maxVelocityAbsolute,:); % retrieve data below
the velocity threshold for foveation

if Prefs.FoveationDefinition.limitDrift % if we're imposing a maximum
foveation drift criterion
    foveationData = limitfoveationdrift(foveationData, Prefs);
end

if Prefs.FoveationDefinition.imposeMinDuration % if we're imposing a
minimum foveation duration criterion
    if ~isempty(foveationData) % if we have detected any foveation data
at all
        x = rot90(diff(foveationData(:,3)) ~=1); % mark the borders
between non-contiguous foveation data
        y = [1, cumsum(x) + 1]; % assign each contiguous group's
elements a reference number
        for i = max(y) : -1 : 1 % for each group of foveation data
(working backwards to avoid deleting elements at the beginning of the
array first)
            if sum(y == i) < Prefs.FoveationDefinition.minDuration %
find those groups with less than the minimum required number of data to
satisfy foveation...
                foveationData(y == i,:) = []; % ...and delete them
            end
        end
    end
end
end

```

```

function foveationData = limitfoveationdrift(foveationData, Prefs)
% Remove foveation data that exceeds
Prefs.FoveationDefinition.maxDriftAbsolute

```

```

if ~isempty(foveationData) % if we have detected any foveation data at
all
    candidatesForDeletion = zeros(size(foveationData,2),1); % initialise
vector which will hold the indices of elements to be removed from
foveationData
    % n.b. in the above line, we preallocate plenty of memory to speed
up this function
    x = rot90(diff(foveationData(:,3)) ~=1); % mark the borders between
non-contiguous elements
    y = [1, cumsum(x) + 1]; % assign each contiguous group's elements a
reference number
    for i = 1 : max(y) % for each foveation
        averagePositionForThisFoveation = median(foveationData(y,1:2));
% get co-ordinates of average foveation position for this foveation
        for j = find(y, i, 'first') : find(y, i, 'last') % for each
datum within this foveation
            differenceInPositionFromAverage =
abs((averagePositionForThisFoveation) - foveationData(j,1:2));
            if differenceInPositionFromAverage >
Prefs.FoveationDefinition.maxDriftAbsolute
                candidatesForDeletion(sum(candidatesForDeletion ~= 0) +
1) = j;
            end
        end
    end
    candidatesForDeletion(candidatesForDeletion == 0) = []; % delete any
unused entries from the candidatesForDeletion memory allocation
    foveationData(candidatesForDeletion,:) = []; % delete the marked
element candidates
end

```

```

function [foveationData, Prefs, errorCode] =
foveationwindowadjustment(positionPeaks, nCycles, Prefs, inputData)
% Check how much foveation data we get with default thresholds. If this
isn't enough, keep increasing the threshold until we get enough

errorCode = false; % default error code from function. If remains 0, no
problems
currentlyMakingPrefs.FoveationDefinitionStricter = true; % we perform
foveation detection iteratively. This value is only 'true' until we have
started to miss foveations
nIterations = 0; % this counts the number of times the foveation
detector has tried to adjust the foveation velocity threshold. If it
gets to a silly number, we give up
nCyclesWithFoveationsDetected = 0; % initialise. Note this variable is
not the actual number of foveations detected, as it doesn't count twice
if two foveations are found in a single beat
while nCyclesWithFoveationsDetected <
(Prefs.FoveationDefinition.percentageOfCyclesThatMustHaveFoveationsFound
/100 * nCycles) || currentlyMakingPrefs.FoveationDefinitionStricter
    nIterations = nIterations + 1;
    if nIterations >
Prefs.FoveationDefinition.maxAttemptsAtFindingAVelocity
        errorCode = true; % if we have an error, produce this error code
so the parent function knows
        return;
    end

    fprintf('.') % each printed dot represents an iteration

```

```

foveationData = identifyfoveations(Prefs, inputData);

if ~isempty(foveationData) % if we have detected any foveation data
at all
    nCyclesWithFoveationsDetected = 0; % reset to zero before we
calculate the number of cycles with foveation data
    for i = 1 : nCycles - 1 % this block checks how many nystagmus
periods we actually have foveation data for
        % n.b. We don't look in the last cycle or we hit an error
due to not having a cycle end-point
        foveationDataFromThisCycle =
identifydatafromthiscycle(foveationData, positionPeaks, i);
        if ~isempty(foveationDataFromThisCycle) % if data exists in
the present cycle
            nCyclesWithFoveationsDetected =
nCyclesWithFoveationsDetected + 1;
        end
    end
end

% First, we make the foveation parameters progressively tighter
until
% we start to lose foveations. Then, we expand them gradually until
we
% have data for at least the percentage desired of cycles. This
keeps
% our definition of foveation as strict as possible in all
individuals
if currentlyMakingPrefs.FoveationDefinitionStricter...
    && nCyclesWithFoveationsDetected >
round((Prefs.FoveationDefinition.percentageOfCyclesThatMustHaveFoveation
sFound/100 * nCycles)) % if too many found, then we first make the
foveation parameters tighter
    Prefs.FoveationDefinition.maxVelocityAbsolute =
Prefs.FoveationDefinition.maxVelocityAbsolute * (1 -
Prefs.FoveationDefinition.iterativeVelocityIncrementPercentage/100);
elseif nCyclesWithFoveationsDetected <=
round((Prefs.FoveationDefinition.percentageOfCyclesThatMustHaveFoveation
sFound/100 * nCycles)) % if not enough found, then we need to make the
foveation parameters more liberal
    currentlyMakingPrefs.FoveationDefinitionStricter = false; % once
we are into this elseif block, we don't want to be making foveation
definition stricter again
    Prefs.FoveationDefinition.maxVelocityAbsolute =
Prefs.FoveationDefinition.maxVelocityAbsolute * (1 +
Prefs.FoveationDefinition.iterativeVelocityIncrementPercentage/100);
end
end

function dataFromThisCycle = identifydatafromthiscycle(data,
positionPeaks, cycleReference)
% Identify consecutive data that lie within the currently analysed
nystagmus cycle

dataAfterLastCycle = find(data(:,3) > positionPeaks(cycleReference,3));
dataBeforeNextCycle = find(data(:,3) < positionPeaks(cycleReference +
1,3));
dataFromThisCycleIndex = intersect(dataAfterLastCycle,
dataBeforeNextCycle);
% At this stage we have any data which exists in the current cycle,
based
% on boundaries defined by 'positionPeaks'. However, it is possible that

```

```

% this boundary could intersect an event. In this case, we still want to
% retain all of the event data. So, we must seek contiguous event data
% about the boundaries. If a foveation lies on the boundary, we keep it
if
% there is data *after* the boundary but not if there is data before the
% boundary. This is to avoid having the same foveation register twice.

```

```

contiguousDataAtStartOfCycleRemoved = false; % this variable is only set
to true once we have removed all contiguous data that lies on the border
of the start of the present cycle
while ~contiguousDataAtStartOfCycleRemoved
    if ~isempty(dataFromThisCycleIndex) && dataFromThisCycleIndex(1) > 1
&& data(dataFromThisCycleIndex(1)-1,3) ==
data(dataFromThisCycleIndex(1),3) - 1 % if the datum prior to the first
datum in this cycle is only separated by one sample
        % If we get here, we must delete all contiguous event data from
the first sample in the cycle onwards
        dataFromThisCycleIndex(1) = []; % remove the first element in
the vector
    else
        contiguousDataAtStartOfCycleRemoved = true;
    end
end

```

```

contiguousDataAtEndOfCycleAdded = false; % this variable is only set to
true once we have included all contiguous data that lies on the border
of the end of the present cycle
while ~contiguousDataAtEndOfCycleAdded
    if ~isempty(dataFromThisCycleIndex) && dataFromThisCycleIndex(end) <
size(data,1) && data(dataFromThisCycleIndex(end)+1,3) ==
data(dataFromThisCycleIndex(end),3) + 1 % if the datum following the
last datum in this cycle is only separated by one sample
        % If we get here, we must include all contiguous event data from
the last sample in the cycle onwards
        dataFromThisCycleIndex(end+1) = dataFromThisCycleIndex(end)+1; %
add the first element from the next cycle to the present cycle vector
    else
        contiguousDataAtEndOfCycleAdded = true;
    end
end
dataFromThisCycle = data(dataFromThisCycleIndex,:); % retrieve the
actual foveation from the indices

```

```

function foveationData = bridgefoveations(foveationData, inputData,
Prefs)
% Find foveations that are separated by a small gap and retrieve the
data from those gaps - combine into a single foveation
x = diff(foveationData(:,3)) ~=1; % mark the borders between non-
contiguous elements in the foveation data timecodes
for i = 1 : size(x)
    if x(i) % if we are at a boundary between non-contiguous elements
        timeGapBetweenFoveations = foveationData(i+1,3) -
foveationData(i,3);
        if timeGapBetweenFoveations <=
Prefs.FoveationDefinition.maxGapToBridge
            y = find(inputData(:,3) == foveationData(i,3)); % 'y' is the
first row of inputData of our gap between foveations
            for j = y + 1 : y + timeGapBetweenFoveations - 1 % for each
line from the inputData that exists between the local foveations...

```

```

        foveationData(end+1,:) = inputData(j,:); %... add it to
the foveationData matrix
        end
    end
end
end

```

```

foveationData = sortrows(foveationData, 3); % arrange the foveation data
in order again, based on the timestamp column (3)

```

```

function foveationData = optimisefoveations(Prefs, positionPeaks,
foveationData, nCycles)
% Take the foveation data and select the best one for each cycle
% This selection can be either based on the slowest or longest (set by
Prefs.FoveationDefinition.optimumFoveationSelectionMethod)
if Prefs.FoveationDefinition.onlyAllowOneFoveationPerCycle
    fprintf('\nOptimising chosen foveations...')
    foveationDataOptimised = []; % this matrix contains only the
shortest foveation period for each cycle

    if ~isempty(foveationData) % if we have detected any foveation data
at all
        for i = 1 : nCycles - 1 % don't look in the last cycle or we
hit an error due to not having a cycle end-point
            % As earlier, we have to separate the cycles out:
            foveationDataFromThisCycle =
identifydatafromthiscycle(foveationData, positionPeaks, i);
            % The next few lines detect the longest contiguous foveation
in the cycle:
            x = rot90(diff(foveationDataFromThisCycle(:,3)) ~=1); % mark
the borders between non-contiguous elements
            y = [1, cumsum(x) + 1]; % assign each contiguous group's
elements a reference number
            if ~isempty(x) % if there is at least one foveation detected
in this cycle
                if
strcmp(Prefs.FoveationDefinition.optimumFoveationSelectionMethod,
'longest')
                    optimumFoveationInThisCycle =
foveationDataFromThisCycle(y==mode(y),:); % find the foveation with the
most data elements
                    % n.b. If two foveations are of equal length, the
reported foveation will be the FIRST detected
                elseif
strcmp(Prefs.FoveationDefinition.optimumFoveationSelectionMethod,
'slowest')
                    foveationMeanVelocity = zeros(size(y,1),1); %
initialise
                    for j = 1 : max(y) % for each contiguous foveation
identified above
                        foveationMeanVelocity(j) =
nanmean(foveationDataFromThisCycle(y == j,4)); % find the average
velocity of the foveation
                    end
                    [unusedVariable, m] = min(foveationMeanVelocity); %
'm' gives the reference number in 'y' of the slowest foveation
                    optimumFoveationInThisCycle =
foveationDataFromThisCycle(y == m,:); % retrieve the data from the
slowest foveation

```

```

        end
        foveationDataOptimised = [foveationDataOptimised;
optimumFoveationInThisCycle];
        end
    end
    end
    foveationData = foveationDataOptimised; % we can now throw away the
old foveationData matrix and replace it with our new one
end

```

```

function plotmainsequence(Saccades)
% Plot #1: amplitude vs. peak velocity
subplot('position', [0.4 0.05 0.2 0.2]);
plot3(Saccades.amplitude, Saccades.peakVelocity, Saccades.duration,
'red. ');
xlabel('Amplitude (°)');
ylabel('Peak velocity (°/s)');
zlabel('Duration (ms)');
title('Saccade analysis');

% Plot #2: amplitude vs. (peak velocity * duration)
subplot('position', [0.7 0.05 0.2 0.2]);
plot(Saccades.amplitude, (Saccades.peakVelocity .* Saccades.duration),
'red. ');
xlabel('Amplitude (°)');
ylabel('Peak velocity x duration');

```

nystagmus_calc_nafx.m

```

function [nafx, tau] = nystagmus_calc_nafx(positionData, velocityData,
eyeTrackerSamplingRate, nCycles, maxDrift, maxVelocity, Foveations,
timestamp)
% Simple calculation of NAFX
% Adapted from code written by Jonathan Jacobs for OMtools

positionLimitPossibleValues = [0.5, 0.75, 1, 1.25, 1.5, 2, 2.5, 3, 3.5,
4, 5, 6];
velocityLimitPossibleValues = [4, 5, 6, 7, 8, 9, 10];

% The NAFX tau surface only allows for a fixed set of velocity and
position
% thresholds. Therefore, we need to check if we're feeding in values
that
% are available in the tau surface lookup table.

if isempty(maxDrift)
    maxDrift = max(positionLimitPossibleValues);
end
if isempty(maxVelocity)
    maxVelocity = max(velocityLimitPossibleValues);
end

if ~any(find(positionLimitPossibleValues == maxDrift)) ||
~any(find(velocityLimitPossibleValues == maxVelocity))
    fprintf('\n')
    warning('Foveation position or velocity limits are not supported by
the NAFX tau surface')
    fprintf('Rounding to the nearest available tau from the tau
surface...')

```

```

% Convert maxDrift to nearest available value in
positionLimitPossibleValues
if maxDrift < min(positionLimitPossibleValues)
    maxDrift = min(positionLimitPossibleValues);
elseif maxDrift > max(positionLimitPossibleValues)
    maxDrift = max(positionLimitPossibleValues);
end
maxDrift =
interp1(positionLimitPossibleValues,positionLimitPossibleValues,maxDrift
,'nearest');

% Convert maxVelocity to nearest available value in
velocityLimitPossibleValues
if maxVelocity < min(velocityLimitPossibleValues)
    maxVelocity = min(velocityLimitPossibleValues);
elseif maxVelocity > max(velocityLimitPossibleValues)
    maxVelocity = max(velocityLimitPossibleValues);
end
maxVelocity =
interp1(velocityLimitPossibleValues,velocityLimitPossibleValues,maxVeloc
ity,'nearest');
end

% Tau surface (version 2) as defined by Jonathan Jacobs:

tauSurface(1,:) = [33.30 33.00 33.00 33.00 33.00 33.00 33.00 33.00 33.00
33.00 33.00 33.00];
tauSurface(2,:) = [38.92 39.04 39.17 39.29 39.41 39.65 39.88 40.11 40.33
40.53 40.87 41.04];
tauSurface(3,:) = [47.14 47.24 47.33 47.42 47.52 47.70 47.88 48.06 48.24
48.41 48.75 49.09];
tauSurface(4,:) = [54.01 54.45 54.76 54.99 55.17 55.45 55.68 55.89 56.10
56.30 56.72 57.13];
tauSurface(5,:) = [61.45 61.96 62.35 62.64 62.88 63.25 63.54 63.80 64.03
64.26 64.72 65.17];
tauSurface(6,:) = [63.76 67.95 69.26 69.76 70.02 70.40 70.75 71.10 71.45
71.80 72.50 73.22];
tauSurface(7,:) = [61.96 69.08 73.20 75.60 77.02 78.45 79.10 79.50 79.82
80.12 80.69 81.26];

tau = tauSurface(velocityLimitPossibleValues == maxVelocity,
positionLimitPossibleValues == maxDrift); % get the tau value from the
tau surface based on the position and velocity criteria being applied

recordingDuration = length(positionData)/eyeTrackerSamplingRate; % in
ms

% Find all the data which exist during foveations
nFoveations = size(Foveations.startTime,2);

foveationTimestamps = [];
for i = 1 : nFoveations
    foveationTimestamps = [foveationTimestamps, find(timestamp ==
Foveations.startTime(i):find(timestamp == Foveations.endTime(i)))]];
end

foveationData.position = positionData(foveationTimestamps);
foveationData.velocity = velocityData(foveationTimestamps);

totalFoveationLength = length(foveationTimestamps); % how much foveation
data we have (in samples)

```

```

totalFoveationDuration = totalFoveationLength * 1000 /
eyeTrackerSamplingRate; % same as above, but in ms
foveationPerSecond = totalFoveationDuration / recordingDuration;
foveationPerCycle = totalFoveationDuration / nCycles;

stdPosition = nanstd(foveationData.position);
stdVelocity = nanstd(foveationData.velocity);

normfac = 0.5 / maxDrift; % normalised to SD

pooledSTD = sqrt(0.5 * ( (stdPosition)^2 + (stdVelocity * (maxDrift /
maxVelocity))^2 ));

% Check to see if enough foveation for realistic results
if foveationPerSecond <= 2000/eyeTrackerSamplingRate
    fprintf('\n')
    warning('Insufficient foveation time for reasonable NAFX analysis')
end

nafx = (1-(pooledSTD*normfac)) * (1 - exp(-foveationPerCycle/tau));

```

nystagmus_calc_noff.m

```

function [noff, timesUsedForCalculation] =
nystagmus_calc_noff(position,velocity,eyeTrackerSamplingRate,useManualOf
fset,foveationPositionConstraint,foveationVelocityConstraint,foveationMi
nDuration,foveationMaxGapToBridge>windowSize>windowStepSize>manualOffset
WindowSize)
% Calculates the Nystagmus Optimal Fixation Function (NOFF) from eye
trace data
% Version 1.0 coded by Matt J Dunn and Joost Felius 2013
%
% *** Required inputs ***
% position: vector, containing eye position data (°)
% velocity: vector, should be same length as 'position', containing eye
velocity (°/s)
% eyeTrackerSamplingRate: int, the eye tracker sampling rate (Hz)
%
% *** Optional inputs ***
% useManualOffset: boolean, set to true if you'd like to use a manual
offset in foveation position calculation
% foveationPositionConstraint: float, maximum position error in
foveation (°)
% foveationVelocityConstraint: float, maximum velocity error in
foveation (°/s)
% foveationMinDuration: int, minimum duration of a foveation (ms)
% foveationMaxGapToBridge: int, maximum gap between foveations that
should be considered as the same foveation (ms)
% windowSize: int, the size of the time window used to calculate NOFF
(ms)
% windowStepSize: int, the amount of time that the time window used to
calculate NOFF should be moved along by for each recalculation (ms)
% manualOffsetWindowSize: int, if using a manual offset, the amount of
data about the selected point that are used to calculate manualOffset
(ms)
%
% *** Outputs ***
% noff: float
% timesUsedForCalculation: vector containing the timestamps of the data
used for NOFF calculation. This may be useful if you want to visualise
the data from your eye trace that were used.

```

```

%
% For further information, see: Felius J, Fu VL, Birch EE, Hertle RW,
Jost RM and Subramanian V (2011) Quantifying nystagmus in infants and
young children: relation between foveation and visual acuity deficit.
Invest Ophthalmol Vis Sci 52: 8724-8731.

% Set defaults (if input not supplied)
% The following parameters are defined in {Felius et al. 2011}:
if ~exist('foveationPositionConstraint', 'var')
    foveationPositionConstraint = 1; % in °
end
if ~exist('foveationVelocityConstraint', 'var')
    foveationVelocityConstraint = 6; % in °/s
end
if ~exist('foveationMinDuration', 'var')
    foveationMinDuration = 7; % in ms
end
if ~exist('foveationMaxGapToBridge', 'var')
    foveationMaxGapToBridge = 35; % in ms
end
if ~exist('windowSize', 'var')
    windowSize = 4000; % in ms
end
if ~exist('windowStepSize', 'var')
    windowStepSize = 500; % in ms
end
if ~exist('manualOffsetWindowSize', 'var')
    manualOffsetWindowSize = 2000; % in ms
end

% Check whether we have the required functions available:
if ~exist('nanmedian','file')
    error('requiredRoutines:nanMedianNotFound','Cannot find nanmedian:
This function relies on the 'nanmedian' function, which is available
as part of the Statistics Toolbox or for free in 'NaN Suite',
available at http://www.mathworks.com/matlabcentral/fileexchange/6837-nan-suite')
end

% Convert everything from ms into samples:
foveationMinDuration = round(foveationMinDuration / 1000 *
eyeTrackerSamplingRate); % in samples
foveationMaxGapToBridge = round(foveationMaxGapToBridge / 1000 *
eyeTrackerSamplingRate); % in samples
windowSize = round(windowSize / 1000 * eyeTrackerSamplingRate); % in
samples
windowStepSize = round(windowStepSize / 1000 * eyeTrackerSamplingRate);
% in samples
manualOffsetWindowSize = round(manualOffsetWindowSize / 1000 *
eyeTrackerSamplingRate); % in samples

recordingDuration = length(position); % in samples

% Manual offset:
manualOffsetWindowHalfSize = round(manualOffsetWindowSize/2);
if exist('useManualOffset','var') && useManualOffset &&
recordingDuration > 2 * manualOffsetWindowHalfSize
    plot(1:recordingDuration,position)
    xlabel('Sample number')
    ylabel('Position')
    disp('Please click approximate foveation position in eye trace')
end

```

```

try
    x = 0;
    while x < manualOffsetWindowHalfSize || x > recordingDuration -
manualOffsetWindowHalfSize
        [x, y] = ginput(1); % get input from cursor
        x = round(x);
        if x < manualOffsetWindowHalfSize || x > recordingDuration -
manualOffsetWindowHalfSize
            warning('offset:invalidPointSelected','Please select a
point not within the first or last 1000ms of the recording')
        end
        end
        manualOffset = y - nanmedian(position(x -
manualOffsetWindowHalfSize : x + manualOffsetWindowHalfSize)); % in °
    catch
        warning('offset:noOffsetSelected','No manual offset selected')
        manualOffset = 0;
    end
    close(gcf);
else
    manualOffset = 0;
end

nSegments = floor((recordingDuration - windowSize) / windowStepSize +
1); % number of steps to be taken to analyse all segments

foveationDataForSegment = cell(1,nSegments); % initialise
nFoveationDataInEachSegment = zeros(1,nSegments); % initialise
for i = 1:nSegments
    segmentStart = (i - 1) * windowStepSize + 1; % segment start time
    segmentEnd = (i - 1) * windowStepSize + windowSize; % segment end
time
    medianPositionForSegment =
nanmedian(position(segmentStart:segmentEnd));
    zeroedPositionForSegment = position(segmentStart:segmentEnd) -
medianPositionForSegment + manualOffset; % position zero'ed on the
median position for segment
    foveationDataForSegment{i} = find(abs(zeroedPositionForSegment) <=
foveationPositionConstraint & abs(velocity(segmentStart:segmentEnd)) <=
foveationVelocityConstraint) + segmentStart - 1; % find foveation data
for segment based on position and velocity criteria
    foveationDataForSegment{i} = cleandata(foveationDataForSegment{i},
foveationMinDuration, foveationMaxGapToBridge); % clean up foveations
    nFoveationDataInEachSegment(i) = length(foveationDataForSegment{i});
% count number of foveation data samples in this segment; append to
record
end

foveationFraction = max(nFoveationDataInEachSegment) / windowSize; % 'p
opt' from {Feliuss et al. 2011}
noff = log(foveationFraction/(1 - foveationFraction));

bestSegmentIndex = find((nFoveationDataInEachSegment ==
max(nFoveationDataInEachSegment)),1); % get the segment index number of
the segment used for NOFF calculation
if ~isempty(bestSegmentIndex)
    timesUsedForCalculation = foveationDataForSegment{bestSegmentIndex};
% get the times of all samples used for NOFF calculation
else
    timesUsedForCalculation = []; % if no foveations were found, return
empty array
end
end

```

```

function foveationTimes = cleandata(foveationTimes,
foveationMinDuration, foveationMaxGapToBridge)
% Clean up foveation data: remove short foveations and bridge short gaps

% 1) Impose minimum foveation duration
if ~isempty(foveationTimes) % if we have detected any foveation data at
all
    x = diff(foveationTimes) ~=1; % mark the borders between non-
contiguous foveation data
    xRotated = [1, rot90(x)]; % diff() created an offset; fix this by
adding an extra element (rotate vector first to allow for this)
    y = cumsum(xRotated); % assign each contiguous group's elements a
reference number
    for i = max(y): -1 : 1 % for each group of foveation data (working
backwards to avoid deleting elements at the beginning of the array
first)
        if sum(y == i) < foveationMinDuration % find those groups with
less than the minimum required number of data to satisfy foveation...
            foveationTimes(y == i) = []; % ...and delete them
        end
    end
end

% 2) Bridge adjacent foveations
x = diff(foveationTimes) ~= 1; % mark the borders between non-contiguous
elements in the foveation data timecodes
for i = 1 : length(x)
    if x(i) % if we are at a boundary between non-contiguous elements
        timeGapBetweenFoveations = foveationTimes(i+1) -
foveationTimes(i); % calculate the time passed between foveations
        if timeGapBetweenFoveations <= foveationMaxGapToBridge
            y = foveationTimes(i); % 'y' is the first row of inputData
of our gap between foveations
            for k = y + 1 : y + timeGapBetweenFoveations - 1 % for each
line from the inputData that exists between the local foveations...
                foveationTimes(end+1) = k; %... add it to the
foveationTimes vector [IGNORE MATLAB WARNING; THIS IS THE MOST EFFICIENT
COMPUTATIONAL METHOD]
            end
        end
    end
end
end

```

nystagmus_calibration_live_eyelink.m

```

function
nystagmus_calibration_live_eyelink(eyeTrackerSamplingRate, nystagmusAxis,
calibrationPositions, subjectInitials, calibrationFileName, autoAcceptCalib
rationPosition, calibrationDuration, crossWidth, ScreenInfo, Prefs)
% Custom calibration procedure for use in subjects with nystagmus
% Version 2.0 by Matt J Dunn 2013

addpath(genpath('resources')); % must have the 'resources' subfolder
present

if ~exist('calibrationPositions', 'var')
    calibrationPositions = [0 0; -5 0; 5 0; 0 3; 0 -3]; % default
positions of the calibration targets (in degrees from centre)

```

```

end
if ~exist('calibrationDuration','var')
    calibrationDuration = 10; % number of seconds at each calibration
point
end
if ~exist('crossWidth','var')
    crossWidth = 0.1; % the width of the calibration cross (in degrees).
n.b. this is line width, so the cross length is 3x this
end
if ~exist('eyeTrackerSamplingRate','var')
    eyeTrackerSamplingRate = input('What is the sampling rate of your
eye tracker (Hz)? > ');
end
if ~exist('subjectInitials','var')
    subjectInitials = input('Please enter subject initials > ','s');
end
if ~exist('ScreenInfo','var')
    ScreenInfo.widthMm = input('What is the screen width in mm? > ');
    ScreenInfo.distance = input('How far is the subject sat from the
screen in mm? > ');
end
if ~exist('nystagmusAxis','var')
    dialogResponse = questdlg('What is nystagmus axis?','Select
nystagmus axis','Horizontal','Vertical','Don't know','Don't know');
    switch dialogResponse
        case 'Horizontal'
            nystagmusAxis = 1;
        case 'Vertical'
            nystagmusAxis = 2;
        case 'Don't know'
            nystagmusAxis = 0;
    end
end
if ~exist('autoAcceptCalibrationPosition','var')
    autoAcceptCalibrationPosition = false;
end
if ~exist('Prefs','var')
    [nystagmusAxis, Prefs.Plot, Prefs.FoveationDefinition,
Prefs.CycleDefinition, Prefs.SaccadeDefinition, Prefs.BlinkDefinition,
Prefs.General, Prefs.FilterDefinition, Prefs.Report] =
nystagmus_setanalysisdefaults;
end

%% Set up screen and EyeLink
whichScreen = max(Screen('Screens')); % set to the primary monitor
ScreenResolution = Screen('resolution', whichScreen); % retrieve info
about the screen
ScreenInfo.widthPx = ScreenResolution.width;
ScreenInfo.heightPx = ScreenResolution.height;
ScreenInfo.window = Screen('OpenWindow', whichScreen); % 'window' will
appear on screen
ScreenInfo.grey = (WhiteIndex(ScreenInfo.window) +
BlackIndex(ScreenInfo.window)) / 2; % calculate grey based on halfway
between B&W
ListenChar(2); % disable key output to MATLAB window
dummymode=0; % set to 1 to run the EL1000 in dummy mode
el=EyeLinkInitDefaults(ScreenInfo.window); % initialise EL1000
if ~EyeLinkInit(dummymode, 1)
    fprintf('EyeLink Init aborted.\n');
    shutdown;
    return;
end

```

```

EyelinkDoTrackerSetup(e1); % begin camera setup procedure for any last
minute adjustments

Eyelink('Message', 'Calibration of %s initialised. Cross width = %s
degrees', subjectInitials, num2str(crossWidth)); % send a message to the
EL1000
fprintf('\nBeginning calibration of %s', subjectInitials)

%% Grab each calibration point
nCalibrationPoints = size(calibrationPositions,1);
if nCalibrationPoints > 6 || nCalibrationPoints < 5

error('impossibleCalibration:wrongNumberOfPointsSelected', 'Calibration
system currently only works with 5 or 6 points!')
end

calibrationLocations = zeros(nCalibrationPoints,2); % initialise an array
which will hold the calibrated co-ordinates for each calibration target
for i = 1 : nCalibrationPoints % for each calibration point
    calibrationPointAccepted = false;
    while ~calibrationPointAccepted
        fprintf('\nPress 'space' to begin recording for calibration
point #i\n', i)
        awaitspacepress;
        fprintf('\nCalibrating based on target presented at (%i, %i)',
calibrationPositions(i,1), calibrationPositions(i,2))
        oculomotorsuite_drawcross(ScreenInfo.window, ScreenInfo.widthPx,
ScreenInfo.heightPx, crossWidth, calibrationPositions(i,:),
ScreenInfo.widthMm, ScreenInfo.distance);
        edfFile = strcat('calPt', num2str(i), '.edf'); % define the name
of our EDF file (must be 8 characters or less)
        oculomotorsuite_beginrecording(edfFile);
        Eyelink('Message', 'New target presented at (%i, %i)',
calibrationPositions(i,1), calibrationPositions(i,2)); % send a message
to the EL1000
        Eyelink('Message', '!V TARGET_POS TARGET (%d, %d) 1 1',
calibrationPositions(i,1) + ScreenInfo.widthPx / 2, -
calibrationPositions(i,2) + ScreenInfo.heightPx / 2); % note new target
position in EDF file
        playtone(0.1,440); % play a tone so we know the recording has
begun
        skippabledelay(calibrationDuration);
        playtone(0.1,880); % play a tone so we know the recording is
complete
        Screen('FillRect', ScreenInfo.window, ScreenInfo.grey); % fill
the screen buffer with grey
        Screen('Flip', ScreenInfo.window); % display the screen (thus
removing the fixation cross)
        oculomotorsuite_receivedatafile;
        ListenChar(0); % restore key output
        [calibrationLocation, calibrationPointAccepted] =
nystagmus_identifycalibrationlocation(edfFile, nystagmusAxis,
eyeTrackerSamplingRate, autoAcceptCalibrationPosition, Prefs);
        movefile(edfFile, strcat(subjectInitials, '_', edfFile)); % rename
the EDF file now that we can use more characters in the filename
        ListenChar(2); % disable key output to MATLAB window
        if calibrationPointAccepted
            calibrationLocations(i,:) = calibrationLocation;
        else
            warning('calibrationPointNotAccepted:userRejected', 'No
calibration determined for this location; repeating...')

```

```

        end
    end
end
shutdown; % turn off EyeLink

[CalibrationResult.xCoefficients, CalibrationResult.yCoefficients] =
nystagmus_calculatecalibration(calibrationPositions(:,1),calibrationPosi
tions(:,2),calibrationLocations(:,1),calibrationLocations(:,2),size(cali
brationPositions,1)); % perform Harris calibration

%% Export calibration file
if ~exist('calibrationFileName','var')
    calibrationFileName = inputdlg('Please specify a name for the
calibration file', 'Enter calibration file name', [1 50]);
    calibrationFileName = strcat(calibrationFileName{1},'.csv');
end
csvwrite(calibrationFileName,[CalibrationResult.xCoefficients,Calibratio
nResult.yCoefficients]); % write calibration coefficients to a CSV file
(X, Y)
fprintf('\nWritten calibration file to %s',calibrationFileName)

function awaitspacepress
% A simple function that awaits a press of the space bar before
continuing

WaitSecs(0.1); % wait a bit so we don't pick up old keypresses
spacePressed = false;
while ~spacePressed % hang the system until the space key is pressed
    [unusedVariable, unusedVariable, keyCode] = KbCheck; % check for
keypress
    if find(keyCode) == 32 % key number 32 is space bar
        spacePressed = true;
    end
end
while KbCheck % wait until user has let go of button before moving on
end

function keyCode = skippabledelay(delay)
% Provides a delay that can be skipped over by pressing any key
% Version 1.0 - 2011 by Matt J Dunn

tStop=GetSecs + delay; % time to stop waiting is decided
while GetSecs < tStop
    [keyIsDown, unusedVariable, keyCode]= KbCheck; % check the keyboard
    if keyIsDown ~= 0 % if a keypress IS detected
        return; % leave the function
    end
end

function shutdown
ListenChar(0); % restore keyboard output to MATLAB
Eyelink('Shutdown'); % switch off EL1000
Screen('CloseAll'); % close screen

```

nystagmus_cycledetection_juhola.m

```

function [positionPeaks, positionTroughs, nCycles, DebugOutput] =
nystagmus_cycledetection_juhola(inputData, nystagmusAxis,
slopeAnalysisLength, smoothingFilterCutOff, eyeTrackerSamplingRate)
slopeAnalysisLength = slopeAnalysisLength / 1000 *
eyeTrackerSamplingRate; % convert from ms to samples

eyeDirection = zeros(1,size(inputData,1)); % initialise vector which
will store the direction of eye travel for the last few samples
leastSquaresSlope = zeros(1,size(inputData,1));
for i = slopeAnalysisLength + 1 : size(inputData,1)
    % Calculate least squares regression slope for the last 100
    (default) samples:
    sumX = sum(inputData(i-slopeAnalysisLength+1:i,3));
    sumY = sum(inputData(i-slopeAnalysisLength+1:i,nystagmusAxis));
    sumXY = sum(inputData(i-slopeAnalysisLength+1:i,3) .* inputData(i-
slopeAnalysisLength+1:i,nystagmusAxis));
    sumXSquared = sum(inputData(i-slopeAnalysisLength+1:i,3) .*
inputData(i-slopeAnalysisLength+1:i,3));
    leastSquaresSlope(i) = (slopeAnalysisLength * sumXY - sumX * sumY) /
(slopeAnalysisLength * sumXSquared - sumX^2);
    eyeDirection(i) = sign(leastSquaresSlope(i)); % we don't actually
care about the slope; just whether it is positive or negative
end

% Fill in any gaps in the eyeDirection vector
for i = 2 : length(eyeDirection)
    if isnan(eyeDirection(i))
        eyeDirection(i) = eyeDirection(i-1);
    end
end

% Remove zeros from the eyeDirection vector
for i = length(eyeDirection)-1 : -1 : 1
    if eyeDirection(i) == 0
        eyeDirection(i) = eyeDirection(i+1);
    end
end

smoothingFilterCutOffInSamples = 1/smoothingFilterCutOff *
eyeTrackerSamplingRate; % convert from Hz to samples
smoothingFilterCutOffInSamples =
2*round((smoothingFilterCutOffInSamples+1)/2)-1; % round to nearest odd
number
eyeDirection = movingaverage(eyeDirection,
smoothingFilterCutOffInSamples); % filter the eyeDirection vector
eyeDirection = sign(eyeDirection); % repolarise eyeDirection values to -
1 or +1

eyeDirectionPositiveReversals = find(diff(eyeDirection) > 0); % find
times when slope changes to positive. This is an approximation; accuracy
comes from seeking for local maxima and minima (next)
eyeDirectionNegativeReversals = find(diff(eyeDirection) < 0); % find
times when slope changes to negative. This is an approximation; accuracy
comes from seeking for local maxima and minima (next)

% Assign variables for optional debug output
DebugOutput.eyeDirection = eyeDirection;
DebugOutput.leastSquaresSlope = leastSquaresSlope;

```

```

if numel(eyeDirectionPositiveReversals) < 2 ||
numel(eyeDirectionNegativeReversals) < 2 % in case of failure to find
cycles
    nCycles = 0;
    positionPeaks = [];
    positionTroughs = [];
    return
end

while eyeDirectionPositiveReversals(1) >
eyeDirectionNegativeReversals(1)
    eyeDirectionNegativeReversals(1) = []; % first negative reversal
should come later
end

while length(eyeDirectionPositiveReversals) >
length(eyeDirectionNegativeReversals)
    eyeDirectionPositiveReversals(end) = []; % equalise the number of
reversals
end
positionPeaks = zeros(length(eyeDirectionPositiveReversals),3); %
initialise
for i = 1 : length(eyeDirectionPositiveReversals)
    % Find the (first) maxima between each negative reversal of eye
position
    positionPeaks(i,:) = inputData(eyeDirectionPositiveReversals(i) +
find(inputData(eyeDirectionPositiveReversals(i):eyeDirectionNegativeReve
rsals(i),nystagmusAxis) ==
max(inputData(eyeDirectionPositiveReversals(i):eyeDirectionNegativeRever
sals(i),nystagmusAxis)),1),1:3);
end

positionTroughs = zeros(length(eyeDirectionPositiveReversals)-1,3); %
initialise
for i = 1 : length(eyeDirectionPositiveReversals)-1
    % Find the (first) minima between each positive reversal of eye
position
    positionTroughs(i,:) = inputData(eyeDirectionNegativeReversals(i) +
find(inputData(eyeDirectionNegativeReversals(i):eyeDirectionPositiveReve
rsals(i+1),nystagmusAxis) ==
min(inputData(eyeDirectionNegativeReversals(i):eyeDirectionPositiveRever
sals(i+1),nystagmusAxis)),1),1:3);
end

nCycles = size(positionTroughs,1); % the number of troughs should now
give a close estimate of the number of cycles in the recording

function outputData = movingaverage(inputData, averagingWindow)
% Simple moving average filter
% Created by Matt J Dunn July 2013

if mod(averagingWindow,2) == 0 || averagingWindow <= 1;
    error('Averaging window must be an odd number > 1');
end

nDataEitherSideOfTestedPoint = (averagingWindow - 1) / 2; % the number
of data either side of the datum being tested

```

```

outputData = nan(length(inputData),1); % initialise a vector of NaNs
for i = 1 + nDataEitherSideOfTestedPoint : length(outputData) -
nDataEitherSideOfTestedPoint
    outputData(i) = nanmean(inputData(i-
nDataEitherSideOfTestedPoint:i+nDataEitherSideOfTestedPoint));
end

```

nystagmus_identifycalibrationlocation.m

```

function [calibrationLocation, calibrationPointAccepted] =
nystagmus_identifycalibrationlocation(inputFile, nystagmusAxis,
eyeTrackerSamplingRate, autoAcceptCalibrationPosition, Prefs)
% Extract calibration point location from a nystagmus eye trace

%% Set defaults
if ~exist('nystagmusAxis','var')
    nystagmusAxis = 0;
end
if ~exist('eyeTrackerSamplingRate','var')
    eyeTrackerSamplingRate = 1000;
end
if ~exist('autoAcceptCalibrationPosition','var')
    autoAcceptCalibrationPosition = false; % set to true if doing batch
processing and want to always accept everything
end
Prefs.General.calibrationFile = 'nullcalibration'; % set calibrationFile
name to 'nullcalibration' to avoid accidentally using an existing
calibration file

if autoAcceptCalibrationPosition
    Prefs.Plot.displayFigure = false; % no need to show a figure if
we're auto-accepting the calibration location
end

%% Get metrics
[nystagmusAxis, Foveations, unusedVariable, unusedVariable, Cycles,
positionPeaks, positionTroughs, inputData] =
nystagmus_analyser(inputFile, eyeTrackerSamplingRate, nystagmusAxis,
Prefs);
nCycles = length(Cycles.startTime);

%% Prompt user
if Prefs.FoveationDefinition.findFoveations
    nFoveationsDetected = length(Foveations.startTime);
    if nFoveationsDetected >= 1
        if ~autoAcceptCalibrationPosition
            fprintf('\n\nCalibration point '%s'' complete!', inputFile)
            if nCycles > 1
                keyPressed = input('\n(A)ccept, (R)etry, use (C)entre of
waveform, (P)eak, (T)rough, (E)ntire waveform, or (M)anual override >
','s');
            else
                keyPressed = input('\n(A)ccept, (R)etry, use (E)ntire
waveform, or (M)anual override > ','s'); % if cycle detection failed,
options are limited
            end
            else % if the program is set to automatically accept the
foveation position
                keyPressed = 'a';
            end
        end
    else
end
else

```

```

if Prefs.FoveationDefinition.findFoveations
    fprintf('\nNo foveations at all were identified for calibration
point '%s'.'.', inputFile)
else
    fprintf('\nCalibration point '%s' complete.', inputFile)
end
if nCycles > 1
    keyPressed = input('\n(R)etry, use (C)entre of waveform, (P)eak,
(T)rough, (E)ntire waveform, or (M)anual override > ','s');
else
    keyPressed = input('\n(R)etry, use (E)ntire waveform, or
(M)anual override > ','s');
end
end
drawnow; % update the screen
switch keyPressed % TODO: Make the unavailable options not respond (eg
when only one cycle is found)
    case 'a'
        inputData(Foveations.startTime:Foveations.endTime);
        % Pull out times of all foveations
        allFoveationTimes = [];
        for i = 1:nFoveationsDetected
            allFoveationTimes = [allFoveationTimes,
Foveations.startTime(i):Foveations.endTime(i)];
        end
        calibrationLocation = median(inputData(allFoveationTimes,1:2));
% output the median co-ordinates all foveations
        calibrationPointAccepted = true;
    case 'm'
        % Manual override
        dataCursor = datacursormode(gcf);

set(dataCursor,'DisplayStyle','datatip','SnapToDataVertex','off','Enable
','on'); % change to 'data cursor mode'
        input('\nPlease select a reference point on the trace, and press
enter to accept > ');
        positionInfo = getCursorInfo(dataCursor); % grab info from the
cursor position
        manualOverride = positionInfo.Position(2);
        manualOverrideTime = positionInfo.Position(1); % we need to know
the time of this sample so we can find out what its other axis value is
        manualOverrideTime = round(manualOverrideTime);
        if nystagmusAxis == 1 % if the axis of nystagmus is horizontal
            calibrationLocation = [manualOverride
inputData(manualOverrideTime,2)]; % arrange the co-ordinates correctly
        elseif nystagmusAxis == 2 % if the axis of nystagmus is vertical
            calibrationLocation = [inputData(manualOverrideTime,1)
manualOverride]; % arrange the co-ordinates correctly
        end
        fprintf('Manually overridden using sample number %s\n',
num2str(manualOverrideTime))
        calibrationPointAccepted = true;
    case 'c'
        % Use centre of waveform for the calibrated axis and the total
mean position in the other axis
        if nystagmusAxis == 1 % if the axis of nystagmus is horizontal
            calibrationLocation = [nanmean(Cycles.amplitude)/2 +
nanmean(positionTroughs(:,2)), nanmean(inputData(:,2))]; % arrange the
co-ordinates correctly
        elseif nystagmusAxis == 2 % if the axis of nystagmus is vertical

```

```

        calibrationLocation = [nanmean(inputData(:,1)),
nanmean(Cycles.amplitude)/2 + nanmean(positionTroughs(:,2))]; % arrange
the co-ordinates correctly
    end
    calibrationPointAccepted = true;
case 'p'
    % Use peak of waveform for calibration (useful in pendular
nystagmus)
    calibrationLocation = mean(positionPeaks(:,1:2));
    calibrationPointAccepted = true;
case 't'
    % Use trough of waveform for calibration (useful in pendular
nystagmus)
    calibrationLocation = mean(positionTroughs(:,1:2));
    calibrationPointAccepted = true;
case 'e'
    % Use the average of the entire waveform (if all else fails)
    calibrationLocation = nanmean(inputData(:,1:2));
    calibrationPointAccepted = true;
otherwise % if the user presses 'n' (or anything else by accident),
restart the function
    calibrationLocation = [];
    calibrationPointAccepted = false;
end
close(gcf); % close graph
drawnow; % update the screen

```

noisechecking.m

```

function noisechecking
% Simple function for checking noise in EL1000 recordings
% Version 1.0 - 2012 by Matt J Dunn

addpath(genpath('resources')); % must have the 'resources' subfolder
present

conditionName = input('Please enter condition name (PHO, SCO or MES) >
','s');

try
    ListenChar(2); % disable key output to MATLAB window

    % ** Screen setup ** %
    whichScreen = max(Screen('Screens')); % set to the primary monitor
    % Retrieve info about the screen:
    screenInfo = Screen('resolution', whichScreen);
    window = Screen('OpenWindow', whichScreen); % 'window' will appear
on screen

    % ** EL1000 setup ** %
    dummymode=0; % set to 1 to run the EL1000 in dummy mode
    el=EyelinkInitDefaults(window); % initialise EL1000

    if ~EyelinkInit(dummymode, 1)
        fprintf('Eyelink Init aborted.\n');
        shutdown;
        return;
    end

    EyelinkDoTrackerSetup(el); % begin camera setup procedure for any
last minute adjustments

```

```

%
***** %
% *           Verification procedure
* %
%
***** %

    edfFile = strcat('noise', conditionName, '.edf'); % define the name
of our EDF file (must be 8 characters or less)
    eye_used = oculomotorsuite_beginrecording(edfFile);

    Eyelink('Message', 'Verification of noise under condition %s',
conditionName); % send a message to the EL1000
    fprintf('Verification of noise under condition %s\n', conditionName)

    for condition = 1:5
        switch condition
            case 1
                positionName = 'central';
            case 2
                positionName = '3° right';
            case 3
                positionName = '3° left';
            case 4
                positionName = '3° up';
            case 5
                positionName = '3° down';
        end
        fprintf('Please set model eye to %s and press any key\n',
positionName)
        Eyelink('Message', 'Model eye is currently being moved to %s',
conditionName); % send a message to the EL1000

        while KbCheck % await no keypress
        end
        while ~KbCheck % await keypress
        end
        while KbCheck % await no keypress
        end
        Eyelink('Message', 'Currently testing at %s', conditionName); %
send a message to the EL1000
        fprintf('Press a key to move on\n')
        while ~KbCheck % await keypress
        end
        while KbCheck % await no keypress
        end
    end

    Eyelink('Message', 'Noise checking complete'); % send a message to
the EL1000
    fprintf('Noise checking complete\n')

    shutdown;
catch
    shutdown;
end

```

```
function shutdown
oculomotorsuite_receivedatafile; % save the edf file
Eyelink('Shutdown'); % switch off EL1000
Screen('CloseAll'); % close screen
ListenChar(0); % restore keyboard output to MATLAB
```

oculomotorsuite_beginrecording.m

```
function eye_used = oculomotorsuite_beginrecording(edfFile)
% Start an EL1000 recording session
% Adapted from code written by SR Research

Eyelink('Command', 'link_sample_data = LEFT,RIGHT,GAZE,AREA'); % define
which data to record to EDF file
Eyelink('Openfile', edfFile); % open the EDF file
Eyelink('StartRecording');
fprintf('\nOpening new recording file '%s'\n', edfFile)
WaitSecs(0.1); % record a few samples before we actually start
displaying mark zero-plot time in data file
Eyelink('Message', 'SYNCTIME'); % we know that we are live once we have
the 'SYNCTIME' message
eye_used = -1; % -1 means we don't yet know which eye we're tracking
```

oculomotorsuite_degrees2px.m

```
function pixels = oculomotorsuite_degrees2px(degrees, screenWidth_mm,
screenWidth_px, distanceFromScreen_mm)
% Converts degrees into pixels
% Version 1.1 - 2011-2013 by Matt J Dunn

millimetres = distanceFromScreen_mm * tand(degrees); % to convert from
degrees to size of area on screen, use trigonometry
sizeOfOnePixel = screenWidth_mm / screenWidth_px; % this gives the size
of one pixel in mm
pixels = millimetres / sizeOfOnePixel; % finally, multiply mm by px/mm
to get px
```

oculomotorsuite_drawcross.m

```
function crossPositionPx = oculomotorsuite_drawcross(window,
screenWidthPx, screenHeightPx, crossWidthDegrees, crossPositionDegrees,
screenWidthMm, screenDistanceMm, crossColour)
% Draw a fixation cross in a given position on screen
% Version 1.0 - 2011 by Matt J Dunn
% n.b. 'crossPosition' and 'crossPositionPx' are relative to the centre
of
% the screen. i.e. the returned value crossPositionPx is NOT the actual
% pixel co-ordinates of the cross, but the displacement from screen
centre

if ~exist('crossColour','var')
    crossColour = 0; % black
end

crossWidthPx = round(oculomotorsuite_degrees2px(crossWidthDegrees,
screenWidthMm, screenWidthPx, screenDistanceMm)); % convert the
crossWidth from degrees to px
crossPositionPx = round(oculomotorsuite_degrees2px(crossPositionDegrees,
screenWidthMm, screenWidthPx, screenDistanceMm)); % convert the
crossPosition from degrees to px

% Prepare the cross:
```

```

Screen(window, 'FillRect', crossColour, [(screenWidthPx/2 +
crossPositionPx(1) - crossWidthPx - crossWidthPx / 2)
(screenHeightPx/2 - crossPositionPx(2) - crossWidthPx / 2) % n.b.
the Y position is minus due to wanting positive to be up
(screenWidthPx/2 + crossPositionPx(1) + crossWidthPx + crossWidthPx
/ 2)
(screenHeightPx/2 - crossPositionPx(2) + crossWidthPx / 2)]); % the
horizontal bar of the cross
Screen(window, 'FillRect', crossColour, [(screenWidthPx/2 +
crossPositionPx(1) - crossWidthPx / 2)
(screenHeightPx/2 - crossPositionPx(2) - crossWidthPx - crossWidthPx
/ 2)
(screenWidthPx/2 + crossPositionPx(1) + crossWidthPx / 2)
(screenHeightPx/2 - crossPositionPx(2) + crossWidthPx + crossWidthPx
/ 2)]); % the vertical bar of the cross

Screen('Flip', window); % actually display the screen

```

oculomotorsuite_findsaccades_behrens.m

```

function Saccades = oculomotorsuite_findsaccades_behrens(position,
velocity, acceleration, eyeTrackerSamplingRate,
standardDeviationsInNSigma)
% Saccade detection algorithm as described in Behrens, MacKeben and
Schröder-Preikschat (2010)
% Coded in MATLAB by Matt J Dunn 2012
% Variable names are as set out in the paper; hence a little more
cryptic than my usual code. See the paper or my comments at
initialisation

if ~exist('standardDeviationsInNSigma', 'var')
    standardDeviationsInNSigma = 3.4; % 3.4 comes from Behrens, MacKeben
and Schröder-Preikschat (2010)
end

durationToCalculateNSigmaFrom = 200; % 200 ms comes from Behrens,
MacKeben and Schröder-Preikschat (2010)
% Note: NSigma is a dynamically-set acceleration threshold for saccade
detection. Under certain circumstances, NSigma is ignored (see paper)
minMonophasicSaccadeDuration = 100; % 100 ms comes from Behrens,
MacKeben and Schröder-Preikschat (2010)
saccadeAccelerationThresholdIncrement = 1; % how much to linearly
increase saccadeAccelerationThreshold (per sample) when returning to
NSigma. This is *not* given in the paper - contact the author

minMonophasicSaccadeDuration = round(minMonophasicSaccadeDuration / 1000
* eyeTrackerSamplingRate); % convert from ms to samples
durationToCalculateNSigmaFrom = round(durationToCalculateNSigmaFrom /
1000 * eyeTrackerSamplingRate); % convert from ms to samples

% The debugTraces can be uncommented and set as an output for debugging
the saccade detector script if for some reason it isn't working:
%debugTraces.saccadeAccelerationThreshold = zeros(length(position), 1);
%debugTraces.NSigma = zeros(length(position), 1);
%debugTraces.MSF = zeros(length(position), 1);
%debugTraces.FmonE = zeros(length(position), 1);
%debugTraces.saccadeDirection = zeros(length(position), 1);

MSF = 0; % membership function; when ~= 0, indicates saccade is taking
place
previousSaccadeEndTime = 0;

```

```

F1 = false; % flag set when the acceleration drops below the threshold
after the initial spike
F2 = false; % indicates a saccade is biphasic
EmonE = false; % marks the end of the monotonic function in the position
trace
positionSinceF1 = []; % record the position trace after F1 is true: used
to determine monotonicity
modifiedThresholdIsRising = false; % following the 200 msec period after
the saccade, threshold acceleration is linearly increased until it
intersects with NSigma
saccadeAccelerationThreshold = 0;

nSamplesInEntireEyeTrace = length(position);
Saccades.startTime = zeros(nSamplesInEntireEyeTrace, 1);
Saccades.endTime = zeros(nSamplesInEntireEyeTrace, 1);
Saccades.direction = zeros(nSamplesInEntireEyeTrace, 1);
Saccades.duration = zeros(nSamplesInEntireEyeTrace, 1);
Saccades.meanVelocity = zeros(nSamplesInEntireEyeTrace, 1);
Saccades.peakVelocity = zeros(nSamplesInEntireEyeTrace, 1);
Saccades.amplitude = zeros(nSamplesInEntireEyeTrace, 1);

listPtr = 1; % keeps track of how far through saccade list we are; used
to save memory when processing saccades

for i = durationToCalculateNSigmaFrom + 1 : nSamplesInEntireEyeTrace %
run through each sample of the input data, starting @ #201 (to allow
calculation of NSigma)
    % Set NSigma based on the preceding samples' acceleration data:
    NSigma = mean(abs(acceleration(i-durationToCalculateNSigmaFrom:i))
+ standardDeviationsInNSigma * nanstd(abs(acceleration(i-
durationToCalculateNSigmaFrom:i)))));
    % NOTE: In the above, why does it use mean and not median?!
    if MSF == 0
        if previousSaccadeEndTime <= i - durationToCalculateNSigmaFrom %
if we're far enough after a saccade to calculate a new NSigma...
            if modifiedThresholdIsRising
                saccadeAccelerationThreshold =
saccadeAccelerationThreshold + saccadeAccelerationThresholdIncrement;
                if saccadeAccelerationThreshold >= NSigma
                    modifiedThresholdIsRising = false;
                end
            else
                saccadeAccelerationThreshold = NSigma;
            end
        end
        if abs(acceleration(i)) >= saccadeAccelerationThreshold
            saccadeDirection = sign(acceleration(i)); % make a note of
the sign of the acceleration spike; we need to know so we know where to
look for the deceleration
            MSF = 1;
            saccadeStartTime = i;
        end
    end
    if MSF == 1 && abs(acceleration(i)) < saccadeAccelerationThreshold %
if acceleration falls below the threshold again
        F1 = true; % then we need to start looking at the position trace
for a monotonic function
    end
    if F1
        if ~F2

```

```

        if (saccadeDirection == 1 && acceleration(i) <= -
saccadeAccelerationThreshold)...
            || (saccadeDirection == -1 && acceleration(i) >=
+saccadeAccelerationThreshold) % if the acceleration transform exceeds
the threshold in the opposite direction to the initial spike
            MSF = -1;
            F2 = true; % indicates saccade is biphasic
        end
    end
    if ~FmonE
        positionSinceF1 = [positionSinceF1, position(i)]; % keep
track of the position since the F1
        % If the position shows a non-monotonic function since the
start of the saccade:
        differentialOfPositionSinceF1 = diff(positionSinceF1); %
used to calculate whether positionSinceF1 is monotonic
        if ~(all(differentialOfPositionSinceF1 > 0) ||
all(differentialOfPositionSinceF1 < 0))
            % n.b. I am looking for strongly monotonic functions,
rather than weak (hence > | < rather than >= | <=). The paper doesn't
specify
            FmonE = true;
        end
    end
    %debugTraces.FMonE(i) = FmonE;
    %debugTraces.MSF(i) = MSF;
    %debugTraces.saccadeDirection(i) = saccadeDirection;
    if FmonE
        if (saccadeDirection == 1 && acceleration(i) > -
saccadeAccelerationThreshold)...
            || (saccadeDirection == -1 && acceleration(i) <
+saccadeAccelerationThreshold) % saccade end is only if both these are
satisfied
                saccadeEndTime = i;
                countsS = saccadeEndTime - saccadeStartTime;
                if countsS < minMonophasicSaccadeDuration && ~F2 % if
saccade is short and monophasic...
                    % ...then it is an artefact and is discarded
                else % otherwise, record it
                    Saccades.startTime(listPtr) = saccadeStartTime;
                    Saccades.endTime(listPtr) = saccadeEndTime;
                    Saccades.direction(listPtr) = saccadeDirection;
                    Saccades.duration(listPtr) = saccadeEndTime -
saccadeStartTime;
                    Saccades.meanVelocity(listPtr) =
nanmean(abs(velocity(saccadeStartTime:saccadeEndTime)));
                    Saccades.peakVelocity(listPtr) =
max(abs(velocity(saccadeStartTime:saccadeEndTime)));
                    Saccades.amplitude(listPtr) =
max(position(saccadeStartTime:saccadeEndTime)) -
min(position(saccadeStartTime:saccadeEndTime));
                    listPtr = listPtr + 1;

                    previousSaccadeEndTime = saccadeEndTime;
                    modifiedThresholdIsRising = true;
                end
                % reset MSF and all flags
                MSF = 0;
                F1 = false;
                F2 = false;
                FmonE = false;
                positionSinceF1 = [];
    end

```

```

        end
    end
    end
    %debugTraces.NSigma(i) = NSigma;
    %debugTraces.saccadeAccelerationThreshold(i) =
saccadeAccelerationThreshold;
end

```

```

% Clear up unused saccade data slots:
Saccades.startTime(listPtr:end,:) = [];
Saccades.endTime(listPtr:end,:) = [];
Saccades.direction(listPtr:end,:) = [];
Saccades.duration(listPtr:end,:) = [];
Saccades.meanVelocity(listPtr:end,:) = [];
Saccades.peakVelocity(listPtr:end,:) = [];
Saccades.amplitude(listPtr:end,:) = [];

```

oculomotorsuite_findsaccades_dunn.m

```

function [Saccades, saccadeVelocityThreshold] =
oculomotorsuite_findsaccades_dunn(position, velocity, acceleration,
standardDeviationsForVelocityThreshold)
% Saccade detector for use in nystagmus data
% position, velocity and acceleration should all be vectors of the same
length
% Version 1.0 - 2013 by Matt J Dunn

% NOTE: This could be improved: find acceleration peaks/troughs first
% (using acceleration threshold set as a function of the mean or
median).
% Then, find which peaks/troughs belong together. Use a reasonable time
% limit to determine which belong to the same saccade

% Initialise output struct:
Saccades =
struct('startTime', [], 'endTime', [], 'duration', [], 'meanVelocity', [], 'peak
Velocity', [], 'amplitude', [], 'direction', []);

velocityStandardDeviation = nanstd(velocity);
accelerationStandardDeviation = nanstd(acceleration);
if velocityStandardDeviation == 0 || accelerationStandardDeviation == 0
    warning('poorData:noVariationInVelocityOrAcceleration', 'No changes
in eye position detected in recording! Aborting...')
    return;
end

if ~exist('standardDeviationsForVelocityThreshold', 'var')
    standardDeviationsForVelocityThreshold = 1;
end

saccadeVelocityThreshold = (standardDeviationsForVelocityThreshold *
velocityStandardDeviation) + nanmean(abs(velocity));

recordingLength = length(position);

% Find saccades by finding peaks of the velocity with the 'peakdet'
function
[velocityPeaks velocityTroughs] = peakdet(velocity,
velocityStandardDeviation, 1:recordingLength);
velocitySpikes = sortrows([velocityPeaks; velocityTroughs]); % combine
into one array

```

```

% Find the start and end of those saccades by finding peaks of the
acceleration transform
[accelerationPeaks accelerationTroughs] = peakdet(acceleration,
accelerationStandardDeviation, 1:recordingLength);
accelerationSpikes = sortrows([accelerationPeaks; accelerationTroughs]);
% combine into one array
% We now have a list of all the times that velocity spikes (probably
saccades) occurred, as well as
% acceleration spikes (their start and finish times).

if isempty(accelerationPeaks)
    warning('poorData:noAccelerationData','No eye acceleration data
detected in recording! Aborting...')
    return;
end

for i = 1 : size(velocitySpikes,1) - 1
    % If a peak/trough exceeds the saccade threshold; we haven't gone
past the end of the data; and the peak/trough isn't at the very
beginning of the data:
    if abs(velocitySpikes(i,2)) > saccadeVelocityThreshold &&
~isempty(find(accelerationSpikes(:,1) > velocitySpikes(i,1), 1)) &&
~isempty(find(accelerationSpikes(:,1) < velocitySpikes(i,1), 1))
        if velocitySpikes(i,2) > 0 % positive velocity spike indicates a
right or upward saccade
            saccadeDirection = 1;
        else
            saccadeDirection = -1;
        end
        % Now we find the start and end of the saccade, using
acceleration spikes:
        saccadeAccelerationStartTime = find(accelerationSpikes(:,1) <
velocitySpikes(i,1), 1, 'last'); % this gives the position in
accelerationSpikes of the saccade acceleration start time
        saccadeAccelerationEndTime = find(accelerationSpikes(:,1) >
velocitySpikes(i,1), 1); % this gives the position in accelerationSpikes
of the saccade acceleration end time
        saccadeAccelerationStartTime =
accelerationSpikes(saccadeAccelerationStartTime,1); % this gives the
sample number of the saccade acceleration start
        saccadeAccelerationEndTime =
accelerationSpikes(saccadeAccelerationEndTime,1); % this gives the
sample number of the saccade acceleration end

        % Now we find the start and end of the saccade, according to the
monotonicity of the position vector:
        positionPtr = velocitySpikes(i,1); % set to index of the saccade
peak
        % We start by finding the beginning of monotonicity, by working
backwards from the saccade peak.
        % n.b. we look for a *strictly* monotonic function
        while positionPtr > 1
            lastTestedPosition = position(positionPtr);
            positionPtr = positionPtr - 1;
            currentTestedPosition = position(positionPtr);
            differenceBetweenPositions = diff([lastTestedPosition
currentTestedPosition]);
            if (saccadeDirection == 1 && differenceBetweenPositions > 0)
|| (saccadeDirection == -1 && differenceBetweenPositions < 0)
                break;
            end
        end
    end
end

```

```

end % when this loop ends, we have left monotonicity or have
disappeared off the end of the eye trace
saccadeMonotonicityStartTime = positionPtr + 1;

% Repeat the above, but to find the *end* of monotonicity this
time:
positionPtr = velocitySpikes(i,1); % set to index of the saccade
peak
while positionPtr < length(position)-1
    lastTestedPosition = position(positionPtr);
    positionPtr = positionPtr + 1;
    currentTestedPosition = position(positionPtr);
    differenceBetweenPositions = diff([lastTestedPosition
currentTestedPosition]);
    if (saccadeDirection == 1 && differenceBetweenPositions < 0)
|| (saccadeDirection == -1 && differenceBetweenPositions > 0)
        break;
    end
end
saccadeMonotonicityEndTime = positionPtr - 1;

% At this point, we have saccade start and end times defined in
two
% ways: by monotonicity of the position vector, and by the peaks
% and troughs of the acceleration transform. We use the most
distal
% of these to define the saccade.
if saccadeMonotonicityStartTime <= saccadeAccelerationStartTime
    saccadeStartIndex = saccadeMonotonicityStartTime;
else
    saccadeStartIndex = saccadeAccelerationStartTime;
end

if saccadeMonotonicityEndTime >= saccadeAccelerationEndTime
    saccadeEndIndex = saccadeMonotonicityEndTime;
else
    saccadeEndIndex = saccadeAccelerationEndTime;
end

if ~any(isnan(position(saccadeStartIndex:saccadeEndIndex))) %
check whether we have any dropped data between start and end. Only
continue if we don't.
    % Keep track of the timestamps of saccades so that later on
we are able to work out metrics of the slow phases by process of
elimination
    Saccades.startTime = [Saccades.startTime,
saccadeStartIndex];
    Saccades.endTime = [Saccades.endTime, saccadeEndIndex];

% Saccadic amplitude, duration and mean/peak velocity are
calculated:
saccadeDuration = saccadeEndIndex - saccadeStartIndex; % in
samples
saccadeMeanVelocity =
nanmean(abs(velocity(saccadeStartIndex:saccadeEndIndex))); % in °/s
saccadePeakVelocity =
max(abs(velocity(saccadeStartIndex:saccadeEndIndex))); % in °/s
saccadeAmplitude = abs(position(saccadeEndIndex) -
position(saccadeStartIndex)); % in °

% Now, add the above metrics to the saccade data arrays

```

```

        Saccades.duration = [Saccades.duration saccadeDuration];
        Saccades.meanVelocity = [Saccades.meanVelocity
saccadeMeanVelocity];
        Saccades.peakVelocity = [Saccades.peakVelocity
saccadePeakVelocity];
        Saccades.amplitude = [Saccades.amplitude saccadeAmplitude];
        Saccades.direction = [Saccades.direction saccadeDirection];
    end
end
end

```

oculomotorsuite_generatecompleteeyetracearray.m

```

function data =
oculomotorsuite_generatecompleteeyetracearray(data, averagingWindow, eyeTrackerSamplingRate, useSingleAxis, axisToUse)
% Convert eye position data to an array with the following columns:
% X pos, Y pos, Timestamp, Velocity, Acceleration
% Created August 2013 by Matt J Dunn
% data should be a two column array with X and Y position

if ~exist('useSingleAxis', 'var')
    useSingleAxis = false;
end

data(:,3) = 1:(size(data,1)); % generate timestamp column, starting at
one. n.b. this is in samples; not ms

fprintf('\nCalculating velocity profile...')
if useSingleAxis % if we're only going to use one axis of the data...
    data(:,4) = oculomotorsuite_datadifferentiator(data(:,axisToUse),
averagingWindow) * eyeTrackerSamplingRate; % take the differential of
the combined nystagmus axis position data and apply it to column 4
    % n.b. we multiply by eyeTrackerSamplingRate since our velocities
    % should be defined in seconds, not samples
else
    data(:,4) = oculomotorsuite_datadifferentiator(data(:,1:2),
averagingWindow) * eyeTrackerSamplingRate; % take the differential of
the combined (X,Y) position and apply it to column 4
end

fprintf('\nCalculating acceleration profile...')
data(:,5) = oculomotorsuite_datadifferentiator(data(:,4),
averagingWindow) * eyeTrackerSamplingRate; % take the differential of
the velocity and apply it to column 5

```

oculomotorsuite_lowpassfilter.m

```

function filteredData = oculomotorsuite_lowpassfilter(inputData, order,
cutoff, eyeTrackerSamplingRate)
% Low pass filter for eye movement position data
% Created by Matt J Dunn in 2012

try
    nyquistFrequency = eyeTrackerSamplingRate/2; % find the Nyquist
frequency
    [b,a] = butter(order, cutoff/nyquistFrequency); % define the filter
    % [b,a] = besself(order, cutoff/nyquistFrequency); % maybe use a
    Bessel filter instead?

    timestampsOfNans = isnan(inputData); % find the timestamps of NaNs

```

```

    inputData = interpolatenans(inputData); % replace NaNs with
interpolated data (filters can't handle NaNs)
    filteredData = filtfilt(b,a,inputData); % filter the data
    filteredData(timestampsOfNans) = NaN; % replace the NaNs back into
the vector
catch
    warning('filterFailed:unableToFilterData','Unable to low pass filter
data. Perhaps you don't have the MATLAB Signal Processing Toolbox?
Continuing using unfiltered data...')
    filteredData = inputData;
end

```

```

function data = interpolatenans(data)
nanPositions = isnan(data);
t = 1:numel(data);
data(nanPositions) = interp1(t(~nanPositions), data(~nanPositions),
t(nanPositions));

```

oculomotorsuite_px2degrees.m

```

function degrees = oculomotorsuite_px2degrees(pixels, screenWidth_mm,
screenWidth_px, distanceFromScreen_mm)
% Converts pixels into degrees
% Version 1.1 - 2011-2013 by Matt J Dunn

sizeOfOnePixel = screenWidth_mm / screenWidth_px;
millimetres = pixels * sizeOfOnePixel;
degrees = atand(millimetres / distanceFromScreen_mm);

```

oculomotorsuite_removeblinks.m

```

function [data, nBlinks] = oculomotorsuite_removeblinks(data,
ColumnNumbers, removeOutliers,
numberOfStandardDeviationsAboveMedianForOutlier)
% Detect and remove blinks from an eye position trace
% Created in 2012 by Matt J Dunn

% Obviously when the eyes are closed, there is no input signal anyway.
% However, we want to remove the eye movements and pupil artefacts
% associated with blinks; i.e. those movements that occur just before
and
% after the data drop.

% Input 'data' should be a n x 5 matrix with the format:
% [x y timestamp velocity acceleration]

% If removeOutliers is true, we also consider large deviations in
position
% or velocity to be blinks. This is useful if using data that never cuts
% out, such as EOG or IR limbal trackers.
%
% The output 'data' is the same as the input 'data', but with blinks
% replaced with NaNs (except the timestamps)

if ~exist('removeOutliers', 'var')
    removeOutliers = false;
end

if ~exist('numberOfStandardDeviationsAboveMedianForOutlier', 'var')
    numberOfStandardDeviationsAboveMedianForOutlier = 5;

```

```

end

% Get 'normal' values for the dataset so we can work out what is unusual
% (and probably constitutes a blink-associated eye movement)
% n.b. There is *some* assumption here
NormativeData.medianXPosition =
nanmedian(data(:,ColumnNumbers.xPosition)); % get median X position
NormativeData.medianYPosition =
nanmedian(data(:,ColumnNumbers.yPosition)); % get median Y position
NormativeData.stdXPosition = nanstd(data(:,ColumnNumbers.xPosition)); %
...and SD
NormativeData.stdYPosition = nanstd(data(:,ColumnNumbers.yPosition)); %
..."
if any(strcmp('xVelocity',fieldnames(ColumnNumbers))) % if 'data' has
velocity and acceleration separated into X and Y
    velocityIsSplitIntoTwoColumns = true;
    NormativeData.medianXVelocity =
nanmedian(abs(data(:,ColumnNumbers.xVelocity))); % get median X velocity
    NormativeData.medianYVelocity =
nanmedian(abs(data(:,ColumnNumbers.yVelocity))); % get median Y velocity
    NormativeData.stdXVelocity =
nanstd(abs(data(:,ColumnNumbers.xVelocity))); % ...and SD
    NormativeData.stdYVelocity =
nanstd(abs(data(:,ColumnNumbers.yVelocity))); % ..."
    NormativeData.medianXAcceleration =
nanmedian(abs(data(:,ColumnNumbers.xAcceleration))); % get median X
acceleration
    NormativeData.medianYAcceleration =
nanmedian(abs(data(:,ColumnNumbers.yAcceleration))); % get median Y
acceleration
    NormativeData.stdXAcceleration =
nanstd(abs(data(:,ColumnNumbers.xAcceleration))); % ...and SD
    NormativeData.stdYAcceleration =
nanstd(abs(data(:,ColumnNumbers.yAcceleration))); % ..."
else % otherwise we assume that there is just a single 'velocity' field
    velocityIsSplitIntoTwoColumns = false;
    NormativeData.medianVelocity =
nanmedian(abs(data(:,ColumnNumbers.velocity))); % get median velocity
    NormativeData.stdVelocity =
nanstd(abs(data(:,ColumnNumbers.velocity))); % ...and SD
    NormativeData.medianAcceleration =
nanmedian(abs(data(:,ColumnNumbers.acceleration))); % get median
acceleration
    NormativeData.stdAcceleration =
nanstd(abs(data(:,ColumnNumbers.acceleration))); % ...and SD
end

if removeOutliers
    outlierTimes = find(data(:,ColumnNumbers.xPosition) >
NormativeData.medianXPosition +
numberOfStandardDeviationsAboveMedianForOutlier *
NormativeData.stdXPosition); % find X axis outliers
    outlierTimes = [outlierTimes; find(data(:,ColumnNumbers.yPosition) >
NormativeData.medianYPosition +
numberOfStandardDeviationsAboveMedianForOutlier *
NormativeData.stdYPosition)]; % add on Y axis outliers
    if velocityIsSplitIntoTwoColumns
        outlierTimes = [outlierTimes;
find(data(:,ColumnNumbers.xVelocity) > NormativeData.medianXVelocity +
numberOfStandardDeviationsAboveMedianForOutlier *
NormativeData.stdXVelocity)]; % add on X velocity outliers
    end
end

```

```

        outlierTimes = [outlierTimes;
find(data(:,ColumnNumbers.yVelocity) > NormativeData.medianYVelocity +
numberOfStandardDeviationsAboveMedianForOutlier *
NormativeData.stdYVelocity)]; % add on X velocity outliers
    else
        outlierTimes = [outlierTimes;
find(data(:,ColumnNumbers.velocity) > NormativeData.medianVelocity +
numberOfStandardDeviationsAboveMedianForOutlier *
NormativeData.stdVelocity)]; % add on velocity outliers
    end
    data(outlierTimes,ColumnNumbers.xPosition) = NaN;
    data(outlierTimes,ColumnNumbers.yPosition) = NaN;
    if velocityIsSplitIntoTwoColumns
        data(outlierTimes,ColumnNumbers.xVelocity) = NaN;
        data(outlierTimes,ColumnNumbers.yVelocity) = NaN;
        data(outlierTimes,ColumnNumbers.xAcceleration) = NaN;
        data(outlierTimes,ColumnNumbers.yAcceleration) = NaN;
    else
        data(outlierTimes,ColumnNumbers.velocity) = NaN;
        data(outlierTimes,ColumnNumbers.acceleration) = NaN;
    end
end
end

droppedDataTimes = find(isnan(data(:,1))); % find times when data was
lost
% We assume that if no X position value was recorded, then the eyes were
% closed. It is possible that the eyes weren't tracked due to some other
% reason, but in any case we're only reducing the amount of data that is
% analysed later, so some false positives won't change reliability of
% the output.

if isempty(droppedDataTimes)
    nBlinks = 0;
else % if there were dropped data
    x = rot90(diff(droppedDataTimes) ~=1); % mark the borders between
non-contiguous dropped data times
    y = [1, cumsum(x) + 1]; % assign each contiguous group's elements a
reference number
    nBlinks = max(y);

    % We now go through the times before and after each blink and
iteratively
    % delete the data rows until we end up with velocities within a SD
of the
    % median both before and after
    for i = 1 : nBlinks % for each group of dropped data
        timeBeforeBlink = droppedDataTimes(find(y == i, 1, 'first')) -
1; % get the timestamp JUST BEFORE the blink began
        lookingBeforeBlink = true; % we are first interested in removing
abnormal data before the blink
        data = removedatabeforeorafterblink(lookingBeforeBlink, data,
timeBeforeBlink, NormativeData, ColumnNumbers,
velocityIsSplitIntoTwoColumns); % remove the data prior to the blink
iteratively until we return to 'normal' values
        timeAfterBlink = droppedDataTimes(find(y == i, 1, 'last')) + 1;
% get the timestamp JUST AFTER the blink ended
        lookingBeforeBlink = false; % we are now looking after the blink
        data = removedatabeforeorafterblink(lookingBeforeBlink, data,
timeAfterBlink, NormativeData, ColumnNumbers,
velocityIsSplitIntoTwoColumns); % remove the data after the blink
iteratively until we return to 'normal' values
    end
end

```

end

```

function data = removedatabeforeorafterblink(lookingBeforeBlink, data,
timeBeforeOrAfterBlink, NormativeData, ColumnNumbers,
velocityIsSplitIntoTwoColumns)
% This is defined as a function as we do it for data before a blink, and
% then again for data after a blink. The only difference is in the first
% condition, we move backwards through the dataset (from the blink),
% whereas after the blink, we are parsing forwards
if lookingBeforeBlink
    eitherPlusOrMinusOne = -1; % if we're looking before the blink, we
need to work backwards through the data
else
    eitherPlusOrMinusOne = 1; % ...otherwise its forwards for after
blinks
end
if timeBeforeOrAfterBlink == 0 || timeBeforeOrAfterBlink >
size(data,ColumnNumbers.xPosition) % if we are trying to remove data
before the beginning or after the end of the dataset
    return; % don't make any changes
else
    positionXBeforeOrAfterBlink =
data(timeBeforeOrAfterBlink,ColumnNumbers.xPosition); % find X position
at that time
    positionYBeforeOrAfterBlink =
data(timeBeforeOrAfterBlink,ColumnNumbers.yPosition); % find X position
at that time
    if velocityIsSplitIntoTwoColumns
        velocityXBeforeOrAfterBlink =
abs(data(timeBeforeOrAfterBlink,ColumnNumbers.xVelocity)); % find the
absolute X velocity at that time
        accelerationXBeforeOrAfterBlink =
abs(data(timeBeforeOrAfterBlink,ColumnNumbers.xAcceleration)); % find
the absolute X acceleration at that time
        velocityYBeforeOrAfterBlink =
abs(data(timeBeforeOrAfterBlink,ColumnNumbers.yVelocity)); % find the
absolute X velocity at that time
        accelerationYBeforeOrAfterBlink =
abs(data(timeBeforeOrAfterBlink,ColumnNumbers.yAcceleration)); % find
the absolute X acceleration at that time
    else
        velocityBeforeOrAfterBlink =
abs(data(timeBeforeOrAfterBlink,ColumnNumbers.velocity)); % find the
absolute velocity at that time
        accelerationBeforeOrAfterBlink =
abs(data(timeBeforeOrAfterBlink,ColumnNumbers.acceleration)); % find the
absolute acceleration at that time
    end
    if velocityIsSplitIntoTwoColumns
        while any(positionXBeforeOrAfterBlink <
(NormativeData.medianXPosition - NormativeData.stdXPosition))... % wait
for X position to be above a SD below the median
            || positionYBeforeOrAfterBlink <
(NormativeData.medianYPosition - NormativeData.stdYPosition)... % wait
for Y position to be above a SD below the median
            || any(positionXBeforeOrAfterBlink >
(NormativeData.medianXPosition + NormativeData.stdXPosition))... % ...
and below a SD above the median
            || any(positionYBeforeOrAfterBlink >
(NormativeData.medianYPosition + NormativeData.stdYPosition))... % ...
and below a SD above the median
        end
    end
end

```

```

        || velocityXBeforeOrAfterBlink >
(NormativeData.medianXVelocity)... % we wait for X velocity to get back
to median (ignoring SD)
        || velocityYBeforeOrAfterBlink >
(NormativeData.medianYVelocity)... % we wait for Y velocity to get back
to median (ignoring SD)
        || accelerationXBeforeOrAfterBlink >
(NormativeData.medianXAcceleration)... % we wait for X acceleration to
get back to median (ignoring SD)
        || accelerationYBeforeOrAfterBlink >
(NormativeData.medianYAcceleration)... % we wait for Y acceleration to
get back to median (ignoring SD)
        || any(isnan(positionXBeforeOrAfterBlink))...
        || any(isnan(positionYBeforeOrAfterBlink))

data(timeBeforeOrAfterBlink,ColumnNumbers.xPosition) = NaN;
data(timeBeforeOrAfterBlink,ColumnNumbers.yPosition) = NaN;
data(timeBeforeOrAfterBlink,ColumnNumbers.xVelocity) = NaN;
data(timeBeforeOrAfterBlink,ColumnNumbers.yVelocity) = NaN;
data(timeBeforeOrAfterBlink,ColumnNumbers.xAcceleration) =
NaN;
data(timeBeforeOrAfterBlink,ColumnNumbers.yAcceleration) =
NaN;

timeBeforeOrAfterBlink = timeBeforeOrAfterBlink +
eitherPlusOrMinusOne;
if timeBeforeOrAfterBlink == 0 || timeBeforeOrAfterBlink >
size(data,1) % if we are trying to remove data before the beginning or
after the end of the dataset
return; % don't make any changes
else
positionXBeforeOrAfterBlink =
data(timeBeforeOrAfterBlink,ColumnNumbers.xPosition); % find X position
at that time
positionYBeforeOrAfterBlink =
data(timeBeforeOrAfterBlink,ColumnNumbers.yPosition); % find Y position
at that time
velocityXBeforeOrAfterBlink =
abs(data(timeBeforeOrAfterBlink,ColumnNumbers.xVelocity)); % find the
absolute X velocity at that time
velocityYBeforeOrAfterBlink =
abs(data(timeBeforeOrAfterBlink,ColumnNumbers.yVelocity)); % find the
absolute Y velocity at that time
accelerationXBeforeOrAfterBlink =
abs(data(timeBeforeOrAfterBlink,ColumnNumbers.xAcceleration)); % find
the absolute X acceleration at that time
accelerationYBeforeOrAfterBlink =
abs(data(timeBeforeOrAfterBlink,ColumnNumbers.yAcceleration)); % find
the absolute Y acceleration at that time
end
end
else
while any(positionXBeforeOrAfterBlink <
(NormativeData.medianXPosition - NormativeData.stdXPosition))... % wait
for X position to be above a SD below the median
|| positionYBeforeOrAfterBlink <
(NormativeData.medianYPosition - NormativeData.stdYPosition)... % wait
for Y position to be above a SD below the median
|| any(positionXBeforeOrAfterBlink >
(NormativeData.medianXPosition + NormativeData.stdXPosition))... % ...
and below a SD above the median

```

```

        || any(positionYBeforeOrAfterBlink >
(NormativeData.medianYPosition + NormativeData.stdYPosition))... % ...
and below a SD above the median
        || velocityBeforeOrAfterBlink >
(NormativeData.medianVelocity)... % we wait for velocity to get back to
median (ignoring SD)
        || accelerationBeforeOrAfterBlink >
(NormativeData.medianAcceleration)... % we wait for acceleration to get
back to median (ignoring SD)
        || any(isnan(positionXBeforeOrAfterBlink))...
        || any(isnan(positionYBeforeOrAfterBlink))

data(timeBeforeOrAfterBlink,ColumnNumbers.xPosition) = NaN;
data(timeBeforeOrAfterBlink,ColumnNumbers.yPosition) = NaN;
data(timeBeforeOrAfterBlink,ColumnNumbers.velocity) = NaN;
data(timeBeforeOrAfterBlink,ColumnNumbers.acceleration) =
NaN;

        timeBeforeOrAfterBlink = timeBeforeOrAfterBlink +
eitherPlusOrMinusOne;
        if timeBeforeOrAfterBlink == 0 || timeBeforeOrAfterBlink >
size(data,1) % if we are trying to remove data before the beginning or
after the end of the dataset
            return; % don't make any changes
        else
            positionXBeforeOrAfterBlink =
data(timeBeforeOrAfterBlink,ColumnNumbers.xPosition); % find X position
at that time
            positionYBeforeOrAfterBlink =
data(timeBeforeOrAfterBlink,ColumnNumbers.yPosition); % find Y position
at that time
            velocityBeforeOrAfterBlink =
abs(data(timeBeforeOrAfterBlink,ColumnNumbers.velocity)); % find the
absolute velocity at that time
            accelerationBeforeOrAfterBlink =
abs(data(timeBeforeOrAfterBlink,ColumnNumbers.acceleration)); % find the
absolute acceleration at that time
        end
    end
end
end
end
end

```

oculomotorsuite_readeyetrace.m

```

function [eyePosition, inputFile] =
oculomotorsuite_readeyetrace(inputFile, inputFile, whichEyeToUse)
% Read in an eye trace file, return position trace (X and Y)
% Created August 2013 by Matt J Dunn

% Input can be a string (pointing to a file), or an array

if ~exist('inputFile', 'var') || isempty(inputFile)
    [inputFileNameWithExtension, inputFile] =
uigetfile({'*.edf;*.mat;*.csv', 'EDF, MAT or CSV files'}, 'Select data
file');
    inputFile = fullfile(inputFile, inputFileNameWithExtension);
end

if isa(inputFile, 'char') % if inputFile is a string
    [inputFilePath, inputFileName, fileExtension] =
fileparts(inputFile); % separate the filename and extension

```

```

fprintf('\nReading file %s...',inputFileName)
if strcmpi(fileExtension, '.edf') % EyeLink data file
    if exist(fullfile(inputFilePath, strcat(inputFileName, '.asc')),
'file') % if the function was terminated halfway through previously, we
need to remove the temp file before continuing

delete(fullfile(inputFilePath, strcat(inputFileName, '.asc')));
    end
    [unusedVariable, unusedVariable] = system(['EDF2ASC -s -miss NaN
"', inputFile, '"']); % convert EDF file to ASCII using SR Research's
EDF2ASC tool
    % If the above line fails, then either EDF2ASC is not installed,
or you need to check your environment variables
    fid =
fopen(fullfile(inputFilePath, strcat(inputFileName, '.asc')));
    nColumnsInFile = numel(regexp(fgetl(fid), '\s*([\s]*)\s*')); %
monocular and binocular ASC files have different numbers of columns
    if nColumnsInFile == 5 % monocular EDF file
        inputData = textscan(fid, '%d %f %f %f %s'); % read the ASCII
file in. The file has the format [timestamp, X, Y, pupilSize, {...}]
        eyePosition = [inputData{2:3}]; % we're only interested in
the X and Y columns
    elseif nColumnsInFile == 8 % binocular EDF file
        inputData = textscan(fid, '%d %f %f %f %f %f %f %s'); % read
the ASCII file in. The file has the format [timestamp, XL, YL,
pupilSizeL, XR, YR, pupilSizeR, {.....}]
        if ~exist('whichEyeToUse', 'var')
            whichEyeToUse = questdlg('Which eye would you like to
analyse?', 'Binocular recording detected', 'Left', 'Right', 'Right');
        end
        switch whichEyeToUse
            case 'Left'
                eyePosition = [inputData{2:3}];
            case 'Right'
                eyePosition = [inputData{5:6}];
        end
    else

error('unrecognisedFileFormat:ascFileUnusualNumberOfColumns', 'Unrecognis
ed EDF file format!')
    end
    fclose(fid);
    delete(fullfile(inputFilePath, strcat(inputFileName, '.asc'))); %
clear up the new file
    elseif strcmpi(fileExtension, '.csv')
        eyePosition = csvread(inputFile); % load the data into MATLAB
    elseif strcmpi(fileExtension, '.mat')
        eyePosition = load(inputFileName); % we assume that the MAT file
only contains one variable (inputData), and that it is already in the
correct format
    end
elseif isa(inputFile, 'numeric') % if our input is an array
    eyePosition = inputFile;
    if ~exist('inputFileName', 'var')
        inputFileName = 'Input Data'; % set a default inputFileName if
none was specified
    end
end
end

% Check that the eyePosition array is of sensible dimensions
if size(eyePosition,2) > 2

```

```

warning('unusualInputFile:tooManyColumns', '\nThere appear to be
more than two columns of data in the input file. Assuming first column
is horizontal eye position, second column is vertical eye position, and
deleting everything else...')
eyePosition(:,3:end) = [];
end
if size(eyePosition,1) < 10
warning('unusualInputFile:veryFewRows', '\nThere appear to be less
than ten samples in your data. Perhaps the input data are structured
incorrectly?')
end
if size(eyePosition,2) == 1 % if we're working with one-dimensional data
fprintf('\nInput data appear to be uniaxial. Assuming this
represents horizontal eye data and setting all vertical axis data to
zero...')
eyePosition(:,2) = 0; % set the other axis to 0
end

```

oculomotorsuite_receivedatafile.m

```

function oculomotorsuite_receivedatafile
% Stop recording and receive data file
% Adapted from code written by SR Research

WaitSecs(0.1); % give the EL1000 a chance to catch up
Eyelink('Stoprecording');
Eyelink('Command', 'set_idle_mode');
WaitSecs(0.5); % give the EL1000 a chance to catch up
Eyelink('CloseFile');
% Download data file
try
fprintf('Receiving data file\n');
status=Eyelink('ReceiveFile');
if status > 0
fprintf('Data file received successfully\n');
end
catch % if data transfer fails, let us know
fprintf('Problem receiving data file\n');
end

```

playtone.m

```

function player = playtone (duration, toneFreq)
% Generate a tone
% Version 1.1 - 2012 by Matt J Dunn

global player; % as a global variable, sound will continue to play after
the function has ended.
samplesPerSecond = 44100; % the bit rate of the tone
y = sin(linspace(0, duration * toneFreq * 2 * pi, round(duration *
samplesPerSecond))); % the equation of the sound wave
player = audioplayer(y, samplesPerSecond); % create an audio object from
the sound wave at the specified bit rate
stop(player); % stop any previous audio
play(player); % play the audio

```

skippabledelay.m

```

function keyCode = skippabledelay(delay)
% Provides a delay that can be skipped over by pressing any key
% Version 1.0 - 2011 by Matt J Dunn

```

```
tStop=GetSecs + delay; % time to stop waiting is decided
while GetSecs < tStop
    [keyIsDown, ~, keyCode]= KbCheck; % check the keyboard
    if keyIsDown ~= 0 % if a keypress IS detected
        return; % leave the function
    end
end
end
```

Appendix II Subject information

II.1 Subjects with nystagmus

Subject Initials	Sex	Date of Birth	Waveform in primary position	Diagnosis	Distance cover test with prescription	Latent component?	Head nodding?
DB	M	20-Nov-58	JR _{EF} (hypermetric quick phases)	IIN	~3Δ XP	FALSE	FALSE
DK	F	01-Aug-61	J _{EF} (PAN) (hypermetric quick phases)	IIN	Ortho	FALSE	FALSE
DP	M	13-Aug-73	PP _{FS}	IIN	LET (sl)	FALSE	FALSE
DT	M	04-Apr-50	J _{EF} (PAN) (hypermetric quick phases)	Achromatopsia	~25Δ LET	FALSE	FALSE
GS	M	02-Sep-84	DJ (PAN)	IIN	Ortho	FALSE	FALSE
GT	M	17-Mar-50	RPC (hypermetric quick phases)	IIN	Ortho	FALSE	FALSE
GT2	M	09-Jul-52	JR _{EF}	IIN	~12Δ alt ET	FALSE	FALSE
IG	M	11-Feb-12	Downbeat	Optic atrophy	Ortho	FALSE	FALSE
JC	M	20-Jul-42	Saccadic intrusions - worse in leftgaze	IIN	Ortho	FALSE	FALSE
JC2	F	20-Jun-58	J _{EF} (PAN) (hypermetric quick phases)	IIN	Ortho	FALSE	FALSE
JS	M	01-Mar-57	JL _{EF}	IIN	Ortho	FALSE	FALSE
JT	M	06-Jan-88	PJ (PAN)	IIN	Ortho	FALSE	FALSE
JX	F	10-Nov-83	BDJR	IIN	Ortho	TRUE	FALSE
KF	M	13-Nov-49	Manifest FMNS	FMNS	~15Δ LET	TRUE	FALSE
KL	F	27-Jun-52	Manifest FMNS (hypermetric quick phases)	FMNS	~5ΔLXT, ~2ΔLHyperT	TRUE	FALSE
LC	M	09-May-84	BDJR	IIN	~7Δ XP	FALSE	FALSE
LL	F	20-Nov-86	Manifest FMNS	FMNS	LHyperT c LET	TRUE	FALSE
MB	F	19-Jan-53	Manifest FMNS	FMNS	~10Δ XP c ~8Δ RHyperP	TRUE	FALSE
MT	F	25-Sep-43	BDJL	IN c fovea plana	Ortho	FALSE	FALSE
NB	M	25-Dec-67	PP _{FS}	Possible macular defect	Ortho	FALSE	TRUE
RC	F	20-Dec-90	PP	Possible albinism	~15Δ RET	TRUE	FALSE
RD	M		JL _{EF}	IIN		FALSE	FALSE
RW	F	02-Nov-29	JR _{EF}	IIN	Ortho	FALSE	FALSE
SW	F	12-Jul-43	J _{EF} (hypermetric quick phases) (PAN)	IIN	Ortho	FALSE	FALSE

Subject Initials	Sex	Date of Birth	Waveform in primary position	Diagnosis	Distance cover test with prescription	Latent component?	Head nodding?
VW	F	31-Jul-90	JR _{EF}	IIN	LET	FALSE	FALSE

Subject Initials	RE VA	LE VA	Binocular VA	Dominant eye at distance	RE Refraction	LE Refraction
DB	0.66	0.64	0.66	=	-7.50/-1.00x177 (VA = 6/18-2)	-9.50/-1.75x3 (VA = 6/18-1)
DK	0.72	0.72	0.64	=	-1.00/-2.00x164	-1.75/-2.25x180
DP	0.60	0.86	0.60	R	-1.75/-3.00x100	-5.00/-1.00x79
DT	0.94	1.20	0.92	R	-11.00	-12.00
GS	0.54	0.56	0.62	R	-7.00/-2.75x22 (VA = 6/18+1)	-8.50/-1.00x169 (VA = 6/24)
GT	0.44	0.44	0.44	=	-1.25/-0.50x25	-0.25/-0.50x120
GT2	0.78	0.84	0.78	R	-3.00/-1.00x150	-3.75/-1.50x160
IG	1.44	1.58	1.24	R	+2.00/-1.00x5	+1.25/-1.00x167
JC	0.06	0.32	0.04	=	+0.75	-1.75
JC2	0.54	0.56	0.46	=	-4.25/-2.00x35 (VA = 6/18-2)	-2.50/-4.75x62 (VA = 6/18-2)
JS	0.36	0.36	0.32	L	-12.25/-1.75x40 (VA = 6/12-2) (BVD 10mm)	-10.75/-1.25x90 (VA = 6/12-1)
JT	0.42	0.48	0.44	R	+0.25/-1.75x148 (VA = 6/18+1)	+1.75/-2.75x26 (VA = 6/18+2)
JX	0.20	0.20	0.18	=	-1.50/-1.50x5 (VA = 6/9-1)	-1.00/-2.00x180 (VA = 6/6-3)
KF	0.42	0.48	0.42	R	-7.00/-4.00x152 (VA = 6/18+1)	-7.00/-3.25x17 (VA = 6/18+1)
KL	0.04	0.24	0.04	R	-0.50/-0.25x165 (VA = 6/5)	+0.25 (VA = 6/9+2)
LC	0.52	0.54	0.46	R	+1.50/-2.25x135	+2.75/-2.50x35
LL	0.18	0.30	0.18	R	∞/-1.00x71	-0.25/-0.25x30
MB	0.84	0.88	0.44	=	∞/-1.75x1 (VA = 6/18-1)	+2.75/-2.25x23 (VA = 6/18)
MT	0.48	0.72	0.48	=	N/K - over-refracted RGPs	N/K - over-refracted RGPs
NB	0.30	0.26	0.22	=	+1.50/-0.50x95 (VA = 6/12+1)	+1.25/-0.75x95 (VA = 6/9-2)
RC	0.66	0.64	0.66	L	+5.50/-3.24x2	+5.50/-3.50x178 (VA = 6/24-1)
RD	0.46	0.42	0.36			
RW	0.86	0.88	0.86	R	+1.25/-1.00x180 (VA = 6/36)	+2.50/-0.50x180 (VA = 6/36-1)
SW	0.16	0.18	0.20	R	-0.50/-0.50x155 (VA = 6/9)	+1.25/-0.25x130 (VA = 6/9-)
VW	0.34	0.44	0.36	R	+2.25/-4.00x23 (VA = 6/12+1)	+2.50/-4.00x155 (VA = 6/12+1)

Subject Initials	Focimetry R	Focimetry L	Age of spectacles	Head turn
DB	-7.25/-1.25x2 add +3.25	-9.25/-2.00x176 add +3.25	3/12	None
DK	N/A	N/A	N/A	Yaw right
DP	-2.25/-3.00x100	-5.50/-1.00x79	1/12	Yaw left (very slight)
DT	N/A	N/A	1/12 (RGPs) - Rx is 15 years old	None
GS	-7.50/-3.00x15 (VA = 6/18)	-8.00/-1.50x174 (VA = 6/18-2)	24/12	Yaw left (slight)
GT	-1.50/-0.50x26	-0.25/-0.75x121	16/12	Pitch up or down (usually up)
GT2	-3.25/-1.00x150	-3.75/-1.50x163	2/12	Yaw right if RE fixing, yaw left if LE fixing
IG	N/A	N/A	N/A	None
JC	+0.75	-1.75	1/12	Yaw left, pitch down
JC2	-3.75/-2.50x35 c 2ΔBO (VA = 6/18-2)	-3.50/-4.50x60 (VA = 6/18-2)	15/12	None
JS	-12.00/-2.00x31	-10.50/-1.25x90	42/12	Yaw left, pitch up (slight)
JT	+0.25/-1.75x143 (VA = 6/18)	+1.25/-2.75x23 (VA = 6/18-1)	36/12	Pitch down, yaw left
JX	-1.50/-1.50x7	-1.00/-1.75x3	36/12	Yaw right
KF	-7.75/-4.25x168	-6.75/-3.25x30	36/12	None
KL	-0.50/-0.25x15 (VA = 6/6+1)	+0.50 (VA = 6/12+3)	10/12	Pitch down, roll left
LC	+3.75/-2.75x163	+3.75/-3.25x37	96/12	Pitch down
LL	∞/-1.00x66	-0.25/-0.50x24	10/12	None
MB	-0.25/-1.50x10	+2.75/-2.00x16	12/12	None
MT	N/K	N/K	7/12 (RGPs)	Yaw right, pitch down
NB	+2.00/-1.00x95 (VA = 6/12-1)	+1.75/-1.25x85 (VA = 6/12-1)	22/12	None
RC	+5.50/-3.75x176 (VA = 6/36-1)	+5.50/-3.50x174 (VA = 6/24-1)	24/12	None
RD	N/A	N/A	N/A	None
RW	N/A	N/A	N/A	None
SW	N/A	N/A	N/A	Yaw left (slight)
VW	+2.25/-3.50x22 (VA = 6/12)	+2.25/-3.50x160	30/12	Yaw left + roll left - sometimes changes to yaw right + roll right (due to changing the fixing eye?)

Subject Initials	Notes
DB	
DK	
DP	
DT	Early LOs. Wears RGPs. Over-refraction: RE -0.50 LE -0.25
GS	Refracted Rx used for experiments. EL1000 stopped working during the day.
GT	Rx not worn
GT2	Alternating ET. RE usually fixates at distance
IG	Hereditary motor and sensory neuropathy (type 2). Unable to perform psychophysical tests due to low VA. Saccade testing and calibration done with 0.5° cross width. Despite this, could not see the target for calibration (but okay for saccade testing)
JC	Rx not worn. Nystagmus was only present in right-gaze.
JC2	
JS	LE dominant @ dist, RE @ near
JT	
JX	
KF	Only covering the RE increases intensity
KL	All tests calibrated using the standard EL1000 method - don't need the calibration files at all. They were done simply because it may be useful to know the level of nystagmus in different positions of gaze. Px experiences oscillopsia when one eye is covered
LC	
LL	Rx not worn
MB	
MT	Early LOs. Wears RGPs. Over-refraction: RE +1.50/-1.25x85 LE +0.75/-1.00x79
NB	
RC	Iris transillumination makes tracking difficult - be aware that all tracking was of the whole pupil AND iris. SaccadeTesting - cross width increased to 0.3°. Unable to track for Flash; poor tracking for absent viewing
RD	Head nodding reported until 12 years of age. LASIK performed to correct ametropia.
RW	Very poor tracking quality. RE distorted pupil. LE mature LO. Fuch's dystrophy
SW	For flash and timeToSee, the refracted Rx was worn
VW	

II.2 Control subjects

Subject Initials	Sex	Date of Birth	RE VA	LE VA	Binocular VA	RE Refraction	LE Refraction
AS	F	23/08/1989	-0.14	-0.14	-0.18	-0.25	-0.25
BF	F	21/08/1986	-0.04	-0.10	-0.10	+0.50/-0.25x120	+0.50/-0.50x60
FE	M	21/05/1965	-0.08	-0.08	-0.08	-2.25/-0.50x160	-2.25/-0.50x30
JG	M	20/02/1970	-0.08	-0.20	-0.20		
JMW	F	15/10/1948	-0.20	-0.18	-0.22	-2.25/- 1.00x180	-2.25/-1.50x145
JS2	M	28/03/1988	-0.06	-0.16	-0.18	+1.00/-4.00x85	+1.00/-4.00x80
JT2	M	21/04/1990	-0.12	-0.14	-0.16	∞ /-0.50x165	∞
JTE	M	08/09/1950	-0.16	-0.16	-0.16		
LP	F	20/04/1989	0.10	0.12	0.06	-0.25/-0.50x180	∞ /-1.00x168
MD	M	17/04/1988	-0.20	-0.20	-0.20	-1.75	-1.75
MU	F	30/05/1991	-0.08	0.02	-0.14	∞ /-0.15x45	+0.25/-0.25x45
NH2	M	06/04/1945	-0.08	-0.12	-0.18		
PG	M	05/03/1992	-0.16	-0.20	-0.26	-1.75/-0.25x65	-1.75/-0.25x135
RE	M	10/08/1941	0.12	-0.18	-0.18	∞ /-1.00x180	∞ /-0.50x12
ROD	M	04/01/1946	-0.14	-0.12	-0.14		
SH2	F	30/07/1955	-0.18	-0.14	-0.18		
SS	M	22/02/1991	-0.12	-0.02	-0.14	+0.25/-0.50x100 (6/4)	+0.25/-0.25x65 (6/4)
TM	M	06/10/1964	-0.12	-0.22	-0.12	-0.25/-0.75x120	+0.25/-1.75x63

Subject Initials	Focimetry R	Focimetry L	Age of spectacles	Distance cover test with prescription	Notes
AS	N/A	N/A	N/A	Ortho	No Rx worn
BF	N/A	N/A	N/A		
FE	-2.25/-0.50x160	-2.25/-0.50x30	N/K		
JG	N/A	N/A	N/A		
JMW	-2.25/- 1.00x180	-2.25/-1.50x145	N/K		
JS2	+1.00/-4.00x85	+1.00/-4.00x80	6/12	Ortho	
JT2	N/A	N/A	N/A		
JTE	N/A	N/A	N/A		
LP	N/A	N/A	N/A	Ortho	
MD	-1.75	-1.75	24/12		
MU	N/A	N/A	N/A	Ortho	
NH2	N/A	N/A	N/A		
PG	-1.75/-0.25x65	-1.75/-0.25x135	1/12	Ortho	
RE	N/A	N/A	N/A		
ROD	N/A	N/A	N/A		
SH2	N/A	N/A	N/A		
SS	N/A	N/A	N/A	Ortho	No Rx worn
TM	N/A	N/A	N/A		Refracted Rx worn

Appendix III **Nystagmus analysis software user manual**

Nystagmus Analysis and Calibration Tool

Matt J Dunn

Version 1.0

Overview

This software package allows for rapid calibration and analysis of nystagmus eye trace data.

1 System Requirements

In order to use the software, you need to have MATLAB installed on your system. The routines work from MATLAB version 7.1 and up, but in order to use the graphical user interface (GUI), a later version is required (fully tested with 2009a).

1.1 Live Calibration

In order to perform a *live* calibration, you will need an EyeLink 1000 and [PsychToolbox](#) installed.

1.2 Reading EDF files

The software can read in data in a variety of formats. One of these formats is the EyeLink Data File (EDF) format. In order to read EDF files, you will need to have the EDF2ASC tool installed on your system. This can be downloaded from the [SR Research Forum](#). Once you have the EDF2ASC application on your system, you will need to set your *Path environment variable* to include the location of EDF2ASC.

2 Getting Started

First, ensure you have the system requirements listed above. Copy the contents of the ZIP file to a new directory and navigate to it in MATLAB. Type `nys` at the MATLAB console. This brings up the GUI (see Figure 1).

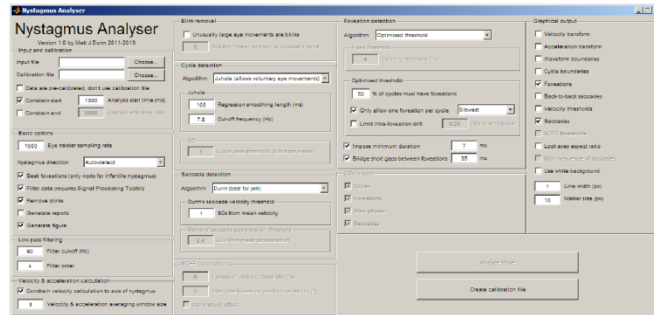


Figure 1: Nystagmus analyser GUI

3 Analyse a recording

From the GUI, you can set various settings, according to how you would like to analyse your eye trace:

3.1 Input and calibration

Input file

Type the name of the file you would like to analyse here, or press the **Choose...** button to manually select. Imported files must reside in the same directory as the Nystagmus Analysis software. This can be a CSV, MAT or EDF file. In order to import an EDF file, you will need to have EDF2ASC installed on your system. For more information, see Section 1.2. CSV files must be in the format of either one or two columns of numbers. The first column is assumed to represent horizontal eye position, whilst the second column is vertical eye position. Any further columns are discarded by the software. If a CSV file only contains a single column of numbers, this is assumed to represent horizontal eye position. MAT files should contain a single array, structured in the same manner as CSV files, described above.

Calibration file

If you have already generated a calibration file using the software, type its name here. You can use the **Choose...** button to browse. As with the eye trace files, the calibration file must also exist in the same directory as the software. If you don't yet have a calibration file, leave this box blank.

Data are pre-calibrated; don't use calibration file

Check this box if the data you are importing are already calibrated in the manner you would like; for example, if you are importing a CSV file containing values that are already in degrees.

Constrain start and end

If you want to analyse only a specific section of your input file, set the start and end times here. For example, during calibration you may wish to ignore the first 1000 ms in order to give participants plenty of time to acquire the new fixation target.

3.2 Basic options**Eye tracker sampling rate**

Enter the temporal resolution of your eye tracker, in Hertz.

Nystagmus axis

If known, select the primary axis of nystagmus here. If you are unsure of the axis of nystagmus, select **Auto-detect**. Assuming there are no voluntary eye movements in the eye trace, the software is capable of automatically detecting the axis of nystagmus.

Seek foveations

Foveation detection will only work in subjects with infantile nystagmus. If you intend on analysing a waveform from any other form of nystagmus, uncheck this box. For more information, see Section 3.9.

Filter data

Filtering an eye trace position signal smooths noise from the resulting plot, especially in the velocity and acceleration transforms. Accurate saccade detection relies on the accuracy of the velocity and acceleration plots; hence, it is better to apply filtering if possible. Note that low pass filtering relies on functions from the MATLAB Signal Processing Toolbox, and will not work unless you have this installed. For more information, see Section 3.3.

Remove blinks

The presence of blinks in an eye trace can affect the accuracy with which nystagmus cycles are detected. Only turn off blink removal if you think data are being removed from your traces unnecessarily. For more information, see Section 3.5.

Generate reports

The software is capable of producing CSV reports relating the parameters of the nystagmus waveform. For more information, see Section 3.10.

Generate figure

The software can produce a graphical figure of the nystagmus waveform, containing several other features. For more information, see Section 3.11.

3.3 Low pass filtering

Low pass Butterworth filtering is applied to the position trace *only*, prior to calculation of velocity and acceleration.

Filter cut-off

This defines the cut-off frequency of the low pass filter. Oscillations with frequencies higher than this value will be attenuated.

Filter order

This defines the order of the low pass filter. Higher orders more strongly attenuate the signal outside the passband.

3.4 Velocity and acceleration calculation

Velocity is calculated by differentiation, using a central difference algorithm. Acceleration is calculated in the same manner, based on the velocity transform.

Constrain velocity calculation to axis of nystagmus

If this box is checked, velocity is calculated based on the position trace in the axis of nystagmus only. If unchecked, velocity is calculated based on the Euclidian norm of the change in position recorded from both position channels.

Velocity and acceleration averaging window size

By default, a three-point central difference algorithm is used to calculate velocity and acceleration. In order to use more points in this calculation, increase the number here. This must be an odd number.

3.5 Blink removal**Unusually large eye movements are blinks**

Some eye tracking systems do not 'drop' the eye position signal during a blink (for example, EOG). In these systems, blinks may be identified by a large 'spike' in eye position. Check this box to turn this detection on.

Number of SDs from mean position to be considered 'unusually large'

If considering large eye movement spikes to be blinks, then spikes that take the eye position this many standard deviations from the mean position will be considered a blink.

3.6 Cycle detection**Algorithm**

Two cycle detection algorithms are available for use with this software. *Juhola's* method of cycle detection is described in [4], and works very well in most cases, even if there are voluntary eye movements within the recording. The alternative method, *SD*, works where *Juhola's* method fails; in waveforms with 'double oscillations', such as a bidirectional jerk waveform with hypermetric quick phases. The *SD* method works by detecting local maxima and minima in the position trace that exceed a certain number of standard deviations from the mean position of the entire recording. An open source peak detection algorithm [2] is used to identify the locations of these positions, and cycles are derived from this.

Juhola: slope analysis length

Juhola's algorithm makes some assumptions about the minimum expected length of a single cycle. In doing so, micro-oscillations in the trace (e.g. due to noise) are ignored. The *slope analysis length* essentially refers to the minimum possible length of a cycle, in ms.

Juhola: cut-off frequency

After calculating the direction of eye movement at any given time, *Juhola's* method then uses a central difference algorithm to filter the resulting number array. This value relates to the inverse of the number of samples used in the central difference algorithm (similar to that used in calculation of the velocity and acceleration transforms).

SD: cycle peak threshold

This is the magnitude of fluctuation that should be considered a part of the nystagmus oscillation, measured in standard deviations from the mean position for the entire recording.

3.7 Saccade detection**Algorithm**

Two saccade detection algorithms are available for use with this software. *Dunn's* method finds saccades by setting a fixed velocity threshold for saccades. This threshold is based on the standard deviation of the velocities present in the

entire recording. Once saccades are detected, their start and end times are calculated by looking for corresponding spikes in the acceleration trace, as well as the beginning and end of monotonicity in the position trace. *Behrens'* method works in a similar way to *Dunn's* method, except the threshold is based on the acceleration transform only. The threshold is dynamic, but the dynamism of the threshold is limited by a minimum expected inter-saccadic interval. The method is described in [1]. *Dunn's* method works better in jerk nystagmus, but it relies on some saccades being present in the trace. i.e. **If there are no saccades present in the eye trace, *Dunn's* method will not work.** As a result, *Behrens'* method is best for use in nystagmus traces in which no saccades are expected, such as pendular waveforms.

Dunn's saccade velocity threshold

This is the number of standard deviations from the mean velocity in the eye trace that should be used as the saccade detection threshold.

Behrens' saccade acceleration threshold

This is the number of standard deviations from the mean acceleration of the preceding 100 ms of data that should be used as the saccade detection threshold.

3.8 NOFF calculation

The software is capable of calculating the Nystagmus Optimum Fixation Function (NOFF) for any eye trace. This function is based on the work described in [3] and was developed with the help of Joost Felijs. NOFF aims to quantify the 'quality' of nystagmus foveation in an eye trace, by performing a calculation on the four-second window in the recording with the most time spent foveating. In order to calculate NOFF, data must be calibrated and contain foveations.

NOFF foveation velocity threshold

This is the velocity threshold used to define foveations.

NOFF max inter-foveation position variability

This is the maximum amount of positional variability allowed between detected foveations.

Use manual NOFF offset

The NOFF function optionally allows the user to manually offset the center of the inter-foveation position variability window (see [3]). Checking this box will prompt the user to mark the centre of expected foveations on the eye trace.

3.9 Foveation detection

Algorithm

Two methods are available to define *foveations*. Please note that these differ not only in their method, but also in their expected outcome. *Foveation* is defined as the period of the nystagmus waveform during which the eyes are moving most slowly. The traditional way of finding foveations has been to define a fixed *velocity threshold*, and to reject all data that exceed this threshold. There has been much debate on the magnitude at which this threshold should be set, as thresholds that work for some individuals might not detect any foveations at all in others. Selecting **Fixed threshold** allows the user to find foveations in this traditional way, by setting a fixed velocity threshold. Alternatively, one may select **Optimised threshold**, which iteratively adjusts the velocity threshold until a foveation is found in a given percentage of nystagmus cycles. This provides the advantage of finding approximately the same number of foveations in all individuals (regardless of overall nystagmus intensity), as well as not requiring data to be pre-calibrated (a paradoxical situation, since one cannot define foveation in the traditional way without first knowing the velocity of the eye, which cannot be known unless the data are calibrated).

Fixed foveation velocity threshold

This is the velocity used to define foveations if using a traditional *fixed velocity* threshold approach to finding foveations.

Optimised threshold: percentage of cycles requiring a foveation

The optimised threshold method can be set to detect a foveation in a given number of the nystagmus cycles detected in the recording, expressed as a percentage of the total number of cycles. Setting this number higher will cause foveations to be detected in a greater percentage of cycles, but as a result, the foveation velocity threshold will be increased. If this value is set too high, you may find that the detected foveations last for the majority of the waveform. If set low, only the very best (slowest) foveations in the entire recording will be detected, and their duration will be very short. A compromise must be made between the number of foveations to be detected and the accuracy with which they truly represent the *slowest* portion of the waveform.

Optimised threshold: only allow one foveation per cycle

Turn this on to ensure that only one foveation is detected in each cycle. Where there is more than one candidate foveation found in any one cycle, you may choose whether the preferred foveation is the *slowest* or the *longest* of the candidates identified.

Optimised threshold: limit intra-foveation drift

Optionally, foveations can be constrained by the amount of positional variability tolerated (within a single foveation). The tolerance is defined by the number of standard deviations of the average amplitude of the nystagmus waveform in the recording.

Impose minimum duration for foveations

If set, any foveations lasting for less than this time (in ms) are considered artefacts and rejected.

Bridge adjacent foveations

If set, any foveations that are separated by a short gap (as defined by the user) are *bridged* to form a single foveation.

3.10 CSV reports

Select here any reports you would like to generate. Output files are in Comma Separated Value (CSV) format, which can be read by any spreadsheet software.

3.11 Graphical output

This section relates to the graphical output produced by the software after analysing an eye trace. The following aspects of the figure output can be controlled:

Velocity transform

Plots eye velocity on the chart. In order to view this on the same axes as the position trace, the velocity plotted is reduced by a factor of 100.

Acceleration transform

Plots eye acceleration on the chart. In order to view this on the same axes as the position trace, the acceleration plotted is reduced by a factor of 1000.

Waveform boundaries

Draws a line between each of the peaks and each of the troughs of the nystagmus waveform, for easy visualisation of overall change in eye position.

Cycle boundaries

Draws a vertical line at the start of each detected nystagmus cycle.

Foveations

Highlights detected foveations on the trace.

Back-to-back saccades

Marks the junction between back-to-back saccades (i.e. saccades without an inter-saccadic interval) on the trace with a vertical dashed line.

Velocity thresholds

Plots the thresholds used to detect foveations and saccades on the trace. May be useful in conjunction with the velocity transform plot.

Saccades

Highlights detected saccades on the trace.

NOFF foveations

Draws the foveations used for the calculation of NOFF on the trace. Note that these foveations will only be within a single four second window, and may be defined differently to the remainder of the foveations on the trace.

Lock axes aspect ratio

Selecting this option will ensure that the X and Y axes are plotted on the same scale. This can be useful if rotating the trace to view in 3D. However, with this option selected, it is only possible to zoom globally; i.e. zooming into a single axis is disabled.

Main sequence of saccades

Selecting this option will create two extra plots containing data from the detected saccades. One such plot is 3D, and shows the relationships between saccade duration, amplitude and peak velocity. The other plot shows the relationship between saccade duration and (saccade duration \times saccade peak velocity).

Use white background

Select this option if producing figures for publication. This will reverse many of the colours in the plot, making them suitable for printing.

Line width

Set the thickness of lines plotted on the figure, in pixels.

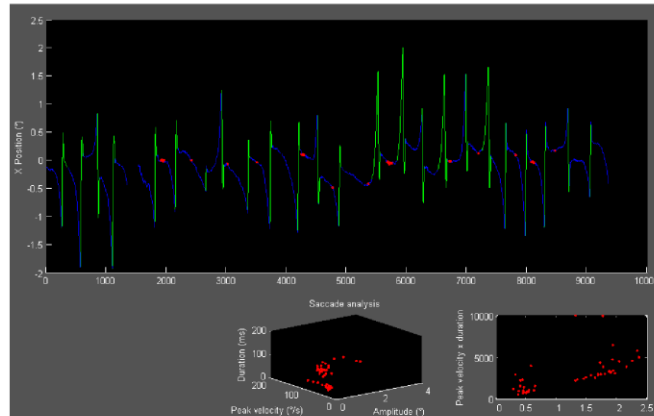


Figure 2: Example of graphical output

Marker size

Set the size of markers plotted on the figure, in pixels.

3.12 Analyse trace

Press this button to analyse an eye trace, using the settings selected above.

Create calibration file

This button allows you to calibrate an eye trace, using the settings selected above for the detection of foveations.

4 Analysis output

An example of the output from the software is shown in Figure 2 and below. Note that this shows the output from a *calibrated* eye trace; however, some of these metrics are still reported even if the data are uncalibrated.

One blink was detected and removed
2.02% of the data were dropped

*** WAVEFORM ANALYSIS ***

21 cycles were detected (20 of these were free from blinks)

Frequency = 2.6Hz (SD = 0.6Hz)
 Amplitude = 1.7° (SD = 0.6°)
 Intensity = 4.4

*** FOVEATION ANALYSIS ***

13 foveations were detected
 Foveation duration = 22.7ms (SD = 21.9ms)
 Foveation velocity threshold (to detect a foveation on >=50% of cycles)
 is 0.9°/s
 Foveation position = (-0.0°, -0.1°) ± (0.3°, 0.2°) (SD = [0.2°, 0.1°])
 Foveation velocity = 0.6°/s (SD = 0.4°/s)
 NOFF = 1.49, using a velocity limit of 6.0°/s and position limit of
 1.0°

*** SACCADIC ANALYSIS ***

46 saccades were detected
 Saccade duration = 29.9ms (SD = 26.2ms)
 21 saccades had no intersaccadic interval
 Saccade velocity threshold is 36.04°/s
 Dominant saccade direction is right: 27 right saccades and 19 left
 saccades were detected
 Saccade peak velocity = 111.7°/s (SD = 52.3°)
 Saccade mean velocity = 53.5°/s (SD = 30.1°)
 Saccade amplitude = 1.2° (SD = 0.7°)

*** SLOW PHASE ANALYSIS ***

Slow phases appear to be accelerating
 Slow phase peak velocity = 23.3°/s (SD = 10.0°)
 Slow phase mean velocity = 4.8°/s (SD = 1.8°)

Note that the nystagmus waveforms can be rotated through three dimensions, as shown in Figure 3.

5 Create a calibration file

Calibration can either be performed *live*, or *post-hoc*. A live calibration requires an EyeLink 1000 and PsychToolbox to be installed on your system. For more information, see Section 1. Figure 4 shows the calibration GUI. Calibration can be performed with either five or six points. In future versions, support for more points may be added. In order to allow your subject chance to take up fixation, you may elect to delete the beginning of each recording before analysing. To do this, make sure you have set *Constrain start* appropriately in the initial GUI window (see Section 3.1).

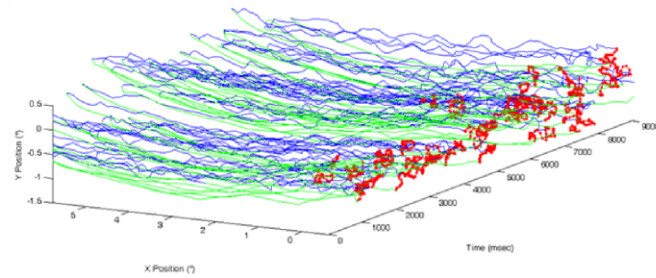


Figure 3: Example of 3D waveform visualisation

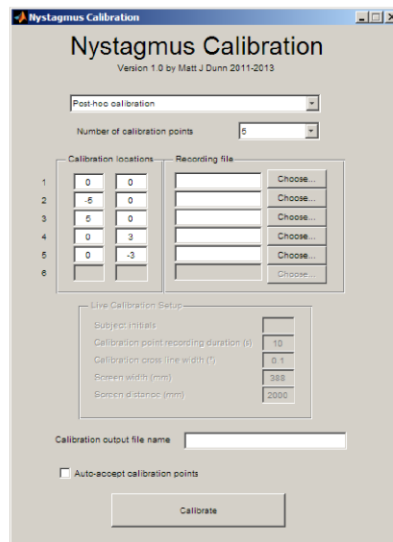


Figure 4: Nystagmus calibration GUI

5.1 Calibration locations

Whether calibrating live or post-hoc, the locations of the calibration points must be specified. These values are typically specified in degrees (although you may use your own units if desired), relative to the straight-ahead position. For example, a calibration value of (-3, 0) refers to a target positioned three degrees to the left of straight ahead.

5.2 Live calibration

To perform a live calibration, it is necessary to specify the dimensions of your screen, as well as the distance that the subject is sat at. This is required in order for the calibration targets to be drawn at the appropriate position on the display screen. In addition, you may specify the subject's initials (to name the output files) and the duration for which you would like to present each calibration point. Longer calibration times will increase the accuracy of the calibration, but may induce fatigue.

5.2.1 Calibration cross line width

For live calibration, fixation targets are presented as a simple black cross on a grey background. The thickness of the cross line width is controlled using this parameter. Use larger cross sizes for subjects with particularly poor visual acuity.

5.3 Post calibration

To perform a post-hoc calibration, specify the names of each of the calibration recordings, as well as the locations at which each target was presented. As with the nystagmus analysis system, these input files may be an EDF, CSV or MAT file. It is assumed that each recording contains simple *fixation* only; i.e. only one calibration location should be included in each recording. If you would like to calibrate using a recording that contains all the calibration locations in a single recording, please split the recording into a different CSV file for each location before attempting to calibrate.

5.3.1 Calibration output file name

Type the desired name of the calibration file here. This is the file that will be later used to calibrate your recordings with the nystagmus analyser system.

5.4 Auto-accept calibration points

Selecting this option will cause each calibration location recording to automatically accept the detected foveations as the calibration location. It is **not** recommended to use this option unless you are repeating a calibration performed

previously, for which you know all the calibration points will have correctly detected foveations.

6 Calibration procedure

If performing a *live* calibration, instruct your subject to fixate the cross for the specified period of time. It is important that subjects do not attempt to make any other voluntary saccades for the duration of the recording, as this might disrupt aspects of the analysis (e.g. cycle detection). Following acquisition of the recording, the eye trace will be displayed graphically (along with any other optional components specified in the analysis setup GUI). Detected foveations (as defined in the analysis setup GUI) will be shown on the trace in **red**. The MATLAB console then prompts the user to decide whether to accept these detected foveations as the calibration location or not. Assuming foveations are detected successfully, the user is presented with seven options:

- Accept the mean position value of the detected foveations as the calibration location (**a**).
- Reject the entire recording, and retry by collecting a new recording (**r**).
- Use the peak of each nystagmus oscillation as the calibration location (**p**).
- Use the trough of each nystagmus oscillation as the calibration location (**t**).
- Use the centre of the nystagmus oscillation as the calibration location (**c**).
- Use the mean position of the eye throughout the entire recording as the calibration location (**e**).
- Manually override the system by selecting a point on the trace by hand (**m**).

For each calibration point, you will be prompted to choose from one of the options above. With the exception of **retry** and **manual override**, each of these options provide an automated calculation of the calibration location. In most cases, you'll want to select **accept**, but there may be situations such as *pendular* nystagmus waveforms in which it is preferable to calibrate to one end of the oscillation (choose **peak** or **trough**). Selecting **manual override** allows the user to place a marker anywhere on the eye position trace.

Calibration files are stored as CSV files, and can be loaded in the nystagmus analyser GUI.

7 Programmatic access of routines

Early versions of MATLAB will not be able to use the GUI to analyse or calibrate data. The calibration and analysis routines used by the software can

be run without the need to invoke the GUI. To analyse a nystagmus eye trace direct from the MATLAB console, type `nystagmus_analyser`. To calibrate *live*, type `nystagmus_calibration_live_eyelink`. To calibrate *post-hoc*, type `nystagmus_calibration_post`. In all cases, the above routines apply some default settings which define the manner in which the traces are analysed. These can be accessed and adjusted in the file `resources\nystagmus_setanalysisdefaults.m`.

8 Support

For support, feel free to contact the author via `DunnMJ1[at]Cardiff.ac.uk`.

References

- [1] F Behrens, M Mackeben, and W Schröder-Preikschat. An improved algorithm for automatic detection of saccades in eye movement data and for calculating saccade parameters. *Behavior research methods*, 42(3):701–708, August 2010.
- [2] Eli Billauer. `peakdet`: Peak detection using MATLAB, 2012.
- [3] J Felius, V L Fu, E E Birch, R W Hertle, R M Jost, and V Subramanian. Quantifying nystagmus in infants and young children: relation between foveation and visual acuity deficit. *Invest Ophthalmol Vis Sci*, 52(12):8724–8731, 2011.
- [4] Giulio Pasquariello, Mario Cesarelli, Maria Romano, Antonio La Gatta, Paolo Bifulco, and Antonio Fratini. Waveform type evaluation in congenital nystagmus. *Computer methods and programs in biomedicine*, 100(1):49–58, October 2010.

Appendix IV **Lay summary of research: letter to participants**

School of Optometry and Vision Sciences
Ysgol Optometreg a Gwyddorau'r Golwg
Head of School *Pennaeth Yr Ysgol* Professor *Yr Athro* Marcela Votruba

College of Biomedical and Life Sciences
Cardiff University
Maindy Road
Cardiff
CF24 4HQ
Wales UK

Tel *Ffôn* +44(0)29 2087 4374
Fax *Ffacs* +44(0)29 2087 4859
<http://www.cardiff.ac.uk/optom/>

Prifysgol Caerdydd
Heol Maindy
Caerdydd
CF24 4HQ
Cymru, Y Deyrnas Gyfunol



Director: Dr Jonathan T. Erichsen



This message is to say thank you for taking part in our studies at Cardiff University's Research Unit for Nystagmus. Over the years, we have conducted numerous experiments examining aspects of perception and eye movement control in individuals with infantile nystagmus (IN). Thanks to your help, we have made significant progress in understanding the difficulties faced by individuals with the condition. Below is a summary of the major findings that have resulted from our work over the last four years:

1. Visual acuity in adults is not limited by motion blur induced by eye movements

By measuring visual acuity (VA) under stroboscopic conditions (with brief flashes of light), we have revealed that nystagmus eye movements do *not* reduce VA in adults. In other words, VA in adults with IN is fixed by some other mechanism, and is unlikely to improve from treatment. The poor VA seen in adults with IN must be the result of either motion blur *during childhood*, or some other pathology of the visual system that we are yet to detect. The results of this study have

recently been published in the journal *Investigative Ophthalmology and Visual Science*.

So, if VA is unlikely to improve from treatment, why do people with nystagmus report improvements to their vision following treatment? The answer to this is that *VA is not an adequate measure of visual function*. VA (a measure of the smallest letters that can be read on a typical optician's chart) is too simple to give the 'full story' in IN, since the eyes are constantly moving. VA is used by eye care professionals as a simple way of measuring visual function, yet no other eye condition causes visual input to change from moment to moment. Since the eyes are constantly moving in IN, it seems that visual perception could be limited by the *time taken to see*.

2. Visual processing in IN is not slow

We investigated the time taken by people with IN to find and respond to visual targets, and discovered that visual *timing* difficulties do indeed exist (a finding that has been reported previously) – people with nystagmus take significantly longer to move their eyes towards and respond to peripherally-presented visual stimuli. We investigated further, by separating the *time taken to move the eyes* from the *time taken to respond to the target after moving the eyes*. We found that the visual *timing* deficit in IN is *entirely* due to difficulties in moving the eyes. In other words, people with IN responded *as quickly* as normally-sighted control subjects once they had 'pointed' their eyes towards the target. Therefore, *visual processing in IN is not slow*; it just takes longer to move the eyes towards objects of interest.

3. Nystagmus 'quick phases' are under subconscious control

Having uncovered the nature of the visual *timing* difficulties faced in IN, we sought to understand what aspects of eye movement control are abnormal. We ran a simple experiment in which participants were asked to move their eyes towards a cross that jumped around a screen. We found that voluntary eye movements towards the cross almost

Appendix V Patient information sheets and consent forms

Visual Perception in Infantile Nystagmus in the Absence of Image Motion

Researchers: Mr Matt Dunn, Dr Jon Erichsen

Consent Form

Please tick

- I have read and understood the Information sheet and have been given the opportunity to ask questions.
- I understand that my participation is voluntary and that I am free to withdraw at any time.
- I agree to take part in the study.
- I would like to receive information on the results of this investigation

Name (Printed):.....

Signed:.....

Date:.....

D.O.B.:.....

Contact Details

Address:.....

..... Postcode:.....

Telephone No. Daytime:.....

Evening:.....

Email Address:.....

Thank You!

Visual Perception in Infantile Nystagmus in the Absence of Image Motion

What is the purpose of this study?

Infantile nystagmus syndrome (also known as INS, congenital nystagmus, and early onset nystagmus) causes involuntary movement of the eyes. It usually presents during early visual development and in the majority of cases causes a reduction in visual function. The number of people believed to be affected by infantile nystagmus syndrome is 14 in every 10,000. In recent years, our understanding of nystagmus has been greatly improved with the aid of eye movement recordings. A recent study from our research unit has shown that a change in nystagmus intensity brought on by stress increases the time taken to identify a visual target, whilst not affecting the actual level of detail that can be resolved using current measures. We have therefore identified 'time to see' as an important factor in nystagmus, and it is our intention to find out why this is. The aims of this study are to measure visual acuity in the absence of image motion, identify the time taken to fixate and identify visual targets, quantify eye movement patterns, and ascertain how visual performance in nystagmus is affected by flicker.

Why have I been chosen?

We are aiming to recruit 10 subjects over the age of 18 with idiopathic infantile nystagmus syndrome. Subjects should not take part if they have a history of light sensitive epilepsy.

Who is organizing the study?

The study is organized by the Research Unit for Nystagmus (RUN) at the Cardiff University School of Optometry and Vision Sciences.

What will happen during the experiments?

Each participant will attend the School of Optometry and Vision Sciences building (Maindy Road) for one session, lasting around four hours.

There are a few different parts to the study. For two of these, your eye movements will be recorded while you view targets which will become increasingly difficult to see. The recording equipment consists of two cameras which monitor the position of the eyes. Apart from an eye patch over one eye, you will not have to wear any equipment as the eye tracker is a remote device. The eye tracker is connected to a camera flash unit which will illuminate the visual targets when the eyes are gazing in specific directions. We will ask you to identify the visual targets as best you can.

A third experiment does not involve an eye tracker at all, although we will ask you to wear a pair of sunglasses whilst identifying targets that flicker.

In addition to this, a qualified optometrist will perform some clinical tests, including measurement of your visual acuity with a letter chart, and acquire a three-dimensional picture of the back of the eye using a special camera known as an optical coherence tomographer, which is often used in eye hospitals.

We are also investigating visual reaction speeds in nystagmus. For this, you will be asked to respond by pressing a button as soon as you notice an image appear on a computer screen.

The final part of the study is a series of experiments designed to look at your eye movement patterns in different situations. One of these involves looking at a dot that moves around on a computer screen. In another, we will ask you to look towards a blank screen for five minutes (we are investigating nystagmus patterns in the absence of a

specific visual task). Another variation involves looking at a static point whilst a peripheral light turns on and off.

What are the possible benefits of taking part?

Although no immediate benefit is likely to arise as a result of this study, we hope that the information obtained will contribute to the long-term understanding of visual perception in nystagmus, and therefore aid the future development of therapeutic and/or rehabilitative techniques designed to maximize the visual potential of people with nystagmus.

Are there any disadvantages to taking part in this study?

No. If you feel uncomfortable at any point during the study, the experiment can be stopped and no further participation is necessary.

Who will know I am taking part in this study?

All information that is collected about you during the course of the research will be kept strictly confidential. Any information about you will be encoded so that you cannot be recognized from it.

Travel expenses

We will pay your travel expenses up to a value of £50.

Ethics

This study has been approved by the School of Optometry Human Research Ethics committee.

What will happen to the results of this study?

We aim to publish the results of this research in scientific journals. If you are interested, we can also summarise the results in an information sheet for you.

Contact information

Please feel free to ask further questions by contacting:

Mr Matt Dunn on 029 2087 0556; email DunnMJ1@cardiff.ac.uk

or

Dr Jon Erichsen on 029 2087 5656; email ErichsenJT@cardiff.ac.uk

Many Thanks

Matt Dunn

Appendix VI Ethical applications and approval documents

Dr. Jeremy Guggenheim
 School of Optometry and Vision Sciences
 Maindy Road
 Cardiff
 CF24 4LU

Request for ethical approval

Dear Dr. Guggenheim,

I would like to request ethical approval for experiments to be undertaken as part of my PhD. I am seeking this from yourself rather than Dr. Woodhouse as she is one of the investigators.

The experiments will involve eye movement recording, for which I already have ethical approval (reference #1269), whilst measuring the visual acuity to the afterimage of a stimulus illuminated by a Metz Mecablitz C-76 camera flash unit. The device is used in photography and has already been approved for use in an experiment undertaken in the School by Ashley Wood (project number 1270; title "The Relationship between retinal structure and function in Age-related Maculopathy"; approved 3rd November 2008). In the above experiment, the flash unit was used to bleach the macula. In our study, we intend to use light *reflected from* the flash in order to illuminate the stimuli for the measurement of visual acuity.

I quote the following regarding the flash unit from Mr. Wood's ethics request document which was previously accepted:

"We intend to produce the photoflash bleach using a Metz Mecablitz C-76 (Metz-Werke GmbH & Co KG, Ohmstr. 55, 90513 Zirndorf) flash unit. Due to the intensity of the flash it was necessary to determine if the flash met the safety standards for ophthalmic light sources as laid out in the British Standard BS EN ISO 15004-2:2007 "Ophthalmic Instruments – fundamental requirements and test methods Part 2 – Light Hazard Protection". Three relevant safety calculations were identified, regarding the safe exposure to UV and IR light as output by our device. The spectral irradiance for the flash was calculated using the maximum output settings and applied to these three safety calculations. In all three cases the output was within the safety limits.

Standard 5.5.1.1 "Weighted corneal and lenticular ultraviolet radiation radiant exposure" 250 – 400 nm (BSI, 2007) the limit was 0.003 j/cm^2 , and the photoflash unit at maximum intensity produced a value of $1 \times 10^{-12} \text{ j/cm}^2$.

Standard 5.5.2.1 "Weighted retinal visible and infrared radiation radiant exposure" 280 – 1400 nm (BSI, 2007) the safety limit was calculated as 0.137 j/cm^2 with the photoflash unit at maximum intensity producing a value of $2.14 \times 10^{-6} \text{ j/cm}^2$.

Standard 5.5.2.2 "Unweighted corneal and lenticular infrared radiation radiant exposure" 770 – 2500 nm (BSI, 2007) the safety limit was calculated as 0.514 j/cm^2 with the photoflash unit at maximum intensity producing a value of $2.67 \times 10^{-4} \text{ j/cm}^2$.

The photoflash used to photobleach the subjects will additionally be attenuated using heat filters, which will further reduce the power output of the flash unit, and reduce the unnecessary infrared output."

Please note, however, that we will **not** be using the heat filters as in the 2008 experiment because the light will be reflected from the stimulus at a much greater distance.

The investigators in the study will be:

- Mr. MJ Dunn
- Dr. JT Erichsen
- Dr. JM Woodhouse
- Dr. TH Margrain

Signature of lead investigator (JT Erichsen):

I look forward to your reply.

Yours Sincerely,

Matt J Dunn

Dr. Jeremy Guggenheim
Cardiff School of Optometry and Vision Sciences
Maindy Road
Cardiff
CF24 4LU

18th July 2011

Request for ethical approval: visual perception in infantile nystagmus in the absence of image motion

Dear Dr. Guggenheim,

I would like to request ethical approval for experiments to be undertaken as part of my PhD. I am seeking this from yourself rather than Dr. Woodhouse as she is one of the investigators.

I am currently approved on ethics document #1269 to use a Metz Mecablitz C-76 flash unit to illuminate a visual target. Whilst this has been approved, I would like to seek clarification on the regularity with which the unit may be discharged. We would like to be able to have the flash fire in response to eye movements. In patients with nystagmus (the main focus of the experiments), this could mean on average a firing rate of around 2-6Hz. We will ensure that photosensitive epilepsy is an exclusion criterion, and that subjects are asked to report any unusual sensations and can end the experiment on request. Testing will always be done monocularly, which will reduce the risk of an epileptic seizure.

Investigators in the study are:

- Mr. MJ Dunn
- Dr. JT Erichsen
- Dr. JM Woodhouse
- Dr. TH Margrain

As per your request, I attach all the necessary documentation for the implementation of a brand new ethical approval, instead of an amendment to the current document.

Signature of lead investigator (JT Erichsen):

I look forward to your reply.

Yours Sincerely,

Matt J Dunn

SCHOOL OF OPTOMETRY AND VISION SCIENCES

SCHOOL RESEARCH/AUDIT ETHICS COMMITTEE



Please complete form for consideration by assessors appointed by the Human Science Ethical Committee. Please submit the completed form, with any related correspondence, to the Departmental Office. **A subject information leaflet and consent form must be included.**

PROJECT TITLE: Visual perception in infantile nystagmus in the absence of image motion

PLEASE REFER TO THE DISTINCTION BETWEEN RESEARCH AND AUDIT ATTACHED TO THIS FORM AND INDICATE INTO WHICH CATEGORY YOUR STUDY FALLS (note that the Committee does not distinguish between audit and service evaluation; both require approval)

<u>RESEARCH</u>	<u>AUDIT</u>
-----------------	--------------

Date of submission: 14th July 2011

INVESTIGATOR(S):	SCHOOL/ADDRESS:	PHONE:
1. Dr. Jon Erichsen	Optometry	75656
2. Dr. Maggie Woodhouse	Optometry	76522
3. Dr. Tom Margrain	Optometry	76118
4. Mr. Matt Dunn	Optometry	70556

5.

SPONSORING/COLLABORATING ORGANISATION (if any): None

DOES THE SPONSORING/COLLABORATING ORGANISATION PROVIDE INSURANCE:

YES/NO*

IF DRUGS ARE USED DO ANY REQUIRE A CLINICAL TRIALS CERTIFICATE OR CLINICAL TRIALS EXEMPTION CERTIFICATE?

YES/NO*

*If YES please provide a copy of the certificate.

Has this project been considered by another Ethical Committee (e.g. NHS)? ~~YES~~/NO

If so, please provide the application, or a summary, and a copy of the decision letter. The School Committee would not normally refuse consent to a project approved by another committee, but requires notification of all work undertaken within the School or by members of the School.

LAY SUMMARY OF PROJECT:

1. Starting date: 18th July 2011
2. Duration 3 Years
3. Description of project:
The project aims to determine the visual acuity of individuals with infantile nystagmus in the absence of image motion. Using a photographic flash unit driven by the position of the eyes, a psychophysical procedure for determining acuity threshold will be used to measure the acuity function with respect to retinal eccentricity.
4. Number of subjects to be used:
- Up to 25
5. Age and gender of subjects:
- Males and females above the age of 18.
6. How will subjects be recruited?
- Letters and emails will be sent to our existing cohort from the RUN (Research Unit for Nystagmus)
7. Will payments be made to the subjects (if so how much)?
- Travel expenses will be paid
8. Will any subjects be excluded and if so on what grounds?
- Individuals known to have photosensitive epilepsy (due to the flash)
9. Is the activity of the subjects to be restricted in any way either before or after the procedure (e.g. diet, driving etc.)
- No.
10. Describe any hazards which could affect the health safety or welfare of any subject or of any researcher and how you propose to minimise these hazards
- The flash unit will be flashing in synchrony with the subject's eye movements. In individuals with nystagmus, this could mean on average a firing rate of around 2-6Hz. Whilst individuals with photosensitive epilepsy will be excluded, we will also ensure that subjects are asked to report any unusual sensations and can end the experiment on request. Testing will always be done monocularly, which will reduce the risk of an epileptic seizure (Anyanwu, 1999).
11. Describe any other ethical issues and how these will be addressed
- N/A
12. What arrangements will there be for subjects to learn of the results of the study?
- The consent form allows subjects to request the results of the investigation are passed on to them.

STATEMENT BY NAMED INVESTIGATORS, HEAD OF DEPARTMENT AND RESEARCH SUPERVISOR (if necessary).

I consider that the details given constitute a true summary of the project, and the hazards and potential risks to any subject are accurately described. I confirm that the relevant health and safety measures, in accordance with University policy and School requirements, have been taken into account for the proposed research

Lead researcher

..... (Signed)..... (Date)

PROJECT DESCRIPTION AND PROTOCOL

PROJECT TITLE: Visual perception in infantile nystagmus in the absence of image motion

Objectives of the study

The objective of the study is to determine the visual acuity of individuals with infantile nystagmus syndrome (INS) in the absence of image motion.

Outline of the study design

Subjects will have their visual acuity measured using both a standard letter chart and by using a psychophysical two-alternative-forced choice method. Eye movements will then be recorded and room lights extinguished. Subjects will attempt to fixate a target and a flash unit will illuminate a visual target when the eyes are detected moving into in a specific angle of gaze. Using similar methods, visual acuity will be obtained at various positions of gaze.

In the event that a subject develops signs or symptoms of epileptic seizure, an ambulance will be summoned and first aid will be sought within the building.

Scientific background to study

It is not known whether visual acuity in individuals with INS (in the absence of underlying pathology) is reduced due to the movement of the retinal image, amblyopia, or both. Secondly, it is not known whether peripheral visual acuity develops in the same way in individuals with nystagmus as those without. Finally, there are currently two theories to explain why people affected by INS do not often experience oscillopsia. This study aims to explain the first two points, and may shed some light on the third.

Subjects

Individuals affected by INS above the age of 18. Both male and female subjects will be used. Subjects who have photosensitive epilepsy will be excluded, due to the frequency of the flashes.

Recruitment procedures

Letters and emails will be sent to our existing cohort from the RUN (Research Unit for Nystagmus).

Substances to be administered

None

Procedures

Standard psychophysical methods will be used to obtain visual acuity thresholds. Eye movements will be recorded. A Metz Mecablitz C-76 will be used to illuminate the visual targets (under monocular viewing conditions only). Please note that ethical approval has already been granted for the use of the flash unit to be used in this study (approval #1269). The purpose of this ethics request is to allow the flash to be fired in synchrony with the subject's eye movements.

References

Anyanwu E (1999) Evaluation of the laboratory and environmental factors that induce seizures in photosensitive epilepsy. *Acta Neurol Belg* 99: 126-132.

Appendix VII Published work

Eye Movements, Strabismus, Amblyopia, and Neuro-Ophthalmology

Grating Visual Acuity in Infantile Nystagmus in the Absence of Image MotionMatt J. Dunn,¹ Tom H. Margrain,¹ J. Margaret Woodhouse,¹ Fergal A. Ennis,¹ Christopher M. Harris,² and Jonathan T. Erichsen¹¹School of Optometry and Vision Sciences, Cardiff University, Cardiff, United Kingdom²Centre for Robotics and Neural Systems, Plymouth University, Plymouth, United Kingdom

Correspondence: Jonathan T. Erichsen, School of Optometry and Vision Sciences, Cardiff University, Maindy Road, Cardiff CF24 4HQ, Wales, UK; ErichsenJT@cardiff.ac.uk

Submitted: October 23, 2013

Accepted: February 16, 2014

Citation: Dunn MJ, Margrain TH, Woodhouse JM, Ennis FA, Harris CM, Erichsen JT. Grating visual acuity in infantile nystagmus in the absence of image motion. *Invest Ophthalmol Vis Sci.* 2014;55:2682–2686. DOI: 10.1167/iov.13-13455

PURPOSE. Infantile nystagmus (IN) consists of largely horizontal oscillations of the eyes that usually begin shortly after birth. The condition is almost always associated with lower-than-normal visual acuity (VA). This is assumed to be at least partially due to motion blur induced by the eye movements. Here, we investigated the effect of image motion on VA.

METHODS. Grating stimuli were presented, illuminated by either multiple tachistoscopic flashes (0.76 ms) to circumvent retinal image motion, or under constant illumination, to subjects with horizontal idiopathic IN and controls. A staircase procedure was used to estimate VA (by judging direction of tilt) under each condition. Orientation-specific effects were investigated by testing gratings oriented about both the horizontal and vertical axes.

RESULTS. Nystagmats had poorer VA than controls under both constant and tachistoscopic illumination. Neither group showed a significant difference in VA between illumination conditions. Nystagmats performed worse for vertically oriented gratings, even under tachistoscopic conditions ($P < 0.01$), but there was no significant effect of orientation in controls.

CONCLUSIONS. The fact that VA was not significantly affected by either illumination condition strongly suggests that the eye movements themselves do not significantly degrade VA in adults with IN. Treatments and therapies that seek to modify and/or reduce eye movements may therefore be fundamentally limited in any improvement that can be achieved with respect to VA.

Keywords: orientation, amblyopia, tachistoscopic

Infantile nystagmus (IN) describes a regular, repetitive movement of the eyes. It usually develops within the first 6 months of life, causing ocular oscillations that are constant and persist throughout life. While many individuals with IN have a comorbid pathology of the visual pathway, approximately 30% appear not to and have been labeled as “idiopathic.”¹ Despite the absence of any other detectable pathology, idiopathic cases of IN are typically associated with a moderate reduction in visual acuity (VA), which has been assumed to be caused by the eye movements themselves. For example, the Nystagmus Acuity Function (NAF) and eXpanded NAF (NAFX) are outcome measures that quantify eye movement characteristics in order to predict VA.^{2,3} Yet, it is not actually known to what extent image motion affects VA in individuals with IN.

Infantile nystagmus waveforms typically exhibit so-called foveations—periods during which the eyes move more slowly. It has been presumed that these periods exist to facilitate better VA by reducing motion blur induced by the eye movements. Nonetheless, the eyes are never truly stable for more than a few milliseconds. In normal subjects, an increase in image velocity (above 2.5 deg/s) causes a concordant reduction in VA and perceived contrast intensity, regardless of the direction of movement.^{4–7} One previous study has examined the effects of comparable (nystagmoid) image motion on the vision of normal subjects, and found a decline in VA at velocities above 3 deg/s.⁸ While many nystagmus waveforms contain foveation periods

with velocities below this threshold, some do not, even in subjects with idiopathic IN. Previous studies^{2,3,9,10} have demonstrated a strong *intersubject* correlation between waveform dynamics and VA. In addition, in experiments in which normally sighted subjects are presented with image motion similar to that produced by nystagmus waveforms, VA improves as simulated foveation period duration increases.^{8,11–13} This wealth of evidence has led to the assumption that poor waveform dynamics (i.e., brief or high-velocity foveations) reduce VA. Many clinical therapies have been predicated on this assumption.^{2,14,15} Nonetheless, in principle, it remains possible that the reverse is true: that poor VA may result in the development of a waveform with less accurate, briefer foveations.¹⁶

Jin and colleagues¹⁷ have demonstrated that a small flash of light is equally likely to be perceived at all times regardless of when it is presented during the nystagmus waveform. Furthermore, images stabilized on the retina, afterimages of bright flashes, and migraine auras are occasionally perceived as continuously moving in individuals with IN.^{18,19} This evidence suggests that visual perception is continuous throughout the slow phases of nystagmus as well as during foveations. Chung et al.²⁰ have found that normal subjects presented with an image moving in a nystagmoid fashion have improved VA when the image is shown during the simulated foveations but hidden for the remainder of the slow phases. One might therefore

expect VA to be similarly degraded by motion blur during the entire slow phase in individuals with IN.

Here, we sought to measure VA in adults with IN in the absence of image motion, by using briefly flashed gratings in an otherwise dark environment. Abadi and King-Smith²¹ have adopted a similar approach. They have determined the luminance required to detect the presence of a single line under continuous and tachistoscopic (0.2 ms) conditions; data were derived from four individuals with IN and three control subjects. Visual stimuli were presented to both groups with a brief flash of light to eliminate image motion, so that the impact of image motion on visual sensitivity could be estimated. They have found that sensitivity to a 16° long line oriented in the same axis as the nystagmus is higher than to a line oriented in the orthogonal axis, which is attributed to meridional amblyopia. However, the relationship between the tachistoscopic and continuous presentations is not discussed, and the sensitivity measure used (i.e., relative sensitivity) cannot be interpreted clinically. Therefore, we used gratings to directly measure the impact of image motion on VA.

METHODS

Seventeen subjects with horizontal idiopathic IN volunteered for the study. First, the diagnosis of idiopathic IN as reported by the subject or by their ophthalmologist was investigated by an optometrist using high-speed eye movement recording, ophthalmoscopy, optical coherence tomography, and a detailed family history. Subjects with nystagmus showing any signs of coexisting ocular pathology other than strabismus were excluded. Following these examinations, four were excluded on the basis of eye movement recordings (one with gaze-evoked nystagmus but no nystagmus in the primary position; three with fusion maldevelopment nystagmus syndrome), two were excluded on the basis of history (achromatopsia and acquired nystagmus), one was excluded owing to iris transillumination (suggesting albinism), and one was excluded owing to having active pathology (Fuchs' endothelial dystrophy). Nine subjects with IN remained to participate in the study (three females, aged 21–69 years; mean, 43 years). Nine normally sighted individuals with no history of ocular disease were recruited (four females, aged 21–48 years; mean, 28 years). The investigation was carried out in accordance with the Declaration of Helsinki; informed consent was obtained from the subjects after explanation of the nature and possible consequences of the study. Ethical approval was granted by the Cardiff School of Optometry and Vision Sciences Human Research Ethics Committee.

First, clinical monocular VA of each eye was measured by using a self-illuminated logMAR chart at 3 m under clinical conditions. The eye with the best VA was then used as the test eye. Subjects with equal VA had their dominant eye tested, as determined by investigation of suppression using a distance Mallett unit. In the case of equidominance, the right eye was tested by default. For the test eye, habitual distance spectacle correction was worn, or refracted correction was provided if refractive error exceeded ± 0.50 diopters (mean sphere) from the habitual correction. The nontest eye was patched.

Subjects were seated 2 m in front of a 12° aperture in the center of a white cardboard mask, through which square-wave gratings were presented (Fig. 1). Large gratings were used in order to ensure that the participant's gaze would be directed toward similar visual stimuli at all times, regardless of eye position during the nystagmus cycle. In addition, gratings provide a robust measure of VA, relying solely on resolution rather than recognition as in the case of optotypes. Twenty square-wave gratings were produced by a high-quality profes-

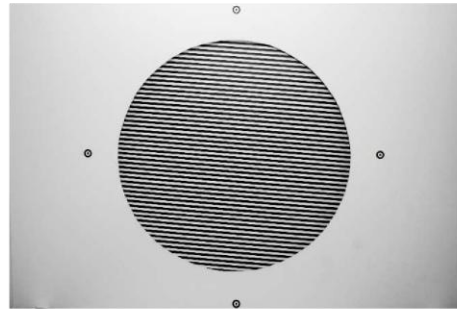


FIGURE 1. Photograph of the aperture frame illuminated by the flash unit, with a grating mounted inside (tilted 5° up to the left), as viewed by subjects. The bull's-eye targets serving as horizontal and vertical axis references can be seen around the grating edge.

sional printer (RA-4 process, Durst Epsilon photographic printer; Durst Image Technology UK Ltd., Surrey, UK) with fundamental spatial frequencies ranging from -0.46 to 1.48 logMAR on heat-treated, nonglossy photographic card large enough to fill the 12° aperture.

Four small bull's-eye targets were arranged around the aperture at 90° intervals, providing reference axes (horizontal and vertical) to aid in judgment of tilt. The bull's-eye targets were illuminated by spots of light from a projector, situated behind the subject.

Gratings were illuminated either constantly, by a lamp providing 1.62 log cd/m², or tachistoscopically by an unlimited number of flashes each lasting 0.76 (± 0.01) ms, from a Metz Mecablitz 76 MZ-5 flash unit (Metz, Zirndorf, Germany) with an output of 4.64 cd-s/m². Flash brightness was empirically adjusted in a pilot experiment to provide VA approximately equal to that obtained under constant illumination for one normally sighted individual. Assuming an eye rotating at 14 deg/s (the average ocular velocity in IN²²), a flash of this duration would cause only 0.01° of image smear (allowing a maximum possible VA of -0.19 logMAR). The flash was strobed, with the delay between flashes varying randomly between 2 to 6 Hz in order to prevent flash-timing prediction.

For each presentation, gratings were automatically tilted on a motorized platform either 5° up/down from horizontal or left/right from vertical. Figure 2 shows the tilting mechanism with the aperture removed. Subjects were allowed as much time (or as many flashes) as desired before reporting the perceived tilt direction of each presentation, using a response box. No feedback was given for correct or incorrect responses. The finest grating available that provided a VA equivalent to or worse than the subject's clinical VA (i.e., slightly coarser) was used for the first presentation. Visual acuity was estimated by using a two-alternative forced choice transformed up-down psychophysical staircase procedure of eight reversals with a three-up/one-down criterion. The direction of tilt for any given presentation was decided by combined Gellerman-Fellows sequences.²³ Grating reorientation and flash delivery was automated and computer controlled. The computer identified which grating was to be used next, and the gratings were then physically replaced. Visual acuity was estimated as the mean of the final six staircase reversals.²⁴

As mentioned above, this procedure was performed under two different lighting conditions, with gratings oriented about two axes:



FIGURE 2. Computer-controlled platform used for automating grating orientation, shown here with the aperture removed.

- *Constant horizontal*: Gratings oriented $\pm 5^\circ$ about the horizontal axis, under constant illumination;
- *Tachistoscopic horizontal*: Gratings oriented $\pm 5^\circ$ about the horizontal axis, illuminated tachistoscopically;
- *Constant vertical*: Gratings oriented $\pm 5^\circ$ about the vertical axis, under constant illumination; and
- *Tachistoscopic vertical*: Gratings oriented $\pm 5^\circ$ about the vertical axis, illuminated tachistoscopically.

Test presentation order was randomized.

RESULTS

The Table shows the data obtained from all 18 subjects, including clinical VA and, for each of the four conditions, grating acuity (logMAR).

The data from the Table are summarized in Figure 3.

Figure 3 shows that, under all illumination conditions and orientations, subjects with idiopathic IN performed significantly worse than controls (all $P < 0.005$). Subjects with idiopathic

IN performed worse for vertically oriented gratings, whereas controls did not show an orientation effect (see below). Most importantly, illumination type did not affect VA for either group. Note that no effect of illumination was expected or observed in the *control* group, since the brightness of the flash was adjusted in a pilot experiment to give approximately the same VA.

Tachistoscopic Versus Constant Illumination

The effect of tachistoscopic presentation on VA was analyzed by using paired samples *t*-tests. Tachistoscopic presentation caused no significant difference in VA in controls for either orientation (horizontal: $P = 0.6224$; vertical: $P = 0.0807$). Similarly, in nystagmats, there was no significant difference between lighting conditions for either orientation (horizontal: $P = 0.2311$; vertical: $P = 0.2431$).

Effect of Orientation

Paired samples *t*-tests indicate a significant orientation effect in nystagmats under both constant ($P = 0.0076$) and tachistoscopic ($P = 0.0188$) conditions. For both lighting conditions, near-horizontal grating acuity was better than that for near-vertical gratings. However, the VA for control subjects was not significantly different regardless of orientation under both conditions ($P = 0.8672$ for constant light and $P = 0.4426$ for tachistoscopic presentation).

DISCUSSION

Under all lighting conditions and stimulus orientations, VA was worse for subjects with idiopathic IN than controls. Crucially, the fact that VA did not improve under tachistoscopic illumination suggests that *image motion may not be the limiting factor to VA in IN*. We found no significant difference in VA between constant and tachistoscopic illumination, *even for vertically oriented gratings*. Since all the nystagmats in this study had primarily horizontal nystagmus, if motion blur were a limiting factor to visual perception, one would have expected vertically oriented gratings to be clearer under tachistoscopic

TABLE. VA (logMAR) Recorded for All Subjects

	Subject	Sex	Age, y	Clinical VA	Constant Horizontal	Constant Vertical	Tachistoscopic Horizontal	Tachistoscopic Vertical
Idiopathic IN	GT2	M	59	0.78	0.80	0.86	0.70	0.91
	DB	M	53	0.64	0.65	0.65	0.80	0.65
	JT	M	24	0.42	0.21	0.33	0.33	0.41
	SW	F	69	0.16	0.21	0.37	0.17	0.34
	JC2	F	54	0.54	0.42	0.53	0.34	0.54
	GS	M	28	0.54	0.39	0.51	0.28	0.42
	NB	M	44	0.26	-0.06	0.31	-0.11	0.33
	DP	M	38	0.60	0.16	0.54	-0.02	0.68
	VW	F	21	0.34	0.36	0.46	0.23	0.52
Mean \pm standard error				0.48 \pm 0.07	0.35 \pm 0.09	0.51 \pm 0.06	0.30 \pm 0.10	0.53 \pm 0.06
Controls	LP	F	23	0.10	0.03	0.01	0.17	0.08
	JS2	M	24	-0.16	-0.04	-0.03	0.01	-0.07
	FE	M	47	-0.08	-0.14	-0.11	-0.08	-0.03
	PG	M	20	-0.20	-0.11	-0.14	-0.17	-0.08
	TM	M	48	-0.22	-0.11	-0.03	-0.11	-0.04
	AS	F	23	-0.14	-0.03	-0.06	-0.01	-0.10
	MU	F	21	-0.08	0.03	-0.07	-0.03	0.02
	BF	F	26	-0.10	-0.08	0.01	0.02	0.07
	JT2	M	23	-0.14	-0.09	-0.09	-0.20	0.00
Mean \pm standard error				-0.11 \pm 0.03	-0.06 \pm 0.02	-0.06 \pm 0.02	-0.05 \pm 0.04	-0.02 \pm 0.02

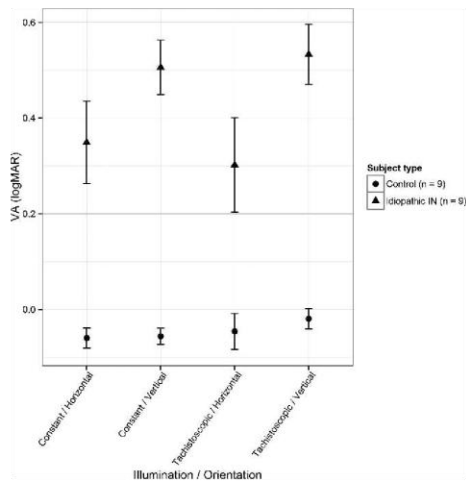


FIGURE 3. Graphical representation of the VAs recorded for all subjects. Error bars indicate standard error.

illumination, resulting in a change in measured VA. Although no effect of illumination was expected in controls (since the flash brightness was set to approximately achieve equality), the absence of a significant improvement in VA in the subjects with idiopathic IN was unexpected.

Under both lighting conditions, subjects with idiopathic IN had significantly poorer VA for vertical gratings than horizontal, whereas controls showed no effect of orientation. This finding is strongly suggestive of meridional amblyopia in IN and has previously been reported under constant illumination.²⁵ Abadi and King-Smith²¹ have found a similar effect under tachistoscopic illumination using a measure of visual sensitivity, although ours is the first study to measure VA under this condition.

Previous studies^{2,3,12} have reported a correlation between foveation quality (e.g., duration, accuracy) and VA, and concluded that eye movement characteristics can be used to predict VA. While this has been shown with simulated waveforms in controls and *between* individuals with IN, the correlation does not appear to be evident in response to waveform changes *within* the same subject.^{26,27} The results of minimizing image motion in the present study strongly suggest that there is an upper limit on the VA possible in adults with idiopathic IN, and that this limit is independent of eye movement characteristics.

Treatments such as biofeedback have been shown to cause increased foveation duration, but were abandoned owing to the lack of an improvement in VA.^{28,29} In light of our unexpected finding indicating that VA cannot be *expected* to improve, it may now be worth revisiting this and other therapies, as there may be other visual benefits that are not captured by VA measurement. For example, we hypothesize that prolonging foveation duration might result in faster visual recognition speed (i.e., reduced visual recognition time), since the retinal locus of highest photoreceptor density would be directed toward the object of interest for a greater proportion of time.

Despite the incessant eye movements, adults with IN usually do not experience oscillopsia,¹⁸ but regardless of this stable percept, retinal anatomy dictates that vision *cannot* be

optimal when the fovea is not directed at the locus of attention. It is hardly surprising therefore that VA, a static measure of visual function in which viewing time is unlimited, cannot adequately represent the visual experience of those with nystagmus.

Algorithmic measures of waveform characteristics (such as Nystagmus Optimal Fixation Function and NAFX) are designed to quantify visual performance, but these are currently predicated on the presumed relationship between VA and foveation characteristics. Alternative assessments might measure other aspects of visual performance, such as processing speed (e.g., time-restricted optotype recognition tasks³⁰ or visual response speed measurements³¹) or target acquisition timing.³² Ideally, these measures would correlate with foveation characteristics and subjective visual experience better than VA.

Image motion blur can have a deleterious effect on vision in normal subjects, which has understandably led to an assumption that the blur induced by the oscillations in IN is, at least partly, responsible for their reduced VA. However, previous studies^{27,33,34} have found little if any significant change in subjects' VA as a result of modifications to their eye movements, whether produced by varying gaze angle, stress, or task demand. Moreover, although treatments for nystagmus are often designed to reduce the velocity of the eye movements, they rarely elicit improvements in VA, whether using optotypes for recognition acuity^{15,35,36} or its prerequisite, resolution acuity, as measured by gratings in the present study.

The results of the present study indicate that removing the image motion blur altogether in subjects with IN also does not change VA, suggesting that their VA may already be fundamentally limited, owing to an underlying pathology and/or stimulus deprivation amblyopia as a result of motion blur during the critical period for visual development. One view on the pathogenesis of IN is that it is a developmental adaptation to enhance contrast in the presence of a pre-existing visual acuity deficit.³⁷⁻³⁹ If this is the case, then the parameters of the adult waveform (foveation duration, average eye velocity, etc.) may well reflect the maximum VA that was available in infancy. This would explain the strong correlation between, for example, foveation duration and VA *across* subjects.¹⁰ In other words, poor-quality nystagmus waveforms may not lead to poor VA; rather, the properties of nystagmus waveforms in adults may reflect the underlying VA, as suggested by a recent study on the development of IN.⁴⁰ For these reasons, interventional studies are likely to require better outcome measures than VA alone if they are to demonstrate an objective change in visual performance.

Acknowledgments

We thank Lawrence Wilkinson for the loan of an EyeLink 1000 (SR Research, Ottawa, Canada) to assess the eye movements of the subjects with IN in this study and the Nystagmus Network (UK) for their help with recruiting subjects for the study.

Disclosure: **M.J. Dunn**, None; **T.H. Margrain**, None; **J.M. Woodhouse**, None; **F.A. Ennis**, None; **C.M. Harris**, None; **J.T. Erichsen**, None

References

- Lorenz B, Gampe E. Analysis of 180 patients with sensory defect nystagmus (SDN) and congenital idiopathic nystagmus (CIN) [in German]. *Klin Monbl Augenheilkd*. 2001;218:3-12.
- Sheth NV, Dell'Osso LF, Leigh RJ, Vandoren CL, Peckham HP, Van Doren CL. The effects of afferent stimulation on congenital nystagmus foveation periods. *Vision Res*. 1995;35:2371-2382.

3. Dell'Osso LF, Jacobs JB. An expanded nystagmus acuity function: intra- and intersubject prediction of best-corrected visual acuity. *Doc Ophthalmol*. 2002;104:249-276.
4. Ludvig E, Miller JW. Study of visual acuity during the ocular pursuit of moving test objects, I: introduction. *J Opt Soc Am*. 1958;48:799-802.
5. Miller JW. Study of visual acuity during the ocular pursuit of moving test objects, II: effects of direction of movement, relative movement, and illumination. *J Opt Soc Am*. 1958;48:803-808.
6. Westheimer G, McKee SP. Visual acuity in the presence of retinal-image motion. *J Opt Soc Am*. 1975;65:847-850.
7. Demer JL, Amjadi F. Dynamic visual acuity of normal subjects during vertical optotype and head motion. *Invest Ophthalmol Vis Sci*. 1993;34:1894-1906.
8. Chung STL, Bedell HE. Effect of retinal image motion on visual-acuity and contour interaction in congenital nystagmus. *Vision Res*. 1995;35:3071-3082.
9. Abadi RV, Worfolk R. Retinal slip velocities in congenital nystagmus. *Vision Res*. 1989;29:195-205.
10. Abadi RV, Pascal E. Visual resolution limits in human albinism. *Vision Res*. 1991;31:1445-1447.
11. Chung STL, Bedell HE. Congenital nystagmus image motion: influence on visual acuity at different luminances. *Optom Vis Sci*. 1997;74:266-272.
12. Currie DC, Bedell HE, Song S. Visual-acuity for optotypes with image motions simulating congenital nystagmus. *Clin Vis Sci*. 1993;8:73-84.
13. Chung STL, Bedell HE. Velocity criteria for "foveation periods" determined from image motions simulating congenital nystagmus. *Optom Vis Sci*. 1996;73:92-103.
14. Dell'Osso LF, Hertle RW, Leigh RJ, Jacobs JB, King S, Yaniglos S. Effects of topical brinzolamide on infantile nystagmus syndrome waveforms: eyedrops for nystagmus. *J Neuroophthalmol*. 2011;31:228-235.
15. Hertle RW, Dell'Osso LF, FitzGibbon EJ, Thompson D, Yang D, Mellow SD. Horizontal rectus tenotomy in patients with congenital nystagmus: results in 10 adults. *Ophthalmology*. 2003;110:2097-2105.
16. Harris CM. Infantile (congenital) nystagmus. *Optom Today*. 2013;48-53.
17. Jin YH, Goldstein HP, Reinecke RD. Absence of visual sampling in infantile nystagmus. *Korean J Ophthalmol*. 1989;3:28-32.
18. Leigh RJ, Dell'Osso LF, Yaniglos SS, Thurston SE. Oscillopsia, retinal image stabilization and congenital nystagmus. *Invest Ophthalmol Vis Sci*. 1988;29:279-282.
19. Dell'Osso LF. The mechanism of oscillopsia and its suppression. *Ann N Y Acad Sci*. 2011;1233:298-306.
20. Chung ST, LaFrance MW, Bedell HE. Influence of motion smear on visual acuity in simulated infantile nystagmus. *Optom Vis Sci*. 2011;88:200-207.
21. Abadi RV, King-Smith PE. Congenital nystagmus modifies orientational detection. *Vision Res*. 1979;19:1409-1411.
22. Bedell HE. Perception of a clear and stable visual world with congenital nystagmus. *Optom Vis Sci*. 2000;77:573-581.
23. Fellows BJ. Chance stimulus sequences for discrimination tasks. *Psychol Bull*. 1967;67:87-92.
24. Levitt H. Transformed up-down methods in psychoacoustics. *J Acoust Soc Am*. 1971;49:467-477.
25. Meiusi RS, Lavoie JD, Summers CG. The effect of grating orientation on resolution acuity in patients with nystagmus. *J Pediatr Ophthalmol Strabismus*. 1993;30:259-261.
26. Erichsen JT, Wiggins D, Woodhouse JM, Margrain TH, Harris CM. Effect of eye orientation on visual acuity in infantile nystagmus (INS). In: *17th European Conference on Eye Movements*. August 11-16, 2013; Lund, Sweden. Poster 514.
27. Jones PH, Harris CM, Woodhouse JM, Margrain TH, Ennis F, Erichsen JT. Stress and visual function in infantile nystagmus syndrome. *Invest Ophthalmol Vis Sci*. 2013;54:7943-7951.
28. Mezawa M, Ishikawa S, Ukai K. Changes in wave-form of congenital nystagmus associated with biofeedback treatment. *Br J Ophthalmol*. 1990;74:472-476.
29. Ciuffreda KJ, Goldrich SG, Neary C. Use of eye movement auditory biofeedback in the control of nystagmus. *Am J Optom Physiol Opt*. 1982;59:396-409.
30. Yang DS, Hertle RW, Hill VM, Stevens DJ. Gaze-dependent and time-restricted visual acuity measures in patients with infantile nystagmus syndrome (INS). *Am J Ophthalmol*. 2005;139:716-718.
31. Hertle RW, Maybodi M, Reed GF, Guerami AH, Yang D, Fitzgibbon EJ. Latency of dynamic and gaze-dependent optotype recognition in patients with infantile nystagmus syndrome versus control subjects. *Ann N Y Acad Sci*. 2002;956:601-603.
32. Wang ZI, Dell'Osso LF. Being "slow to see" is a dynamic visual function consequence of infantile nystagmus syndrome: model predictions and patient data identify stimulus timing as its cause. *Vision Res*. 2007;47:1550-1560.
33. Wiggins D, Woodhouse JM, Margrain TH, Harris CM, Erichsen JT. Infantile nystagmus adapts to visual demand. *Invest Ophthalmol Vis Sci*. 2007;48:2089-2094.
34. Cham KM, Anderson AJ, Abel LA. Task-induced stress and motivation decrease foveation-period durations in infantile nystagmus syndrome. *Invest Ophthalmol Vis Sci*. 2008;49:2977-2984.
35. Kumar A, Shetty S, Vijayalakshmi P, Hertle RW. Improvement in visual acuity following surgery for correction of head posture in infantile nystagmus syndrome. *J Pediatr Ophthalmol Strabismus*. 2011;48:341-346.
36. McLean RJ, Proudlock F, Thomas S, Degg C, Gottlob I. Congenital nystagmus: randomized, controlled, double-masked trial of memantine/gabapentin. *Ann Neurol*. 2007;61:130-138.
37. Harris CM, Berry D. A developmental model of infantile nystagmus. *Semin Ophthalmol*. 2006;21:63-69.
38. Harris CM, Waddington J. Optimal control theory of normal and pathological slow eye movements. *J Control Eng Technol*. 2013;3:181-188.
39. Harris CM. Oculomotor developmental pathology: an evo-devo perspective. In: Liversedge S, Gilchrist ID, Everling S, eds. *Oxford Handbook of Eye Movements*. Oxford: Oxford University Press; 2011:663-686.
40. Felius J, Muhanna ZA. Visual deprivation and foveation characteristics both underlie visual acuity deficits in idiopathic infantile nystagmus. *Invest Ophthalmol Vis Sci*. 2013;54:3520-3525.